MOLECULAR CYTOGENETICS AND GENETIC CHARACTERISATION OF CHROMOSOMAL REARRANGEMENTS

by

SALWATI SHUIB

A thesis submitted to
The University of Birmingham
for the degree of
DOCTOR OF PHILOSOPHY

Department of Medical and Molecular Genetics
School of Clinical and Experimental Medicine
College of Medicine and Dental Sciences
The University of Birmingham
July 2010

MOLECULAR CYTOGENETICS AND GENETIC CHARACTERISATION OF CHROMOSOMAL REARRANGEMENTS

Abstract

In this thesis I report three related studies that utilise state-of-the-art technologies to investigate germline and somatic chromosomal rearrangements in humans. Firstly, 16 patients with cytogenetically detectable deletions of 3p25-p26 were analysed with high density single nucleotide polymorphism (SNP) microarrays; Affymetrix 250K SNP microarrays (n=14) and Affymetrix SNP6.0 (n=2). Assuming complete penetrance, a critical region for congenital heart disease (CHD) susceptibility gene was refined to approximately 200 kb and a candidate critical region for mental retardation was mapped to ~1 Mb interval containing *SRGAP3*. Secondly, I used SNP microarray and molecular cytogenetic studies to characterise chromosome 11p15 in 8 patients with the imprinting disorder Beckwith-Wiedemann syndrome (BWS). In addition to characterising 11p duplications in three patients, the breakpoints in two patients with balanced rearrangements were mapped to two distinct regions. Thirdly, I used high resolution SNP arrays (Affymetrix 250K Sty1 and 6.0 arrays) to identify copy number changes in renal cell carcinoma (RCC) primary tumours (n=81) and cell lines (n=23). Copy number changes most frequently involved large segments (>10Mb) and loss of 3p and gain of 5q were the most common copy number changes. A comparison of copy number changes in RCC cell lines and inherited and sporadic primary tumours was made.

Dedication

For my dearest family, who has always been a source of love, encouragement and support throughout my study.

Acknowledgements

There are many people who have contributed directly and indirectly towards the realisation of this thesis. It is a pleasure to convey my gratitude to them all in my humble acknowledgements.

I would like to express my deepest gratitude to both of my supervisors, Professor Eamonn R. Maher and Professor Farida Latif for given me the opportunity to be their student. I cannot thank you enough for all their support and guidance throughout the course of my studies.

This thesis would not have been possible without the help and support from the staff at the Birmingham Womens Hospital. I am so grateful especially to Fiona MacDonald and Dominic McMullan for allowing me to use the lab and the facilities in the Cytogenetic Department. I am thankful to Eleanor Rattenberry and Fatima Rahman for teaching me how to do the arrays, Mary Strachan and her staff for helping me with the cell culture, Angela Harris for her guidance in FISH and Richard Barber for helping me with the MLPA.

To my friends Neil, Sarah, Manju, Louise, Esther, Derek, Jane, Hakan, Dewi, Mark, Dean, Fiona, Chris Ricketts, Chris Bruce, Emma, Malgosia, Wendy, Julie, Andrew and Tom, many thanks for your help and I truly appreciate our friendship.

Words cannot describe how thankful I am to God for blessing me with a wonderful family. I couldn't have achieved this far without their love, continuous support, patience and encouragement. To my mother, my father, my beloved husband and wonderful children, thank you so much for always being there for me and for making my life complete.

This work received financial support from the Ministry of Higher Education of Malaysia and the Universiti Kebangsaan Malaysia.

Table of Contents

Index of figures

Index of tables

Preface

Part of the work presented in this thesis was published in the following papers. These are included at the end of this thesis.

Peer-reviewed journal articles

Shuib S, McMullan D, Rattenberry E, Barber RM, Rahman F, Zatyka M, Chapman C, Macdonald F, Latif F, Davison V, Maher ER. Microarray based analysis of 3p25-p26 deletions (3p- syndrome) Am J Med Genet A. 2009 Oct;149A(10):2099-105

Morris MR, Hughes DJ, Tian YM, Ricketts CJ, Lau KW, Gentle D, Shuib S, Serrano-Fernandez P, Lubinski J, Wiesener MS, Pugh CW, Latif F, Ratcliffe PJ, Maher ER. Mutation analysis of hypoxia-inducible factors HIF1A and HIF2A in renal cell carcinoma. Anticancer Res. 2009 Nov;29(11):4337-43

Peer-reviewed journal articles not relating to this thesis

Kurian MA, Meyer E, Vassallo G, Morgan NV, Prakash N, Pasha S, Hai NA, Shuib S, Rahman F, Wassmer E, Cross JH, O'Callaghan FJ, Osborne JP, Scheffer IE, Gissen P, Maher ER. Phospholipase C beta 1 deficiency is associated with early-onset epileptic encephalopathy. Brain. 2010 Oct;133(10):2964-70.

Abbreviations

Standard international units of measurement and standard chemical formulae are used. In addition the following abbreviations are referred to in this thesis.

A	adenine
aCGH	array comparative genomic hybridisation
AVSD	atrioventricular septal defect
BAC	bacterial artificial chromosome
C	cytosine
cDNA	complementary DNA
CGH	comparative genomic hybridisation
CHD	congenital heart disease
CNAT	copy number analysis tool
CNV	copy number variation
COBRA-FISH	Combined Binary Ratio fluorescence *in situ* hybridisiation
DAPI	4',6-diamidino-2-phenylindole
del	deletion
der	derivative
DMSO	dimethyl sulfoxide
DNA	deoxyribonucleic acid
dNTP	deoxyribonucleotide triphosphate
EDTA	ethylenediaminetetraacetic acid
FACS	fluorescent activated cell sorting
FISH	fluorescence *in situ* hybridization

G	guanine
GCOS	GeneChip Operating Software
gDNA	genomic DNA
GTC	Genotyping Console
HSDNA	herring sperm DNA
inv	inversion
ish	*in situ* hybridisation
LCD	liquid crystal display
LOH	loss of heterozygosity
LOI	loss of imprinting
mat	maternal
MES	2-(N-morpholino) ethanesulfonic acid
MFISH	multiplex fluorescence *in situ* hybridisation
MLPA	multiplex ligation-dependent probe amplification
MM	mismatch
OD	optical density
PAC	P1-derived artificial chromosomes
pat	paternal
PCR	polymerase chain reaction
PM	perfect match
RNA	ribonucleic acid
SKY	spectral karyotyping
SNP	single nucleotide polymorphisms
SSPE	saline-sodium phosphate-EDTA

T	thymine
t	translocation
TE	tris EDTA
TMACL	tetramethylammonium chloride
TSG	tumour suppressor gene
UPD	uniparental disomy

1 General introduction

1.1 The history of human cytogenetics

The concept of chromosomes was first introduced in 1873 by a German zoologist, Anton Schneider who described the process of mitosis. Later, in 1882, a detailed description of mitosis in animals was published by Walther Flemming and he was the first to use the term mitosis. In 1888, an anatomy professor in Germany, Heinrich Waldeyer, introduced the term, *chromosome* which was derived from the Greek words for 'coloured body'. Subsequently, Walter Sutton and Theodor Boveri, independently proposed that chromosomes carry the hereditary factors in accordance with Mendelian laws. The suggestions were put forward by the observation of the behaviour of chromosomes at cell division which they thought could provide an explanation of how genes could segregate. Sutton referred to the study of chromosomes as cytogenetics; a combination of the disciplines of cytology and genetics.

Significant discoveries in tissue culture techniques eventually led to the important findings by Tjio and Levan in 1956. They worked on human embryonic lung fibroblasts cultures and optimized the colchicines/hypotonic method. They then determined for the first time the correct number of human chromosomes as 46.

With the new technique, congenital anomalies associated with chromosomal number started to be identified for example Down syndrome associated with trisomy 21 (Lejeune et al., 1959), Turner syndrome in females with 45,X karyotype (Ford et al., 1959), Klinefelter syndrome in males with 47,XXY karyotype (Jacobs and Strong, 1959), triple X

(XXX) syndrome (Jacobs et al., 1959), Patau syndrome which also known as trisomy 13 and Edward syndrome or trisomy 18 (Edwards et al., 1960; Patau et al., 1960; Smith et al., 1960). Nowell and Hungerford reported the presence of the 'Philadelphia chromosome' in chronic myelogenous leukemia demonstrating, for the first time, an association between chromosomes and cancer (Nowell and Hungerford, 1960). Lejeune et al (1963 and 1964) identified partial deletion of the short arm of chromosome 5 in cri du chat (cat-cry) syndrome patients.

Moorhead et al (1960) introduced the short-term culture technique using peripheral lymphocytes from blood samples. The effectiveness of the technique was based on the mitosis-inducing ability of phytohemagglutinin, a bean extract. The technique eliminated the need for bone marrow aspiration that had previously been the best way to obtain a sufficient number of spontaneously dividing cells.

Identification of each of human chromosomes was made possible by Caspersson et al (1970). They discovered the nucleobase-specific fluorochrome quinacrin. When stained with quinacrin, each chromosome will show a specific pattern of bands, the Q-bands. These bands allowed for the first time the identification of all 22 human autosomal pairs and the two human sex chromosomes. Sumner, Schnedl, Seabright (1971) introduced additional stains and preparation methods, that brought forward new banding types: Giemsa banding (G-banding), Reverse banding (R-banding), Telomere banding (T-banding), centromere banding (C-banding). Banding greatly improved the accuracy of chromosome analysis (Caspersson et al., 1970; Seabright, 1972) by permitting the analysis of many different tissues and diseases which led to the discovery of a large number of

different chromosome aberrations including terminal deletions, interstitial deletions and duplications.

1.2 Chromosome rearrangements

Chromosomal rearrangements encompass several different classes of events: deletions, duplications, inversions, insertions and translocations. They result from chromosome breakage with subsequent reunion in a different configuration. Chromosomal rearrangements originating in the germ line, whether inherited from the parents or from a *de novo* mutation in the gametes, are referred to as constitutional. On the other hand, any changes in the chromosomes which arise during development or during the life of an organism are referred as acquired chromosomal rearrangements. In human live births, the presence of a chromosome aberration is ~0.5-0.6% and, of these, 0.1–0.3% corresponds to structural chromosome rearrangements such as translocations, inversions, insertions and deletions (De Braekeleer and Dao, 1991; Nielsen and Wohlert, 1991).

Chromosome rearrangements can be categorised as a balanced or unbalanced. It is estimated that 1 in 200 live births have an apparently balanced translocation and 1 in 500 have an unbalanced translocation (Jacobs et al., 1992). In a balanced rearrangement the chromosome complement is complete with no gain or loss of genetic material. Although balanced reciprocal translocation carriers are usually phenotypically normal (with the exception of rare cases which involve breakpoint in an important functional gene), they are often at risk of having offspring with an unbalanced chromosomal complement or reproductive failure. On the other hand, unbalanced rearrangements involve gain or loss of genetic materials and very often resulted in phenotypic abnormalities.

Conventional cytogenetics enabled the identification of the chromosomes and the specific bands involved in the rearrangements (Caspersson et al., 1972; Yunis, 1976) while molecular cytogenetic methods ie. fluorescence *in situ* hybridisation (FISH) and comparative genomic hybridisation (CGH) are required to visualize microdeletions which cannot be detected by the conventional method. Analysis of rearrangement breakpoints in relation to the banding pattern observed along Giemsa banded metaphase chromosomes showed that 84% of breakpoints occurred in Giemsa negative, gene rich regions of the genome (Warburton, 1991; Niimura and Gojobori, 2002).

1.2.1 Translocations

Translocations involve a transfer of genetic material from one chromosome to another and consequently join two otherwise separated genes. The frequency of various chromosomal rearrangements in the general population varies from 1/625 to 1/5,000 (Bandyopadhyay et al., 2002). Translocations can be classified into two different types: reciprocal and Robertsonian. It was found that reciprocal translocations occur more frequently than Robertsonian (Bandyopadhyay et al., 2002). The major impact of translocations is that they can generate significant chromosome imbalance during segregation at meiosis, predisposing the carrier to the birth of abnormal child, stillbirth, miscarriage or infertility.

Many published translocation breakpoints have shown that direct disruption of a gene can lead to an associated phenotype (Bhalla et al., 2004; Bocciardi et al., 2005; Klar et al., 2005) but studies also showed that translocation breakpoints can cause an effect on genes several kilobases away. Examples include a t(2;8)(q31;p21) which affects the *HOXD* gene 60 Kb away from the chromosome 2 breakpoint in a patient with mesomelic dysplasia and vertebral defects (Spitz et al., 2002) and a t(6;11)(q14.2;q25) translocation affecting the

B3GAT1 gene which lies 299 Kb centromeric to the chromosome 11 breakpoint in a patient with psychosis (Jeffries et al., 2003). The position effect phenomenon arises from the disruption of *cis*-acting regulatory elements such as promoters, enhancers and silencers which can be directly altered, distanced from the gene they influence or brought into proximity of a gene not normally under their control when a chromosome undergoes a rearrangement. These elements have been observed as far away as 1.1 Mb from the gene they regulate as in the case of the SOX9cre1 element which was identified upstream of the *SOX9* gene (Bien-Willner et al., 2007).

1.2.1.1 Reciprocal translocations

These involve breakage of at least two non-homologous chromosomes and exchange of the fragments. The incidence of reciprocal translocations is ~1/625 in the general population (Van Dyke et al., 1983). The first reciprocal translocation to be associated with human cancer is t(9;22) which formed a shortened derivative chromosome 22, also known as Philadelphia chromosome (Ph) (Nowell and Hungerford,1960; Rowley,1973).

Most reciprocal translocations are nonrecurring rearrangements except for the t(11;22) reported in more than 160 unrelated families (Fraccaro et al., 1980; Zackai et al., 1980; Iselius et al.,1983). Breakpoint studies on both 11q and 22q have demonstrated a common site for rearrangement (Edelmann et al., 1999b; Shaikh et al., 1999). It was later suggested that a highly specific Alu-mediated recombination in the breakpoints could be the cause in the translocation (Hill et al., 2000).

The breakpoint on chromosome 22 maps within a low-copy region-specific repeat (LCR22) that is also associated with the breakpoints seen in del(22)(q11.2) in

DiGeorge/VCF syndrome (Edelmann et al., 1999a). The breakpoint on the long arm of chromosome 11 is consistently found between two genetic markers, in a genomic region of about 185–190 kb (Edelmann et al., 1999b; Shaikh et al., 1999), and then narrowed to a 190-bp region harbouring an AT-rich repeat (Edelmann et al., 1999b; Kurahashi et al., 2000). The repetitive sequence found in the low-copy repeats on 22q also has multiple copies of an AT-rich sequence (Edelmann et al., 1999b). These findings suggest that AT-rich regions may be prone to recombination events that lead to rearrangements.

1.2.1.2 Robertsonian translocations

Robertsonian translocation (abbreviation rob) is named after the American insect geneticist, W.R.B. Robertson, who first described the translocation in grasshoppers in 1916. They are found in ~1 in 1,000 individuals (Hamerton et al., 1975; Blouin et al., 1994) making it the most common, recurrent structural rearrangements in human. These translocations involve exchanges of the whole arm of acrocentric chromosomes (13-15, 21 and 22). The result is one long chromosome with a single centromere and the total number of chromosomes is reduced to 45. In the short arm, the p11 includes satellite DNAs I, II, III, IV and β; the p12 region contains multiple copies of the genes coding for the 18S and 28S ribosomal RNA (nucleolar organizer region); and the p13 region terminates with β-satellite DNA and telomeric sequences (Page et al., 1996; Bandyopadhyay et al., 2001). Thus, the short-arm regions of the five pairs of human acrocentric chromosomes have extensive sequence homology although some sequences are not common to all acrocentric chromosomes (Bandyopadhyay et al., 2001).

Although all acrocentric chromosomes are capable of participating in the translocation, the distribution of chromosomes was shown to be non-random (Therman et al., 1989). rob (13q;14q) and rob(14q21q) are the most common, constituting ~85% of all Robertsonian translocations (Therman et al., 1989). In ~50% of Robertsonian translocations, the rearrangements occur *de novo* (Shaffer et al., 1992) and in ~95% of the *de novo* cases, rob(13q14q) and rob(14q21q) originate during maternal meiosis (Page and Shaffer, 1997).

1.2.2 Deletions

Deletion involves loss of part of a chromosome either terminal or interstitial, resulting in monosomy in that region of the chromosome. Deletion therefore is an unbalanced rearrangement. It can involve deletion of a single base to an entire piece of chromosome (Lewis, 2005). In most cases, large cytogenetically visible deletions cause embryopathy which presents after birth as mental retardation, growth failure and multiple malformations.

In humans, cytogenetically visible autosomal deletions have a live birth incidence of about 1 in 7,000 (Jacobs et al., 1992). The first chromosomal deletions identified in humans were the deletion of distal 5p associated with the cri-du-chat syndrome (Lejeune et al., 1963; Lejeune et al., 1964) and the distal deletion of 4p, subsequently named the Wolf-Hirschhorn syndrome (Wolf et al., 1965).

A principal method of producing deletions is by unequal crossing-over between region specific low copy-number repeat sequences that flank the deleted regions (figure 1.1) (Lupski et al., 1996; Chen et al., 1997; Lupski, 1998; Shaikh et al., 2000).

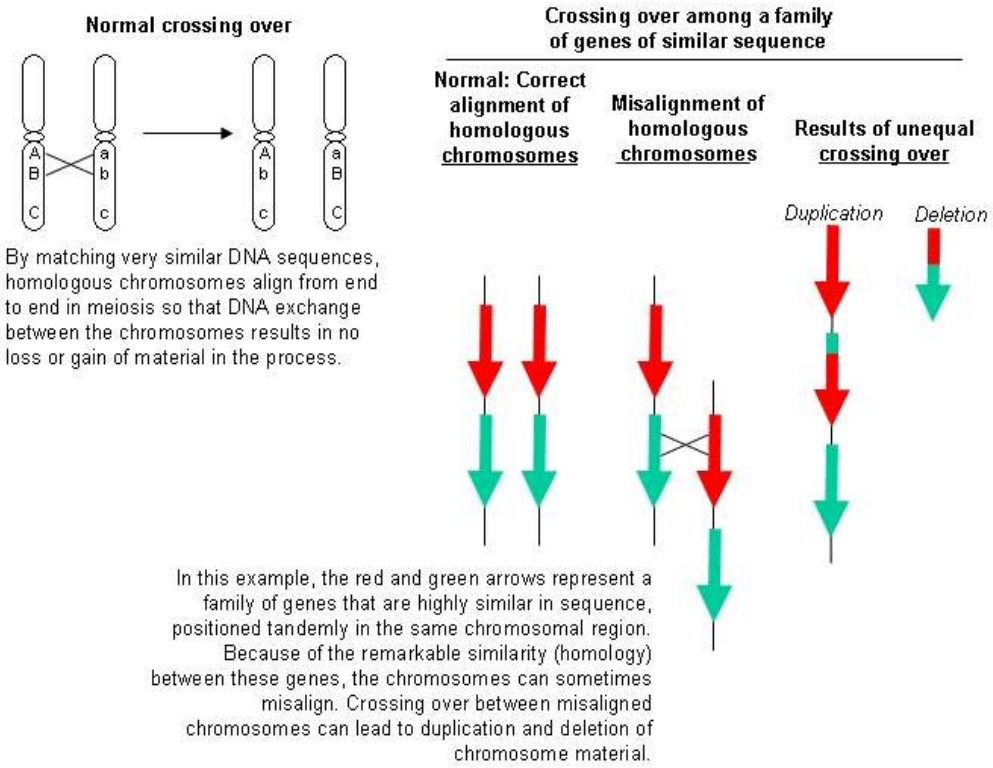

Figure 1.1: Unequal crossing over results in deletion and duplication rearrangements (Adapted from Nussbaum, McInnes and Willard, 2001).

1.2.2.1 Terminal deletions

Even though terminal deletions have been identified for all human chromosomes, only a few have a significant incidence. Common terminal deletions include 1p-, 4p-, 5p-, 9p-, 11q-, 17p-, 18q-, and 22q- (Shaffer and Lupski, 2000). Terminal deletions usually do not occur at a single site but involve breakpoints at various regions with variable sizes (Shaffer and Lupski, 2000). However, some cases of terminal deletion demonstrated clustering at a number of locations (Christ et al., 1999; Wu et al., 1999). In Jacobsen syndrome (deletion 11q23) , molecular investigations have shown that the terminal 11q23 deletions cluster in a defined region in most patients (Jones et al., 1994; Tunnacliffe et al., 1999; Jones et al., 2000).

Breakage of fragile site can cause terminal deletions in chromosomes (Jones et al., 1994; Jones et al., 1995). In Jacobsen syndrome, the 11q23 region contains the proto-oncogene *CBL2*, which also contains a CCG trinucleotide repeat (Jones et al., 1994; Jones et al., 1995; Jones et al., 2000). Expansion of this repeat may result in the folate-sensitive fragile site *FRA11B* that is potentially the site of breakage for terminal deletions of 11q23. Analysis on five Jacobsen syndrome patients and their parents found two cases of deletion to be derived from a *FRA11B*-expressing chromosome (Jones et al., 1995; Jones et al., 2000). However, for the remaining three families investigated, the site of breakage was proximal to *FRA11B* (Jones et al., 1995).

Terminal deletion can also be due to double-strand DNA breaks of unknown cause followed by the addition of the telomeric sequence (TTAGGG)n as described in an α thalassemia mutation associated with terminal truncation of chromosome 16p13.3 (Wilkie et al., 1990; Lamb et al., 1993; Flint et al., 1994). Another characteristic of terminal deletions may be a preference for the maternal or paternal chromosome and it was found that in deletion 1p36, 78% of the cases involve a deletion on the maternally inherited chromosome (Wu et al., 1999).

1.2.2.2 Interstitial deletions

A number of genetic syndromes have been recognised to be caused by interstitial deletions and in majority of the patients, the deletion size is similar (Greenberg et al., 1991; Guzzetta et al., 1992; Mutirangura et al., 1993; Chen et al., 1995; Juyal et al., 1996; Carlson et al., 1997; Chen et al., 1997; Wu et al., 1999). The common deletion in 7q11.23 found in Williams syndrome is about 1.6 Mb in size (Peoples et al., 2000) and is present in more than 99% of patients (Morris and Mervis,

2000). The deletion size in most patients with Prader-Willi syndrome or Angelman syndrome is about 4 Mb (Mutirangura et al., 1993). However, two different proximal breakpoints have been identified in both the maternally derived deletions of Angelman syndrome and the paternally derived deletions of Prader-Willi syndrome (Christian et al., 1995). The common Smith-Magenis syndrome deletion within 17p11.2 is approximately 5 Mb (Trask et al., 1996; Chen et al., 1997) and is found in the vast majority of patients (Juyal et al., 1996; Chen et al., 1997). For most patients with DiGeorge syndrome/VCFS, the deletion in 22q11.2 is about 3Mb (Morrow et al., 1995; Carlson et al., 1997). Some patients have an alternate distal deletion breakpoint, resulting in a smaller, 1.5-Mb deletion (Carlson et al., 1997). Although altered sized deletions, or even rarer unique deletions, can be found in patients with these syndromes, the finding of the same-sized deletions in the majority of patients points to a specific mechanism giving rise to most of these structural rearrangements.

1.2.3 Duplications

Crossing over between nonallelic, directly repeated, homologous segments between sister chromatids (intrachromosomal) or between homologous chromosomes (interchromosomal) would be expected to produce two reciprocal products: a tandem or direct duplication and a deletion (Figure 1.1). Duplication in 17p12 results Charcot-Marie tooth disease type 1A (CMT1A) while Smith Magenis syndrome is cause by the corresponding deletion. Homologous recombination between 24-kb flanking repeats, termed CMT1A−REPs, results in a 1.5-Mb deletion that is associated with hereditary neuropathy with liability to pressure palsy (HNPP) and the reciprocal duplication product is associated with CMT1A (Lupski, 1998). del(17)(11.2) causes Smith-Magenis syndrome (SMS) and this same region was identified to be duplicated in seven unrelated patients (Potocki et al., 2000).

Molecular analyses on dup(p11.2) or Potocki-Lupski syndrome (PTLS syndrome), suggest that the *de novo*17p11.2 duplication is preferentially paternal in origin, arises from unequal crossing over due to homologous recombination between flanking repeat gene clusters and probably represents the reciprocal recombination product of the SMS deletion (Potocki et al., 2000). Further study involving 35 patients has shown that 22 of them harbour the homologous recombination reciprocal product of the common SMS microdeletion (~3.7 Mb), 13 subjects (~37%) have nonrecurrent duplications ranging in size from 1.3 to 15.2 Mb.

1.2.4 Inversions and insertions

An inversion involves two breaks in a chromosome and the segment is reversed or inverted in the position. If the inversion is outside the centromere, it is termed a paracentric inversion whereas inversion spanning the centromere, involving both the chromosome arms, is known as pericentric inversion. Since it is a balanced rearrangement, it usually has no adverse effect on the carriers unless one of the breakpoint disrupts an important gene. Pericentric inversion of chromosome 9 is an example of a common structural variant or polymorphism and is not thought to be of any functional importance. A study of 377,357 amniocentesis estimated the rate of inversions to be 1 in 10,000 with a 9.4% risk of an associated congenital abnormality (Warburton, 1991).

An insertion occurs when a segment of a chromosome is inserted in another chromosome. If the inserted material has moved from another chromosome then the karyotype is balanced. Otherwise it causes an unbalanced chromosome complement. It can be hazardous if it involves the coding region of a gene.

1.2.5 Copy number variations (CNVs)

Recently, Redon et al (2006) has discovered copy number variations (CNVs) in 270 normal individuals using microarray platforms. They identified almost 1,500 regions of the genome which were variable in copy number, encompassing 360 Mb and thousands of genes. CNVs can be caused by genomic rearrangements such as deletions, duplications, inversions and translocations. Low copy repeats (LCRs), which are region-specific repeat sequences are susceptible to such genomic rearrangements resulting in CNVs. Although CNVs is a widespread and common phenomenon in humans, some of them have been associated with susceptibility or resistance to disease. For example, a higher copy number of *CCL3L1* has been associated with lower susceptibility to human HIV infection (Gonzalez et al., 2005) and a low copy number of *FCGR3B* (the CD16 cell surface immunoglobulin receptor) can increase susceptibility to systemic lupus erythematosus and similar inflammatory autoimmune disorders (Aitman et al., 2006). CNV has also been associated with autism (Sebat, 2007; Cook and Scherer, 2008; Pinto et al., 2010) schizophrenia (Cook and Scherer, 2008; St Clair, 2008) and idiopathic learning disability (Knight, 1999).

1.3 Analysis of chomosome rearrangements

Different methods of chromosome analysis have been applied to the analysis of chromosome rearrangements. Conventional method is generally applied for the initial identification of rearrangements. Molecular methods such as fluorescence *in situ* hybridisation (FISH) can be used to identify precise breakpoints, but more recently microarray based techniques have been developed which allows genome wide analysis of the chromosomes.

1.3.1 Metaphase chromosome banding

This method is universally applied in cytogenetic laboratories to analyse the chromosome constitution of an individual. The method involved tissue culture from samples of peripheral blood, skin, bone marrow, chorionic villi or cells from amniotic fluid (amniocytes). The metaphase chromosomes obtained from the cells are treated with Trypsin and then stained for example with Giemsa. This creates unique banding patterns on the chromosomes that enable them to be analysed. Analysis of this pattern in relation to the human genome reference sequence showed that Giemsa positive bands (dark) were AT rich and gene poor and Giemsa negative bands (light) were GC rich and gene rich (Niimura and Gojobori, 2002). Analysis of chromosome banding patterns can identify chromosome rearrangements and localise the breakpoints to within approximately 3Mb depending on the quality and length of the prepared chromosomes (Lichter et al., 2000). Although conventional method examines the whole genome at once, chromosomal changes smaller than ~5 Mb cannot usually be detected by the method (Lupski, 2007). Subsequently, molecular genetics methods were introduced to address this problem.

1.3.2 Flow cytometry

Fluorescent dyes are used to bind specifically to GC (gene rich) or AT (gene poor) sequences in the chromosomes. Due to the differing size and DNA composition, chromosomes bind different amounts of the dye and allow it to be separated by the process of flow cytometry or fluorescent activated cell sorting (FACS). Rearrangements such as reciprocal translocations which alter the size and basepair constitution of chromosomes can be detected using flow cytometry.

1.3.3 Multiple ligation-duplex probes amplification (MLPA)

Multiplex ligation-dependent probe amplification (MLPA) is a multiplex PCR method that detects abnormal copy numbers of up to 50 different genomic DNA or RNA sequences, and which is able to distinguish sequences differing in only one nucleotide (Schouten et al., 2002). This makes it suitable to be applied in both diagnostic laboratories and cancer studies for detection of deletions and duplications in a gene, gains and losses of chromosomal regions, trisomies, SNP and mutation detection (Schouten et al., 2002; Gille et al., 2002; Taylor et al., 2003; Kluwe et al., 2005; Gerdes et al., 2005; Aldred et al., 2006; Aretz et al., 2007; Kanno, et al., 2007; Depienne et al., 2007; Redeker et al., 2008; Kozlowski et al., 2009).

This technology is based on the identification of target sequences by hybridisation of pairs of MLPA probes. Each probe consists of a two oligonucleotides which recognise adjacent target sites on the DNA. One probe oligonucleotide contains the sequence recognised by the forward primer, the other the sequence recognised by the reverse primer. When both probe oligonucleotides are hybridised to their respective targets, they are then ligated into a complete probe. Each complete probe has a unique length (130-472 bp) so that its resulting amplicons can be separated and identified on a capillary sequencer or on a gel, resulting in size separated chromatograms. Since the forward primer used for probe amplification is fluorescently labelled, each amplicon generates a fluorescent peak which can be detected by a capillary sequencer. Comparing the peak pattern obtained on a given sample with that obtained on various reference samples, the relative quantity of each amplicon can be determined (figure 1.2). This ratio is a measure for the ratio in which the target sequence is present in the sample DNA.

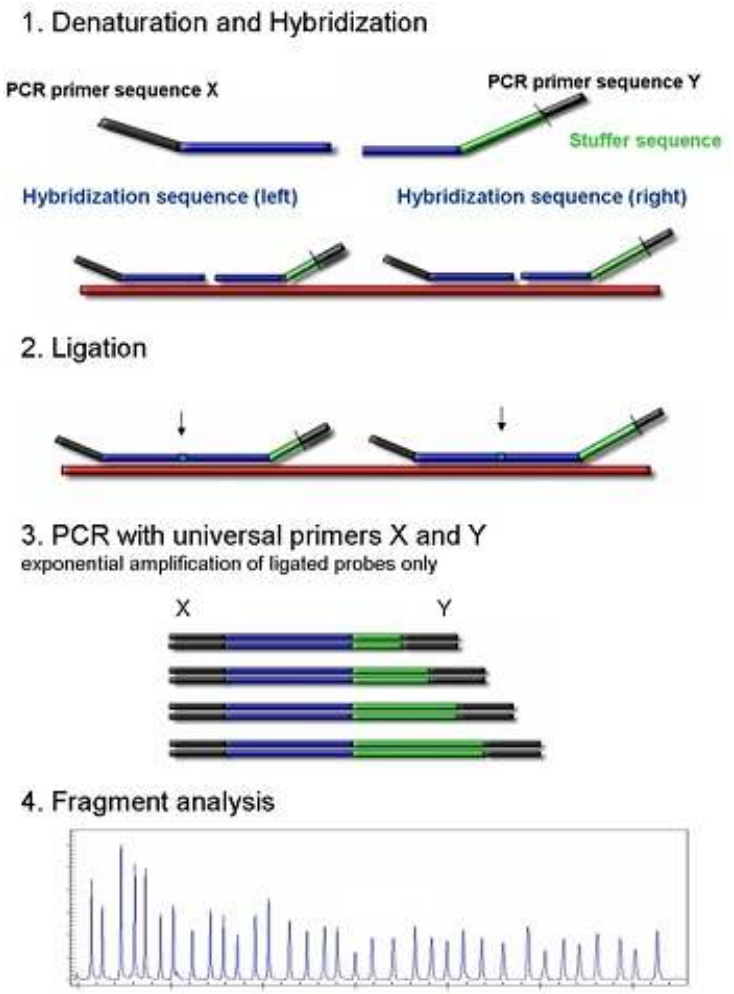

Figure1.2: Steps in multiplex ligation-dependent probe amplification (MLPA). Denatured genomic DNA is hybridised with a mixture of probes. Each MLPA probe consists of two oligonucleotides. The two parts of each probe hybridise to adjacent target sequences and are ligated by a thermostable ligase. All probe ligation products are amplified simultaneously by PCR using a single primer pair. The amplification product of each probe has a unique length (130–472 bp). Amplification products are separated by capillary electrophoresis. Relative amounts of probe amplification products reflect the relative copy number of target sequences.

Compared to conventional karyotyping and fluorescence *in situ* hybridisation (FISH), the MLPA method is technically uncomplicated, less expensive, less laborious, has shorter turnaround time and allows for relative quantification of up to 40 DNA target sequences in one PCR (Schouten et al., 2002). In addition, it does not require living cells or cell culture, but the input of 20 ng or more DNA. As the probe target sequences are small (50-70 nt),

MLPA can identify single gene aberrations and have proven to be useful for studies involving archival formalin fixed paraffin embedded tissue (van Dijk et al., 2005).

1.3.4 Fluorescence *in situ* hybridisation (FISH)

This method is based on the ability of a portion of single-stranded DNA (ie. a probe) to anneal with its complementary target sequence on a metaphase spread or interphase cells. In principle, the DNA probe is conjugated with modified nucleotides which after hybridisation with the patient sample allow the region where hybridisation has occurred to be visualised using a fluorescent microscope.

FISH is routinely used to identify, confirm and characterise chromosomal abnormalities or confirm the clinical suspicion of known microdeletion syndromes (Speicher and Carter, 2005). However, this method is targeted and can only screen individual DNA targets rather than the entire genome (Vermeesch et al., 2007). To overcome this problem, multicolour FISH-based karyotyping (SKY, MFISH and COBRA FISH) was developed, which enables simultaneous detection of all chromosomes (Speicher et al., 1996; Speicher and Carter, 2005; Szuhai and Tanke, 2006). Another technology allowing genome wide detection of copy number aberrations was introduced in 1992 and termed comparative genomic hybridisation (Kallioniemi et al., 1992).

1.3.5 Comparative genomic hybridisation (CGH)

The method has been widely used for the analysis of tumour genomes and constitutional chromosomal aberrations since it was first reported by Kallioniemi and colleagues (Kallionemi et al., 1992). It involves competitive hybridisation of differentially labeled total genomic DNA from control tissue and tumour DNA to normal chromosome spreads.

Hybridisation of repetitive sequences is blocked by the addition of Cot-1 DNA. The ratio of the fluorescence intensities, generated by two different fluorochromes incorporated into test and control DNA is used to differentiate chromosomal regions between the normal and tumour DNA. The fluorescence ratio of the test and reference hybridisation signals is determined at different positions along the genome and provides information on the relative copy number of sequences in the test genome compared with a normal diploid genome.

CGH is applied for identifying regions of chromosomes associated with amplification, loss and gain in specific tumours (Forozan et al., 1997; Knuutila et al., 1998), particularly for solid tumours where, it is often technically difficult to obtain sufficient G-banded metaphases of good quality for detailed analysis (Bejjani and Shaffer, 2006). However, one disadvantage of CGH is that it is unable to detect balanced rearrangements such as inversions or translocations (Pandita et al., 1999). Subsequently microarray-based formats for CGH (array CGH) were introduced and are beginning to be widely used in preference to chromosome-based CGH. The main advantages of array CGH are higher resolution and dynamic range, direct mapping of aberrations to the genome sequence and higher throughput (Pandita et al., 1999).

1.3.6 Microarray-based comparative genomic hybridisation (array CGH)

Array comparative genome hybridisation (array CGH) was developed based on DNA microarrays and dedicated to the investigation and mapping of changes in DNA copy number (Solinas-Toldo et al., 1997; Pinkel et al., 1998; Snijders et al., 2001; Ishkanian et al., 2004). The technique uses cDNAs (Pollack et al., 1999) or genomic fragments that are cloned in a variety of vectors such as plasmids, fosmids, cosmids (Pinkel and Albertson,

2005), bacterial artificial chromosomes (BAC) (Pinkel et al., 1998; Bejjani et al., 2005) or P1-derived artificial chromosomes (PAC) (Fiegler et al., 2003; Bejjani et al., 2005) arrayed onto a glass slides as the hybridisation targets. Following hybridisation of differentially labelled test and reference genomic DNAs to the target sequences on the microarray, the slide is scanned to measure the fluorescence intensities at each target on the array. The normalised fluorescent ratio for the test and reference DNAs is then plotted against the position of the sequence along the chromosomes. Gains or losses across the genome are identified by values increased or decreased from a 1:1 ratio ($\log_2$ value of 0) (figure 1.3). The resolution of the array is limited only by the size and the number of the cloned DNA targets and the natural distance between these sequences located on the chromosome (Bejjani and Shaffer, 2006; Vermeesch et al., 2007).

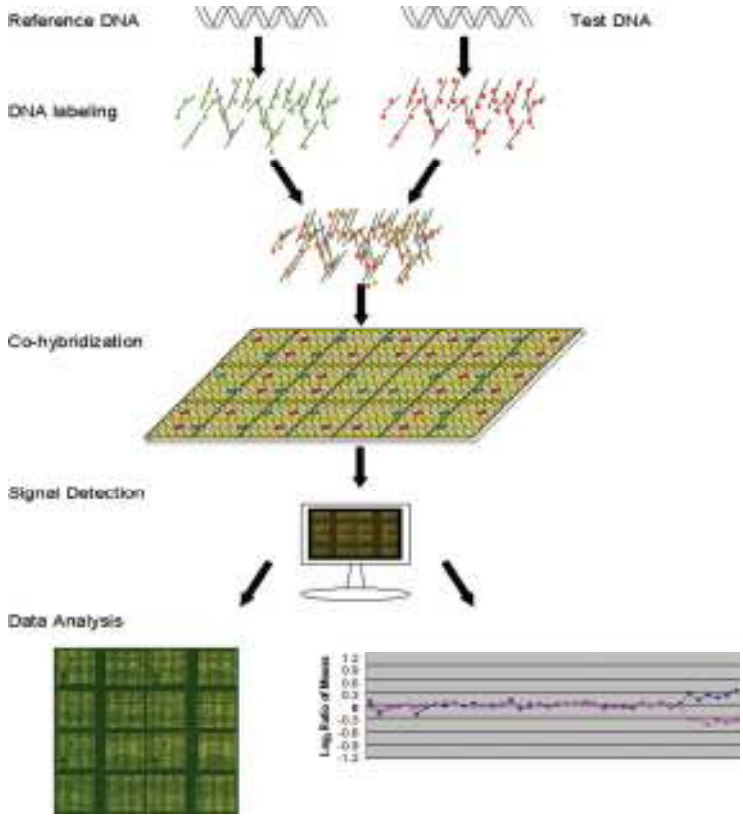

Figure 1.3: Schematic representation of CGH microarray technology. Whole genomic DNA from a control or reference (left) and genomic DNA from a test or patient (right) are differentially labeled with two different fluorophores. The two genomic DNA samples are competitively cohybridized with large-insert clone DNA targets. Computer imaging programs assess the relative fluorescence levels of each DNA for each target on the array (lower left). The ratio between control and test DNA for each clone can be linearly plotted using data analysis software to visualise dosage variations (lower right), indicated by a deviation from the normal $\log_2$ ratio of zero. (Adapted from Bejjani and Shaffer,2006).

Recently, a high-density oligonucleotide-based single nucleotide polymorphism arrays (SNP arrays) have been introduced and applied particularly in cancer studies to identify copy number and LOH of chromosomal regions throughout the entire genome (Zhao et al., 2004; Huang et al., 2004). One of the main advantages of a combined SNP-CGH approach is the identification of allele specific gain and loss by SNP array and the robust copy number detection by array CGH (Kloth et al., 2007).

1.3.7 Single nucleotide polymorphism (SNP) arrays

Single nucleotide polymorphisms (SNPs) are a form of genome variation. Each polymorphism, or variant, occurs at a frequency of greater than 1% in the population (Brookes 1999). SNPs are common throughout the genome, have relatively high levels of heterozygosity and can be easily genotyped. SNPs were recognised as the most frequent type of variation in the human genome and therefore would provide a powerful tool for human genetic studies (Risch et al., 1996; Kruglyak, 1999). Due to their abundance, estimated to be 10 million in the human genome (Kruglyak and Nickerson, 2001), even spacing and stability across the genome, SNPs provide a significant diagnostic potential for human diseases and cancers compared to restriction fragment length polymorphisms and microsatellite markers (Zhao X et al., 2004). This feature also makes it easier for automation.

SNP arrays were developed in 1998 for genotyping (Wang et al., 1998). With the improvement of the arrays in the subsequent years, their use has been successfully extended from investigation of genomic alterations in cancer and cell lines (Lindblad-Toh et al., 2000; Hodgson et al., 2001; Cai et al., 2002; Wilhelm et al., 2002; Fiegler et al., 2003; Kraus et al., 2003; Paris et al., 2003; Albertson and Pinkel, 2003; Bignell et al., 2004; Huang et al., 2004; Janne et al., 2004; Rauch et al., 2004; Zhou et al., 2004; Gibbs and Singleton, 2006; van Beers, 2006) to identification of unbalanced constitutional rearrangements (Vissers et al., 2003; Shaw-Smith et al., 2004), single copy gains and losses in specific chromosomal regions (Bruder et al., 2001; Yu et al., 2003; Veltman, 2003), telomeres and subtelomeres (Veltman et al., 2002; Schoumans et al., 2005; de Vries et al., 2005) and an entire chromosome (Buckley et al., 2002). Importantly, this technique

can detect copy neutral loss of heterozygosity (LOH) events, which comprise 50–70% of the LOH detected in human tumours (Huang et al., 2004; Ishikawa et al., 2005; Beroukhim et al., 2006).

Currently, Affymetrix and Illumina are among the main manufacturers of SNP arrays. Although the technology applied in producing the arrays is different, they both rely on the basic principle that nucleotides bases bind to their complementary partners, A-T and G-C. Both array protocols call for the hybridisation of fragmented single-stranded DNA to arrays containing hundreds of thousands of unique nucleotide probe sequences. Each probe is designed to bind to a target DNA subsequence. Following hybridisation, signal intensity associated with each probe and its target is measured using specialized equipment and software (figure 1.4).

The underlying principle is that the signal intensity depends upon the amount of target DNA in the sample, as well as the affinity between target and probe. For example, the Affymetrix Mapping 500K Array Set includes more than 6.5 million features, each consisting of more than one million copies of a 25-bp oligonucleotide probe of a defined sequence, synthesized in parallel by proven photolithographic manufacturing. Each SNP is interrogated by 6- or 10-probe quartets where each probe quartet is comprised of a perfect match (PM; perfectly complementary to one of the target alleles), and a mismatch probe (MM; identical to a perfect match probe except that the centre base is altered so as to be perfectly complementary to neither allele) for each allele. In total, there are 24 or 40 different 25-bp oligonucleotides per SNP (http://www.affymetrix.com/) (Zhao et al., 2004). The scheme yields quartets comprised of four types of probes: PM_A, MM_A, PM_B and

MM_B. The computational goal is to convert these probe quartet intensity measures from raw array data into a genotype inference *AA*, *AB* or *BB*.

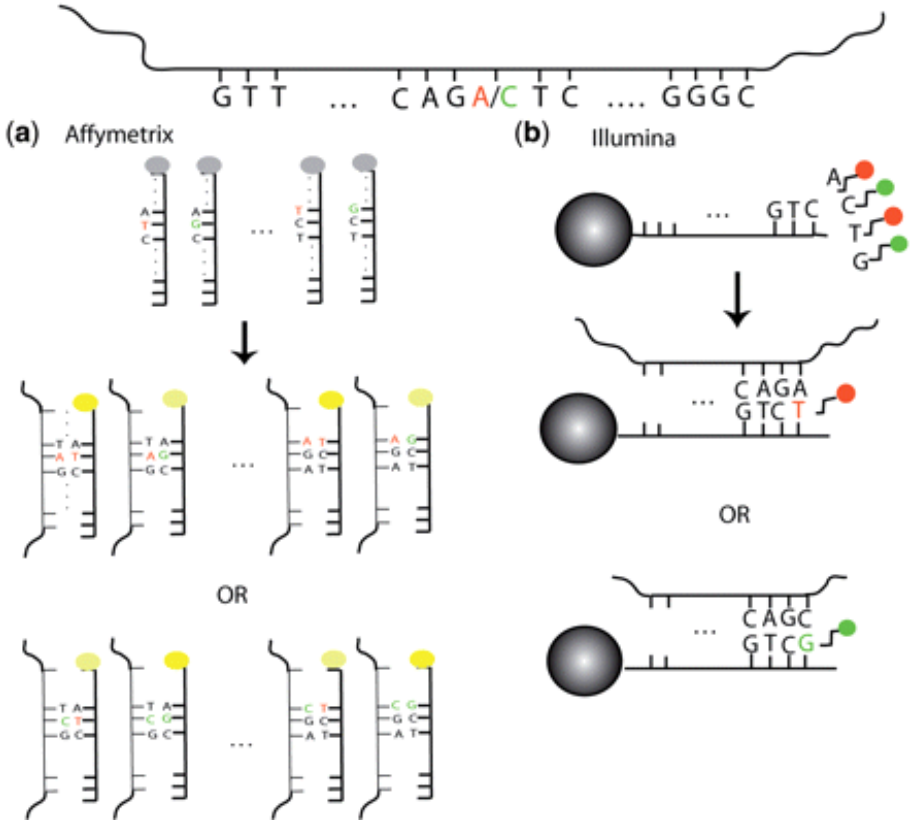

Figure 1.4: Overview of SNP array technology. At the top is the fragment of DNA harbouring an A/C SNP to be interrogated by the probes shown. (**a**) In the Affymetrix assay, there are 25-mer probes for both alleles, and the location of the SNP locus varies from probe to probe. The DNA binds to both probes regardless of the allele it carries, but it does so more efficiently when it is complementary to all 25 bases (bright yellow) rather than mismatching the SNP site (dimmer yellow). This impeded binding manifests itself in a dimmer signal. (**b**) Attached to each Illumina bead is a 50-mer sequence complementary to the sequence adjacent to the SNP site. The single-base extension (T or G) that is complementary to the allele carried by the DNA (A or C, respectively) then binds and results in the appropriately-colored signal (red or green, respectively). For both platforms, the computational algorithms convert the raw signals into inferences regarding the presence or absence of each of the two alleles. (Adapted from LaFramboise, 2009)

1.4 Genetic alterations and human cancers

The idea that numerical alterations in the chromosome contribute to tumourigenesis was put forward by David von Hansemann in 1890 from his study on 13 different carcinoma samples. In each of the cases, he found examples of aberrant mitotic figures that showed asymmetric distribution of 'chromatin loops' or chromosomes. He postulated that these aberrant cell divisions were responsible for the decreased or increased chromatin content found in cancer cells. His idea was abandoned for many decades until Theodor Boveri (Boveri, 1914) pursued the concept by inducing multipolar mitoses on sea urchin eggs. From his observation of the abnormal cells bearing abnormal chromosomal number, he suggested that individual chromosomes were qualitatively dissimilar and transmitted different inheritance factors. He proposed that aberrant mitoses led to the unequal distribution of chromosomes, which, in most cases, would be detrimental. Yet, on occasion, a "particular, incorrect combination of chromosomes" would generate a malignant cell endowed with the ability of unlimited growth, which would pass the defect on to its progeny. This idea has laid a foundation for viewing cancer as a genetic disease.

However, the hypotheses only became evident almost 40 years later when it was discovered that all tumour cell lines had chromosomal aberrations, frequently containing more than 100 chromosomes per cell including ring and dicentric chromosomes (Levan, 1967; Rowley, 2001). The identification of Philadelphia chromosome (Ph) due to t(9;22)(q34;q11) in bone marrow patients with chronic myelogenous leukaemia (CML) (Nowell and Hungerford, 1960; Rowley, 1973) further supported the findings. It is also well established that abnormal chromosome segregation in cell division is one way by which tumour cells may accumulate the many genetic abnormalities required for tumour progression (Lengauer et al., 1998; Brinkley 2001; Saunders, 2005). Now, with the advent

of high throughput and high resolution technologies to identify genetic and epigenetic alterations in cancers, it has been reported that some 45,000 cytogenetic aberrations are associated with human neoplasms (Mitelman et al., 2004). It has also been observed that most recurrent aberrations and rearranged genes have been found in hematological disorders whereas numerous genomic imbalances have been identified in solid tumours (Look, 1997; Mertens et al., 1997; Rowley, 2001; Rabbits, 2003; Helman and Meltzer, 2003; Albertson et al., 2003).

In 1971, Alfred G. Knudson proposed a 'two-hit' hypothesis to explain the genetic mechanism underlying retinoblastoma (a childhood form of retinal cancer) which occurs in both hereditary and nonhereditary forms. He performed statistical analysis on his data of 48 patients with retinoblastoma combined with similar data from two previous publications (Vogel, 1957; Schappert-Kimmijser et al., 1966). He found that in the hereditary form, most children with an affected parent develop bilateral retinoblastoma, however some develop unilateral and others are not affected but have an affected child. These observations led to the theory that a single mutation is not sufficient for tumourigenesis. He hypothesized that in children with hereditary retinoblastoma, the first hit was inherited in the DNA and the second hit would rapidly cause cancer. His findings also led to conclusions that patients who inherit the mutation would develop tumours earlier, and they would often develop more than one tumour. In contrast, individuals who did not inherit a mutation would almost always be affected by a single tumour. This statement, which called the two-mutation hypothesis is now known as the two-hit hypothesis (Knudson, 1971). Later, cloning of retinoblastoma gene confirmed the requirement for two mutations and that the gene, *RB,* occur on the two alleles on chromosome 13q14 (Benedict et al., 1983; Cavenee et al.,1983; Friend et al., 1986).

Disruption of the gene on both alleles causes loss of RB1 protein and subsequently leads to cancer formation. Following this seminal findings, more tumour suppressor genes (TSG) were later identified for example *p53, BRCA1, BRCA2, APC, PTEN, VHL*.

A variety of genetic alterations leading to tumour suppressor gene inactivation, including point mutations, small insertions, deletions, structural changes of the chromosome, or chromosomal loss, can constitute the first hit. All of these events plus mitotic recombination can occur as the second hit (Nowak et al., 2004). However, usually large deletions or chromosome loss do not account both for the first and second step in one cell, because large homozygous deletions are often lethal for a cell (Nowak et al., 2004).

Experiments in mice, however, have highlighted some exceptions to this rule such that deletion of a single tumour suppressor gene allele can lead to cancer. Such haploinsufficiency is observed in *p53* and $p27^{Kip1}$ (Venkatachalam et al., 1998; Fero et al., 1998). In the p53 study, the penetrance of spontaneous tumours in p53+/- mice was 95%, with a median age of morbidity of 460 days and less than half of the tumours had lost the wild-type p53 allele. Thus approximately 50% of the tumours harvested before 550 days, and 85% of the late-arising tumours, retained one expressed allele (Venkatachalam et al., 1998).

The alleles retained in two of the p53+/- tumours were completely sequenced in the coding region, and found to be wild-type. Five tumours were examined in a wide range of tests of *p53* function and all of the results were consistent with the presence of a functional p53 protein, as were the Western blot data. The evidence suggests that fatally malignant tumours retaining the wild-type *p53* allele appear slightly later than tumours which have

lost it, but significantly more frequently and earlier than tumours in the +/+ mice. This study is consistent with the earlier reports which implied that although *p53* hemizygous cells respond to DNA damage signals, the efficiency of the response is lower, allowing some cells to escape and continue to proliferate, and thus become targets for further mutations in other genes (Clarke et al., 1993, 1994; Gottlieb et al., 1997).

Similar findings were observed in mice hemizygous for $p27^{Kip1}$ in which 32% of them were shown to develop tumours. Despite a relatively late onset (median 570 days), all arose before any appeared in the +/+ control mice. None of the tumours examined showed loss of the second allele, whose sequence was shown to be wild-type (complete coding regions sequenced from one spontaneous tumour and from 13 tumours induced by radiation or ethyl nitrosourea). The gene product was expressed at levels comparable to those of normal tissues, and was appropriately localised to the nucleus. And so it was concluded that for both *p53* and $p27^{Kip1}$, loss of two alleles was more tumourigenic than loss of one and tumours arose more quickly in homozygous than hemizygous deficient mice (Venkatachalam et al., 1998; Fero et al., 1998). Several other examples of haploinsufficiency for tumour suppression have been demonstrated, for example $p16^{Ink4a}$ (Krimpenfort et al., 2001) and *PTEN* (Sulis and Parsons, 2003; Trotman et al., 2003).

In contrast to the usual function of a tumour suppressor gene, somatic mutation on one allele or 'one hit' is believe to be sufficient for oncogene to confer a selective growth advantage on the cell (Vogelstein and Kinzler, 2004). Oncogenes were first identified in oncogenic retroviruses that had picked up a cellular oncogene (*c-onc*) and incorporated it into the viral genome to produce a viral oncogene (*v-onc*) (Stehelin et al., 1976a; Stehelin

et al., 1976b; Stehelin et al., 1977). An oncogene can be the result of several DNA alterations; mutation, structural rearrangement or gene copy number gains (Albertson et al., 2003; Vogelstein and Kinzler, 2004). *K-ras* point mutation has been shown to be associated with poor prognosis of lung adenocarcinoma (Slebos et al., 1990), mutation of *BRAF* in human cancers changes a valine to a glutamate at codon 599 which is a residue within the activation loop of the kinase domain (Davies et al., 2002), translocation t(8;14)(q24;q32) found in about 85% of cases of Burkitt lymphoma places the c-*myc* gene located at chromosome 8q24 under control of regulatory elements from the immunoglobulin heavy chain locus located at 14q32 resulting in transcriptional activation of c-*myc*, which encodes a nuclear protein involved in the regulation of cell proliferation (Siebert et al., 1998; Mann et al., 2002).

Peter Nowell in 1976 has proposed a model for the evolution of tumour cell populations in terms of stepwise genetic variation based from his observation that (1) in many primary tumours, all cells show the same abnormal karyotype, and even when several chromosome patterns are present within a single tumour, marker chromosomes in each cell often indicate that the different subpopulations derive from a common stemline (Sandberg, 1970) (2) the isoenzymes of glucose-6-phosphate dehydrogenase in a variety of neoplasms in heterozygous women have indicated that typically the same member of the X chromosome pair is functional in all cells of a given tumour (Linder and Gartler, 1965). (iii) the immunoglobulin produced by plasma cell tumours (and perhaps other lymphoproliferative neoplasms as well) has in almost every case the homogeneity characteristic of a single clone (Linder and Gartler, 1965; Milstein et al., 1967). Nowell suggested that, following an initiating event that converts a normal cell to a neoplastic cell, cancer progression results from the acquisition of genetic instability, leading to the

accumulation of genetic alterations and the continual selective outgrowth of variant subpopulations of tumour cells with a proliferative advantage.

In 1997, Kinzler and Vogelstein proposed a division of TSG genes to ‘gatekeepers’ and ‘caretakers’. Gatekeeper genes function by directly controlling cell growth, thus inhibiting proliferation, leading to apoptosis and/or promoting terminal differentiation (Russo et al., 2003). These genes are frequently mutated in both sporadic and hereditary tumours and their functional loss is rate limiting for tumour growth of a specific tissue type. Alteration of a particular gatekeeper gene can lead to the development of a particular form of predisposition to cancer (Kinzler and Vogelstein, 1997). Caretaker genes are involved in the maintenance of genomic stability by reducing the mutation rates in gatekeepers and oncogenes. Mutations in these genes are frequently found in hereditary tumours (Kinzler and Vogelstein, 1997). Consequently, an altered gatekeeper gene could affect mainly tumour initiation, while a caretaker gene could accelerate the tumour progression, even if in certain cases their functions may partly overlap; as such the same gene may act either as a gatekeeper or as a caretaker.

1.5 Aims of this thesis

The principal aim of my thesis is to apply molecular cytogenetic technique and high resolution SNP array to characterise constitutional and acquired cytogenetic abnormalities in specific human disease situations i.e. developmental disorders (3p- syndrome and Beckwith-Wiedemann syndrome) and human renal cancers.

1.5.1 Array CGH analysis of 3p25-p26 deletion (3p- syndrome)

The two main aims of this study are to investigate phenotype-genotype correlations and to accurately map the deletion breakpoints on the chromosome 3p using 250K SNP array (in 14 patients) and SNP 6.0 (in 2 patients).

1.5.2 Cytogenetics and molecular genetic analysis of Beckwith Wiedemann syndrome (BWS)

To define and characterise the region of chromosome 11p15 involved in Beckwith-Wiedemann syndrome (BWS), I have carried out a high resolution 250K SNP array analysis on seven patients and SNP6.0 on one patient with features of BWS. Conventional and molecular cytogenetic techniques were also applied in two of the cases with chromosome rearrangements.

1.5.3 Analysis of copy number changes in primary tumours of clear cell renal cell carcinoma (cRCC) and renal cell carcinoma (RCC) cell lines using 250K SNP Array

This study is aim to identify copy number changes and characterise chromosomal changes in primary tumours of clear cell renal cell carcinoma

from sporadic, VHL disease and renal cell carcinoma cell lines using 250K SNP Array.

1.5.4 Identification of copy number changes in sporadic clear cell renal cell carcinoma (cRCC) using high resolution array SNP6.0

The main aim of this study is to precisely characterise and identify copy number changes associated with sporadic clear cell renal cell carcinoma (cRCC). Therefore, I took advantage of the latest microarray technology, Affymetrix array SNP6.0, to study copy number changes of 37 samples of sporadic cRCC. The data was then compared with the results of sporadic cRCC obtained using the 250K SNP array.

2 General methods

2.1 250K SNP array (Sty1)

The experiment was carried out following the manufacturer's protocol (Affymetrix, USA) (summarized in Figure 2.1) to minimize possible sources of contamination that would reduce genotyping accuracy, call rate and consequently genetic power.

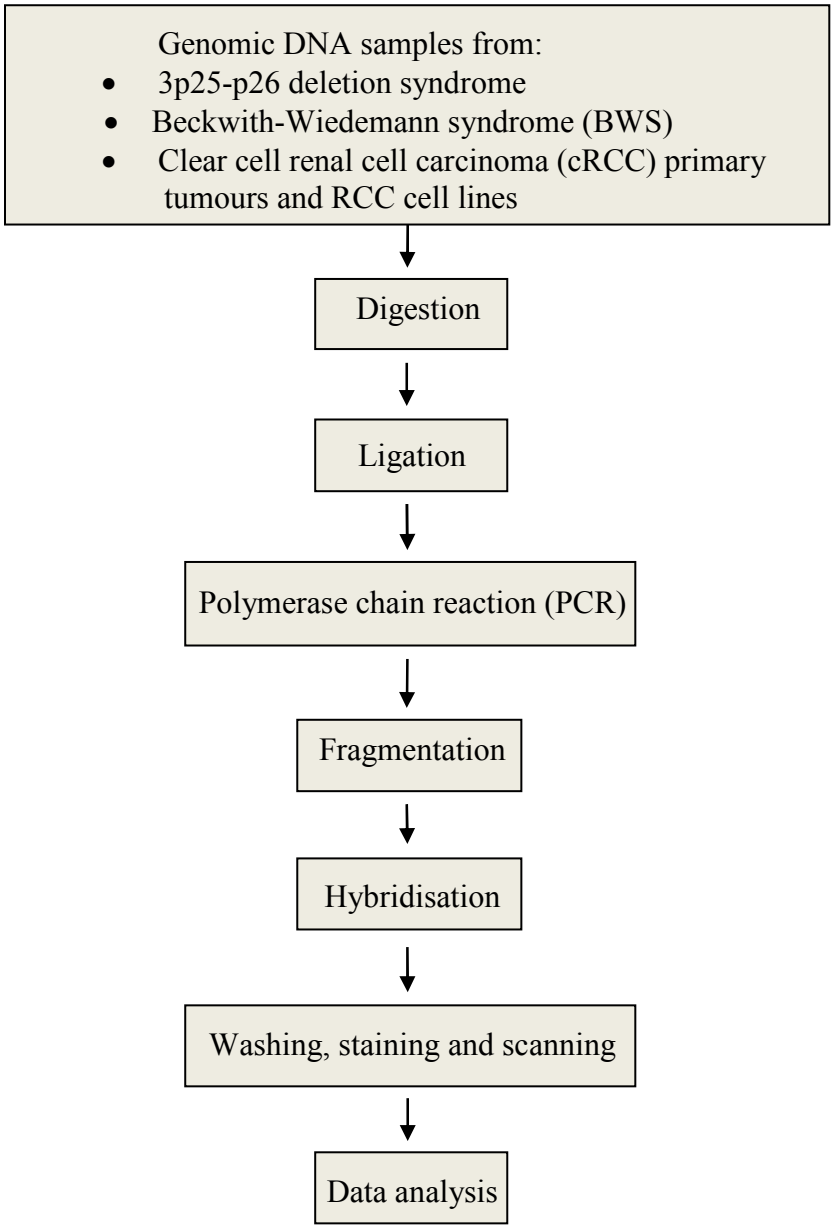

Figure 2.1: Steps involved in 250K SNP array

All the samples used for this study follows the guidelines and requirements specified by the manufacturer (Affymetrix, USA). Please refer appendix A1.

2.1.1 Sample preparation

Location: Pre-PCR clean area

The samples were thoroughly mixed by vortexing at high speed for 3 seconds and spun down at 2000 rpm for 30 seconds. The concentration of each sample was determined using Nanodrop 1000 spectrophotometer (Thermo Scientific, USA). Based on OD measurements, the samples were diluted to 50ng/ul using DNase/RNase free molecular grade water. The diluted DNA was then thoroughly mixed by vortexing at maximum speed for 3 seconds. 5 ul DNA was aliquoted to the corresponding 96-well reaction plate which was placed in a double cooling chamber on ice. If the next step was not proceeded to directly, the samples were stored in -20°C.

2.1.2 Restriction enzyme digestion

Location: Pre-PCR clean area

Before starting this step, the reagents, equipment and consumables required were prepared as follows:

- Genomic DNA was thawed on ice if frozen. When thawed, the centre of the plate was vortexed at high speed for 3 seconds, spun down at 2000 rpm for 30 seconds and placed back on ice.
- BSA (Bovine Serum Albumin) and NE Buffer 3 (New England Biolab, UK) were thawed on ice. When thawed, they were vortexed at high speed for 3 seconds, then spun for 3 seconds and placed on ice.

- 2 mL of AccuGENE® water was placed on ice.
- The thermocycler was on to preheat the lid at room temperature.
- A 2.0 mL Eppendorf tube was labeled *Dig MM* and placed on ice.

2.1.2.1 Preparation of the digestion master mix

All the reagents required were kept on ice. For 1 sample, 11.55 ul AccuGENE water, 2 ul NE Buffer 3 and 0.2 ul BSA (10X;1 mg/ml) were added to the 2.0 mL eppendorf tube. Sty1 enzyme (10 U/ul) was removed from the freezer, immediately placed on ice and then spun for 3 seconds. 1 ul of the enzyme was then added to the master mix. The master mix was then vortexed at high speed for 3 seconds, spun for 3 seconds and then placed on ice. Any remaining enzyme was then returned to the freezer. When preparing multiple samples, 5% extra of each component were added.

2.1.2.2 Addition of digestion master mix to samples

This step was handled on ice. 14.75 µL of Digestion Master Mix was added to each DNA sample making the total volume in each well 19.75 µL. The plate was sealed tightly using 96-well Clear Adhesive Films (Applied Biosystems, USA) and vortexed at the centre at high speed for 3 seconds. It was then spun down at 2,000 rpm for 30 seconds and loaded onto the preheated thermal cycler and the 500K Digest program was run as follows:

120 minutes 37°C
20 minutes 65°C
Hold 4°C

The plate was then removed and spun down at 2000 rpm for 30 seconds and the samples were stored in -20°C if not proceeding directly to the next step.

2.1.3 Ligation

Location: Pre-PCR clean area

Before starting, the reagents, equipment and consumables required for this step were prepared as follows:

Adaptor Sty (50 µM; 1 vial) (Affymetrix, USA) and T4 DNA Ligase Buffer (10X; 1 vial) (Affymetrix, USA) were thawed on ice. They were then vortexed at high speed for 3 seconds then pulse spun for 3 seconds and placed back on ice.

If frozen, the Digestion Stage plate was thawed on ice. It was then vortexed at the centre at high speed for 3 seconds, spun down at 2000 rpm for 30 seconds and placed back on ice.

The thermal cycler was powered on to preheat the lid.

A 2.0 mL eppendorf tube was labeled *Lig MM* and placed on ice.

2.1.3.1 Preparation of ligation master mix

Keeping all reagents and tubes on ice, 0.75 ul Adaptor Sty1 (50 uM) and 2.5 ul T4 DNA Ligase Buffer (10X) were added to the 2.0 mL eppendorf tube labeled *Lig MM.* T4 DNA Ligase (400 U/ul) was removed from the freezer and immediately placed on ice. It was then pulse spun for 3 seconds and immediately 2 ul of the enzyme was added to the master mix. The master mix was then vortexed at high speed for 3 seconds, pulse spun for 3 seconds and placed in the cooling chamber. Any remaining enzyme was placed back in the -20C freezer.

2.1.3.2 Addition of ligation master mix to samples

The addition was done on ice. The seal of the Digestion Stage plate was carefully removed and 5.25 µL of Ligation Master Mix was aliquoted to each reaction. The plate was then tightly sealed again using 96-well Clear Adhesive Films (Applied Biosystems, USA), vortexed at the centre at high speed for 3 seconds then spun down at 2000 rpm for 30

seconds. The plate was loaded onto the preheated thermal cycler and the 500K Ligate program was run as follows:

180 minutes 16°C
20 minutes 70°C
Hold 4°C

2.1.3.3 Dilution of the samples

10 mL of the AccuGENE® water was placed on ice for 20 minutes prior to use. When the program was finished, the ligation plate was removed from the thermal cycler, spun down at 2000 rpm for 30 seconds and placed on ice. The seal of the plate was carefully removed and 75 µL of water was added to each reaction. The plate was then tightly sealed again using 96-well Clear Adhesive Films (Applied Biosystems, USA), vortexed at the centre at high speed for 3 seconds and then spun down at 2000 rpm for 30 seconds. If not proceeding directly, the samples were stored in -20°C.

2.1.4 Polymerase Chain Reaction (PCR)

Location: Pre-PCR clean area

The following reagents, equipment and consumables were prepared before starting this step:

10X TITANIUM™ *Taq* PCR Buffer (Clontech, USA), dNTPs (Takara, USA), PCR Primer 002 (Affymetrix, USA), G-C Melt (5M) (Clontech, USA) were thawed on ice. Once thawed, they were vortexed at high speed for 3 seconds, pulse spun for 3 seconds and placed back on ice.

15 mL of AccuGENE water was placed on ice.

The Ligation Stage plate was thawed on ice if frozen. It was then labelled *Lig*, vortexed at the centre at high speed for 3 seconds, spun down at 2000 rpm for 30 seconds and placed back on ice.

The thermal cycler was powered on and preheated.

Three 96-well reaction plates were labeled *P1*, *P2*, *and P3*

A 50 mL Falcon tube was labeled *PCR MM*

2.1.4.1 Addition of DNA to the reaction plates

Location: Pre-PCR clean area

10 µL of sample from each well of the Ligation Stage plate was transferred to the corresponding row and well of each reaction plate (as shown in figure 2.2). The transfer was done on ice. Each plate were tightly sealed and left on ice.

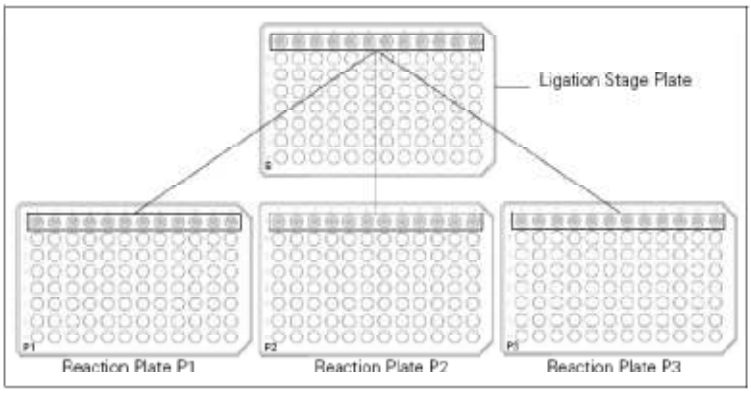

Figure 2.2: Transfer of ligation stage plate to the corresponding row and well of reactions plates 1, 2 and 3.

2.1.4.2 Preparation of PCR master mix

Location: Pre-PCR clean area

Keeping the 50 mL Falcon tube on ice, all of the reagents (except for Taq DNA polymerase) were added in the order shown in table 2.1. The TITANIUM Taq DNA Polymerase was then removed from the freezer and immediately placed on ice. It was then pulse spun for 3 seconds and immediately added to the master mix. The master mix was vortexed at high speed for 3 seconds. For multiple samples, 5% excess of each reagent was added. Any remaining of Taq DNA polymerase was returned to the -20C freezer.

Table 2.1: PCR master mix

Reagent	1 PCR	3 PCR	Final conc. in sample
AccuGENE water	39.5 ul	118.5 µL	
TITANIUM Taq PCR Buffer (10X)	10 ul	30 µL	1X
GC-melt (5M)	20 ul	60 µL	5M
dNTPs (2.5 mM)	14 ul	42 µL	350 uM
PCR primer 002 (100 uM)	4.5 ul	13.5 µL	4.5 uM
TITANIUM Taq DNA polymerase (50X)	2 ul	6 µL	1X
Total	**90 ul**	**270 µL**	

Abbreviation: conc., concentration

2.1.4.3 Addition of PCR master mix to samples

Location: PCR staging area

The reaction plates P1, P2 and P3 and PCR Master Mix were transferred to PCR staging area on ice. 90 µL of PCR Master Mix was added to each sample making the total volume in each well 100 µL. Each reaction plate was sealed tightly, vortexed at medium speed for 2 seconds and spun at 2,000 rpm for 1 minute.

2.1.4.4 PCR reaction

Location: Main lab

Reaction plates P1, P2 and P3 were transferred to the Main Lab. Each plate was loaded onto a preheated thermal cycler MJ Tetrad PTC-225 and the program was run as follows:

3 minutes 94°C 1 cycle
30 minutes94°C ┐
30 minutes60°C } 30 cycles
15 seconds68°C ┘
7 minutes68°C 1 cycle
Hold 4°C

Each reaction plate was then removed from the thermal cycler and spun down at 2000 rpm for 30 seconds then placed on ice. Three fresh 96-well reaction plates were labelled *P1Gel*, *P2Gel* and *P3Gel*. 3 µL of 2X Gel Loading Dye was added to each well of the three plates. 3 µL of each PCR product from plates *P1*, *P2* and *P3* was transferred to the corresponding plate, row and wells of plates *P1Gel*, *P2Gel* and *P3Gel*. Plates *P1Gel*, *P2Gel* and *P3Gel* were sealed and vortexed at medium speed for 3 seconds then spun down at 2000 rpm for 30 seconds. 6 µL from each well of plates *P1Gel*, *P2Gel* and *P3Gel* was loaded onto 2% TBE gels and run at 120V for 40 minutes to 1 hour. The gels were examined to verify that the PCR product distribution is between 250 bp to 1100 bp (figure 2.3). If not proceeding directly to the next stage within 60 minutes, the plates were sealed and stored at −20 °C.

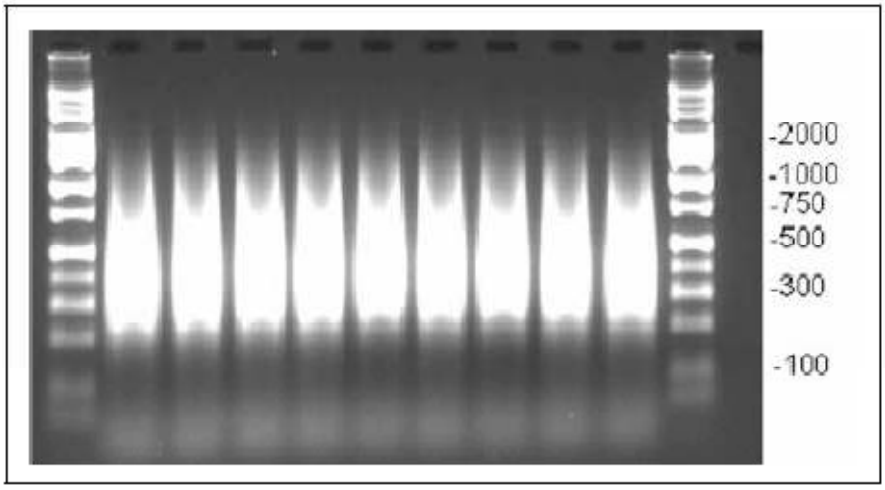

Figure 2.3: Typical example of PCR products run on 2% TBE agarose gel at 120V for 1 hour, with average size between 200 and 1,100 bp

2.1.5 PCR purification and elution

Location: main lab

Before starting this step, the following were done:

The PCR product was thawed at room temperature if frozen. Once thawed, it was vortexed at the centre at medium speed for 3 seconds and spun down at 2000 rpm for 30 seconds.

The manifold-QIAvac multiwell unit (Qiagen, USA) was set up as follows:

a. the manifold was connected to a vacuum source QIAGEN Vacuum Regulator (Qiagen, USA) able to maintain 600 mbar.

b. a waste tray was placed inside the base of the manifold.

8 µL of diluted EDTA (0.1M) was aliquoted into each well on each PCR product plate. They were then tightly sealed and vortexed at medium speed for 2 seconds and spun at 2000 rpm for 1 minute.

Next, the samples from the same row and well of each PCR product plate were transferred and pooled to the corresponding row and well of the Clontech Clean-Up Plate (figure 2.4).

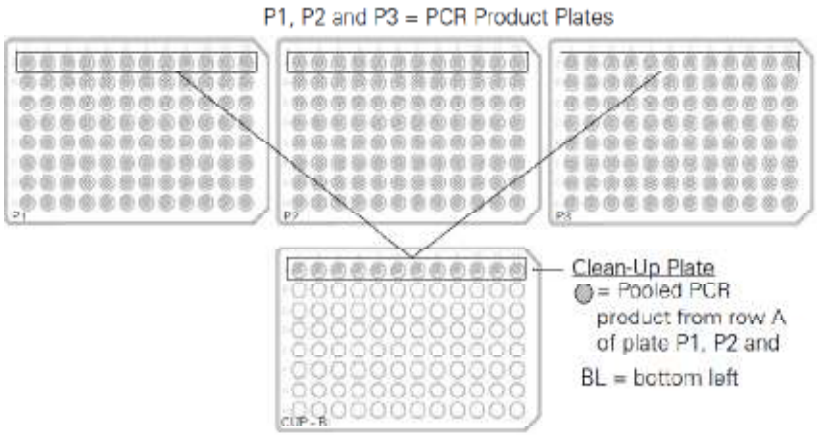

Figure 2.4: Pooling of PCR products

The vacuum was then turned on and maintained at 600 mbar until all of the wells were dry (approximately 1.5 to 2 hours). The PCR products were washed by adding 50 µL molecular biology grade water and the wells completely dry in approximately 20 minutes. This step was repeated 2 additional times for a total of 3 water washes. After the third wash, the manifold was tapped firmly on the bench to force any drops on the sides of the wells to move to the bottom and be pulled through the plate. The samples were allowed to dry completely which took 45 to 75 minutes in the third wash. The vacuum was then turned off and was carefully removed from the manifold. The bottom of the plate was immediately blotted on a stack of clean, absorbent paper to remove any remaining liquid. Next, 45 µL RB Buffer (Clontech, USA) was added to each well of the plate. It was then tightly sealed and then loaded onto a plate shaker, e.g., Jitterbug (Boekel Scientific, model 130000), for 10 minutes at room temperature. Approximately 45 µL of each eluted sample was then transferred from the Clontech Clean-Up Plate to the corresponding well of a fresh

96-well plate. If not proceeding immediately to the next stage the plate was sealed and stored at −20 °C.

2.1.6 Quantification of purified PCR product and normalization

2 µL of the purified PCR product was added to 198 µL molecular biology grade water (100-fold dilution) and mixed well. Nanodrop 1000 spectrophotometer (Thermo, USA) was utilized to determine the purified PCR product yield. Water was used as blank. The absorbance at 260 nm was read for each sample. The convention that 1 absorbance unit at 260 nm equals 50 µg/mL (equivalent to 0.05 µg/µL) was applied for double-stranded PCR products. For accurate concentration measurement, three independent dilutions of each sample were made and *Average Sample OD* was obtained by average the 3 readings.

Average Sample OD:

Sample Concentration in µg/µL = Average Sample OD X (0.05 µg/µL) X 100

A typical average sample OD is 0.5 to 0.7. This OD range is equivalent to a final PCR product concentration of 2.5 to 3.5 µg/µL.

Next, the samples were normalized by adding appropriate volume of RB Buffer (Clontech, USA) by using the formula as shown below:

X µL RB Buffer = 45 µL – (Y µL purified PCR product)

Where:

Y = The volume of purified PCR product that contains 90 µg

The value of Y is calculated as:

Y µL purified PCR product = (90 µg) ÷ (Z µg/µL)

Z = the concentration of purified PCR product in µg/µL

Calculated volume of RB Buffer (the value of X) was added to each well of the reaction plate in the cooling chamber on ice. The calculated volume of purified PCR product (the value of Y) was added to the corresponding well with RB Buffer. The total volume of each well was 45 µL. After normalization, each well contains 90 µg of purified PCR product in a volume of 45 µL (or 2 µg/µL). The plate was then sealed with a clear adhesive film, vortexed at medium speed for 2 seconds and spun down at 2000 rpm for 1 minute. If not proceeding immediately to the next step, the plate was sealed and stored at –20 °C.

2.1.7 Fragmentation

Location: main lab

Before starting, reagents, equipments and consumables were prepared as follows:

The thermal cycler block was preheated to 37 °C for 10 minutes prior to loading reactions.

The Fragmentation Buffer (10X) (Affymetrix, USA) was thawed on ice. Once thawed, it was vortexed at medium speed for 3 seconds, pulse spun for 3 seconds and placed on ice.

2 mL of the AccuGENE water was placed on ice.

One 1.5 mL Eppendorf tube labeled *Frag MM*

Plate of purified, normalized PCR product from the previous stage.

Two strips of 12 tubes labeled *Buffer* and *FR*.

5 µL of Fragmentation Buffer was added to each sample on ice. The label of the Fragmentation Reagent (Affymetrix, USA) tube was examined to define the concentration (U/ul). Based on the concentration, the Fragmentation Reagent was diluted to 0.05 U/µL by adding water and fragmentation buffer in a 1.5 ml tube labelled *Frag MM* placed on ice. The mix was then vortexed at medium speed for 2 seconds and placed back on ice.

Example of the dilution for two different concentrations of fragmentation reagent is shown in table 2.2.

Table 2.2: Dilution of fragmentation reagent

Reagent	**Fragmentation Reagent Concentration**	
	2 U/ul	**3 U/ul**
Water, molecular grade	525 ul	530 ul
10X Fragmentation buffer	60 ul	60 ul
Fragmentation Reagent	15 ul	10 ul
Total (enough for 96 samples)	600 ul	600 ul

The Fragmentation Reagent was removed from the freezer and immediately placed on ice. It was pulse spun for 3 seconds and immediately added to the mix, vortexed at high speed for 3 seconds then pulse spun for 3 seconds and immediately placed on ice. On ice, 5 µL of diluted Fragmentation Reagent was added to each sample and pipetted up and down several times to mix. The plate was tightly sealed, vortexed at medium speed for 2 seconds and spun briefly at 2000 rpm at 4°C. The plate was immediately loaded onto the preheated block of the thermal cycler (37 °C) and the 500K Fragment program was run as follows:

35 minutes 37°C
15 minutes 95°C
Hold 4°C

The plate was then removed from the thermal cycler, spun down at 2000 rpm for 30 seconds and placed back on ice. 4 µL of each fragmented PCR product was diluted with 4 µL gel loading dye. It was then loaded and run on a 4% TBE gel with the BioNexus All Purpose Hi-Lo Ladder at 120V for 30 minutes to 1 hour. If the gel matches the example shown in figure 2.5, the process was continued immediately to the next step.

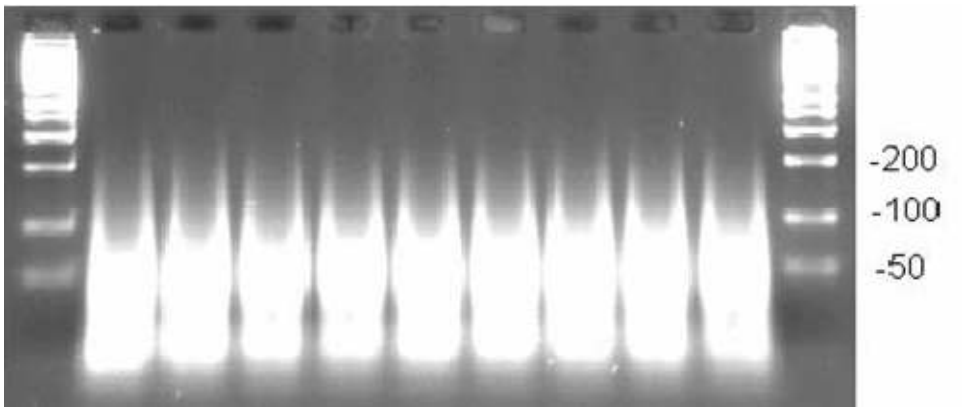

Figure 2.5: Typical example of fragmented PCR products run on 4% TBE agarose gel at 120V for 30 minutes to 1 hour. Average fragment size is < 180 bp.

2.1.8 Labeling

Location: Post-PCR clean area

The following were done before starting this stage:

The 5X TdT Buffer (Affymetrix, USA) and the GeneChip® DNA Labeling Reagent (30 mM) (Affymetrix, USA) were thawed on ice. Once thawed, they were vortexed at medium speed for 3 seconds, pulse spun for 3 seconds and placed on ice.

The thermal cycler was turned on and the block preheated to 37°C for at least 10 minutes before samples are loaded.

One 1.5 mL centrifuge tube marked *Label MM*

For 1 sample, 14 ul 5X TdT Buffer and 2 ul Labeling Reagent (30 mM) were added to the 1.5 mL centrifuge tube on ice. The TdT enzyme (30 U/µL) was removed from the freezer and immediately spun for 3 seconds. Immediately 3.5 ul of the enzyme was added to the master mix, vortexed at medium speed for 3 seconds and then pulse spun for 3 seconds. Next, 19.5 µL of Labeling Master Mix was aliquoted to each fragmented DNA samples from the previous step. The mixture was pipetted up and down one time. The plate was

sealed tightly, vortexed at medium speed for 3 seconds and spun down at 2000 rpm for 30 seconds. The plate was placed onto the preheated thermal cycler block, and the 500K Label program was run as follows:

4 hours 37°C
15 minutes 95°C
Hold 4°C

The plate was then removed from the thermal cycler and spun down at 2000 rpm for 30 seconds. If not proceeding directly to the next stage, the samples were freeze at −20 °C.

2.1.9 Hybridisation

The following reagents, equipments and consumables were prepared prior hybridisation:

The hybridisation oven was turned on and allowed to preheat for 1 hour. The temperature was set to 49 °C, the rpm was set to 60 and the rotation was turned on.

Two heat blocks were turned on; one was preheated to 99 °C and the other to 49 °C.

If the labelled samples from the previous stage were frozen, they were thawed on the bench top, then vortexed at high speed for 3 seconds, spun down at 2000 rpm for 30 seconds and placed back on ice.

The arrays were unwrapped and placed on the bench top, septa side up, to warm to room temperature for 10–15 minutes.

Each array was marked with a meaningful designation (e.g., a number) to know which sample is loaded onto each array.

A 200 µL pipet tip was inserted into the upper right septum of each array.

1000 ml 12X MES stock solution was prepared by adding 70.4 g MES hydrate (Sigma-Aldrich, USA) and 193.3 g MES Sodium Salt (Sigma-Aldrich, USA) to 800 mL molecular biology grade water. The reagents and the water were mixed together and volume was adjusted to 1,000 mL. The pH should be between 6.5 and 6.7. The solution was filtered through a 0.2 μm filter, stored in 2-8ºC and shield from light.

Preparation of hybridisation master mix

The reagents were added to a 50 mL centrifuge tube in the order as shown in table 2.3 and mixed well. For multiple samples, 5% excess was made.

Table 2.3: Hybridisation cocktail master mix

Reagent	**1 array**	**Final concentration in sample**
MES (12X;1.22M)	12 ul	0.056 M
Denhardt's solution (50X) (Sigma-Aldrich, USA)	13 ul	2.50X
EDTA (0.5M) (Ambion, USA)	3 ul	5.77 mM
HSDNA (10 mg/ml) (Promega, USA)	3 ul	0.115
Oligo Control Reagent, 0100 (Affymetrix, USA)	2 ul	1X
Human Cot-1 DNA (1 mg/ml) (Invitrogen, USA)	3 ul	11.55 ug/ml
Tween-20 (3%) (Surfact-Amp, USA)	1 ul	0.0115%
DMSO (100%) (Sigma-Aldrich), USA)	13 ul	5.0%
TMACL (5 M) (Sigma-Aldrich, USA)	140 ul	2.69M
Total	**190 ul**	

Each of the labelled samples was transferred from the plate to a 1.5 mL eppendorf tube. 190 μL of the Hybridisation Cocktail Master Mix was aliquoted into the labelled DNA samples. The hybridisation mix and labeled DNA were heated at 99°C for exactly 10 minutes to denature. It was then cooled on crushed ice for 10 seconds, spun briefly at 2000

rpm in a microfuge to collect any condensate. The tubes were then placed in a heat block at 49°C for 1 minute. 200 µL denatured hybridisation cocktail was injected into the array and each septa was then covered with a Tough-Spot (figure 2.6). The arrays were then hybridised at 49°C for 16 to 18 hours at 60 rpm.

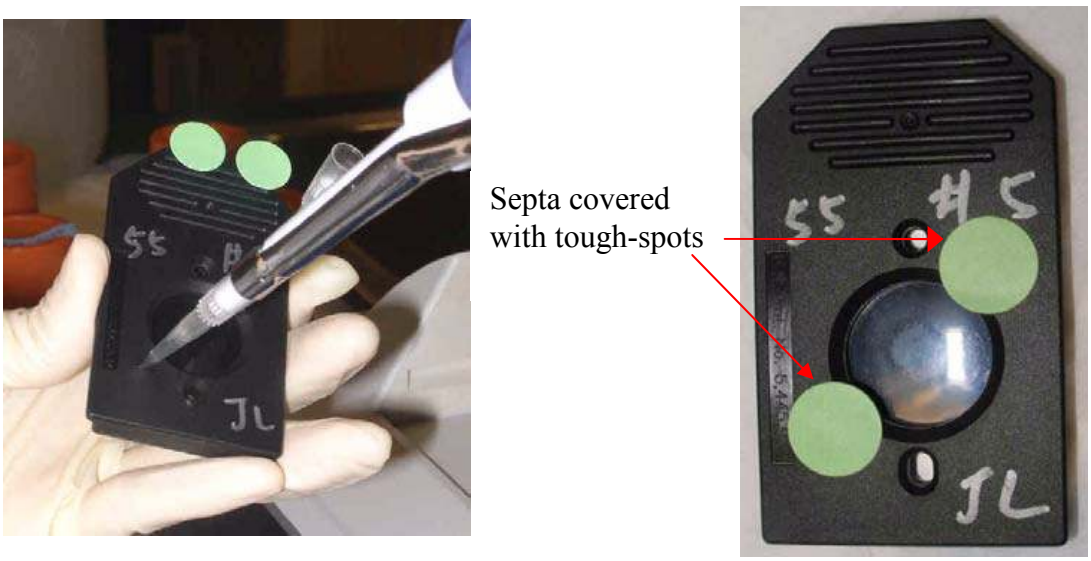

Figure 2.6: Loading samples onto arrays

2.1.10 Washing, staining and scanning arrays

The automated fluidics station used for washing and staining the arrays was the GeneChip® Fluidics Station 450 (Affymetrix, USA). The arrays were scanned using GeneChip® Scanner 3000 7G (Affymetrix, USA). The scanned data were collected and extracted by the Affymetrix GeneChip Operating Software (GCOS) v 1.4.

2.1.10.1 Preparation of reagents required for washing and staining

Wash A: Non-stringent wash buffer (6X SSPE, 0.01% Tween 20)

For 1000 mL, 300 mL of 20X SSPE (BioWhittaker Molecular Applications/Cambrex, USA), 1.0 mL of 10% Tween-20 and 699 mL of water were added together. The solution was filtered through a 0.2 μm filter and stored at room temperature.

Wash B: Stringent Wash Buffer (0.6X SSPE, 0.01% Tween 20)

For 1000 mL, 30 mL of 20X SSPE, 1.0 mL of 10% Tween-20 and 969 mL of water were added together. The solution was filtered through a 0.2 μm filter and stored at room temperature.

0.5 mg/mL Anti-Streptavidin Antibody

0.5 mg of Anti-Streptavidin Antibody was resuspend in 1 mL of water and stored at 4°C.

12X MES solution

The solution was prepared following the method mentioned previously in section 2.1.9.

Stain Buffer

Stain buffer was prepared by adding 800.04 ul H2O, 360 ul SSPE (20X), 3.96 ul Tween 20 (3%) and 24 ul Denhardt's. The solution was mixed.

Streptavidin Phycoerythrin (SAPE) (Sigma-Aldrich, USA) Stain Solution

6.0 ul Streptavidin Phycoerythrin (SAPE) was added to 594 ul Stain buffer and stored in the dark at 4°C. The solution was always prepared immediately before use. A vial containing SAPE Stain Solution must be placed in sample **holder 1** for each module used.

0.5 mg/mL biotinylated antibody solution mix

6 µL of 5 µg/mL biotinylated antibody (Vector Laboratories, USA) was added to 594 µL Stain buffer. A vial containing Antibody Stain Solution must be placed in sample **holder 2** for each module used.

1X Array Holding Buffer:

The solution was prepared by adding together 8.3 ml MES stock buffer (12X), 18.5 ml 5 M NaCl, 0.1 ml Tween-20 (10%) and 73.1 ml water. It was mixed and stored at 2°C to 8°C, shield from light. A vial containing 820 ul of Array Holding Buffer must be placed in sample **holder 3** for each module used.

2.1.10.2 Experiment and fluidics station setup

The following instructions were followed for GeneChip® Operating Software (GCOS) 1.4 client (1.3 server).

STEP 1: REGISTERING A NEW EXPERIMENT IN GCOS

From the File menu click New Experiment.

The New Experiment window appears in the display pane (figure 2.7).

• The top half of the display pane refers to the sample and then bottom half refers to the experiment.

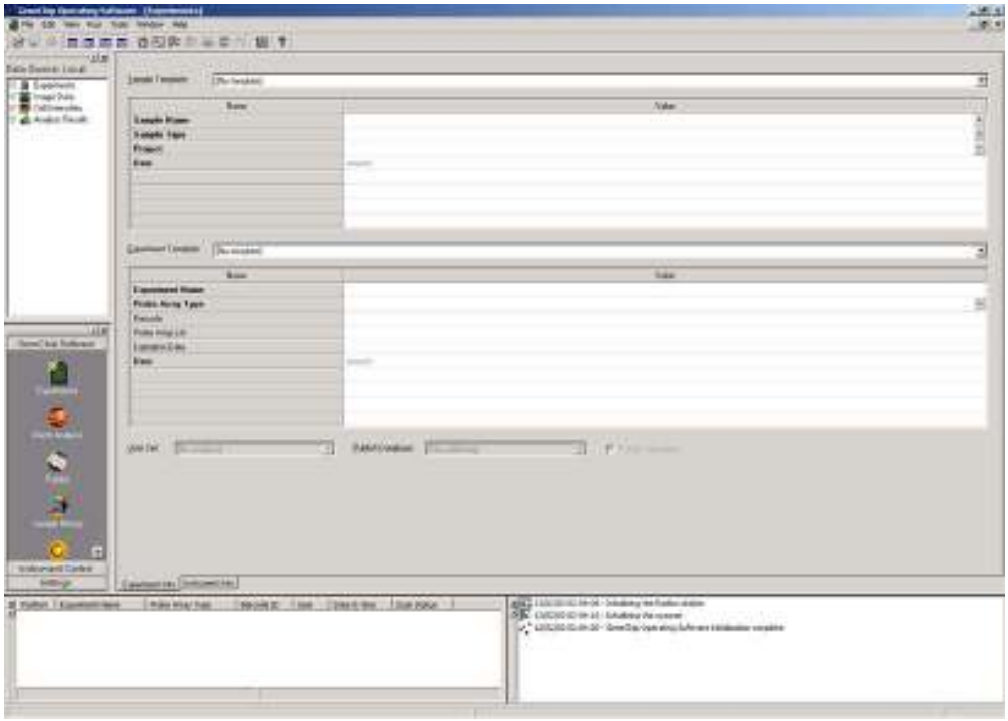

Figure 2.7: GCOS sample entry pane

Enter information into the appropriate boxes.

• Fields that are highlighted in bold require an entry.

• Drop-down menus are available for Sample/Project information (default information can be used or new information can be entered).

• The Experiment Name must be unique.

• Appropriate library files must be installed for a probe array to appear in the drop-down menu.

From the File menu click Save As, or click the Save icon on the tool bar to register the experiment into the database.

STEP 2: PREPARING THE FLUIDICS STATION

1. Turn on the Fluidics Station using the toggle switch on the lower left side of the machine.

2. Select Run → Fluidics from the menu bar in GCOS.

The Fluidics Station dialog box appears with a drop-down list for selecting the experiment name for each of the fluidics station modules. A second drop-down list is accessed for choosing the Protocol for each of the fluidics station modules. Use the radio buttons to access each module.

Priming the Fluidics Station

Priming ensures the lines of the fluidics station are filled with the appropriate buffers and the fluidics station is ready to run fluidics station protocols.

Priming should be done:

• when the fluidics station is first started.

• when wash solutions are changed.

• before washing, if a shutdown has been performed.

• if the LCD window instructs the user to prime.

1. To prime the fluidics station, select Protocol in the Fluidics Station dialog box.

2. Choose **Prime_450** for the respective modules in the Protocol drop-down list.

3. Change the intake buffer reservoir A to Non-Stringent Wash Buffer, and intake buffer reservoir B to Stringent Wash Buffer.

4. Click Run for each module to begin priming.

5. Follow LCD instructions.

Probe Array Wash and Stain

After 16 to 18 hours of hybridisation, the hybridisation cocktail was removed from the probe array and set aside in a microcentrifuge vial. It was stored on ice during the procedure or at –80°C for long-term storage. The probe array was filled completely with 270 µL of Array Holding Buffer. The following instructions were followed for washing and staining the arrays using the Fluidics Station 450.

Using the Fluidics Station 450

1. In the Fluidics Station dialog box on the workstation, select the correct experiment name from the drop-down Experiment list. The Probe Array Type appears automatically.

2. In the Protocol drop-down list, select **Mapping500Kv1_450**, to control the washing and staining of the probe array.

3. Choose Run in the Fluidics Station dialog box to begin the washing and staining. Follow the instructions in the LCD window on the fluidics station.

4. Insert the appropriate probe array into the designated module of the fluidics station while the cartridge lever is in the Down or Eject position. When finished, verify that the cartridge lever is returned to the Up or Engaged position.

5. Remove any microcentrifuge vials remaining in the sample holders of the fluidics station module(s) being used.

6. When prompted to "Load Vials 1-2-3," place the three vials into the sample holders 1, 2 and 3 on the fluidics station.

• Place one vial containing 600 µL Streptavidin Phycoerythrin (SAPE) stain solution mix in sample holder 1.

• Place one vial containing 600 µL anti-streptavidin biotinylated antibody stain solution in sample holder 2.

• Place one vial containing 820 µL Array Holding Buffer in sample holder 3.

• Press down on the needle lever to snap needles into position and to start the run.

Once these steps are complete, the fluidics protocols begin. The Fluidics Station dialog box at the workstation terminal and the LCD window displays the status of the washing and staining steps.

7. When staining is finished, remove the microcentrifuge vials containing stain and replace with three empty microcentrifuge vials as prompted.

8. Remove the probe arrays from the fluidics station modules by first pressing down the cartridge lever to the eject position.

9. Check the probe array window for large bubbles or air pockets.

• If bubbles are present, the probe array should be filled with Array Holding Buffer manually, using a pipette. Take out one half of the solution and then manually fill the probe array with Array Holding Buffer.

• If the probe array has no large bubbles, it is ready to scan on the GeneChip® Scanner 3000 7G. Pull up on the cartridge lever to engage wash block and proceed to Probe Array Scan.

If the arrays cannot be scanned promptly, keep the probe arrays at 4°C and in the dark until ready for scanning. Scan must be preformed within 24 hours.

The fluidics station was shut down after the washing and staining of the probe arrays completed (appendix A2).

2.1.10.3 Probe array scan

Before the probe array was scanned, the following were done:

The GeneChip Scanner 3000 7G laser was turned on to warmed up the laser at least 10 minutes prior to scanning.

Tough-Spots®, label spots was applied to each of the two septa on the probe array cartridge to prevent leaking of fluids from the cartridge during scanning. Excess fluid was cleaned from around the septa.

If necessary, the glass surface of the probe array was clean with a non-abrasive towel or tissue before scanning.

If the probe array was stored at 4°C, it was allowed to warm to room temperature before scanning.

Scanning the probe array

1. Select Run → Scanner from the menu bar. Alternatively, click the Start Scan icon in the tool bar. The Scanner dialog box appears with a drop-down list of all unscanned experiments.

2. Select the experiment name that corresponds to the probe array being scanned. A previously run experiment can also be selected by using the Include Scanned Experiments option box. After selecting this option, previously scanned experiments appear in the drop-down list.

3. Click the Load/Eject button and place the array in the scanner. Only one scan is required for the GeneChip Scanner 3000 7G.

4. Once the experiment has been selected, click the Start button. A dialog box prompts to load the array into the scanner.

5. Pixel resolution and wavelength for the GeneChip Scanner 3000 7G are preset and cannot be changed.

6. Open the sample door of the scanner and insert the probe array into the holder. The door of the GeneChip Scanner 3000 7G closes automatically.

7. Click OK in the Start Scanner dialog box. The scanner begins scanning the probe array. When Scan in Progress is selected from the View menu, the probe array image appears on the screen as the scan progresses.

2.1.11: Data analysis

Data analysis was done using Genotyping Console (GTC) 3.0.2

2.2 SNP Array 6.0

The genomic DNA general requirement for SNP array 6.0 is the same as in 250K SNP array (refer to Appendix A1). The experiment was carried out following the manufacturer's protocol (Affymetrix, USA) (as summarized in section 2, figure 2.1).

2.2.1 Sample preparation

The genomic DNA and Ref 103 were thawed on the bench top at room temperature. Once thawed, they were placed in the cooling chamber on ice. OD measurement of each sample was taken using Nanodrop spectrophotometer. The convention that 1 absorbance unit at 260 nm equals 50 µg/mL for double-stranded DNA.was applied. This convention assumes a path length of 1 cm. Based on OD measurements, each sample was diluted in a separate well of the 96-well plate to 50 ng/µL using reduced EDTA TE buffer (10 mM Tris, 0.1 mM EDTA, pH 8.0). The plate was sealed, vortexed at high speed for 3 seconds then spun down for 30 seconds. It was then placed back on the top half of the cooling chamber.

2.2.2: Aliquoting the prepared genomic DNA (gDNA) and controls

A 96-well plate was marked as shown in Figure 2.8 (a blue marker was used for Nsp (N) and a red marker for Sty (S) and placed on the bottom half of the cooling chamber.

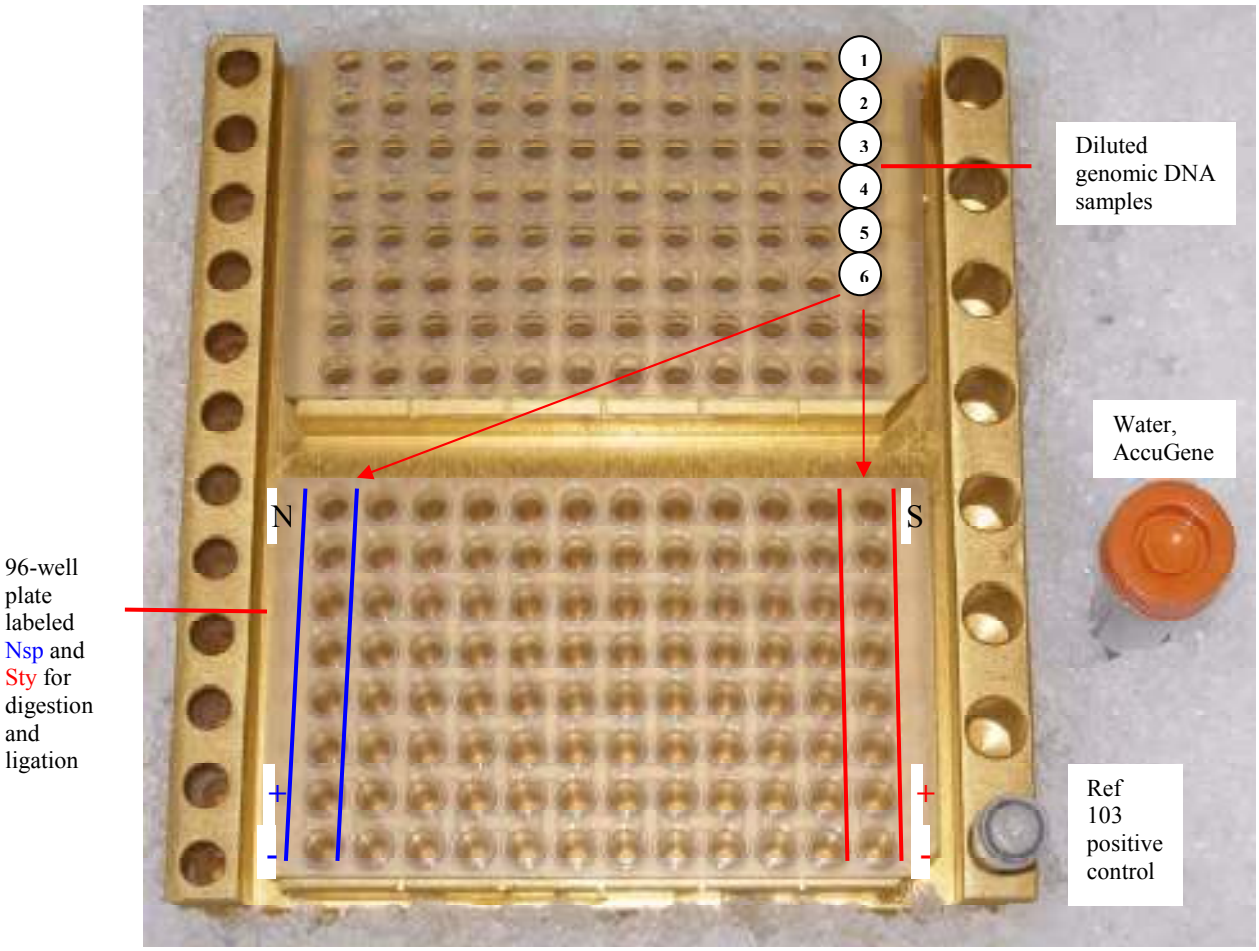

Figure 2.8: Setup for aliquoting diluted gDNA and controls to a 96-well plate labeled for Nsp and Sty digest and ligation

Two 5 µL aliquots of the first sample were transferred to wells A1 and A12 of the digest/ligate plate (figure 2.8). The remaining samples were transferred in the same manner into the appropriate wells. The Ref 103 (positive control) was vortexed for 3 seconds then spun down for 30 seconds. 5 ul of the control sample was transferred to wells G1 and G12. 5 ul of water which served as negative control was transferred into wells H1 and H12. The plate was tightly sealed. If the next step was not continued immediately, it was stored in -20°C.

2.2.3 Nsp and Sty restriction enzyme digest

Before starting this step, the following reagents, equipment and consumables were prepared:

NE Buffer 2, NE Buffer 3 and BSA were thawed on ice. They were then vortexed 3 times, 1 second each time, pulse spun for 3 seconds and placed in the cooling chamber on ice.

If the plate of genomic DNA and controls were frozen, it was thawed in a cooling chamber on ice. Once thawed, they were vortexed at high speed for 3 seconds and spun down at 2000 rpm for 30 seconds.

The thermal cycler was powered on to preheat the lid. The block was left at room temperature.

A 1.5 mL Eppendorf tubes was labeled *NSP* and another one labelled *STY.*

Preparation of the Nsp Digest Master Mix:

Usually 8 samples were processed at one time. Therefore, the preparation of the master mix was made for 8 samples+15% extra. All the reagents and tubes were placed on ice while preparing the master mix. 106.3 ul AccuGene water, 18.4 ul NE Buffer (10X), 1.8 ul BSA (100X;10 mg/ml) were added together. The NspI enzyme (10U/ul) was removed from the freezer and pulse spun for 3 seconds. 9.2 ul of the enzyme was immediately added to the master mix and vortexed at high speed 3 times, 1 second each time. It was pulse spun for 3 seconds and placed in the cooling chamber. The tube was labeled *NSP.*

14.75 µL of Nsp Digest Master Mix was then added to each sample and control for Nsp digest.

Preparation of the Sty Digest Master Mix:

The volumes and the reagents used for the preparation of the master mix was the same as Nsp Digest Master Mix, except for the enzyme. The StyI (10U/ul) was added to the solution and the tube was labeled *STY*. 14.75 µL of Sty Digest Master Mix was added to each sample and control for Sty1. The total volume in each well is now 19.75 µL. The plate was then sealed tightly. Next, the plate was vortexed at high speed for 3 seconds then spun down at 2000 rpm for 30 seconds. It was then loaded onto the thermal cycler and the Cyto Digest program was run as follows:

120 minutes 37°C
20 minutes 65°C
Hold 4°C

Then, the plate was removed and spun down at 2000 rpm for 30 seconds. The plate was stored at –20°C if not proceeding directly to the next step,

2.2.4 Nsp and Sty Ligation

Location: Pre-PCR clean area

The following were prepared before starting this step:

Adaptor Nsp, Adaptor Sty and T4 DNA Ligase Buffer were thawed on ice, then vortexed at high speed 3 times, 1 second each time and pulse spun for 3 seconds.

The digested samples were thawed on ice. They were then vortexed at high speed for 3 seconds and spun down at 2000 rpm for 30 seconds.

One 1.5 mL Eppendorf tube was labeled *NSP* and another was labelled *STY*.

The thermal cycler was powered on to preheat the lid and the block was left at room temperature.

Preparation of the Nsp Ligation Master Mix:

The preparation of the master mix was done on ice. For 8 samples+15% extra, 23.0 ul T4 DNA Ligase Buffer (10X) and 6.90 ul Adaptor Nsp were added together in the 1.5 mL eppendorf tube labeled *NSP*. T4 DNA Ligase (400 U/ul) was removed from the freezer and immediately pulse spun for 3 seconds. 18.4 ul of the enzyme was immediately added to the master mix. The solution was vortexed at high speed 3 times, 1 second each time, pulse spun for 3 seconds and placed on ice. 5.25 µL of Nsp Ligation Master Mix was then added to each Nsp digested sample and control.

Preparation of the Sty Ligation Master Mix:

The preparation of the master mix was done on ice. For 8 samples+15% extra, 23.0 ul T4 DNA Ligase Buffer (10X) and 6.90 ul Adaptor Sty (50 uM) were added together in the 1.5 mL eppendorf tube labeled *STY*. T4 DNA Ligase (400 U/ul) was removed from the freezer and immediately pulse spun for 3 seconds. 18.4 ul of the enzyme was immediately added to the master mix. The solution was vortexed at high speed 3 times, 1 second each time, pulse spun for 3 seconds and placed on ice. 5.25 µL of Sty Ligation Master Mix was then added to each Sty digested sample and control.

The plate was then sealed tightly. It was then vortexed at high speed for 3 seconds, spun down at 2000 rpm for 30 seconds and loaded onto the pre-heated thermal cycler and the Cyto Ligate program was run as follows:

180 minutes 16°C
20 minutes 70°C
Hold 4°C

Dilution of the Ligated Samples:

Before the dilution was done, the water was placed on ice 20 minutes prior to use. When the Cyto Ligate program is finished, the plate was removed and spun down at 2000 rpm for 30 seconds and placed in a cooling chamber on ice. 75 µL of water was added to each reaction. The plate was then sealed tightly, vortexed at high speed for 3 seconds then spun at 2000 rpm for 30 seconds. If not proceeding directly to the next step, the plate was stored at –20 °C.

2.2.5 Nsp and Sty PCR

Location: Pre-PCR clean area

The following were done before starting this step:

A double cooling chamber was placed on ice.

A 50 mL centrifuge tubes was labelled *PCR*.

The thermal cycler in the Post-PCR Area was power on to preheat the lid. The blocks were left at room temperature.

Water (AccuGENE) and GC-Melt were placed on ice.

TITANIUM Taq, PCR Buffer, dNTPs and PCR Primer 002 (Affymetrix, USA) were thawed on ice. They were then vortexed at high speed 3 times, 1 second each time, pulse spun for 3 seconds and placed on ice or in the cooling chamber.

If the diluted ligated samples were frozen, they were thawed in a cooling chamber on ice, vortexed at high speed for 3 seconds then spun down at 2000 rpm for 30 seconds. It was placed in the top half of the cooling chamber.

A fresh 96-well plate was labelled as shown in figure 2.9 (blue for Nsp; red for Sty). The plate was placed in the lower half of the cooling chamber.

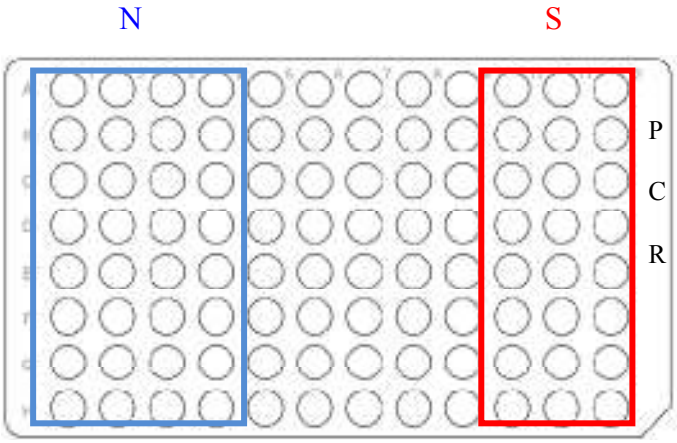

Figure 2.9: Labeling the 96-well plate for PCR.

10 µL of each Nsp ligated sample was transferred to the corresponding four wells of the PCR plate. 10 µL of each Sty ligated sample was transferred to the corresponding three wells of the PCR plate. The remaining ligated Nsp and Sty samples in the plate were sealed, labeled and stored at –20 °C.

Keeping the 50 mL centrifuge tube in the cooling chamber, PCR master mix was prepared for 8 samples+15% extra by adding 2544 ul AccuGene water, 644 ul TITANIUM Taq PCR Buffer (10X), 1288 ul GC-Melt (5M), 902 ul dNTP (2.5 mM each), 290 ul PCR primer 002 (100 uM). The TITANIUM Taq DNA polymerase (50X) was removed from the freezer and immediately pulse spun for 3 seconds. Immediately 129 ul of the enzyme was added to the master mix. The mix was then vortexed at high speed 3 times, 1 second each time. 90 µL PCR Master Mix was added to each sample and control on the PCR plate.

The plate was then sealed tightly, vortexed at high speed for 3 seconds then spun down at 2000 rpm for 30 seconds. It was then loaded onto the thermal cycler with preheated lid and the Cyto PCR program was run as follows:

3 minutes 94°C 1 cycle
30 seconds 94°C
30 seconds 60°C } 30 cycles
15 seconds 68°C
7 minutes 68°C 1 cycle
Hold 4°C

The plate was then removed from the thermal cycler and spun down at 2000 rpm for 30 seconds and placed in a cooling chamber on ice.

A fresh 96-well plate was labeled as *gel plate*. 3 µL of 2X Gel Loading Dye was aliquot to each well to be used. 10 µL BioNexus Hi-Lo Ladder was loaded to the first lane of the gel. 3 µL of Nsp PCR product was transferred from each well in one column only to the corresponding wells of the gel plate. The step was repeated for Sty PCR product. The plate was sealed, vortexed and then spun down at 2000 rpm for 30 seconds. The total volume from each well of the gel plate was loaded onto a 2% TBE gel. The gel was run at 120V for 40 minutes to 1 hour. The PCR product distribution was verified between ~250 bp to 1100 bp (figure 2.10). If not proceeding directly to the next stage, the plate was sealed with PCR product and stored at –20 °C.

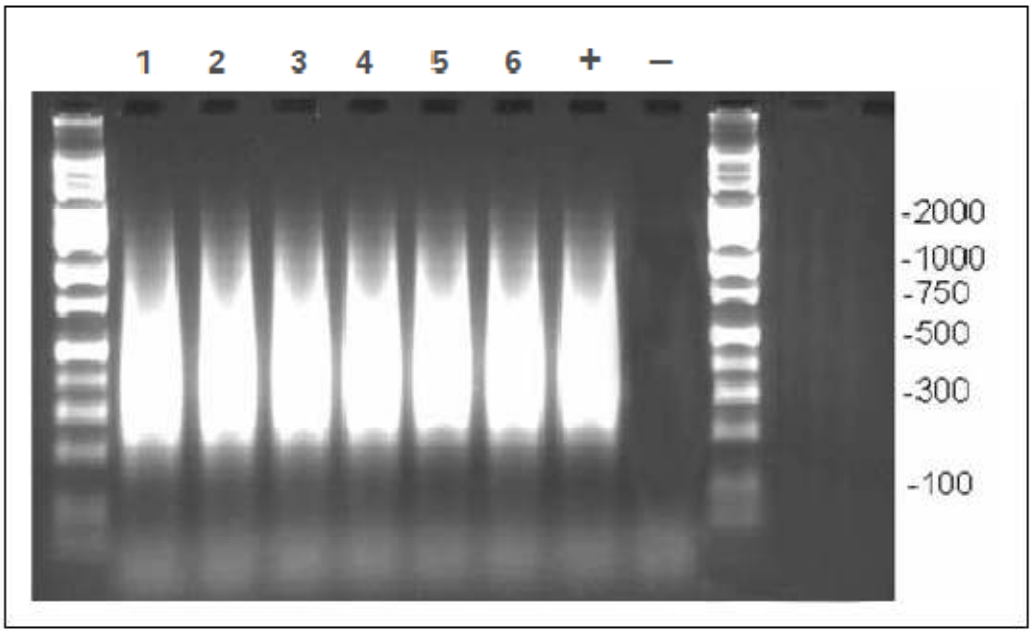

Figure 2.10: Example of PCR products run on 2% TBE agarose gel at 120V for 1 hour. Average product distribution is between ~200 to 1100 bp.

2.2.6 PCR product purification

Location: Post PCR Area

If frozen, the PCR products were thawed in a plate holder on the bench top to room temperature. The plate was then vortexed at high speed for 3 seconds then spun down at 2000 rpm for 30 seconds. Seven aliquots of each sample were transferred to the appropriately marked 2.0 mL microcentrifuge tube (figure2.11). The PCR plate was then examined to ensure that the total volume in each well has been transferred and pooled.

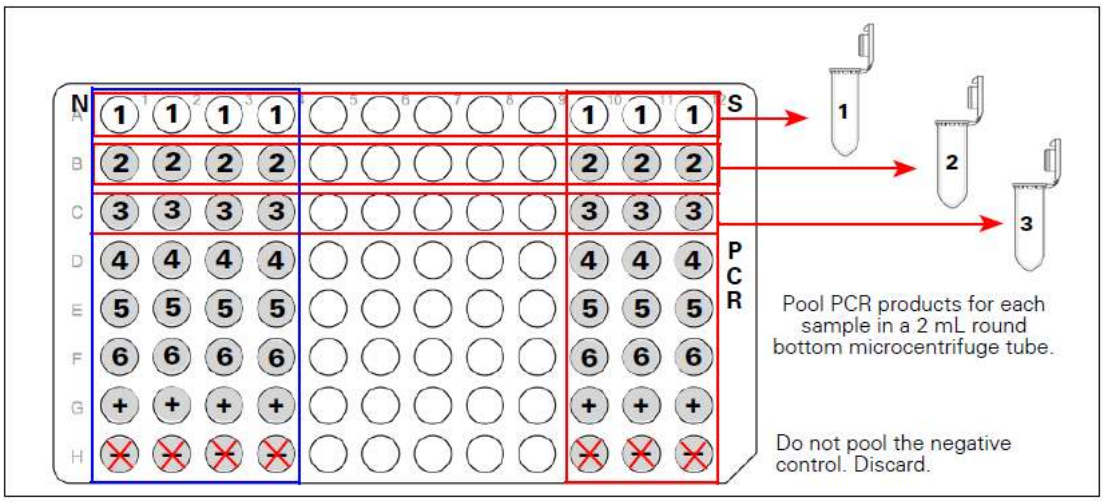

Figure 2.11: Pooling PCR products

The magnetic bead (Agencourt Bioscience, Beverly, Massachusetts, USA) stock was thoroughly mix by shaking the bottle vigorously. The bottom of the bottle was examined to ensure that the solution appears homogenous. Magnetic beads were poured into a 50 mL conical tube. 1 mL of magnetic beads was aliquot to each pooled sample. Each tube was securely capped and mixed well by inverting 10 times. It was then incubated at room temperature for 10 minutes to allow the DNA binds to the magnetic beads. The tubes were then loaded with cap hinge facing out onto the microcentrifuge and spun for 3 minutes at maximum speed (16,100 rcf). They were then placed on the magnetic stand (Invitrogen Corporation, Carlsbad, CA, USA). Leaving the tubes in the rack, the supernatant was pipetted off without disturbing the bead pellet and discard.

Next, 1.5 mL of 75% EtOH was added to each tube. The tubes were capped and loaded into the foam tube adaptor, fully inserted into the foam to ensure they are secured and spaced adequately to balance. The tubes were vortexed at 75% power for 2 minutes, then centrifuge for 3 minutes at maximum speed (hinges facing out; 16,100 rcf). They were

then placed on the magnetic stand and the supernatant was pipetted off without disturbing the bead pellet and discard. The tubes were then spun for 30 seconds at maximum speed (hinges facing out; 16,100 rcf) and placed back on the magnetic stand. Remaining drops of ethanol was removed from the bottom of each tube. The tubes were left uncapped at room temperature for 15 minutes to allow the remaining ethanol to evaporate.

55 µL of Buffer EB (Qiagen, USA) was added to each tube and they were then capped and loaded into the foam tube adaptor. The tubes were then vortexed at 75% power for 10 minutes to resuspend the magnetic beads. Each tube was examined to ensure that the beads were resuspended in homogeneous slurry. If the beads were not fully resuspended, the tube was flicked to dislodge the pellet and vortexed an additional 2 minutes. It was then re-examined. The tubes were centrifuged for 5 minutes at maximum speed (hinges facing out; 16,100 rcf) and placed on the magnetic stand for 5 minutes. When all the beads had been pulled to the side in each tube, 47 µL of eluted sample was transferred to the appropriate well on a fresh 96-well plate. The plate was sealed tightly.

2.2.7 Quantitation

18 µL of water was added to the corresponding wells of a 96-well plate. 2 µL of each purified sample was transferred to the corresponding well of the 96-well plate and pipette up and down a few times. The result was a 10-fold dilution. The NanoDrop 1000 spectrophotometer (Thermo, USA) was blanked with water. 2 µL of the diluted sample was taken and the OD of each sample at 260, 280 and 320 nm was measured. OD280 and OD320 were used as controls. The undiluted concentration for each sample was calculated as follows:

Undiluted sample concentration in µg/µL = OD X 10

An acceptable OD should fall within 0.9 to 1.4.

DNA yield equivalent = 4.5 to 7.0 μg/μL

This OD range is based on the use of a conventional UV spectrophotometer plate reader and assumes a path length of 1 cm.

• The OD260/OD280 ratio should be between 1.8 and 2.0.

• The OD320 measurement should be very close to zero (≤ 0.1).

If not proceeding immediately to the next step, the plate was sealed and stored at –20 °C.

2.2.8 Fragmentation

Location: post-PCR area

Equipment, reagents and consumables required in this step were prepared as follows:

A cooling chamber and the water were placed on ice.

The Fragmentation Buffer (10X) (Affymetrix, USA) was thawed on ice. It was then vortexed 3 times, 1 second each time, pulse spun for 3 seconds and placed in the cooling chamber.

The plate of purified, quantitated samples was placed in the cooling chamber.

A 1.5 mL eppendorf tube was labelled *Frag* and placed in the cooling chamber.

The thermal cycler block was powered on and the block preheated to 37 °C.

5 μL of Fragmentation Buffer was added to each sample on ice.

Preparation of the fragmentation master mix:

The concentration of the Fragmentation Reagent written on the tube label was identified and recorded. For 8 to 16 samples, the volume of reagents used is as shown in table 2.4.

Table 2.4: Fragmentation master mix

Reagent	Fragmentation Reagent Concentration				
	2 U/µL	2.25 U/µL	2.5 U/µL	2.75 U/µL	3 U/µL
AccuGENE water	85.00 µL	96.25 µL	107.50 µL	118.75 µL	130.00 µL
10X Fragmentation Buffer	10.00 µL	11.25 µL	12.50 µL	13.75 µL	15.00 µL
Fragmentation Reagent (enzyme)	5.00 µL	5.00 µL	5.00 µL	5.00 µL	5.00 µL
Total	**100 µL**	**112.50 µL**	**125 µL**	**137.50 µL**	**150 µL**

The appropriate volume of water and fragmentation buffer were added to the *Frag* tube on ice. It was allowed to cool on ice for 5 minutes. The fragmentation reagent (enzyme) was removed from the freezer and immediately pulse spun for 3 seconds. Immediately the appropriate volume of fragmentation reagent was then added (refer to table 2.4). The master mix was vortexed at high speed 3 times, 1 second each time, pulse spun for 3 seconds and immediately placed on ice. 5 µL of fragmentation master mix were transferred to each sample - mixing was not allowed at this stage. The plate was then sealed tightly, vortexed at high speed for 3 seconds then spun down for 30 seconds. The samples were immediately loaded onto the pre-heated block of the thermal cycler (37°C) and the Cyto Fragment program was run as follows:

35 minutes 37°C
15 minutes 95°C
Hold 4°C

The samples were then removed from the thermal cycler, spun down for 30 seconds and placed in a cooling chamber on ice. 2.0 µL of each sample was removed and placed in a 96-well plate. 4 µL gel loading dye was added to each sample. 10 µL BioNexus All Purpose Hi-Lo Ladder was loaded to the first and last lanes. The samples were loaded and run on a 4% TBE gel at 120V for 30 minutes to 1 hour. The gel was inspected and compared against the example shown in figure 2.12.

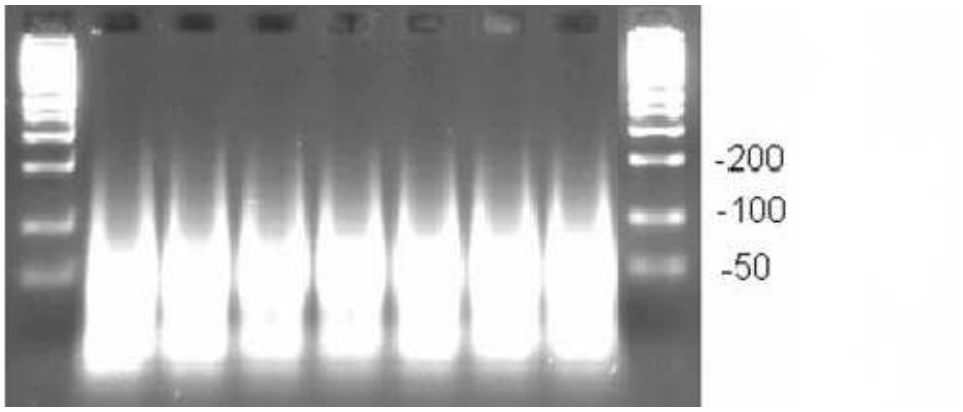

Figure 2.12: Typical example of fragmented PCR products run on 4% TBE agarose gel at 120V for 30 minutes to 1 hour. Average fragment size is < 180 bp.

2.2.9 Labeling

Location: Post-PCR area

The equipment, reagents and consumables required for this step were prepared as follows:

5X TdT Buffer (Affymetrix, USA) and DNA Labeling Reagent (Affymetrix, USA) were thawed on ice. When thawed, each reagent was vortexed at high speed 3 times, 1 second each time, pulse spun for 3 seconds then place in the cooling chamber.

The thermal cycler block was heated to 37 °C before samples were loaded.

A cooling chamber was placed on ice.

A 1.5 mL centrifuge tube was labeled *LBL* and placed in the cooling chamber.

All reagents and tubes were kept on ice while preparing the Labeling Master Mix. For 8 samples+15% extra, 128.8 ul 5X TdT Buffer and 18.4 ul DNA Labeling Reagent were added to the 1.5 mL centrifuge tube on ice. The TdT enzyme (30 U/ul) was removed from the freezer and immediately pulse spun for 3 seconds then immediately placed back in the cooler. 32.2 ul TdT enzyme was added to the master mix, vortexed at high speed 3 times, 1

second each time, pulse spun for 3 seconds. 20 µL of Labeling Master Mix was aliquot to each sample and pipetted up and down one time to ensure that all of the mix were added to the samples. The plate was sealed tightly, vortexed at high speed for 3 seconds then spun down for 30 seconds. It was then placed on the pre-heated thermal cycler block and the Cyto Label program (table 28) was run as follows:

4 hour 37°C
15 minutes 95°C
Hold 4°C

The plate was then removed from the thermal cycler and spun down for 30 seconds. If not proceeding directly to the next stage, the samples were stored at –20°C.

2.2.10 Target hybridisation

The equipment, reagents and consumables required for this step were prepared as follows:

The labeled samples from the previous stage were allowed to thaw on the bench top at room temperature if frozen. It was then vortexed at high speed for 3 seconds then spun down for 30 seconds and placed in a cooling chamber on ice.

The oven was turned on and the temperature set to 50°C. The rpm was set to 60. The rotation was turned on and allowed to preheat for 1 hour before loading arrays.

The thermal cycler was powered on to preheat the lid. The block was left at room temperature.

The arrays were unwrapped and placed on the bench top, septa-side up.

The front or back of each array was marked with a designation that will identify which sample was loaded onto each array.

The arrays were allowed to warm to room temperature on the bench top 10 to 15 minutes.

A 200 µL pipet tip was inserted into the upper right septum of each array.

500 mL 12X MES stock solution (1.25 M MES, 0.89 M [Na+]) was prepared. The recipe is the same as in the section 2.1.9.

Preparation of hybridisation master mix for 8 samples+15% extra was done by adding 110.4 ul MES (12X;1.25 M), 119.6 ul Denhardt's solution (50X), 27.6 ul EDTA (0.5 M), 27.6 ul Herring Sperm DNA (10 mg/ml), 18.4 ul Oligo Control Reagent 0100, 27.6 ul Human Cot-1 DNA (1 mg/ml), 9.2 ul Tween-20, 119.6 ul Dimethyl sulfoxide (DMSO) (100%), 1288.0 ul 5 M Tetramethylammonium Chloride (TMACL). The solution was mixed and placed on ice.

190 µL of Hybridisation Master Mix was added to each sample. The plate was then sealed tightly, vortexed for 30 seconds then spun down for 30 seconds and placed onto the thermal cycler. The Cyto Hyb program was run as follows:

10 minutes 95°C
Hold 49°C

The lid of the thermal cycler was opened when the temperature reached 49°C. 200 µL of the first sample were removed and immediately injected into an array. The septa on the array were covered with a Tough-Spot. It was pressed firmly to ensure a tight seal to prevent evaporation and leakage. When 4 arrays were loaded and the septa were covered, the arrays were loaded into an oven tray evenly spaced. The tray was then immediately placed into the hybridisation oven. It was not allowed to sit at room temperature for more than approximately 1 minute. The oven was ensured balanced and the trays were rotating at 60 rpm. This process was repeated until all samples were loaded onto arrays and were placed in a hybridisation oven. The arrays were allowed to rotate at 50 °C, 60 rpm for 16 to 18 hours.

2.2.11 Washing, staining and scanning arrays

The Fluidics Station 450 was used to wash and stain the arrays. It is operated using either GCOS or Affymetrix GeneChip® Command Console (AGCC) software.

Detail information on these applications can be found in Affymetrix GeneChip® Command Console™ User's Guide (http://www.affymetrix.com/support/technical/byproduct.affx?product=commandconsole)

Before washing and staining were performed, the fluidics station was primed using AGCC software.

Prime the Fluidics Station

The Fluidics Station 450 was used to wash and stain the arrays.

To prime the Fluidics Station:

1. The Fluidics Station turned on.

2. The Fluidics Station was primed by:

• Select protocol **Prime_450** for each module

• Intake buffer reservoir: use **Non-Stringent Wash Buffer**

• Intake buffer reservoir B: use **Stringent Wash Buffer**

After 16 to 18 hours of hybridisation, the arrays were removed from the oven. The hybridisation cocktail from each array was extracted and transferred to the corresponding well of a 96-well plate. It can be stored on ice during the procedure or at –80 °C for long-term storage. Each array was filled completely with 270 µL of 1X Array Holding Buffer. The arrays were allowed to equilibrate to room temperature before washing and staining.

Buffers and solutions required for washing and staining are the same as used in 250K array in section 2.1.10.

To wash and stain the array using fluidics station 450 for AGCC:

1. Sample name was selected in AGCC.

2. The protocol **GenomeWideSNP6_450** was **s**elected.

3. The protocol was then started and the instructions in the LCD were followed on the fluidics station.

Details on how to handle the arrays on the fluidics station can be found in the appropriate Fluidics Station User's Guide, or Quick Reference Card (P/N 08-0093 for the Fluidics Station450)

(https://www.affymetrix.com/support/downloads/quick_reference_cards/fs450_agcc_qrc.pdf).

4. An array was inserted into the designated module of the fluidics station while the cartridge lever was in the Down or Eject position.

5. When finished, the cartridge lever was returned to the Up or Engaged position.

6. Any vials remaining in the positions of the fluidics station module(s) being used were removed.

7**.** When prompted to "Load Vials 1-2-3," the three vials were placed into positions 1, 2 and 3 on the fluidics station.

a. One vial containing 600 µL Streptavidin Phycoerythrin (SAPE) stain solution mix was placed in position 1.

b. One vial containing 600 µL anti-streptavidin biotinylated antibody stain solution was placed in position 2.

c. One vial containing 1 mL Array Holding Buffer was placed in position 3.

d. the needle lever was pressed down to snap needles into position and to start the run.

Once these steps are complete, the fluidics protocol begins. The Fluidics Station dialog box at the workstation terminal and the LCD window displays the status of the washing and staining steps.

8. When staining was finished, the microcentrifuge vials containing stain were removed and replace with three empty vials as prompted.

9. The arrays were removed from the fluidics station by first pressing down the cartridge lever to the eject position.

10. Presence of large bubbles or air pockets was checked by looking at the array window. If there were bubbles, these steps were taken:

1) One-half of the solution was manually removed, then

2) The array was manually filled with Array Holding Buffer.

11. If there were no bubbles, the array is ready for scanning.

If the arrays cannot be scanned promptly, they were store at 4°C in the dark until ready for scanning. Scan must be performed within 24 hours.

12. When finished washing and staining, the fluidics station was shut down following the procedure in appendix A2.

Scanning Arrays

The GeneChip Scanner 3000 7G was used in this experiment. It is controlled by GCOS or AGCC software. The scanner has to be turned on at least 10 minutes before use. If the arrays were stored at 4°C, they were allowed to warm to room temperature before scanning. The glass surface of the array was cleaned with a non-abrasive towel or tissue

before scanning. Any excess fluid from around the septa on the back of the array cartridge was cleaned. Both septa were carefully covered with Tough Spots. The spots were pressed firmly to ensure they remain flat. An array was inserted into the scanner and tests the autofocus to ensure the spots do not interfere with the focus. If a focus error message was observed, the spot was removed and a new spot was applied. The arrays were scan by following these steps:

1. The sample name that corresponds to the array being scanned was selected from AGCC.
2. Following the AGCC instructions as appropriate, the array was loaded into the scanner and the scan begin.

2.2.12 Data analysis

Data analysis was done using Genotyping Console (GTC) 3.0.2

2.3 Multiplex ligation-dependent probe amplification (MLPA)

This protocol is based by the procedure recommended by MRC-Holland. It has five parts:

-DNA denaturation and hybridisation of SALSA probes to DNA

-ligation reaction

-PCR of ligation products

-separation by capillary electrophoresis

-data analysis

2.3.1 DNA denaturation and hybridisation of the SALSA probes

A set of 0.2 ml thin-walled PCR tubes were labeled with patient's initials or lab number on the lid or on the side of the tube. Each DNA sample (50-250 ng) was diluted with TE to 2.5 ul in a 0.2 ml labelled tube (for example, 0.5 ul of a 500 ng/ul DNA sample and 2 ul TE). A drop of mineral oil was added to each tube. The tubes were then loaded onto a PCR machine with a heated lid and the MLPA program was started as follows:

5 minutes 98°C
25°C pause
1 minute 95°C
60°C pause

SALSA probe mix and MLPA buffer tubes were taken out of the freezer to thaw. For one sample, 0.75 ul SALSA probe mix and 0.75 ul MLPA buffer was added together. The solution was pipetted up and down to mix. 1.5 ul of the mix was added to PCR tube whilst still at 25ºC on the PCR block and pipetted up and down gently to mix. Lids were closed firmly and proceed to next step of the program – incubation for 1 minute at 95ºC then 16 hours at 60ºC.

2.3.2 Ligation reaction

A master mix for the ligase reaction was prepared less than 1 hour before use. For 1 reaction, 1.5 ul ligase-65 buffer A was added with 1.5 ul ligase 65 buffer, 0.5 ligase 65 and 12.5 ul water. Temperature of the PCR machine was reduced to 54ºC by proceeding to the next step of the PCR program. The ligation reaction program was started as follows:

15 minutes 54ºC
5 minutes 98ºC
4ºC pause

Whilst at 54ºC, 15 ul of the ligase 65 mix was added to each sample whilst still on the block and mixed by repeated pipetting. This was done as quickly as possible. The tubes were close firmly. It was then incubated for 10-15 minutes at 54ºC then heated for 5 minute at 98ºC to deactivate the ligase enzyme. Following 98ºC ligase inactivation treatment, samples can be stored at 4ºC for up to 1 week or for longer at –20ºC.

2.3.3 Polymerase chain reaction (PCR)

A second set of 0.2 ml thin walled PCR tubes were labeled as previously. PCR Buffer master mix was prepared by adding 2 ul 10X SALSA PCR Buffer and 13 ul water. 15 ul of the master mix was transferred into the labeled 0.2 ml thin walled PCR tubes. 5 ul of each of the MLPA ligation reaction was transferred to the correctly labeled tube.The tubes were then loaded onto the PCR machine with heated lid and heat to 60ºC by proceeding to the next step of the MLPA program. The PCR program applied was as follows:

60ºC pause
30 seconds 95ºC
30 seconds 60ºC } 33 cycles
60 seconds 72ºC
20 minutes 72ºC
4ºC pause

Next, Polymerase master mix was prepared by adding 1 ul SALSA PCR primers, 1 ul SALSA enzyme dilution buffer, 0.25 ul SALSA polymerase and 2.75 ul water. While at 60ºC 5 ul polymerase mix was added to each tube and mix by pipetting up and down. The lids were then closed firmly. The PCR cycles was run by proceeding to the next step of the MLPA program. The PCR products may be stored for 1 week at 40ºC or indefinitely at –20ºC.

2.3.4 Separation of amplification products by capillary electrophoresis

0.2 ml tubes were labelled with sample/lab name. 90 ul of water was added into each tube. 10 ul of the PCR product was then transferred into the tube to make a dilution of 1:10. Hi-Di (Applied Biosystem, USA) master mix was prepared by adding 500 ul Hi-Di formamide and 4 ul LIZ-500 (Applied Biosystem, USA). 1 ul of the diluted PCR products were then pipette out into the well of the plate. Only the uneven rows of the plate were used. 10 ul of Hi-Di mix was added into the PCR products in the well. The plate was then sealed and pulse spin for 30 seconds. It was then loaded into a thermal cycler to denature the DNA. The program used was 96ºC for 5 minutes with no heated lid.

The plate was then immediately snap-chilled and ready to be loaded on capillary electrophoresis for fragment analysis. The amplified products were separated by capillary electrophoresis equipped with fragment analysis software. Relative amounts of probe

amplification products as compared to a control DNA sample reflect the relative copy number of target sequences. Intensity peaks or electropherograms were produced and analysed to determine genomic deletion or amplification.

2.3.5 Data analysis

SoftGenetics GeneMarker v1.85 (ABI) software was used to analyse MLPA worksheets ran on the capillary electrophoresis system. The analysis was done according to the steps described in the website http://www.softgenetics.com/GeneMarkerMLPA.html

3 Array CGH analysis of 3p25-p26 deletion (3p- syndrome)

3.1 Introduction

Distal 3p25-p26 deletion (3p- syndrome) is a rare contiguous gene disorder and less than 30 cases have been reported since it was first described by Verjaal and de Nef (Verjaal and De Nef, 1978; Merrild et al., 1981; Schwyzer et al., 1987; Narahara et al., 1990; Nienhaus et al., 1992; Mowrey et al., 1993; Phipps et al., 1994; Knight et al., 1995; Drumheller et al., 1996; McClure et al., 1996; Angeloni et al., 1999; Benini et al., 1999; Green et al., 2000; Kariya et al., 2000; Cargile et al., 2002; Endris et al., 2002; Fernandez et al., 2004; Higgins et al., 2004; Malmgren et al., 2007). Characteristic feature of distal 3p- syndrome include low birth weight, microcephaly, trigonocephaly, hypotonia, psychomotor and growth retardation, ptosis, telecanthus, downslanting palpebral fissures and microagnathia. In addition, postaxial polydactyly, renal anomalies, cleft palate, congenital heart defects especially atrioventricular septal defects (AVSDs), preauricular pits, sacral dimple and gastrointestinal anomalies occur variably. Although intellectual deficits are almost invariably associated with cytogenetically visible 3p deletions, rare patients with a 3p25-p26 deletion and normal intelligence or only mild abnormalities have been described (Knight et al., 1995; Jervis et al., 2002; Sklower-Brooks et al., 2002; Takagishi et al., 2006).

The two main aims of my studies were to investigate phenotype-genotype correlations and to accurately map the deletion breakpoints on the chromosome 3p. Previous studies had used microsatellite markers and molecular cytogenetic methods to accomplish this. Thus in a study of five patients, it was found that congenital heart defects were present only in the

three patients with the most centromeric deletions (Phipps et al., 1993). Further mapping studies suggested that the 3p25 congenital heart disease (CHD) susceptibility locus mapped between D3S1263 and D3S3594, a distance of 3.7 cM (Green et al., 2000). Subsequently Malmgren et al., (2007) further refined the CHD gene localization interval to a 450 kb region and following a report that three of 50 subjects with sporadic AVSD had a *CRELD1* missense substitution, *CRELD1* was proposed as a candidate 3p25 CHD gene (Robinson et al., 2003). However, *CRELD1* maps outside the 3p- CHD target intervals identified by both Green et al., (2000) and Malmgren et al., (2007) and in a previous study from Birmingham there was no evidence of pathogenic *CRELD1* mutations in 49 sporadic AVSD cases (Zatyka et al., 2005). A number of genes have been implicated in the pathogenesis of mental retardation associated with 3p- syndrome including: *CHL1(CALL)* (at 213 kb from p-telomere), *ITPR1* (4,700 kb), and *SRGAP3* (9,000 kb) (Angeloni et al., 1999; Endris et al., 2002; Higgins et al., 2004). In addition, Fernandez et al., (2004) reported a balanced t(3;10)(p26;q26) translocation associated developmental delay (full scale IQ of 73) and some features of 3p deletion syndrome (short stature, downslanting palpebral fissures and ptosis) that disrupted *CNTN4*.

3.2 Materials and methods

3.2.1 Patients

Sixteen cases of 3p25-p26 deletion were studied. The clinical details of 10 patients were reported previously (Green et al., 2000; Zatyka et al., 2005). Four of these cases (P1, P2 and P4, P5) had a congenital heart defect and all had mental retardation. Three of the four new cases (P13, P14, and P15) showed characteristic features of 3p- syndrome (microcephaly, developmental delay, mental retardation, ptosis, micrognathia) and in addition P15 also had congenital heart disease (AVSD). One patient, P16, was ascertained

incidentally via recurrent miscarriages and did not show any features of 3p- syndrome (in particular there was no evidence of mental retardation). Following the publication of Shuib et al (2009), two further cases were ascertained (P17 and P18). P17 had an unbalanced 3,7 translocation (karyotype 46,XX,der(3)t(3;7)(p25.3;p21.3)). P18 was presented with a tetralogy of fallot and has abnormal karyotype 47,XXY add(3)p25.3.ish add(3)(D3S4559)mat.

Information on clinical phenotype was obtained from the referring clinicians and hospital records. The studies were approved by the South Birmingham Research Ethics Committee and informed consent was obtained (from parents except for the one case without mental retardation).

3.2.2 Array analysis

250K Sty1 SNP mapping arrays were applied in 14 (P1-P16) cases and SNP 6.0 arrays in two cases, P17 and P18. The methods applied are described in detail in sections 2.1 and 2.2.

For 250K SNP arrays, genotypes were generated using the BRLMM algorithm using default settings. Copy number analysis was performed with Affymetrix Genotyping Console 2.0 (GTC v2.0) using the CNAT v4.0 algorithm. Deletion intervals were automatically called by Hidden Markov Model (HMM) generated Copy Number (CN) state intervals with genomic smoothing set at 100 kb. In addition to this automated calling estimate I also derived an estimate of the breakpoint by analyzing the unsmoothed Affymetrix genotyping console log2 ratios with the Nexus 3.1 copy number analysis software (Biodiscovery, El Segundo, CA). This utilizes a rank segmentation algorithm.

The deletion breakpoint estimates (approximated to the nearest 50 kb) from both analyses are presented but the discussion is based on the Nexus estimates.

The SNP Array 6.0 platform offers the genotype calling algorithm "Birdseed" to determine the genotypes of 909,622 SNPs (Affymetrix, Inc. http://www.affymetrix.com/index.affx). The Birdseed algorithm performs a multiple-chip analysis to estimate signal intensity for each allele of each SNP, fitting probe-specific effects to increase precision, and then makes genotype calls by fitting a Gaussian mixture model in the two-dimensional A-signal vs. B-signal space, using SNP-specific models to improve accuracy. In addition, this array also contains 945,826 copy number probes designed to interrogate CNVs in the genome; 115,000 of these probes interrogate previously identified CNVs while the remaining 831,000 are distributed across the genome for improved CNV detection (Affymetrix, Inc. http://www.affymetrix.com/index.affx). Copy number analysis was performed with Affymetrix Genotyping Console v3.0.2 (GTC v3.0.2)

3.2.3 MLPA analysis

MLPA was applied using a SALSA P016B VHL kits (MRCHolland, Amsterdam, The Netherlands) that contains specific probes to detect deletions of four genes: *FANCD2* (at 10043.1 kb from pter), *VHL* (10158.3 kb), *IRAK2* (10181.6 kb), and *GHRL* (10302.4 kb) on chromosome 3p25. The analysis was performed according to the manufacturer's instructions (for full details see section 2.3). The ligation products were amplified on a Tetrad thermal cycler (Peltier 225 from MJR). PCR products were then separated by capillary electrophoresis on a Beckman Coulter CEQ 8000 genetic analyser. Electropherograms were analysed using Beckman Coulter Fragment Analysis software all from Beckman Coulter. DNA dosage was estimated using an in house developed Excel

dosage calculator using peak heights. All results which fell outside of a predetermined dosage range were highlighted. Deletions were indicated by a relative dosage value of 0.5 and duplications by 1.5.

3.3 Results

3.3.1 Array analysis results and correlation with MLPA copy number analysis

The reference set for 250K Sty1 mapping arrays was 48 samples from the HapMap project (www.hapmap.org/downloads/raw_data/affy500k/) and 270 HapMap individuals of various populations for SNP 6.0 (Goldstein and Cavalleri, 2005). Six normal controls were used for MLPA. The average genotype call rate for the 14 samples of 250K Sty was 97.70±1.95% and 96.11±1.82 for the two samples of SNP6.0 (P17 and P18). Analysis of 3p copy number status on the 14 samples was performed with Affymetrix Genotyping Console v2.0 and Nexus 3.1 copy number analysis software (Table 3.1, figure 3.1 and figure 3.2) while Affymetrix Genotyping Console v3.0.2 was used for the two samples of SNP6.0 (figure 3.3). Microarray and the MLPA copy number analysis results were concordant (see table 3.1).

Table 3.1: Clinical and molecular cytogenetics features of 3p- syndrome patients studied

	Clinical features			Deletion size by Affymetrix Genotyping Console v2.0 or v3.0.2 (Mb)*	Deletion breakpoints by Nexus 3.1 copy number analysis software (El Segundo, CA)*	MLPA probes deleted	Deletion type
	Congenital heart disease	Mental retardation	Chrom. region affected				
P1	Yes	Yes	3p25.2-pter	12.65	0-12.55	FANCD2,VHL, IRAK2,GHRL	terminal
P2	Yes	Yes	3p25.2-pter	12.25	0-12.20	FANCD2,VHL, IRAK2,GHRL	terminal
P4	Yes	Yes	3p25.2-pter	12.05	0-12.05	FANCD2,VHL, IRAK2,GHRL	terminal
P5	Yes	Yes	3p25.3-pter	11.35	0-11.30	FANCD2,VHL, IRAK2,GHRL	terminal
P6	No	Yes	3p25.3-pter	11.15	0-11.10	FANCD2,VHL, IRAK2,GHRL	terminal
P7	No	Yes	3p25.3-pter	11.10	0-11.05	FANCD2,VHL, IRAK2,GHRL	terminal
P8	No	Yes	3p25.3-pter	10.20	0-10.31	FANCD2,VHL, IRAK2,GHRL	terminal
P9	No	Yes	3p25.3-pter	9.95	0-10.01		terminal
P10	No	Yes	3p25.3-pter	9.55	0-9.50		terminal
P11	No	Yes	3p25.3-pter	9.60	0-9.55		terminal
P13	No	Yes	3p25.3-pter	10.90	0-10.90	FANCD2,VHL, IRAK2,GHRL	terminal
P14	No	Yes	3p25.3-p26.1	6.30	4.40-10.65	FANCD2,VHL, IRAK2,GHRL	interstitial
P15	Yes	Yes	3p25.3-pter	11.50	0-11.55	FANCD2,VHL, IRAK2,GHRL	terminal
P16	No	No	3p26.1-pter	8.60	0-8.55		terminal
P17	Yes	NA	3p26.1-pter	7.67	ND		terminal
P18	NA	NA	3p26.1-pter	8.53	ND		terminal

The size of the deleted region was estimated by Affymetrix Genotyping Console 2.0 (GTC v2.0) or GTCv3.0.2 using the CNAT v4.0 algorithm and Birdseed v1 algorithm respectively. In addition to this automated calling estimate, primary unsmoothed log 2 ratios of 250K Sty data were imported into Nexus 3.1 and analysed using the Rank Segmentation algorithm and estimates of the deletion breakpoints obtained.

Abreviations: pter, p terminal; Mb, megabase; ND, not done; NA, not available

*both the deletion size and Nexus deletion breakpoints were approximated to the nearest 50kb. MLPA results reported for probes at FANCD2 (at 10043.1 kb from pter), VHL (10158.3 kb), IRAK2 (10181.6 kb) and GHRL (10302.4 kb)

Figure 3.1: Mapping of the extent of deletions at chr 3p25-p26 in the 14 patients studied. Relative genomic locations of 3p deletions is shown using Nexus 3.1 software (El Segundo, CA), calculated from unsmoothed log2 ratios generated in Genotyping Console v2.0 using the Rank Segmentation algorithm with default settings. The consensus region of overlap is a 4.2 Mb region (shown as an aggregate bar at 100%) containing 7 HGNC mapped genes. The percentage penetrance for all cases within the area of analysis is illustrated by the solid red area. The open boxes and solid bars below the percentage penetrance represent genes within the area of analysis. The horizontal pink lines represent copy number variants within the area of analysis. The horizontal red lines at the bottom of the figure represent the extent of deletion within the area of analysis for each individual case. Please refer to table 3.1 for the genomic coordinates and deletion size for each individual case.

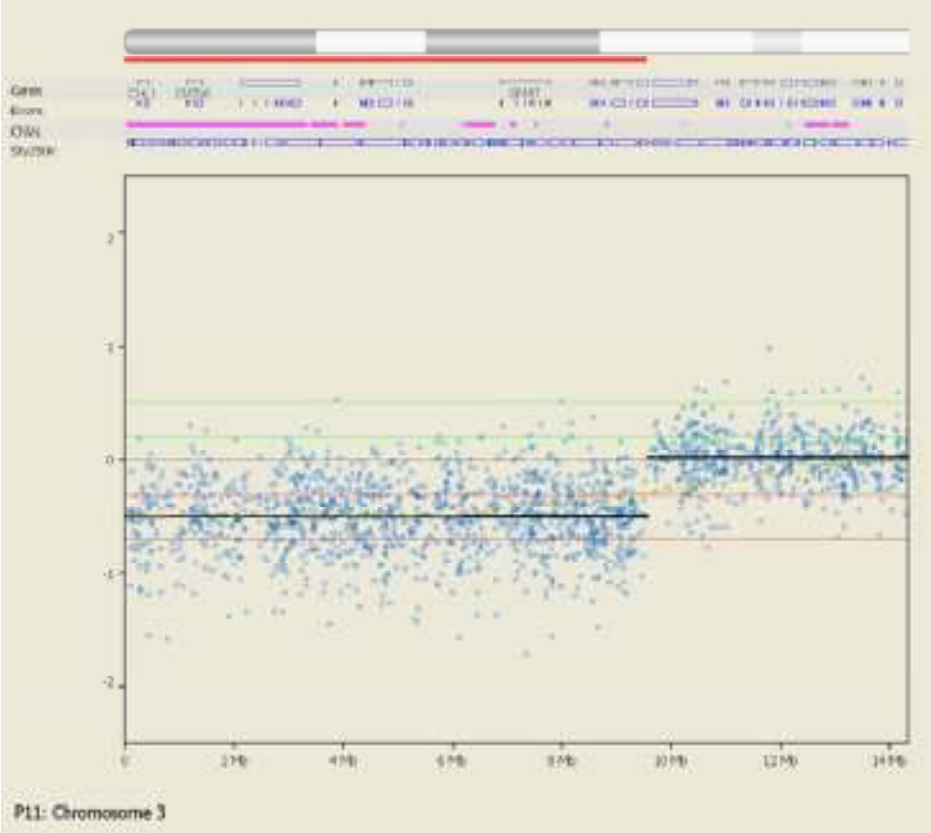

Figure 3.2: Sample P11 chromosome 3 unsmoothed log2 ratios imported into Nexus 3.1 and analysed using the Rank Segmentation algorithm. The horizontal red line at the bottom of the ideogram represents the extent of deletion within the area of analysis. Probe-level view of the focused chromosome 3p25.3-pter array indicating the boundaries of the breakpoint in the 3p25.3-pter is shown in the lower panel. Blue dots depict single SNP signal intensity while horizontal black segmentation bar present an average value of SNP signal intensity. The deletion 3p25.3-pter is observed as a reduction in copy number (-0.5=heterozygous deletion, 0= diploid DNA copy number) as denoted by the black segmentation bar. The proximal breakpoint denoted by the black segmentation bar is called at 9.56 Mb.

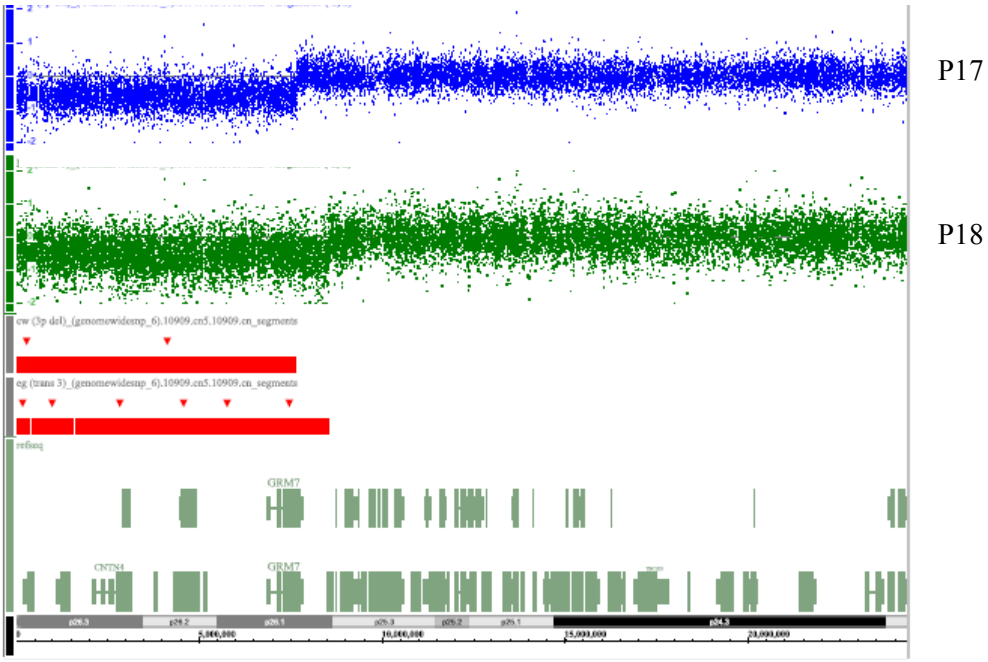

Figure 3.3: Sample P17 (upper panel) and P18 (lower panel) chromosome 3 log2 ratio analysed using the Birdseed v1 algorithm for SNP 6.0 arrays. Blue and green dots depict single SNP signal intensity in P17 and P18 respectively. The horizontal red bars represent the extent of deletion within the area of analysis for each individual case. The proximal breakpoint in P17 and P18 is called at 7.67 Mb and 8.53 Mb respectively. Ideogram of chromosome and genes within the area of analysis are displayed at the bottom of the figure.

3.3.2 Array-based 3p25-p26 deletion analysis and genotype–phenotype correlations

Deletions ranged from ~6.3 Mb (P14) to 12.65 Mb (P1) (see Table 3.1). Fifteen of 16 deletions were terminal and the only interstitial deletion (P14) was also the smallest. No clear breakpoint hotspots were detected. Ten patients (P1–P8 and P13–P15) were hemizygous for *VHL*, however to date none of these children have yet been reported to have features of von Hippel–Lindau disease. Array based analysis refined the 3p deletion breakpoints in the four previously reported patients with *CHD* to between 11.3 and 12.55 Mb. In addition, a new 3p- syndrome patient (P15) with *CHD* was investigated and found to have a terminal deletion with a breakpoint at 11.55 Mb. The most centromeric breakpoint in the nine patients without *CHD* (P6–P14) was ~11.1 Mb and thus there was

an ~200 kb interval in the breakpoints between P5 and P6 (with and without *CHD* respectively). All but one of the 16 patients with cytogenetically visible distal 3p deletions for whom detailed psychomotor status was available had psychomotor retardation.

The exception (P16) had the smallest terminal deletion with a breakpoint at ~8.6 Mb from pter. The smallest terminal deletion associated with psychomotor delay was detected in P10 and this suggested that the critical interval for mental retardation associated with distal 3p deletions was ~950 kb interval between the breakpoints in P16 and P10. This interval was deleted in the one patient with an interstitial deletion (P14) who also had developmental delay.

3.4 Discussion

This is the first report of high resolution (~238,000 probes, mean inter-probe distance within ~12.0 kb for 14 patients and more than 1.8 million markers, mean inter-probe distance within 680 bases for 2 patients) array-based analysis of a cohort of distal 3p deletion syndrome patients. The results of 14 patients have been published (Shuib et al., 2009). Previously Affymetrix 250K oligonucleotide arrays have been used successfully to map constitutional deletions (Ballif et al., 2007; Kirov et al., 2008) and the results of MLPA and array analyses were concordant in this study. The SNP6.0 arrays have been applied for studies of common diseases such as diabetes and heart disease (McPherson et al., 2007; Saxena et al., 2007; Zeggini et al., 2007), detection of UPD and characterisation of chromosome breakpoint in chronic lymphocytic leukemia (Hagenkord et al., 2010) and identification of copy number alterations and LOH in tumours (Gorringe et al., 2009; Greenman et al., 2010). The arrays were also successfully applied on fresh frozen tissue (Tuefferd et al., 2008) as well as archived samples (Tuefferd et al., 2008; Bucasas et al., 2009).

The majority of distal 3p deletions are terminal deletions and only one interstitial deletion was detected. Although a patient analysed by Dijkhuizen et al., (2006) had a complex 3p abnormality in which an ~4 Mb distal deletion was accompanied by a more proximal duplication, all of the patients in my study appeared to have ‘‘pure’’ deletions. In contrast to disorders such as Jacobsen syndrome (Tunnacliffe et al., 1999; Jones et al., 2000), there was no close clustering of terminal deletion breakpoints (although the breakpoints in P6 and P7 mapped within an ~50 kb interval) in my study.

I found that the candidate interval for a 3p25 CHD susceptibility locus mapped to an ~200 kb interval. Two known genes contained in the region are *HRH1* and *ATG7*. The histamine receptor H1 (*HRH1*) gene encodes a G protein-coupled receptor that mediates diverse neuronal and peripheral actions of histamine. The H1 receptor is expressed by various peripheral tissues, such as smooth muscle, and by neurons in the brain, where histamine may be involved in the control of wakefulness, mood, and hormone secretion. ATG7/APG7L is the human homolog of yeast Apg7, an ubiquitin-activating enzyme E1-like protein essential for the Apg12 conjugation system that mediates membrane fusion in autophagy (Tanida et al., 2001). To date neither of these genes has been linked to cardiovascular development and several known genes such as *ATP2B2, FBLN2, TIMP4,* and *SEC13R*, which are expressed in the heart, were shown to map outside the target interval. Potential complicating factors in the mapping of a 3p25 CHD locus using 3p deletions include (a) that some patients with more telomeric deletions might be non-penetrant and (b) that genes that are outside of the CHD critical interval might have altered expression as a result of deleted regulatory regions. The latter possibility is difficult to exclude since regulatory regions may exert long-range influences over gene expression (Crolla and Van Heyningen, 2002; Velagaleti et al., 2005). Although *CRELD1* has been suggested as a 3p25 AVSD susceptibility locus (Robinson et al., 2003), it maps ~1Mb distal to the ~200kb target interval that I found and *CRELD1* was deleted in four patients without CHD (Zatyka et al., 2005). Although such cases might be non-penetrant, to date all 3p- patients with CHD have had the most centromeric breakpoints and so there is no direct evidence for non-penetrance (although this possibility cannot be exclude formally) (Malmgren et al., 2007). Analysis of further 3p- patients with and without CHD would be helpful in confirming this interpretation.

Another potential strategy for identifying the precise 3p25 AVSD gene would be to undertake mutation analysis of candidate genes in sporadic AVSD cases. Similar studies of *CRELD1* identified missense substitutions (not present in >200 control chromosomes) in ~4% of sporadic AVSD patients (Robinson et al., 2003; Zatyka et al., 2005). However the relevance of these rare substitutions to AVSD pathogenesis is unclear. One intriguing possibility is that CHD in 3p- cases might result from deletion of two genes (e.g. *CRELD1* and a gene within the more centromeric target interval). Such a model, although consistent with the 3p deletion mapping data would imply that a single mutation in either gene would not be sufficient to cause AVSD and so analysis of sporadic AVSD cases would not unequivocally identify a single 3p25 AVSD susceptibility gene.

Previously a number of genes (e.g., *CHL1 (CALL), CNTN4, LRRN1, SRGAP3/MEGAP,* and *ITPR1*) have been suggested to be responsible for psychomotor retardation in 3p- syndrome. In addition, a locus for non-syndromic autosomal recessive mental retardation (MRTA-OMIM 607417) was mapped to 4.2 Mb in 3p26.3-p26.1 between loci D3S3630 and D3S1304 containing nine known genes (Higgins et al., 2004). Although most patients with a cytogenetically visible 3p deletion have psychomotor retardation, a few rare individuals with normal intelligence have been described (Knight et al., 1995; Endris et al., 2002; Takagishi et al., 2006).

P16 is a phenotypically normal patient with a terminal deletion of ~8.6 Mb. The deleted region contains 16 known genes which included *ITPR1, CNTN4, CHL1, LRRN1, SETMAR, IL5RA,* and *TRNT1*. Takagishi et al (2006) reported a mother and daughter with a cytogenetically visible deletion of 3pter. The mother showed only a mild phenotype (simple-formed ears, a high arched palate, fourth and fifth toe clinodactyly, and a history

of moderate scoliosis) while, at age 15 months, the daughter had mild hypotonia and joint laxity, fourth and fifth toe clinodactyly but no developmental delay. A terminal deletion with a breakpoint between ~8.65 and 10.16 Mb was detected. Patients P1-P15 had marked intellectual disability and so, assuming the most parsimonious explanation of complete penetrance for deletion of a psychomotor retardation gene, candidate genes for terminal 3p- associated mental retardation should map centromeric to the P16 deletion breakpoint (~8.6 Mb) and telomeric to the breakpoint in P10. *SRGAP3(MEGAP)* (a GTPase-activating protein that acts towards Rac1 and Cdc42 in vitro and in vivo and regulates cell migration by affecting actin and microtubule cytoskeleton dynamics (Yang et al., 2006), maps ~9Mb from the telomere and so is retained in P16 and is possibly retained in the family reported by Takagishi et al (2006). Endris et al (2002) reported that *SRGAP3* was disrupted in a patient with a constitutional translocation associated with hypotonia and severe mental retardation and *SRGAP3* was deleted in all our patients with mental retardation and the three patients reported by Malmgren et al (2007). Two patients further with a relatively mild phenotype have also been reported. Thus Shrimpton et al (2006) described an unbalanced der(3)t(3;8)(p26;q24.3) translocation associated with a terminal 3p deletion and 8q duplication in a boy with a mild cognitive deficit (IQ score of 97). The 3p deletion breakpoint mapped distal to *SRGAP3* (between 6.89 and 8.16 Mb). Rivera et al., (2006) reported a 3p26 to 3pter deletion in a 14-year old boy with a full scale IQ of 95 but an unusual cognitive and behavioral profile. However the deletion has not been characterized in detail.

The findings of my study are consistent with the hypothesis that *SRGAP3 (MEGAP)* is a prime candidate for 3p- syndrome psychomotor retardation. A number of genes previously implicated in 3p- associated mental retardation are deleted in P16 and the family of

Takagishi et al (2006) (*CHL1/CALL* at 2.14 Mb, *CNTN4* at 3.06 Mb, *LRRN1* at 3.86 Mb, and *ITPR1* at 4.51Mb). Of these candidate genes the most convincing case has been made for *CNTN4* (contactin 4) that encodes a GPI-anchored neuronal membrane protein that functions as a cell adhesion molecule. Dijkhuizen et al (2006) reported a patient with severe mental retardation (IQ score 30), upslanted palpebral fissures, a small nose with a short philtrum, macrostomia with prominent everted lips, small cup-shaped ears and small hands (metacarpal and phalanges lengths were particularly small). Array-CGH demonstrated a complex rearrangement with a 4.0-Mb deletion (3p26.2-3pter), 1.3-Mb amplification (3p26.1-3p26.2) and 6.0-Mb duplication (3p25.3-3p26.1) (all on the same chromosome 3 homologue), *CNTN4* and *CRBN* were deleted and duplicated in this patient and it is difficult to evaluate detailed genotype–phenotype correlations in this case. Although Cargile et al (2002) reported on a child with features of 3p- syndrome (ptosis, microcephaly, growth retardation, and developmental delay) and an interstitial deletion mapping somewhere betweenD3S3630 (at 2.67Mb) and D3S1304Mb (at 6.89Mb) the deletion was characterized by FISH studies and it is possible that a high resolution microarray analysis might have discovered additional abnormalities. Fernandez et al (2004) reported a balanced t(3;10)(p26;q26) translocation associated with borderline intellectual disability (full scaleIQ of 73) and some features of 3p- syndrome (short stature, downslanting palpebral fissures and ptosis) that mapped within the first intron of *CNTN4* and was predicted to disrupt the 5' UTR of the mature mRNA of one of three of *CNTN4* isoforms that is highly expressed in human brain leading to the suggestion that deletion of *CNTN4* was causally associated with the pathogenesis of the 3p- syndrome phenotype. However this conclusion is at odds with our results and those of Takagishi et al (2006). In addition, Roohi et al (2009) reported on two patients with autistic spectrum disorder with germline deletions involving *CNTN4*. Neither demonstrated phenotypic features of a 3p-

syndrome and the copy number variant was inherited from a normal phenotype father. This could suggest that loss of *CNTN4* is not sufficient to cause a 3p- syndrome phenotype but, in combination with other autistic susceptibility alleles, could contribute to autistic spectrum disorder. If this hypothesis is correct, then the translocation reported by Fernandez et al (2004) may have been associated with a 3p- phenotype because of position effects of the translocation on other genes, unmasking of recessive alleles or through an oligogenic effect whereby the phenotypic effects of loss of *CNTN4* depended on loci outside of 3p25-p26.

In summary, currently most evidence is in favour of *SRGAP3* being the major determinant of mental retardation in 3p- syndrome. However, the interpretation of genotype–phenotype studies for distal 3p deletions is complex (Barber, 2008), and analysis of such cases on genome-wide high density arrays will provide better characterisation of the deletions in individual cases and exclude the possibility of coexistent unrecognised copy number abnormalities.

4 Cytogenetics and molecular genetic analysis of Beckwith-Wiedemann syndrome (BWS)

4.1 Introduction

Most genes are expressed equally from the paternal and maternal alleles ie. biallelic gene expression is the usual physiological state. However, a minority of genes, probably numbering about 100 in humans and in mice are imprinted genes and show differences in expression according to the parental origin of the allele. This parent-of-origin genomic imprinting phenomenon is heritable at a cellular level and, when complete, only one of the alleles is expressed ie. monoallelic gene expression. Imprinted genes often have a critical role in prenatal growth and development (Charalambous et al., 2007). The process of genomic imprinting is initiated during the formation of germ cells. Thus imprints are erased and re-established based on the sex of the transmitting parent (Barlow, 1994). The establishment and maintenance of genomic imprinting involves a number of epigenetic mechanisms including differential DNA methylation, allele-specific RNA transcription, antisense transcripts, histone modifications as well as differences in replication timing (Weksberg et al., 2003).

The first evidence for genomic imprinting was provided by classical mouse experiments using the technique of pronuclear transplantation (McGrath and Solter, 1984). Mouse embryos that were diploid but with the nuclear material derived solely from the maternal (gynogenetic) or paternal (androgenetic) genomes were created but failed to develop post-implantation. In gynogenotes, development of the extraembryonic tissues was poor although the embryo was present. In contrast, embryonic development in androgenotes was considerably retarded but substantial growth of the trophoblast and yolk sac was

evident (McGrath and Solter, 1984; Barton et al., 1984). These experiments demonstrated that diploidy alone is not sufficient for normal embryonic development and the presence of both of maternal and paternal genomes is required. In addition, they also showed that the maternal genome appears to be biased towards fetal development whereas the paternal genome contributes more towards the development of extra embryonic structures (McGrath and Solter, 1984). Evidence for the differential contribution of maternal and paternal genomes is also clearly demonstrated by the reciprocal phenotypes observed in ovarian teratomas and complete hydatidiform moles in humans. These occurred from parthenogenotes and androgenotes, respectively. Ovarian teratomas are composed of a disorganised mass of differentiated embryonic tissues but do not contain any placental tissue (Linder et al., 1975). Complete hydatidiform moles are characterised by extensive growth of the trophoblast in the absence of an embryo (Kajii and Ohama, 1977).

Imprinted genes are members of several gene families and encode gene products involved in a diversity of physiological processes, many of which are involved in growth control and development (Tycko and Morison, 2002). In mammals, they tend to occur in clusters in distinct regions on chromosomes which are referred as imprinted domains (Weksberg et al., 2005). These domains are characterized by regulatory systems known as imprinting centre which control expression of closely linked imprinted genes (Nicholls, 2000). Imprinting centres in these domains are characterized by the presence of differential methylation on the paternal and maternal chromosomes which result in differential *cis*-regulation and transcription of imprinted genes. This results in different epigenotypes on the maternal and paternal alleles. To date, >50 imprinted genes have been identified in the human genome (Morison et al., 1998; Morison et al., 2005; Glaser et al., 2006).

Imprinting is a normal mechanism of gene regulation. However, deregulation of imprinting is associated with genetic diseases, for example abnormalities in the imprinted domain on chromosome 15q11-q13 are associated with Prader-Willi and Angelman syndromes (Nicholls, 2000) and with the imprinted domains on chromosome 11p15 with the imprinting disorder Beckwith-Wiedemann syndrome (BWS), a variety of human cancers including Wilm's tumour and Silver-Russell syndrome (Reik and Maher, 1997; Tycko, 2000). A number of mechanisms may cause an imprinting disorder including a failure to establish a normal genomic imprinting epigenotype, uniparental disomy (UPD), gene mutations and chromosome rearrangements such as inversion, duplication, deletion and translocation can also give rise to the syndromes. Chromosomes 7 and 14 also contain imprinted genes and imprinting defects associated with UPD of the chromosomes have been confirmed to cause certain diseases in humans (table 4.1).

Table 4.1: Genetic diseases caused by imprinting effects in humans

Imprinted region	**Disease**	**References**
mUPD7	Silver-Russel syndrome	Kotzot et al, 1995;Eggermann et al,1997;Preece et al,1997
Segmental pUPD11p15.5	Beckwith-Wiedemann syndrome	Henry et al,1993;Henry et al,1991;Slatter et al,1994
mUPD14	MatUPD14 syndrome	Healey et al,1994;Sanlaville et al,2000
pUPD14	PatUPD14 syndrome	Cotter et al, 1997
mUPD15;chromosomal region 15q11-q13	Angelman syndrome	Malcolm et al,1991;Nicholls et al,1992
pUPD15; chromosomal region 15q11-q13	Prader-Willi syndrome	Nicholls et al,1989; Robinson et al,1991

The list of imprinted genes is regularly being updated and can be found at the University of Otago's Imprinted Gene Catalogue (http://igc.otago.ac.nz/home.html).

4.1.1 Clinical genetics of Beckwith-Wiedemann syndrome (BWS)

Beckwith-Wiedemann syndrome (BWS; MIM 130650) is a paediatric overgrowth disorder involving a predisposition to tumour development with an estimated incidence of 1 in 13,700 livebirths (Junien, 1992). It was first described by Beckwith in 1963 and Wiedemann in 1964 on children with features of exomphalos, macroglossia and gigantism. BWS is a prototypic imprinting disorder resulting from mutations or epimutations in genes from the imprinted cluster at chromosome 11p15.5 (Reik and Maher, 1997). Chromosome 11p15.5 was first implicated by the finding of paternally derived duplications of 11p15.5 in BWS patients (Turleau et al., 1984; Brown et al., 1992; Nystrom et al., 1992; Slavotinek et al., 1997). Subsequently, maternally inherited balanced rearrangements of 11p15 were also demonstrated to be associated with BWS (Norman et al., 1992; Tommerup et al., 1993). The finding of chromosome 11 paternal uniparental disomy in a subset of sporadic BWS patients provided further evidence that BWS is an imprinting disorder (Henry et al., 1991; Slatter et al., 1994).

The penetrance and clinical presentation of BWS is highly variable but most frequently it is characterized by pre- and postnatal overgrowth, macroglossia and anterior abdominal wall defects (omphalocoele, umbilical hernia and diastasis recti). Additional features include visceromegaly (particularly kidneys, liver and pancreas), hypoglycaemia, hemihyperplasia, genitourinary abnormalities and embryonal tumours which occur in 5% of patients (most frequently, Wilm's tumour) (Engel et al., 2000). Other embryonal tumours include rhabdomyosarcoma, adrenocorticol carcinoma and neuroblastoma

(Sotelo-Avila et al., 1980; Pettenati et al., 1986; DeBaun et al., 1998; Lapunzina, 2005; Tan and Amor, 2006). Most of the tumours associated with BWS appear in the first 8-10 years of life with very few reported beyond this age (DeBaun et al., 1998; Tan and Amor, 2006). Clinical findings associated with higher risks of tumour development include hemihyperplasia, nephromegaly and nephrogenic rests (DeBaun et al., 1998; Coppes et al., 1999).

Three major groups of BWS are distinguished: sporadic (about 85%), familial (about 15%) and those with chromosome abnormalities (about 2%) (Slatter et al., 1994; Reik and Maher, 1997; Maher and Reik, 2000). The majority of BWS cases are sporadic with ~20% of these having paternal isodisomy which always includes the 11p15.5 imprinted gene cluster (Henry, 1991; Slatter, 1994; Catchpoole et al., 1997). Segmental UPD arises from post-zygotic somatic recombination event and therefore has a mosaic distribution (Cooper et al., 2007).

The majority of familial and sporadic cases show no cytogenetic abnormality but about 2% of cases involve duplications, inversions, and translocations affecting distal 11p. Duplications are invariably derived from paternal whereas inversions and translocations always involve the maternal homologue (Maher and Reik, 2000). Based on the maternally inherited rearrangements in BWS, three distinct breakpoint cluster regions (*BWSCRs*) have been identified (figure 4.1).

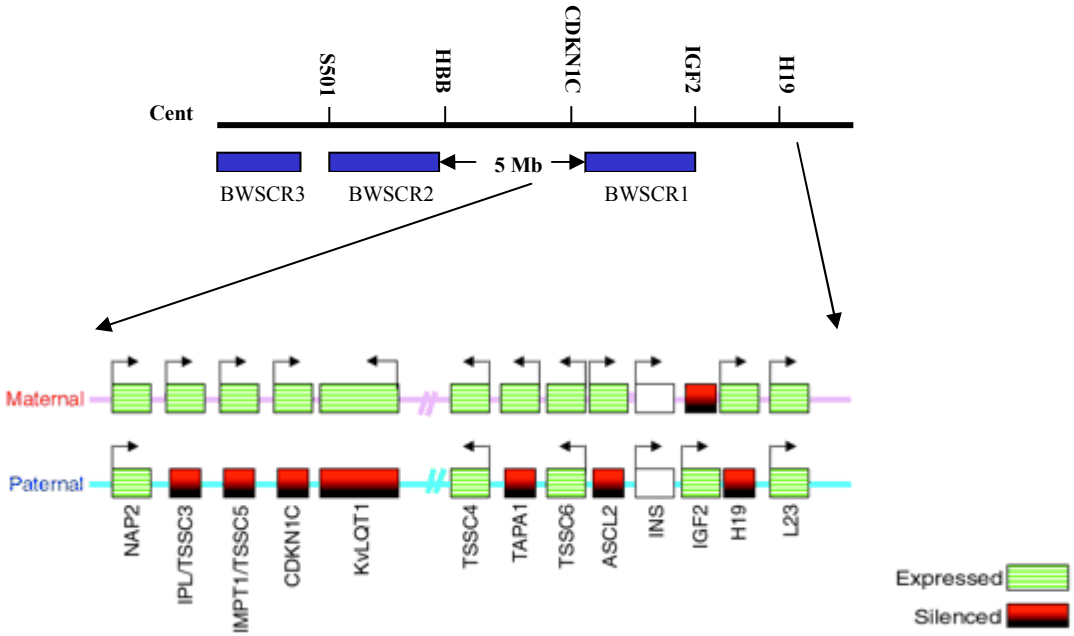

Figure 4.1: The imprinting cluster on human chromosome 11p15.5. The distal breakpoint cluster region (BWSCR1) is indicated. Breakpoints within BWSCR1 disrupt *KvLQT1*. Solid red symbols indicate allelic silencing; green/white symbols indicate allelic transcription. (Adapted from: Maher and Reik, 2000)

The most frequent of these is *BWSCR1* which map at 200-300 kb proximal to *IGF2* (Hoovers et al., 1995). *BWSCR1* is in the centre of a region that contains multiple imprinted genes including *IGF2, H19, CDKN1C* (also known as $p57^{kip2}$), *ASCL2* (also known as *HASH2*), and *KCNQ1* (also known as *KVLQT1*). All breakpoints in *BWSCR1* disrupt the imprinted *KCNQ1* gene which is maternally expressed (Lee et al., 1997b). However, in at least two patients, loss of imprinting (LOI) of *IGF2* has also been shown to associated with a *BWSCR1* breakpoint (Brown et al., 1996; Smilinich et al., 1999). The less frequent breakpoint cluster regions, *BWSCR2* and *BWSCR3* map respectively, 5 Mb and 7 Mb centromeric to *BWSCR1* (Redeker et al., 1995). *BWSCR2* is defined by two breakpoints and maybe associated with a distinct phenoytype (Alders et al., 2000). In a

study of two BWS patients, Alders et al (2000) have isolated cDNAs encoding 2 zinc finger genes, *ZNF214* and *ZNF215* in the *BWSCR2*. *ZNF215* gene is imprinted in a tissue-specific manner whereas *ZNF214* is not imprinted. Two of the five alternatively spliced *ZNF215* transcripts are disrupted by both *BWSCR2* breakpoints. Parts of the 3-prime end of these splice forms are transcribed from the antisense strands of *ZNF214*. These data supported a role for *ZNF215* and possibly *ZNF214* in the aetiology of BWS.

4.1.2 BWS candidate genes in chromosome 11p15.5

Sex bias in the transmission of BWS in families whereby the clinical features are passed on from mother to offspring two to three times more frequently than from father to offspring, the finding of UPD in BWS patients, and the sex bias in the chromosome anomalies associated with BWS (the duplications of 11p are always paternal and the balanced translocations and inversions are maternal) led to the hypothesis that the responsible gene(s) is imprinted (Niikawa et al., 1986; Elliott et al., 1994).

A number of imprinted genes in 11p15.5 have been implicated in the aetiology of BWS including the paternally expressed (maternally imprinted) *IGF2, KCNQ1OT1 (LIT1)* genes and the maternally expressed (paternally imprinted) *H19* and *CDKN1C (p57^{kip2})* genes (Engel et al., 2000).

The association of *IGF2* with BWS was demonstrated by Weksberg et al (1993). Control skin fibroblasts were shown to maintain monoallelic expression of paternal *IGF2* but skin fibroblasts from 3 out of 5 patients of BWS demonstrated biallelic *IGF2* expression. Their study has led to a conclusion that biallelic expression reflects disruption of *IGF2* imprinting and BWS can result from the loss of normal suppression of the maternally

inherited *IGF2* gene. Biallelic expression of the gene was also detected in tumours including Wilm's tumour (Ogawa et al., 1993; Rainier et al., 1993). *IGF2* encodes a fetal growth factor and overgrowth in BWS is restricted to tissues in which *IGF2* is expressed.

H19 is a gene encoding a biologically active non-translated RNA that may function as tumour suppressor (Hao et al, 1993). The imprinted region at 11p15.5 includes regions that are differentially methylated between the parental genomes. The *H19* differentially methylated region (DMR; located at 1.98 Mb) is paternally methylated and in the methylated state is proposed to promote the expression of *IGF2* (Cui et al., 2001).

KCNQ1OT1 is a non-coding RNA with antisense transcription to *KCNQ1*. The promoter for *KCNQ1OT1* is located in intron 10 of *KCNQ1*. The 5' end of this imprinted transcript overlaps with the differentially methylated imprinting centre for Domain 2 (IC2) or *KvDMR* (as it was originally called for 'KvLQT1 DMR') (Lee et al., 1999; Smilinch et al., 1999). Normally the maternal allele of ICR2 is methylated and *KCNQ1OT1* is silenced and the paternal allele is unmethylated allowing transcription of the *KCNQ1OT1* transcript (Lee et al., 1999b; Smilinich et al., 1999). Maternal methylation at the *KvDMR1* is thought to prevent transcription of the *KCNQ1OT1* gene and enable expression of *KCNQ1* and *CDKN1C* (Smilinich et al., 1999; Lee et al., 1999; Horike et al., 2000; Fitzpatrick et al., 2002; Diaz-Meyer et al., 2003).

CDKN1C is a member of the cyclin dependent kinase inhibitor and encodes a protein known as $p57^{kip2}$ (Bhuiyan et al., 1999). The protein is involved in the negative regulation of the cell cycle (Lee et al., 1995; Matsuoka et al., 1995) and is critical during mouse embryogenesis (Zhang et al., 1997; Yan et al., 1997). In human, *CDKN1C* is imprinted and primarily expressed from the maternal allele, though some expression (5–30%) is observed

from the paternal chromosome (Chung et al., 1996; Hatada et al., 1996). Other imprinted genes including *TSSC3* and *IMPT1* were both hypothesized to have negative growth regulatory functions and are thought to be regulated by ICR2 (Fitzpatrick et al., 2002).

4.1.3 Epigenetics, genetics and cytogenetic basis of BWS

4.1.3.1 Genomic imprinting of 11p15

The genetics of BWS are complex, but all causes to date are associated with alterations in the expression or function of one or more imprinted genes in the 11p15.5 imprinted gene cluster (Maher and Reik, 2000). Up to 60% of sporadic cases are due to epigenetic mutations involving two imprinting centres (ICs), IC1 and IC2. Both of the ICs regulate the expression of the imprinted genes on 11p15 over a long distance (Weksberg et al., 2003; Murrell et al., 2004).

IC1 controls the imprinting of the *H19* and *IGF2* genes (Bell and Felsenfeld, 2000; Hark et al., 2000) while IC2 controls the imprinting of *KCNQ1, CDKN1C, ASCL2, PHLDA2, TSSC4* and *SLC22A1L* (figure 4.2) (Smilinich et al., 1999; Lee et al., 1999; Maher and Reik, 2000).

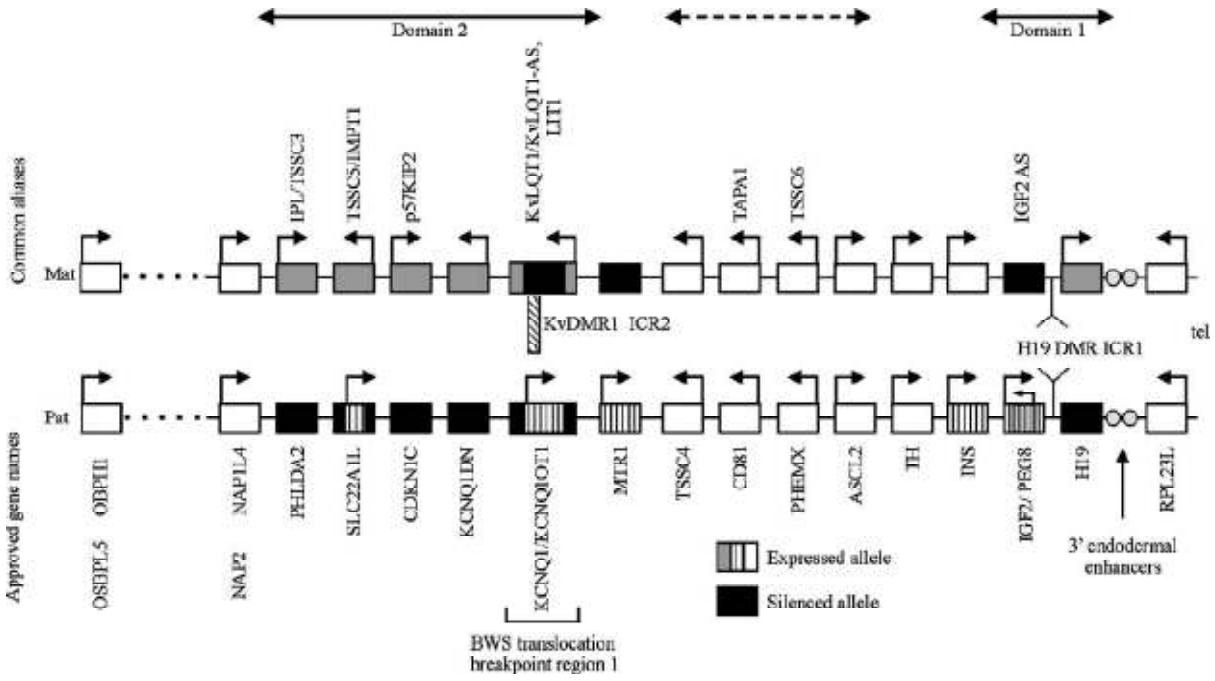

Figure 4.2: The cluster of imprinted genes on human chromosome 11p15.5. The maternal (Mat) and paternal (Pat) chromosomes are shown. The silenced allele is shown as a black box and the expressed alleles are shown as vertically striped boxes or white or grey boxes. The horizontal arrows indicate the direction of transcription. The diagonally striped box indicates the location of the CpG island that is studied here and is differentially maternally methylated (KvDMR1 or ICR2). The H19 DMR (ICR1) along with the 3' enhancers (circles) are indicated. Some genes (e.g., TSSC4, TAPA1, ASCL2, NAP1L4, and OSBPL5) are imprinted in mouse but not human. MTR1 is imprinted in human but not mouse. The dashed lines between NAP1L4 and OSBPL5 indicate the presence of intervening non-imprinted genes. Domains 1 and 2, indicated by the horizontal arrows at the top of the figure, are controlled by ICR1 and ICR2, respectively. The dashed arrow indicates that Domain 2 in mouse extends further to the right. (Adapted from: Minjie Du et al., 2003)

IC1 (or ICR1) consists of a differentially methylated region (DMR1) positioned upstream of *H19* and containing target sites for the insulator protein CTCF, which regulates access to the same enhancers of the two reciprocally imprinted genes *H19* and *IGF2* (Bell and Felsenfeld, 2000). Methylation on the paternal allele prevents CTCF from binding DMR1, permitting expression of *IGF2* and silencing of *H19*. On the unmethylated maternal allele, insulator protein binding prevents *IGF2* promoters interacting with the enhancers downstream of *H19* (Bell and Felsenfeld 2000; Lewis and Murrell, 2004), thus *IGF2* is silenced and *H19* is expressed. This region is known as domain 1 (figure 4.2).

Gain of methylation at the maternal *H19* and IC1 is associated with loss of *H19* expression and biallelic *IGF2* expression (Joyce et al., 1997). This alteration is called *H19*-dependent *IGF2* biallelic expression and is seen in approximately 5–10% of sporadic BWS cases (Catchpoole et al., 1997; Weksberg et al., 2001). Gain of methylation is almost always seen in sporadic cases without family history. However, three families with clinical features of BWS have also been reported to carry heritable DNA sequence abnormalities in IC1 that can disrupt imprint regulation in domain 1 (Sparago et al., 2004; Prawitt et al., 2005). Another alteration is referred to as H*19*-independent biallelic expression and can be found in many cases of BWS as well as in isolated Wilm's tumour. This alteration, first observed by Brown et al (1996) involved biallelic *IGF2* expression accompanied by monoallelic *H19* expression. BWS cases with this alteration show normal methylation and expression of *H19* from the maternal allele with biallelic *IGF2* expression (Weksberg et al., 2001).

IC2 (or ICR2) is associated with a maternally methylated differentially methylated region (*KvDMR1*) and a paternally expressed untranslated RNA (*KCNQ1OT1* (*LIT1*)) (Smilinich et al., 1999). Loss of maternal methylation of IC2 is seen in 50%-60% of patients with sporadic BWS (Lee et al., 1999; Engel et al., 2000) and in these cases there is *KCNQ1OT1* loss of imprinting (biallelic *KCNQ1OT1* expression) reduced *CDKN1C* expression (Diaz-Meyer et al., 2003) and variable loss of imprinting (LOI) of *IGF2* (Lee et al., 1999). Deletion of the orthologous sequence in mice results in loss of imprint for several genes neighbouring *KCNQ1* suggesting that IC2 is critical for maintaining imprinted gene expression in domain 2 (Fitzpatrick et al., 2002).

4.1.3.2 Mutations in CDKN1C

There are however, cases of BWS which arise from germline mutations in *CDKN1C* which include missense and frameshift mutations (Hatada et al., 1996). It has been reported in 5%-10% of sporadic BWS (Hatada et al., 1996) and approximately 40% of BWS cases with positive family history (Lam et al., 1999). These cases provide evidence that, mutation in a single gene is sufficient to implicate the disease in some individuals with BWS.

4.1.3.3 11p15 segmental uniparental disomy (UPD)

Approximately 20-28% of patients with BWS have paternal UPD ie. two paternally derived copies of 11p15 and no maternal contribution for that region (Henry et al., 1991; Slatter and Elliott, 1994). The region of paternal UPD invariably includes the imprinted gene cluster at 11p15.5; however, the extent of isodisomy along chromosome 11 is variable (Catchpoole et al., 1997; Dutly et al., 1998). In a cohort of 52 children with BWS and UPD, it was found that all cases demonstrated mosaic paternal isodisomy, and *IGF2* and *H19* were included in the segment of UPD in all cases. While the extent of segmental disomy was variable, there was no evidence of clustering of the proximal UPD breakpoint. In most cases (92% of those informative) UPD did not involve 11q, but 4 patients demonstrated UPD for the whole of chromosome 11 (Cooper et al., 2007). The findings that all cases demonstrated mosaic paternal disomy implies that UPD arises post-zygotically as a result of a somatic recombination in early embryogenesis. A comparison of patients with BWS and UPD for chromosome 11 with BWS patients without UPD showed an increased incidence of hemihypertrophy (6/9 v 1/23) and a decreased incidence of exomphalos (0/9 v 13/23) (Elliott and Maher, 1994). Other studies have reported an

increased incidence of tumours in BWS patients with UPD (Henry et al., 1993; Schneid et al., 1993).

4.1.3.4 11p15 chromosome rearrangements

Cytogenetic abnormalities have been found in 2-3% of individuals with BWS (Elliott and Maher, 1994). Translocations and inversions are usually maternally inherited and are always balanced (Sait et al., 1994). Duplication of chromosomal region 11p13–p15 responsible for BWS most frequently results from unbalanced segregation of a paternal translocation (Slavotinek et al., 1997) but de novo duplications of the paternally derived 11p15 were also found (Slavotinek et al., 1997). The most common aberration is duplications involving chromosome 11p15.5 due to unbalanced segregation of a paternal translocation (most frequent) or paternal inversion or de novo (table 4.2). The clinical features in these patients are thought to be due to increased *IGF2* expression from the extra paternal copy (Mannens et al., 1994). Additional types of chromosome rearrangements in BWS are translocations, inversions and deletions. Balanced chromosome translocations or inversions in 11p can be transmitted from a phenotypically normal parent to their offspring who then develop BWS. The breakpoints of these translocations and inversions have been found to cluster in two regions, *BWSCR1*, a 450 kb 200-400 kb centromeric to the *IGF2* at 11p15.5 and *BWSCR2*, a 2000 kb region proximal to *BWSCR1* at 11p15.3-p15.4 which is subdivided into at least two regions (Weksberg et al., 1993; Mannens et al., 1994; Lee et al., 1997). With the advent of more sensitive and high resolution molecular methods, for example array CGH, microdeletions (Niemitz et al., 2004; Sparago et al., 2004; Prawitt et al., 2005) and microduplication (Algar et al., 2007) of 11p15 in BWS patients have been identified.

Table 4.2: Summary of published chromosome rearrangements in BWS

Reference	Chromosome rearrangement	Karyotype of proband	Cytogenetic anomaly
Falk et al., 1973	Pat translocation	46,XY,t(2q +pat)	Dup 11p
Bajolle et al., 1978	Pat translocation	46,XY,der(5),t(5;11) (pl5;pl4)pat	Dup 11pl5-pter
Turleau et al., 1984	Pat translocation	46,XY,-4,+der(4) t(4;11)(q33;pl4)pat	Dup 11pl4-pter
Journel et al., 1985	Pat translocation	46,XY,-18,+der(11;18), t(11;18)(p15.4;p11. 1)pat	Dup 11p15.4-pter
Wales et al., 1986	Pat translocation	46,XY,-5, +der(5), t(5;11)(p15;p15.1)pat	Dup 11p15.1 - pter
Okano et al., 1986	Pat translocation	46,XX,-4,+der(4), t(4;1 1)(q35;p13)pat	Dup 11p13-pter
Tonoki et al., 1991	Pat translocation	46,XX,-14,+der(l4)t(11;14)(p15.3;q32.3)	Dup 11p15.3-pter
Brown et al., 1992	Pat translocation	46,XY,der(5)t(5;11) (p15.2;p14)pat	Dup 11p14-pter
Drut et al., 1996	Pat translocation	46,XY,-10,+der(10) t(10;11)(q26;p15)	Dup 11p15-pter
Krajewska-Walasek et al., 1996	Pat translocation	46,XY,-21,+der(21)t(11;21)(p15.2;q22.3)pat	Dup 11p15.2 - pter
Slavotinek et al., 1997	Pat translocation	46,XY,der(5)t(5;11)(p15.3;p15.3)pat	Dup 11p15.3-pter
Fert-Ferrer et al, 2000	Pat translocation		Dup 11p15.5
Russo et al., 2006	Pat translocation		Dup 11p11.5
Delicado et al., 2005	Pat translocation	47,XX, inv (Y) (p11.2 q11.23), der(18)t (11;18) (p15.5;q23) pat. ish der(18) (D11S2071+, D18S1390-)	Dup 11p15.5-pter
Bliek et al., 2009	Pat translocation		Dup 11p15.5
Kubota et al., 1994	De novo translocation	46,X,-X,+der(X) t(X;11)(p22.l;p13)	Dup 11p13-pter
Waziri et al., 1983	pat inversion	46,XY,rec(11), dup(pl3-pl5),del(q23-q25)	Dup 11p13-p15.5
Rethore et al., 1980	De novo duplication	Trisomy l1p (excluding 11p13)	Dup 11p (excluding 11p13)
Waziri et al., 1983	De novo duplication		Dup 11p15
Turleau et al., 1984	De novo duplication		Dup 11p15
Estabrooks et al., 1989	Mat duplication	46,XX,dup(15)(q11.2-ql3)mat	Dup 15q11.2-q13
Han et al., 2006	Pat duplication		Dup 11p13-p15.5
Russo et al., 2006	Pat duplication		Dup 11p15.5
Algar et al., 2007	Pat micro duplication		Dup 11p15.5
Pueschel and	Mat	46,XX,t(11p;22q)	Breakpoint 11p

Padre-Mendoza, 1984	translocation		
Tommerup et al., 1993	Mat translocation	46,XX,t(9;11) (p11.2;p15.5)	Breakpoint 11p15.5
Weksberg et al., 1993	Mat translocation	46,XX,t(11;16)(p15.5;q12)	Breakpoint 11p15.5
Mannens et al., 1994	Mat translocation	46,XX,t(4;l1)(p15.2;p15.4)	Breakpoint 11p15.4
Hoovers et al., 1995	Mat translocation	46,XX,t(11;12) (pl5.5;q13.1)	Breakpoint 11p15.5
Hoovers et al., 1995	Mat translocation	46,XX,t(l0;11)(p13;p15.5)	Breakpoint 11p15.5
Newsham et al., 1995	Mat translocation	46,XX,t(11;16)(p15;q13)	Breakpoint 11p15
Norman et al., 1992	Mat inversion	46,XX,inv(11)(p11.2p15.5)	Breakpoint 11p15.5
Mannens et al., 1994	Mat inversion	46,XX,inv(l1)(p15.4;q22.3)	Breakpoint 11p15.4
Grundy et al., 1998	Pat translocation		Breakpoint 11p14
Alders et al., 2000	Mat translocation		Breakpoint 11p15.5
Alders et al., 2000	Mat translocation		Breakpoint 11p15.4
Squire et al., 2000	Mat translocation		Breakpoint 11p15
Haas et al., 1986	De novo deletion	46,XY,del(11)(p11.1p11.2)	Del 11p11.1-11.2
Schmutz, 1986	De novo deletion	46,XX,del(11)(p11p13)	Del 11p11-p13
Zollino et al., 2009	De novo deletion		Del 11p15
Niemitz et al., 2004	Mat microdeletion		Del 11p15.5
Niemitz et al., 2004	Pat microdeletion		Del 11p15.5
Sparago et al., 2004	Mat microdeletion		Del 11p15.5
Prawitt et al., 2005	Mat microdeletion		Del 11p15.5

Abbreviations: mat, maternal; pat, paternal; inv, inversion; del, deletion; der, derivative; dup, duplication; t, translocation.

4.1.4 Phenotype – genotype/epigenotype correlations

The clinical expression of BWS may differ between patients with different molecular mechanisms and also between patients similar molecular abnormalities (e.g. from different levels of mosaicism in patients with UPD) (Itoh et al., 2000). Hemihyperplasia is highly positively correlated with UPD 11p15 (Engel et al., 2000; DeBaun et al., 2002; Cooper et al., 2005). This most likely reflects the somatic mosaicism associated with the chromosome alteration. Alterations in IC2 and mutations in *CDKN1C* are positively correlated with exomphalos (omphalocoele) and, possibly, cleft palate (Lam et al., 1999; Bliek et al., 2001; Gaston et al., 2001; Li et al., 2001; Weksberg et al., 2001, Bliek et al., 2004). However, there was no association between germline *CDKN1C* mutations and risk of embryonal tumours (Lam et al., 1999). Patients with UPD 11p15 and those with *H19* hypermethylation have the highest tumour risks especially for Wilm's tumour. In contrast, patients with loss of methylation at *KvDMR1* (IC2) have a lower tumour risk, are apparently not at risk for Wilms tumour but are susceptible to non-Wilm's tumours including hepatoblastoma, rhabdomyosarcoma and gonadoblastoma (Weksberg et al., 2001, Bliek et al., 2004, Cooper et al., 2005). The only tumour reported in patients with mutation of *CDKN1C* is neuroblastoma (Lee et al., 1997; Gaston et al., 2001).

To define and characterise the region of chromosome 11p15 involved in Beckwith-Wiedemann syndrome (BWS), I have carried out a high resolution 250K SNP array analysis on seven patients and SNP6.0 array on one patient with features of BWS. Conventional and molecular cytogenetic techniques were also applied in two of the cases with chromosome rearrangements.

4.2 Materials and Methods

4.2.1 Patients

A total of eight BWS cases were studied which include two lymphoblast cell lines from patients BWSCA1 and BWSCA2 carrying the der(11)t(3;11)(q22;p15.4) and inv(11)(p15.4;q23.3) respectively and six genomic DNA samples from BWS patients. The DNA was extracted using standard methods and stored at -80^{o}C. The two cell lines were cultured following standard protocol as described below. The DNA from the two cell lines were extracted following manufacturer's (Qiagen, Germany) recommended procedure. The parents give consent for all diagnostic procedures.

4.2.2 Cell culture

500 ml RPMI 1640 medium (Gibco BRL, Grand Island, NY, USA) was added with 50 ml fetal bovine serum, 5 ml 200 mM L-Glutamine and 5 ml penicillin/streptomycin. The medium was warmed in 37°C water bath and the class II cabinet was switched on at least 15 minutes before starting. The inside of the cabinet was swab with 70% ethanol as well as all bottles that have been in the water bath before placing them in the cabinet. The frozen cell lines (BWSCA1 and BWSCA2) were thawed at 37°C as quickly as possible and placed in the cabinet. The cells (~1 ml) were then pipetted into a 25 cm^2 cell culture flasks. 9 ml of the warmed medium was slowly pipetted into the flasks and placed upright in the 37°C CO_2 incubator. The cells survival rate was checked the next day and the medium was replaced with fresh 10 ml medium and placed back in the incubator. The cells were checked every 3-4 days, healthy cultures should appear orange to yellow in colour. When the cells were already confluence, they were transferred to 50 ml sterile tubes and centrifuge at 2000 rpm for 10 minutes at room temperature. The excess medium was

siphoned out with serological pipette attached to the vacuum system. The cells were then harvested following standard procedure.

4.2.3 Chromosome analysis

Chromosome were stained with Giemsa and karyotyped. Twenty five metaphases were completely analysed. Karyotypes were described according to ISCN (1995).

4.2.4 Fluorescence *in situ* hybridisation (FISH)

Fluorescence *in situ* hybridisation (FISH) analysis was applied on both of the two cell lines to locate the breakpoints in chromosome 11p15. Bacterial artificial chromosome (BAC) clones spanning the region of breakpoint in chromosome 11p15.4-p15.5 were selected according to Ensemble Genome Browser (February 2007 release) (figure 4.3). The clones were obtained from Roswell Park Cancer Institute (RPCI, Buffalo NY, USA) and Bluegnome Limited (Cambridge, UK). For BWSCA1 cell line, eight BAC clones were used: RP11-295K3, RP11-847E17, RP4-608B4, RP11-38L8, RP11-774H09, RP11-699D10, RP11-211E17 and RP11-89D4. Ten BAC clones were applied on BWSCA2 cell lines which include RP11-295K3, RP5-1075F20, RP11-847E17, RP11-304P12, RP11-211E17, RP11-560B16, RP11-413N10, RP11-715M10, RP11-324J3 and RP11-89D4. The BAC probes purchased from Bluegnome include RP4-608B4, RP11-38L8, RP11-774H09, RP11-699D10, RP5-1075F20 were prelabelled with spectrum orange. The remaining of the RPCI BAC clones were labelled with Cy3-dUTP (Amersham Biosciences, USA) and the method is explained in detail in the next section. Telomeric probe for chromosome 11p (chr11:145,611-345,808) and centromeric probe for chromosome 11 (CEP11) (Vysis, USA) in spectrum green were used as controls. Chromosomes were then counterstained with 4'-6-Diamidino-2-phenylindole (DAPI) (Abbott Molecular, Illinois, USA).

Hybridized metaphase spreads were analysed using a fluorescence microscope (Olympus, USA) coupled to a CCD camera and FISHView EXPO 2.0 software (Applied Imaging, USA). Fifteen metaphase spreads were evaluated.

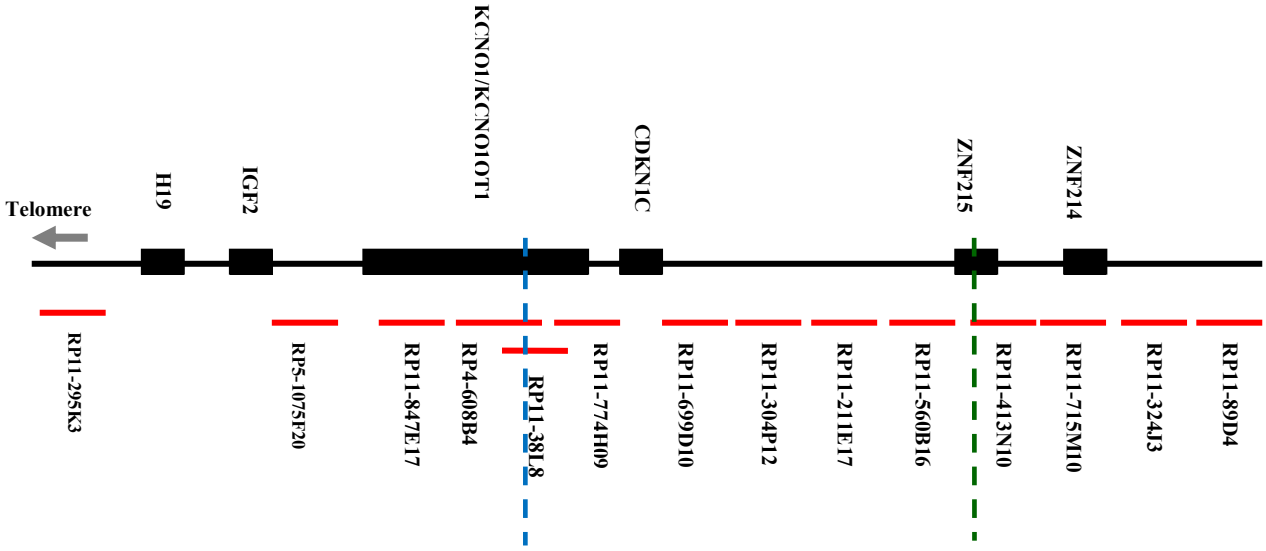

Figure 4.3: Imprinted gene map of chromosome 11p15.4-p15.5 and the localisation of the BAC clones applied in patients BWSCA1 and BWSCA2. The breakpoint in patient BWSCA1 and BWSCA2 is indicated by dashed blue line and dashed green line respectively.

4.2.4.1 Labeling of RPCI BAC probes with Cy3

Bioprime Labelling Kit (Invitrogen, USA) contains Klenow polymerase, 2.5X random primers and stop buffer (EDTA) and Cy3-dUTP (1mM) (Amersham Biosciences, USA) were used for BACs labelling. The DNA of the BAC clones was quantified using the NanoDrop 1000 spectrophotometer (Thermo Scientific, USA). The DNA was diluted to 1000ng/ul using molecular grade water. Dilution was made depending on the concentration of the stock BAC DNA. For BACs with a concentration of >2000ng/ul, 20 ul of 1000ng/ul DNA was made. For BACs with concentration <2000ng/ul, 10 ul of 1000ng/ul was prepared. The 1000ng/ul BAC DNA was then pre-denatured by incubating

at 98°C for 5 minutes. It was then left in ice until ready to use. The labelling master mix was prepared by adding these reagents in an eppendorf tube:

For 1 sample, 20 ul 2.5 X random primers
18.5 ul sterile water
1 ul Cy3
5 ul low-C dNTPs (refer appendix A3 for preparation)

The denatured BAC DNA was pulse spin and transferred 4 ul into the prepared master mix. The solution was then denatured in a hot block at 98°C for 5 minutes. It was then transferred immediately to ice and incubated for at least 5 minutes and then pulse spun. Klenow was taken out from the freezer, vortexed, spun and added 1ul to the solution. The solution was then vortexed, spun and incubated at 37°C overnight (16-18 hours) in a hot block covered with aluminium foil. The next day, the reaction was stopped by adding 5 ul of stop buffer, and then vortexed and pulse spun.

Autoseq G50 (GE Healthcare, USA) was vortexed with the column inverted. The bottom closure was snapped and the lid unscrewed and refits to the column ¼ turn. The column was placed in a collection tube, spun at room temperature (~22°C) at 2000g for 1 minute. The gel column was then transferred to a new 1.5 ml eppendorf tube. The screw lid and recovery tube was discard. The labelling reaction master mix was carefully loaded onto the centre of the gel bed. Then, it was loaded into the Beckman 22R centrifuge, orientating the column so that the gel face is away from the centre. It was spun at room temperature at 2000g for 1 minute. The used column was then discarded and the eppendorf tube containing the flow through was sealed. The measurement of dye incorporation was then made using the NanoDrop 1000 spectrophotometer (Thermo Scientific, USA). Ideally the

DNA BAC concentration is ≥100ng/ul and dye incorporation is ≥3 pmol/ul. The reaction can be stored in the -20°C freezer if not proceeding to the next step which is precipitation. Precipitation process was done in a low light to prevent fading of the fluorescent dye. The volume equivalent to 200ng of BAC was required in a precipitation. The volume was determined by using the formula:

Precipitation volume (200ng) = 200/labelled BAC concentration (ng/ul)

The reagents required per BAC were 5 ug of Cot-1 DNA (5 ul of 1 ug/ul stock), 1 ug of herring sperm DNA (1 ul of a 1/10 dilution of 10 ug/ul stock), appropriate amount of the BAC and the total volume of the precipitation should be topped up to 100 ul with sterile water (BAC volume + Cot-1 DNA + HS DNA + sterile water = 100 ul). The specified amounts of water, Cot-1 DNA, 1/10 HS dilution followed by BAC were pipetted in an eppendorf tube. 10 ul of 3M sodium acetate (retrieved from the fridge) followed by 200 ul 100% cold ethanol (retrieved from the freezer) was then added to the reaction and mixed gently by inverting the tube several times. The tube was then placed in a polystyrene box with elastic band on the lid and stored in the -80°C freezer for at least 30 minutes. Alternatively, it can be precipitated at -20°C for at least 2 hours or on dry ice for 15 minutes. The tube was then loaded in the centrifuge, hinge face outwards and centrifuged at 4°C for 30 minutes at full speed. The supernatant was discard and replaced with 200 ul of 70% ethanol to wash the pellet. The tube was inverted a few times and centrifuge again at full speed for another 10 minutes. The supernatant was discard. The tube was pulse spun and the excess ethanol was removed with a fine tip pipette. The pellet was air dried for 5 minutes.

Next, the BAC pellet was resuspended in 5 ul hybridisation buffer (Vysis Inc., USA). The type of the hybridisation buffer used depends on the type of control probe applied: Vysis LSI buffer with site specific control probe and Vysis CEP buffer if centromeric was used. The resuspended pellet was then incubated in the 73°C/75°C water bath for 1 minute, then vortexed and pulse spun. The step was repeated if the pellet was not completely dissolved. The dissolved BAC can be stored in -20°C freezer if not proceeding to the next step.

Before starting the hybridisation, the slide was incubated in the oven overnight at 60°C. If using centromeric or site specific probe, 0.5 ul of the probe was added to the BAC and 1 ul if using telomeric probe. The probe mix (approximately 6 ul per slide) was then transferred onto the slide and covered with a 22 X 22 mm coverslip. Any air bubbles were removed and the edges of the coverslip were sealed with rubber glue. The slide was then incubated overnight on Hybrite (Vysis Inc., USA), program1. The following day, the rubber glue and cover slip were removed. The slide was washed in 0.4XSSC/0.3% NP-40 (refer appendix A4 for preparation) for 2 minutes at 73°C, then 2XSSC/0.1% NP-40 (refer appendix A4 for preparation) for 30 seconds at room temperature. The reverse of the slide was wiped and allowed to dry slightly in the dark. 7.5 ul of DAPI was pipette onto the slide and covered with 22 X 32 mm coverslip. Any air bubbles were removed and the slide was ready for analysis.

4.2.5 Array analysis

250K Sty1 SNP mapping arrays were applied in seven cases (BWSCA1, BWSCA2, BWSCA3, BWSCA4, BWSCA5, BWSCA7 and BWSCA8) and SNP 6.0 arrays in one case (BWSCA6). The methods applied were according to the manufacturer's recommendations (Affymetrix, Inc., Santa Clara, CA) and described in detail in sections

2.1 and 2.2. The reference set for 250K Sty1 mapping arrays was 48 samples from the HapMap project (www.hapmap.org/downloads/raw_data/affy500k/) and 270 HapMap individuals of various populations for SNP 6.0 (Goldstein and Cavalleri, 2005). Copy number analysis was done using the Affymetrix Chromosome Copy Number Analysis Tool 4.0 (CNAT 4.0).

4.3 Results

4.3.1 Chromosome analysis

BWSCA1 has a reciprocal translocation involving the long arm of chromosome 3 and the short arm of chromosome 11 (figure 4.4). The karyotype of BWSCA1 was described as 46,XY,der(11)t(3;11)(q22;p15.4). BWSCA2 has a pericentric inversion in chromosome 11 (figure 4.5) and the karyotype was described as 46,XX,inv(11)(p15.4;q23.3).

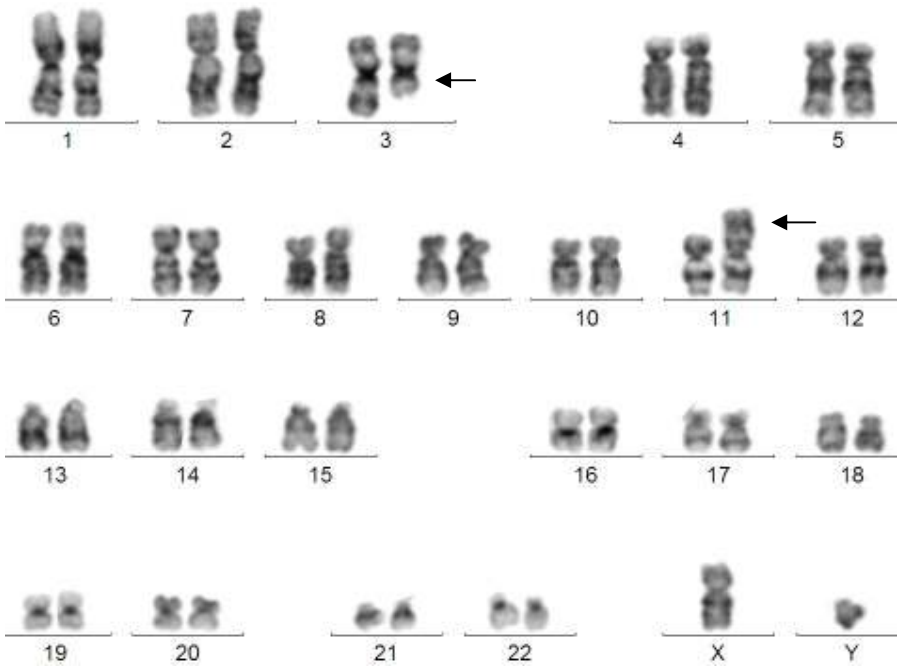

Figure 4.4: Karyotype of BWSCA1 46,XY,der(11)t(3;11)(q22;p15.4) showing translocation of the long arm of chromosome 3 and the short arm of chromosome 11 (arrows).

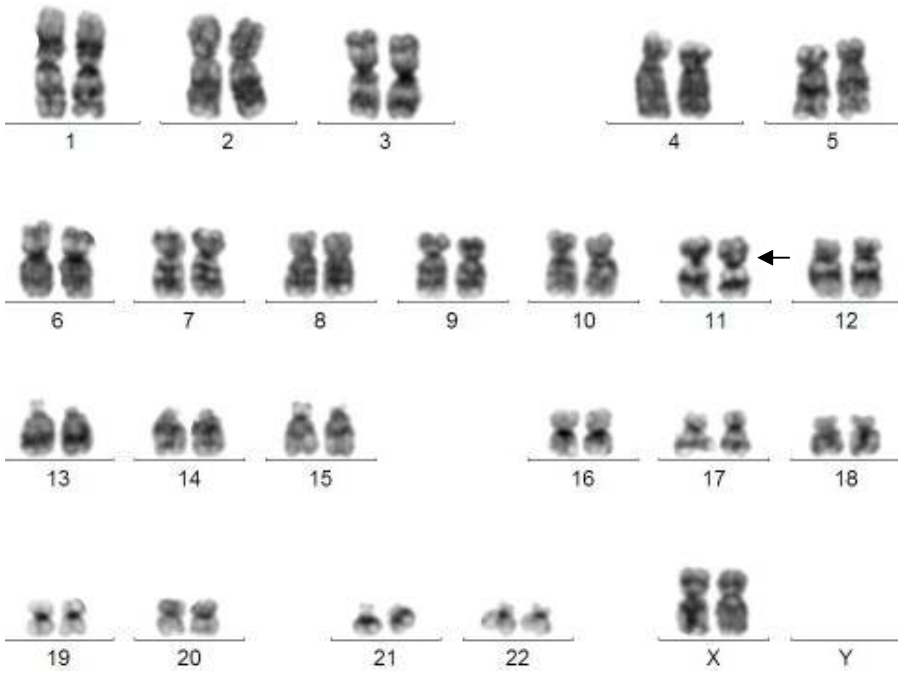

Figure 4.5: Karyotype of BWSCA2 46,XX,inv(11)(p15.4;q23.3) with a pericentric inversion of chromosome 11 (arrow)

4.3.2 FISH analysis

4.3.2.1 Patient BWSCA1

Eight BAC probes labelled with spectrum orange were used for FISH analysis to localise the breakpoint in chromosome 11p15.5 or 11p15.4 of patient BWSCA1. Centromeric 11 or telomeric 11p in spectrum green (Vysis, USA) were applied as controls. The hybridisation signals observed for each of the BAC probe used are shown in table 4.3.

Table 4.3: Patterns of the hybridisation signals of the BAC clone probes applied on the metaphase spreads of patient BWSCA1

BAC probe	Start position	End position	Length (bps)	Pattern of BAC probe hybridisation signals
RP11-295K3	1672662	1785148	112487	Translocated to the aberrant chromosome 3
RP11-847E17	2426546	2542863	116318	Translocated to the aberrant chromosome 3
RP4-608B4	2542864	2676679	133816	Split signal
RP11-38L8	2624666	2805691	181026	Split signal
RP11-774H09	2627884	2812495	184611	Retained in der(11)
RP11-699D10	2849462	2999871	150409	Retained in der(11)
RP11-211E17	6433969	6580309	146341	Retained in der(11)
RP11-89D4	7249883	7402046	152164	Retained in der(11)

Abbreviation: bps, base pairs

Examples of the pattern of FISH signal on the metaphase spreads of some of the BAC probes are shown in figure 4.6. Based on the results of FISH analysis of the BAC probes, the breakpoint in chromosome 11p15.5 was identified within RP4-608B4 and RP11-38L8, ~2.62-2.67 Mb (or ~400 kb centromeric to *IGF2*) which is in the *KCNQ1* gene (figure 4.3).

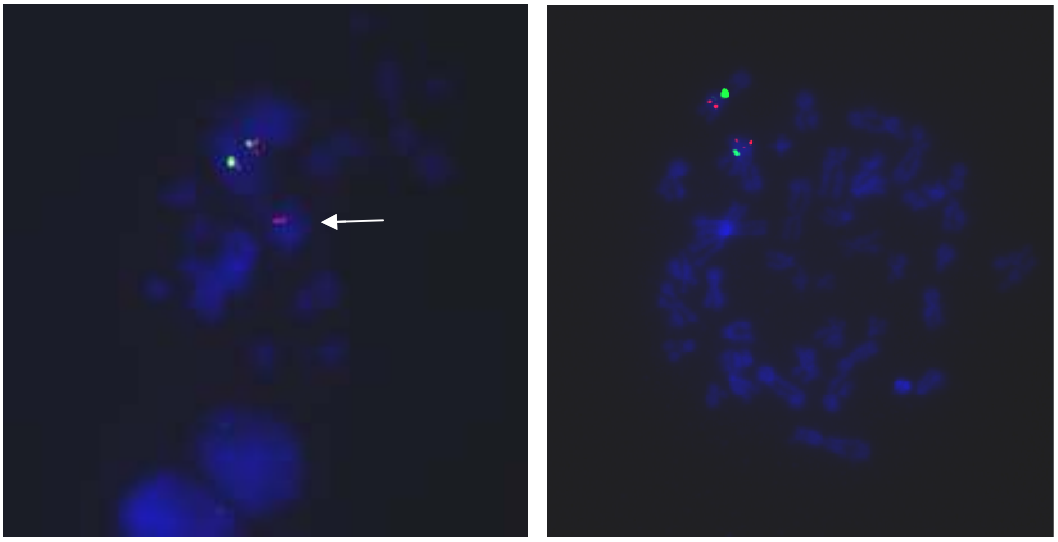

A B

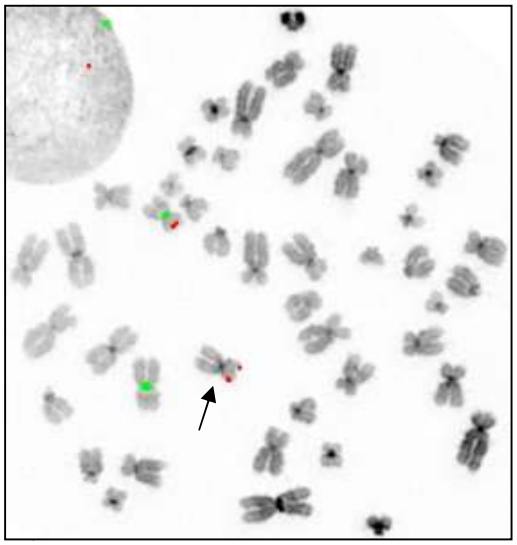

C

Figure 4.6: FISH analysis with BAC clone probes in spectrum orange and control probes in spectrum green on BWSCA1 metaphase spreads **(A)** BAC probe RP4-608B4 and centromeric 11 (CEN11) as control probe. The normal chromosome 11 has both of the green and orange signals. Split signals of the BAC probe are seen on the der(11) and the aberrant chromosome 3 (arrow) indicating a breakpoint in the probe locus of chromosome 11p15.5. **(B)** Hybridisation of RP11-699D10 and control centromic 11. Both of the signals are seen on the normal chromosome 11 and der(11 **(C)** Hybridisation of RP11-847E17 and control (CEN11). Normal chromosome 11 exhibits both of the signals while RP11-847E17 is seen translocated onto the aberrant chromosome 3(arrow).

4.3.2.2 Patient BWSCA2

Ten BAC probes (spectrum orange) and control telomeric 11p (spectrum green) (Vysis, USA) were used to map the breakpoint. The hybridisation signals observed for each of the BAC probe used are shown in table 4.4.

Table 4.4: FISH results using BAC probes in patient BWSCA2

BAC probe	**Start position**	**End position**	**Length (bps)**	**Pattern of FISH signals on the inv(11)**
RP11-295K3	1672662	1785148	112487	Fusion (green and orange) on chromosome inv(11)
RP5-1075F20	2266878	2406238	139361	Fusion (green and orange) on chromosome inv(11)
RP11-847E17	2426546	2542863	116318	Fusion (green and orange) on chromosome inv(11)
RP11-304P12	3060165	3236511	176347	Fusion (green and orange) on chromosome inv(11)
RP11-211E17	6433969	6580309	146341	Fusion (green and orange) on chromosome inv(11)
RP11-560B16	6790739	6934157	143419	Fusion (green and orange) on chromosome inv(11)
RP11-413N10	6934158	6984344	50187	Break apart
RP11-715M10	6984345	7179441	195097	Break apart
RP11-324J3	7179442	7293306	113865	Break apart
RP11-89D4	7249883	7402046	152164	Break apart

Abbreviations: inv, inversion; bps, base pairs

Probe configurations for detection of breakpoint on the inverted chromosome 11 by fluorescence *in situ* hybridisation (FISH) are shown in the diagrams below.

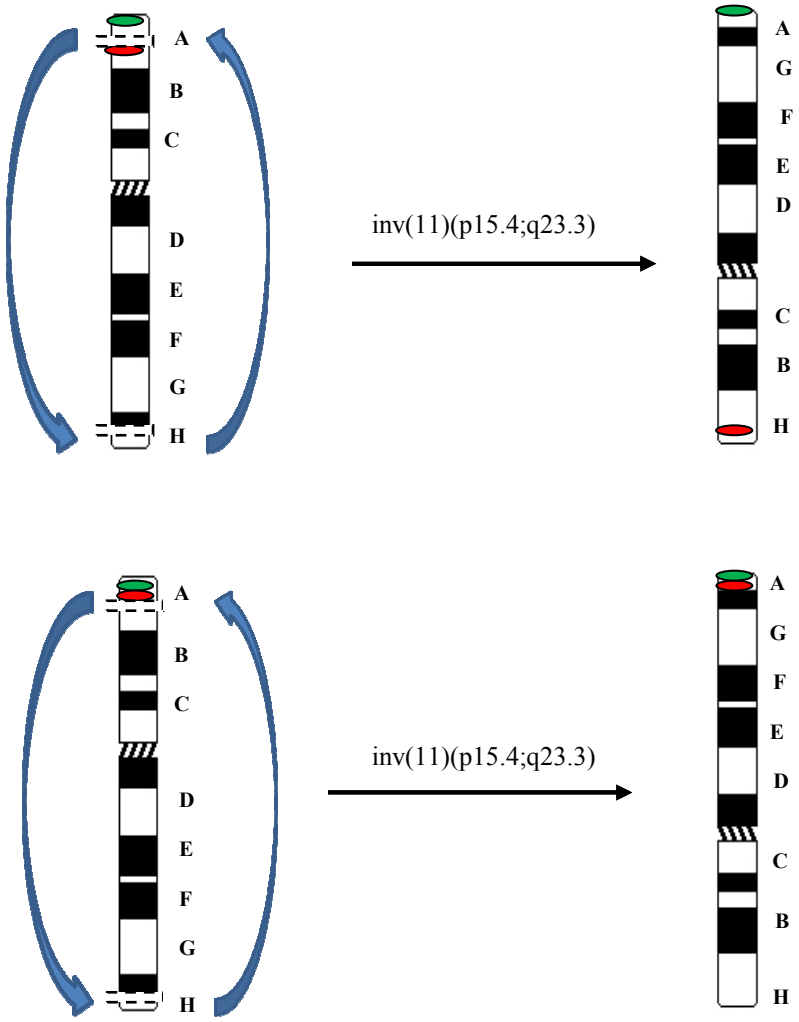

Figure 4.7: Probe configurations for detection of breakpoint by fluorescence *in situ* hybridisation (FISH). The green oval represents control probe 11p and the red oval represents BAC probe. Diagrams in the top section show the configuration of the signals if the breakpoint occurs distal to the BAC probe (spectrum orange). On the inv(11), the orange signal will be seen apart from the green signal (control 11p). If the break occurs proximal to the BAC probe, the signals will be seen or fused together (orange and green) on the inv(11) as shown in the diagrams in the bottom section.

Based on the pattern of FISH signals exhibited by each of the BAC probes and control 11p probe on the metaphase spreads of BWSCA2, the breakpoint on chromosome 11p15 of the patient was determined (figures 4.8, 4.9 and table 4.4).

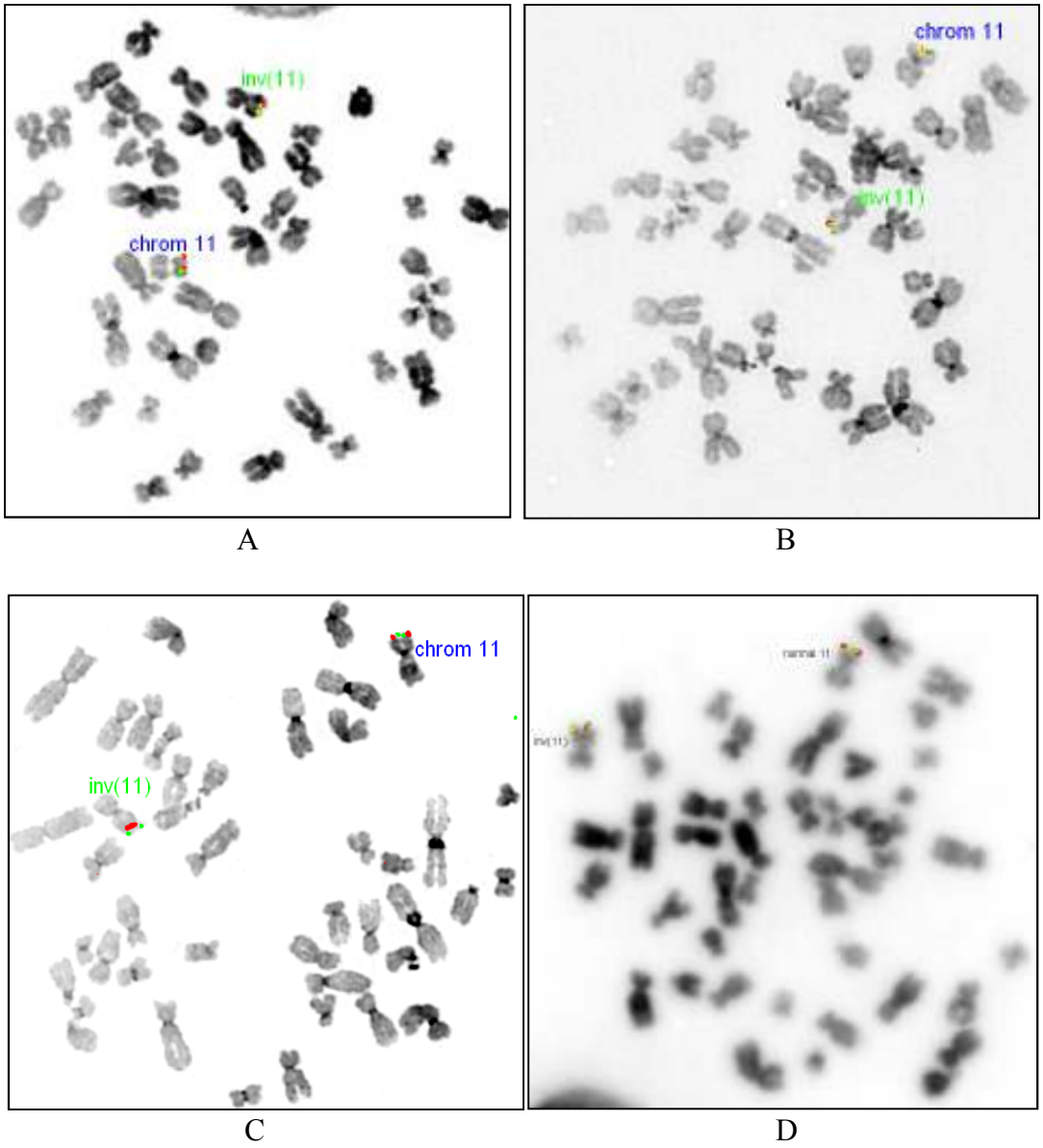

Figure 4.8: FISH analysis with telomeric probe for chromosome 11p (spectrum green) and BAC probes (spectrum orange) on BWSCA2 metaphase spreads. (A, B, C and D) RP11-295K3, RP11-847E17, RP11-211E17 and RP11-560B16 respectively, hybridised together with control probe telomeric 11p on the metaphase spreads. Both of the signals are seen together with the control telomeric 11 probe on the inv(11) indicating that the breakpoint is proximal to the BAC probes.

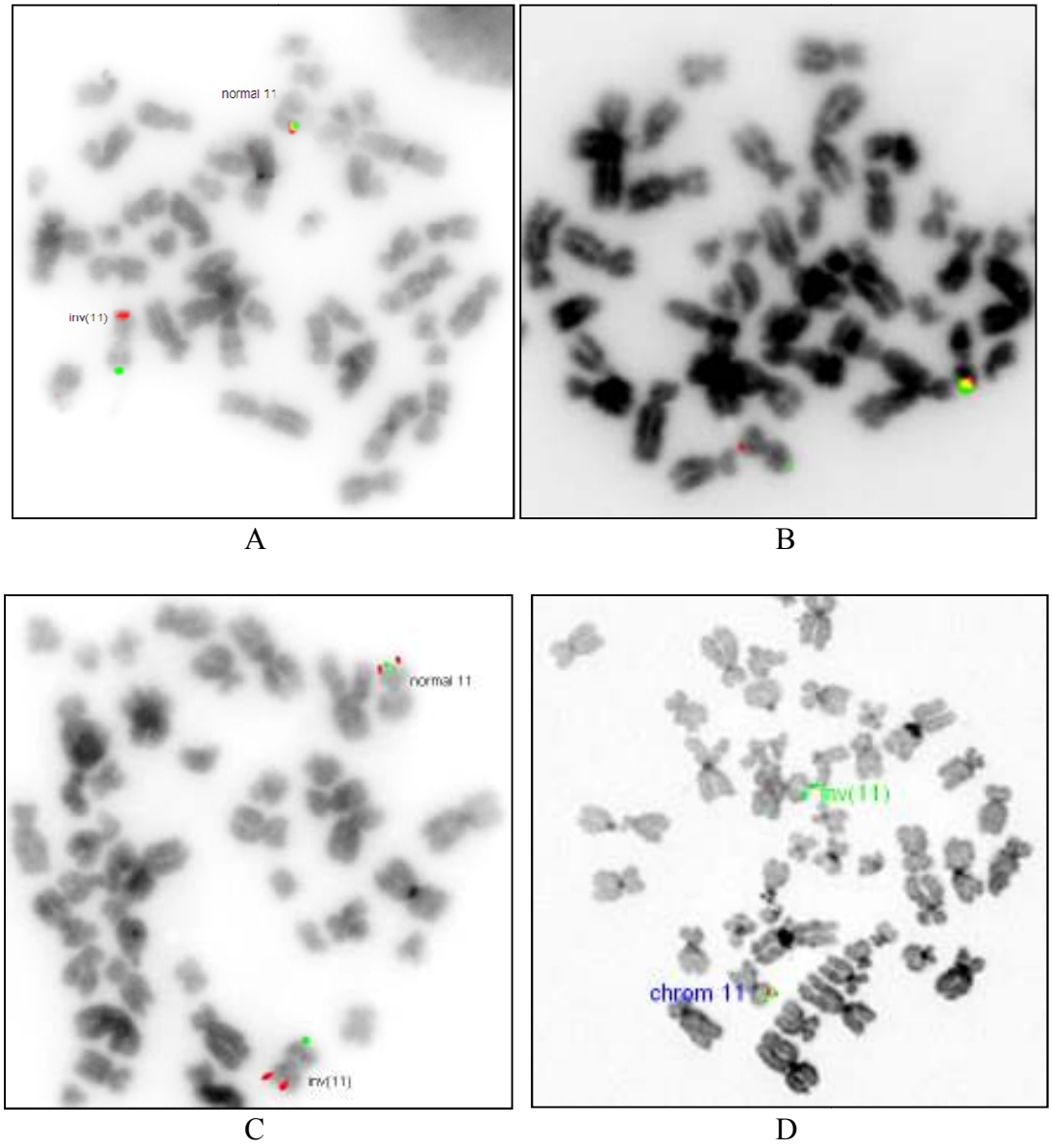

Figure 4.9: FISH analysis using BAC probes (spectrum orange) on BWSCA2 metaphase spreads. (A, B, C and D) Hybridisation of RP11-413N10, RP11-715M10, RP11-324J3, RP11-89D4 respectively and the control telomeric 11p probe (spectrum green) show split signals of green and orange in the inv(11) indicating a breakpoint in between the BAC probes and the control probe. The breakpoint was determined to localise from RP11-413N10 as the split signal starts to be observed from there onwards.

All the BAC probes telomeric to RP11-413N10 showed fusion (red and green) signals indicating the region telomeric to RP11-413N10 are intact and not rearranged (figures 4.8A-D). Green and orange signals were seen apart and on both ends of the inv(11) starting

from RP11-413N10. Thus the breakpoint was localised in ~6.93-6.98 Mb of 11p15.4 (figures 4.9A-D) which maps to the *ZNF215* gene (figure 4.3).

4.3.3 Array analysis

The reference set for 250K Sty1 mapping arrays was 48 samples from the HapMap project (www.hapmap.org/downloads/raw_data/affy500k/) and 270 HapMap individuals of various populations for SNP 6.0 (Goldstein and Cavalleri, 2005). The average call rate for the seven samples (BWSCA1, BWSCA2, BWSCA3, BWSCA4, BWSCA5, BWSCA7 and BWSCA8) was 96.46±2.88. Two cases, BWSCA4 and BWSCA3, showed duplication in the 11p region. The duplication in BWSCA4 was observed in chromosome 11p15.4 to telomeric 11p with the size of ~10.3 Mb (figure 4.10).

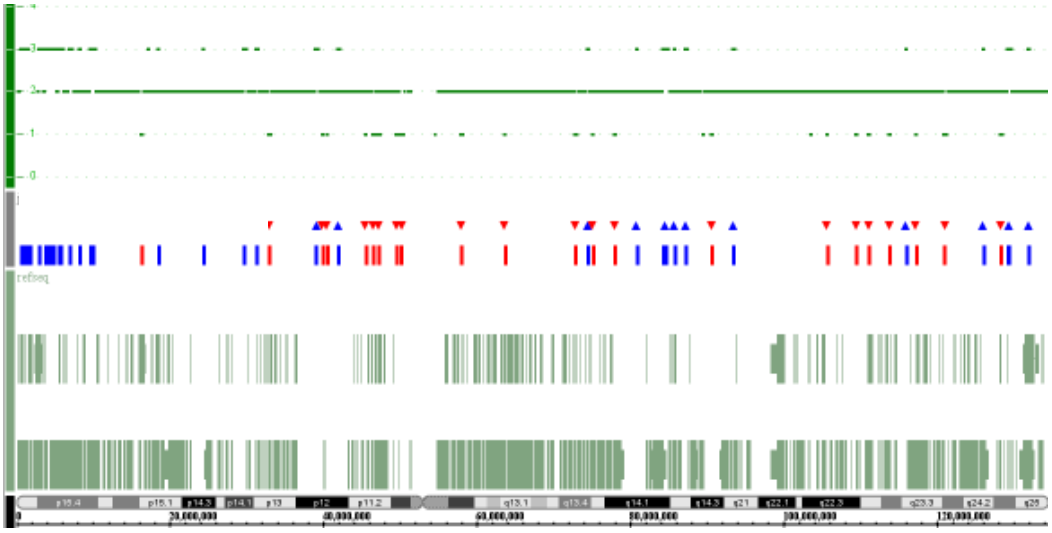

Figure 4.10: Copy number analysis using Affymetrix CNAT v4.0 on patient BWSCA4. Green horizontal line represents copy number state (2= diploid copy number, 1= haploid copy number). The duplicated region of 11p15.4-pter is observed as an increase in copy number (copy number state= 3). Size of the duplicated region is called at 10.3 Mb. Blue and red vertical bars below the green horizontal lines represent region of gain and loss respectively. Ideogram of chromosome and genes within the area of analysis are displayed at the bottom of the figure.

BWSCA3 had a smaller size of duplication, about 7.0 Mb in 11p15.4 to the telomere (figure 4.11). The duplicated region in both of the cases involved the imprinted genes in two imprinting domains regulated by IC1and IC2.

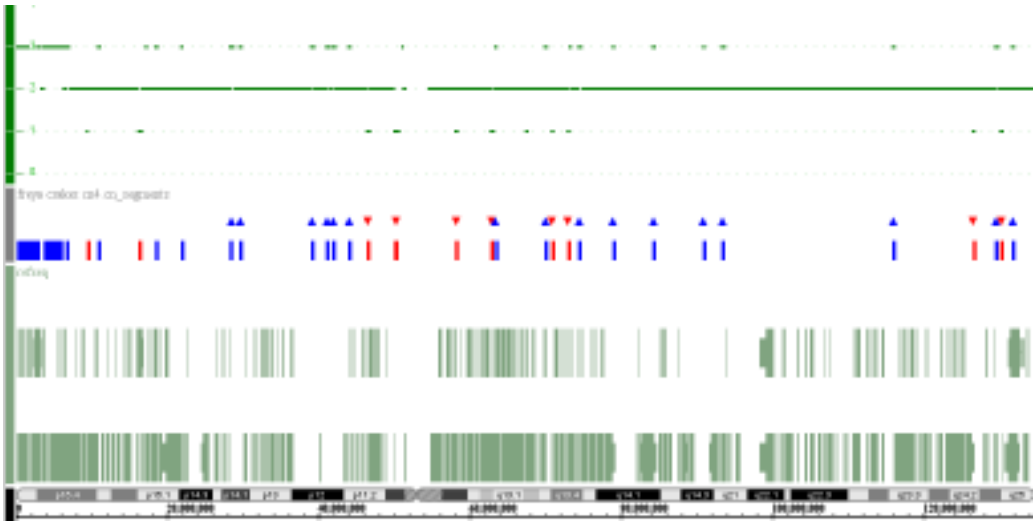

Figure 4.11: Copy number analysis using Affymetrix CNAT v4.0 on patient BWSCA3. Green horizontal line represents copy number state (2= diploid copy number, 1= haploid copy number). The duplicated region of 11p15.4-pter is observed as an increase in copy number (copy number state= 3). Size of the duplicated region is called at 7.0 Mb. Blue and red vertical bars below the green horizontal lines represent region of gain and loss respectively. Ideogram of chromosome and genes within the area of analysis are displayed at the bottom of the figure.

Although patient BWSCA5 has a normal copy number of chromosome 11 but there was loss of heterozygosity (LOH) detected involving almost the whole short arm of the chromosome (figure 4.12). This is caused by uniparental disomy (UPD) most probably inherited from the father.

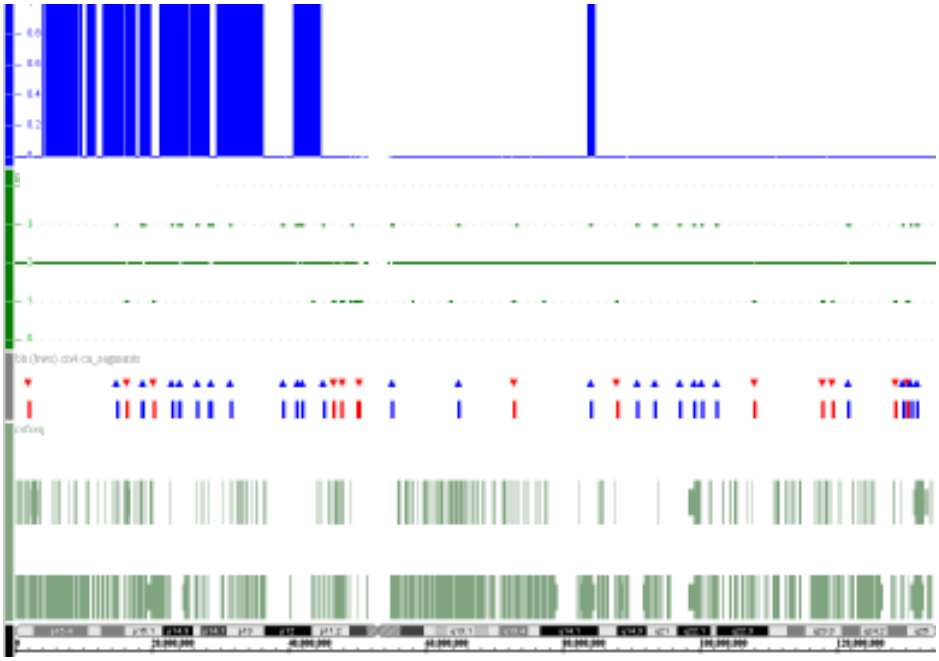

Figure 4.12: Region of LOH (represented by a continuous blue bars in the top panel) in patient BWSCA5 identified using Affymetrix CNAT v4.0. The region spanning from 11p11.2-pter with a normal copy number (copy number state= 2) represented by the horizontal green line. Ideogram of chromosome and genes within the area of analysis are displayed at the bottom of the figure.

No copy number changes or LOH were detected in chromosome 11 of patients BWSCA8 and BWSCA7. This could be due to epigenetic mechanisms such as loss of methylation or loss of imprinting in the BWS imprinting centre or unidentified genetic mechanisms. There were also no copy number alterations identified in patients BWSCA1 and BWSCA2, suggesting of a balanced rearrangement.

SNP6.0 arrays were applied on one patient, BWSCA6. Duplication with the size of 3.4 Mb in chromosome 11p15.4-pter (figure 4.13) and a deletion in chromosome 4p16.2-pter with the size of 3.8 Mb were observed (figure 4.14).

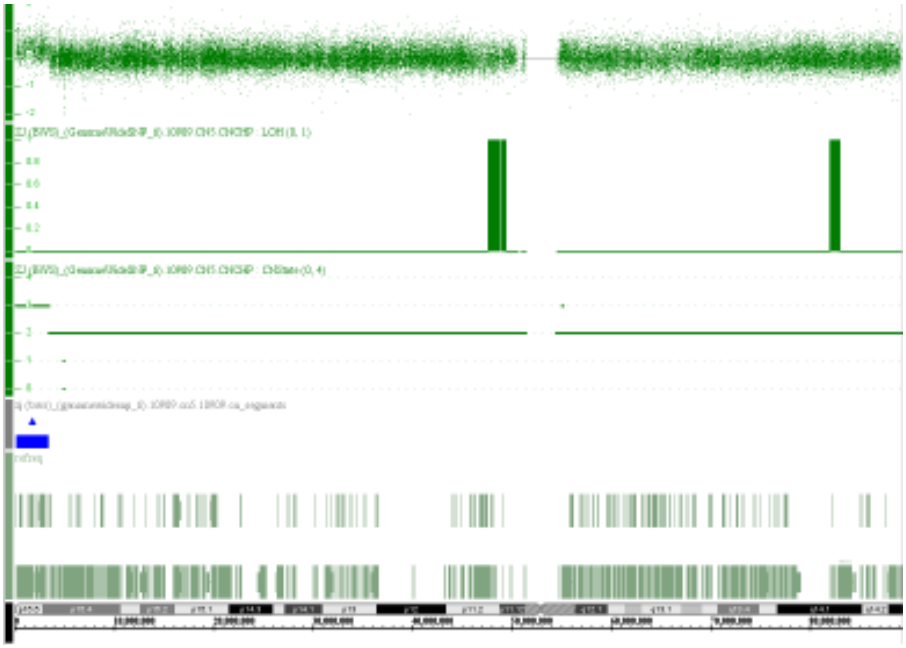

Figure 4.13: Chromosome 11 log2 ratio analysed using the Birdseed v1 algorithm for SNP 6.0 arrays for patient BWSCA6. The duplicated region is shown as an increase in copy number state (copy number state= 3) represented by the horizontal green line. Blue horizontal bar represents region of gain in the chromosome. Size of the duplicated region in 11p15.4-pter is called at 3.4 Mb. Ideogram of chromosome and genes within the area of analysis are displayed at the bottom of the figure.

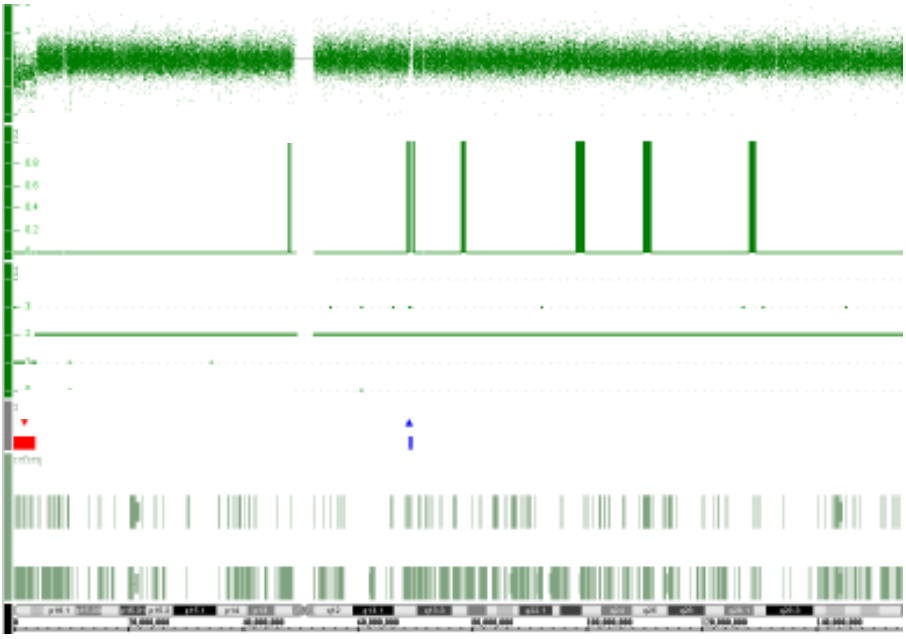

Figure 4.14: Chromosome 4 log2 ratio analysed using the Birdseed v1 algorithm for SNP 6.0 arrays for patient BWSCA6. The deleted region is shown as a decrease in copy number state (copy number state= 1) represented by the horizontal green line. Red horizontal bar represents region of loss in the chromosome. The size of the deleted region in 4p16.2-pter is called at 3.8 Mb. Ideogram of chromosome and genes within the area of analysis are displayed at the bottom of the figure.

Copy number analysis on the eight patients of BWS described above is summarized in table 4.5.

Table 4.5: Array analysis in the eight BWS patients studied.

Patient	Chromosome aberration	LOH	Start position (Mb)	End position (Mb)	Size (Mb)
BWSCA1	46,XY,t(3;11)(q22;p15.4)	No	-	-	-
BWSCA2	46,XX,inv(11)(p15.4;q23.3)	No	-	-	-
BWSCA3	Dup(11)(p15.4p15.5)	No	0	7.057	7.0
BWSCA4	Dup(11)(p15.4p15.5)	No	0	10.307	10.3
BWSCA5	No	Yes	0	48.0	48.0
BWSCA6	Dup(11)(p15.4p15.5) Del(4)(p16.2-p16.3)	No	0	3.435 3.845	3.4 3.8
BWSCA7	No	No	-	-	-
BWSCA8	No	No	-	-	-

Abbreviations: Mb, megabase; t, translocation; dup, duplication; del, deletion; inv, inversion; p, short arm; q, long arm

4.4 Discussion

BWS due to chromosome translocations, duplications or inversions is rare, encountered in approximately 2% of the cases (Elliott and Maher, 1994). In this study, chromosomal rearrangements involving chromosome 11p15.4-p15.5 were observed in five out of the eight cases (these were highly selected cases derived from a large cohort (~400) of BWS patients). One of the advantages of using 250K SNP array is that the method allows simultaneous identification of LOH and copy number alterations in a single experiment. In the present study, region of LOH with normal copy number was detected in chromosome 11p of patient BWSCA5. This indicates that both of the copies were derived from the same parent, also known as uniparental disomy (UPD). No copy number gain or loss observed in the two cell lines (BWSCA1 and BWSCA2) indicating the rearrangements are balanced (or the imbalance is very small).

It cannot be ascertained whether the rearrangements in BWSCA1 and BWSCA2 are inherited or *de novo*, as the parents samples were not available for testing. However, it has been reported that patients with BWS who have cytogenetic abnormalities involving chromosome 11p15.5 duplications, inversions in distal 11p or balanced translocations that break in this region - genomic imprinting effects are evident in the parental origin of the affected chromosomes. Duplications in this group of patients are invariably derived from the patient's father, whereas inversions and translocations always involve the maternal homologue (Maher and Reik, 2000).

Evidence from the FISH mapping shows that the breakpoint in chromosome 11p15.5 of patient BWSCA1 occurs in *BWSCR1* and disrupts the maternally expressed *KCNQ1* gene which spans >400 kb. This is consistent with the report that *BWSCR1* contains multiple

balanced chromosomal translocation breakpoints associated with BWS, which were proposed to affect an imprinting control element (Lee et al., 1997). Several studies (Sait et al., 1994; Brown et al., 1996; Joyce et al., 1997; Li et al., 1998) have described chromosomal rearrangements including translocation and inversion involving chromosome 11p15.5 in patients with BWS. Among the alteration observed were biallelic expression of *IGF2* and normal imprinting of *H19* in an affected BWS patients with maternally inherited inv(11)(p11.2;p15.5) (Brown et al., 1996). Data from a large series of sporadic BWS cases analysed by Engel et al (2000) suggested that loss of methylation of *KvDMR1* on maternal allele results in epigenetic silencing of *CDKN1C* and variable loss of imprinting of *IGF2*. In another study, loss of methylation of *KvDMR1* in maternal allele is associated with expression of the antisense transcript, *KCNQ1OT1* from the maternal copy (Maher and Reik, 2000). Loss of maternal allele methylation at *KvDMR1* and biallelic *KCNQ1OT1* expression occurs in 50–60% of BWS patients (Lee et al., 1999; Engel et al., 2000). Relating these findings with BWSCA1, the BWS phenotype of the patient could be caused by loss of methylation of *KvDMR1* on the maternal allele which altered the normal expression of *KCNQ1* or *CDKN1C* or *KCNQ1OT1* or *IGF2*. Further investigation such as methylation status of the genes can provide the information of the exact cause of BWS in this patient.

Breakpoint in BWSCA2 was localised in *ZNF215* in *BWSCR2* by FISH mapping. It is very rare to find breakpoint in this region correlated with BWS and to date, only one report demonstrated association of *ZNF215* in BWS (Alders et al., 2000). They analysed the breakpoints in two patients – one with inv(11p15.4) and the other with t(10,11)(p13;p15.4), both presented with hemihyperplasia together with other minor BWS features which is not seen in patients with chromosomal breakpoint in *BWSCR1* and

BWSCR3. In both of the patients, the chromosomal rearrangements disrupt *ZNF215*. *ZNF215* is imprinted and expressed preferentially from the maternal allele. The gene is expressed in a tissue specific manner and contains 4 zinc fingers, a KRABA domain, sequences similar to a KRABB domain, an N-terminal SCAN box and a nuclear localisation signal. The breakpoint in *BWSCR2* disrupts alternative spliced *ZNF215* transcripts which encode a truncated protein lacking the zinc fingers but retaining the KRAB and SCAN box functional domains (Alders et al., 2000). They suggested that there is a gene(s) at *BWSCR2* and *BWSCR3* that interacts with some components of the *IGF2*/*BWSCR1* systems and influences the BWS phenotype through this mechanism. Although FISH results of this study agrees with the findings of Alders et al (2000), more tests have to be done to verify the results.

Approximately 20% of sporadic BWS cases have segmental paternal uniparental disomy involving the imprinted gene cluster at 11p15.5 (Henry et al., 1991; Slatter et al., 1994). Previous reports (Slatter et al., 1994; Catchpoole et al., 1997; Dutly et al., 1998; Cooper et al., 2007) have also shown that all cases of BWS UPD are mosaic isodisomy. Thus, the process of UPD occurs postzygotically due to mitotic recombination in early embryogenesis and lack of one or more chromosome 11 maternally expressed genes may lead to embryonic lethality. The region of paternal UPD invariably includes the imprinted gene cluster at 11p15.5, however, the extent of isodisomy along chromosome 11 is variable (Catchpoole et al., 1997; Dutly et al., 1998; Cooper et al., 2007). Cases of BWS UPD involving the whole chromosome 11 has also been reported and to date there are only five such cases; 4 identified by Cooper et al (2007) and 1 by Dutly et al (1998). These suggest that BWS UPD due to mitotic recombination is more common than mitotic nondisjunction in early embryo. In the present study, the patient (BWSCA5) has UPD

spanning from the telomeric region 11p to p11.2 (48.0 Mb) identified by high resolution SNP array. Genotyping analysis on chromosome 11 shows homozygous region in the chromosome (data not shown). Although high resolution SNP array is useful in giving a precise region of LOH in this case, it is unable to give information whether the segment was derived from paternal or maternal. However, based from the previous reports (Maher and Reik, 2000; Cooper et al., 2007), it is presumed that the LOH segment of chromosome 11p in BWSCA5 was paternal in origin. BWS UPD cases are predicted to have increased *IGF2,* reduced *H19* and reduced *CDKN1C* expression (Cooper et al., 2005). Hemihyperplasia is highly positively correlated with UPD 11p15 in BWS (Engel et al., 2000; DeBaun et al., 2002; Cooper et al., 2005) and in some cases, isodisomy can be detected in only a small subset of tissue in the patient (Weksberg et al., 2001). There is no known instance of recurrence of segmental UPD 11 and as a postzygotic event, it is assume no increased risk would apply.

Paternally inherited cases of overgrowth have been described previously; in these cases, unbalanced translocations leading to trisomy for 11p with paternal duplication have been responsible (Slavotinek et al., 1997), however *de novo* duplications of the paternally derived 11p15 region were also found. Using microsatellite analysis, Russo et al. (2006) have identified a small duplication at 11p15.5 involving IC1 and excluding IC2, spanning 1.8 Mb in a patient with features of BWS who had a *de novo* paternal tandem duplication. This was proposed to result from an unequal recombination at paternal meiosis 1. In the present study, patient BWSCA6 has an unbalanced translocation t(4;11)(p16.2;p15.4) leading to paternal duplication of 11p15.4-pter (3.4 Mb) and deletion of 4p16.2-pter (3.8 Mb). In addition to BWS, deletion of 4p16.3 contributes to the Wolf-Hirschhorn syndrome features in BWSCA6. Wolf-Hirschhorn syndrome is characterised by severe

growth and mental defect, microcephaly, 'Greek helmet' facies, and closure defects (cleft lip or palate), coloboma of the eye and cardiac septal defects (Hirschhorn et al., 1965; Wolf et al., 1965). Two other reports (Russo et al., 2006; Mikhail et al., 2007) have also described overlapping phenotype of Wolf-Hirschhorn and BWS in their patients. The duplication 11p15.4-pter identified in BWSCA3 and BWSCA4 involved large segments, 7.0 Mb and 10.3 Mb respectively, spanning from 11p15.4 to the telomere 11p. No copy number changes were detected in the other chromosomes, indicating that the duplication was not due to unbalanced translocation. Although the extent of the duplicated region in these patients is variable, the phenotypic expression of BWS is presumably due to the presence of a common duplicated region.

The duplicated region 11p15.4-pter identified in BWSCA3, BWSCA4 and BWSCA6 involved both of the ICs, therefore, all of the genes implicated with BWS in 11p15.4-p15.5 were duplicated. The duplication is predicted to disrupt the dosage and expression of normally paternally and maternally expressed genes as well as non-imprinted genes. The paternally expressed gene, *IGF2* is thought to be overexpressed while effective dosage of maternally expressed genes including *H19, KCNQ1* and *CDKN1C* are predicted to remain unchanged. The *IGF2* gene encodes a fetal growth factor and overgrowth in BWS is restricted to those tissues in which *IGF2* is expressed. In mice, over-expression of *IGF2* results in most of the symptoms of BWS, including prenatal overgrowth, polyhydramnios, fetal and neonatal lethality, disproportionate organ overgrowth and macroglossia (Sun et al., 1997). Cases with maternal duplication 11p15 were also been reported but none of the patients showed features of BWS; three patients had growth retardation, in contrast to the overgrowth characteristic of BWS (Fisher et al., 2002) and two patients represented with Silver-Russel syndrome (Eggermann et al., 2006). These observations support the

hypothesis that paternally expressed genes promote growth and maternally expressed genes have the opposite effects. There were no copy number changes or LOH observed in BWSCA8 and BWSCA7, thus the BWS phenotype in the patients could be due to epimutations which alter the methylation or expression of the imprinted gene(s) in 11p15.

The findings of this study is consistent with the previous reports; the breaks identified in 11p15.4 due to inversion and translocation disrupts the imprinted genes in that region and alterations in the normal doses of genes caused by duplications of paternal allele or paternal UPD can also contribute to the BWS phenotype. To the best of my knowledge, patient BWSCA2 is the third BWS found with breakpoint in *ZNF215*. Thus, further studies should be taken to elucidate the role of *ZNF215* in BWS.

5 Analysis of copy number changes in primary tumours of clear cell renal cell carcinoma (cRCC) and renal cell carcinoma (RCC) cell lines using 250K SNP array

5.1 Introduction

Kidney cancer constitutes about 2% of all malignant tumours in adults (Clifford et al., 1998). It is the seventh most common cancer in men and ninth most common in women, a male-predominant (2:1) disease with a typical presentation in the sixth and seventh decades of life (median age about 60 years) (Maher et al., 1990a). Incidence rates for the cancer have been rising steadily each year in Europe and the United States (Mathew et al., 2002) and it is estimated to account for about 209,000 new cases per year and 102,000 deaths per year (Gupta et al., 2008). Incidence is generally highest in Western and Eastern European countries, Scandinavia, parts of Italy, North America and in Australia/New Zealand. The lowest incidence is reported in Asia and Africa (Ferlay et al., 2004).

Several environmental factors have been reported to be associated with an increased risk of renal cell carcinoma (RCC). Active and passive cigarette smoking is an established risk factor for RCC (Yuan et al., 1998; Hunt et al., 2005). Obesity, specifically body mass index, also has a positive association with risk of RCC (Bjorge et al., 2004; van Dijk et al., 2004). Another known risk factor is hypertension (Lipworth et al., 2006) with data showing hypertensive medication such as diuretic medications are not independently associated with the risk of the development of the cancer (McLaughlin et al., 1995; Grossman et al., 1999; Grossman et al., 2002). Patients with end stage renal failure, acquired renal cystic disease and various hereditary kidney cancer syndromes have a higher risk of developing RCC than in the general population (Ishikawa et al., 2003; Rakowski et al., 2006). Exposure to asbestos or trichloroethylene has not been

convincingly associated with RCC (McCredie et al., 1995). Other factors such as alcohol consumption, vegetable and fruit consumption, intake of micronutrients and vitamins showed less consistent association with the risk of RCC (Wolk et al., 1996; Mellemgaard et al., 1999; Dhote et al., 2000; Lindblad et al., 2004).

Renal parenchyma (renal cell) cancer accounts for about 85% of kidney cancers diagnosed in the United states from 1992 to 2002 The remainder was composed mainly of renal pelvis cancer (approximately 12%) and other rare malignancies (approximately 2%). All renal cell cancers are adenocarcinomas and the majority of the renal pelvis cancers are transitional cell carcinomas (Lipworth et al., 2006). Renal cell carcinomas (RCC) are adenocarcinomas derived from tubular epithelium. Most cases of RCC occur sporadically, only about 2%-3% of cases are inherited (Maher, 1996a) RCC is divided into 5 subtypes based on histological pattern: clear cell (conventional) is the most common type (70%-80%), papillary occurs in 10%-15% and chromophobe renal carcinoma occurs in 3%-5%, with the remaining being made up of collecting duct (1%) and unclassified (1%). Papillary is further divided into type 1 (5% of the cases) and type 2 (10% of the cases) (Kovacs et al., 1997). These different types of RCC have different histological patterns, different clinical courses and each have a distinct genetic basis (Linehan et al., 2003).

5.1.1 Classification of renal cell carcinoma (RCC)

Renal cell carcinoma (RCC) originates from the tubular epithelial cells of the renal cortex and accounts for 80-85% of primary malignancies in kidney (Motzer et al., 1996). RCC comprises of different types of tumours, each derived from different parts of the nephron. The nephron consists of the renal corpuscle and renal tubule which is divided into four histo-

physiological zones: proximal convoluted tubule, loop of Henle, distal convoluted tubule and collecting duct (figure 5.1).

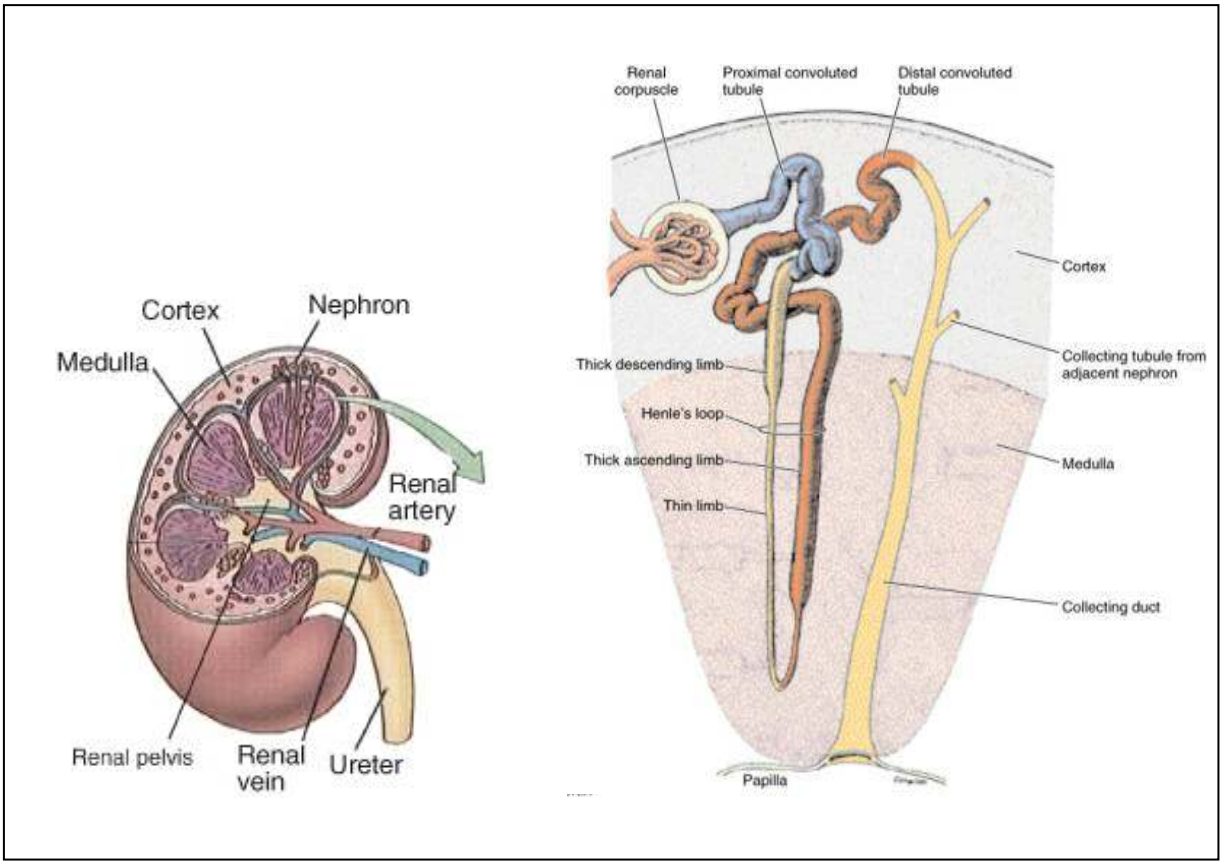

Figure 5.1: Anatomy of the kidney. The kidney is divided into two major structures: superficial is the renal cortex and deep is the renal medulla. Nephrons consist of the renal corpuscle and renal tubules and span the cortex and medulla.

In 1996, the Heidelberg classification of RCC was proposed with the aim of integrating histological criteria and an understanding of genetic alterations (Kovacs et al., 1997). According to the classification, RCC can be classified into three major subtypes: clear cell RCC (also known as conventional RCC), papillary RCC and chromophobe RCC. Other less frequent subtypes include multilocular cRCC, collecting duct carcinoma, medullary carcinoma and unclassified type. The WHO classification of 2002 is more comprehensive and in addition to the previous subtypes also includes renal carcinoma associated with

neuroblastoma, Xp11 translocation carcinoma and mucinous tubular and spindle cell carcinoma (figure 5.2).

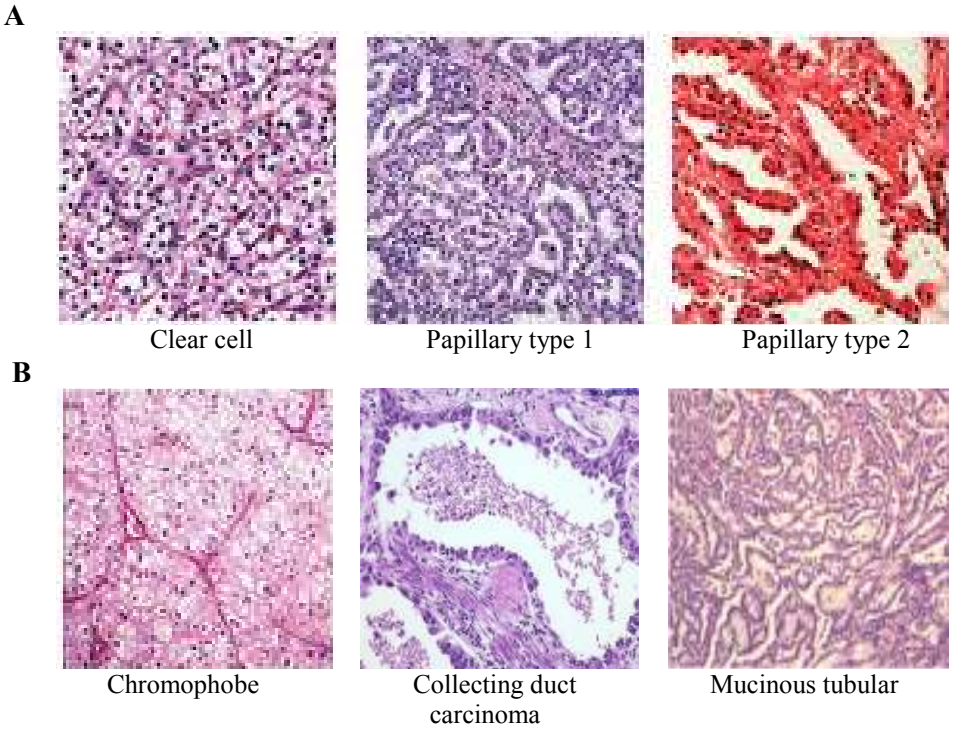

Figure 5.2: The different RCC subtypes. **(A)** Clear cell RCC and papillary RCC from the proximal convoluted tubule **(B)** chromophobe RCC, collecting duct carcinoma and mucinous tubular and spindle cell carcinoma from the collecting tubule.

The most common (~80%) forms of RCC are clear cell carcinoma (cRCC) and among the nonclear cell type, papillary (chromophilic) and chromophobic tumours are the most frequent (Thoenes et al., 1986). Most cases of cRCC are sporadic and the tumours are unilateral and unifocal. Papillary RCC are often bilateral and multifocal. The chromophobe variant of RCC accounts for 5% of all cases of RCC and is thought to originate from type B intercalated cells of renal collecting ducts (Crotty et al., 1995; Storkel et al., 1997). Papillary RCC is further divided into type 1 and type 2. Type 1 tumours are usually of lower-grade and stage than type 2 tumours (Amin et al., 1997; Delahunt et al., 2001). Collecting duct (Bellini duct) carcinomas are thought to originate

from the collecting ducts within the renal medulla (Rumpelt et al., 1991; Storkel et al., 1997). Collecting duct RCC are very aggressive and tend to occur in younger patients. Medullary carcinoma is a variant of collecting duct carcinoma (Swartz et al., 2002) which preferentially appear in younger patients with sickle trait and regarded as a more aggressive variant of collecting duct carcinoma with a mean survival time after surgery of 15 weeks (Srigley and Eble, 1998). The unclassified RCCs which accounts for 4-5% of all cases (Storkel et al., 1997; Kovacs et al., 1997) are a diagnostic category of renal tumours which do not fit into one of the other subtypes.

Mucinous tubular and spindle cell carcinoma are thought to originate from the distal nephron (Argani et al., 2001) and are reported to be a low-grade renal epithelial neoplasm characterized by an indolent course and female predominance. RCC associated with neuroblastoma occurs in long term survivors of childhood neuroblastoma, is morphologically heterogeneous and prognosis correlates with tumour grade and stage (Koyle et al., 2001).

5.1.2 Genetics of clear cell renal cell carcinoma (cRCC)

Zbar et al (1987) examined tumours from 18 patients with non-hereditary renal cell carcinoma and found loss of alleles at loci on the short arm of chromosome 3 in eleven of the patients. By studying loss of alleles at different chromosomal loci on normal and tumour tissue from 60 patients with various stages of renal cell carcinoma, Anglard et al (1991) suggested that the disease genes for sporadic renal cell carcinoma and for familial renal cell carcinoma associated with von Hippel-Lindau disease are in the same location. More importantly, they had refined the specific region in 3p21-p26. Subsequently, genetic linkage studies in families with von Hippel-Lindau disease followed by physical mapping

analyses resulted in the identification of the von Hippel-Lindau (*VHL*) tumour suppressor gene in the 3p25-p26 region (Latif et al., 1993).

Clear cell renal cell carcinoma is genetically characterized by deletions of the short arm of chromosome 3 and this was reported to be as the only karyotypic changes in about 10% of cases (Bodmer et al., 2002). Complete or partial loss of chromosome 3p is the most frequent alteration in cRCC suggesting the presence of one or more tumour suppressor gene(s) in this chromosome responsible for tumour development (Presti et al., 1998; Huebner, 2001; Sukosd et al., 2003). Deletions of 3p occur commonly in renal cell carcinoma associated with VHL disease and although von Hippel-Lindau disease is a rare cause of RCC, somatic inactivation of the *VHL* gene occurs in a high percentage of clear cell RCC tumours and cell lines from patients with sporadic (nonhereditary) clear cell renal carcinoma (Foster et al., 1994; Gnarra et al., 1994; Clifford et al., 1998; Zbar et al., 2003; Kim et al., 2004; van Houwelingen et al., 2005; Weiss and Lin, 2006; Banks et al., 2006). Inactivation of *VHL* can be due to somatic mutations, deletions, LOH or epigenetic inactivation such as promoter DNA methylation.

Chromosome 3p deletions in cRCC are large and are not limited to the *VHL* gene region (3p25-p26). Loss of heterozygosity (LOH) study on sporadic cRCC identified three regions on chromosome 3p that are recurrently affected: 3p12-p14, 3p21-p22 and 3p25-p26 (Van den Berg and Buys, 1997). It was suggested that an allelic loss in either 3p25 or 3p12-p14 is associated with adenomas whereas in carcinoma also involved losses in 3p21 together with 3p25 or 3p12-p14. In another studies to evaluate whether *VHL* gene inactivation is essential for tumour formation, the patterns and extent of allelic losses on 3p were compared in a set of cRCCs both with and without *VHL* mutations. This study

revealed that although the frequency of 3p12-p22 LOH was similar in both tumour types, LOH at 3p25-p26 was significantly less than LOH at 3p12-p22 in tumours without *VHL* mutation, whereas LOH at 3p25-p26 and 3p12-p22 was similar in tumours with *VHL* mutation (Teh et al., 1997; Martinez et al., 2000; Woodward et al., 2000a). These results supported the presence of both *VHL*-dependent and *VHL*-independent tumourigenic pathways and suggested that inactivation of a tumour suppressor gene at 3p12-p22 may play an important role in both these pathways. Subsequently the *RASSF1A* tumour suppressor gene that maps to 3p21 was found to be methylated in many RCC (Morrissey et al., 2001).

Predisposition to clear cell carcinoma may be associated with constitutional cytogenetic rearrangements involving chromosome 3p. The first report was of an Italian-American family who was affected with renal carcinoma in multiple family members (Cohen et al., 1979). Upon investigation of the affected family members, it was found that they had a germline balanced translocation involving chromosome 3p, t(3;8)(p14;q24). In another family, several siblings carried a constitutional t(3;6)(p13;q25) and one of them developed multiple bilateral RCCs (Kovacs et al., 1989). Positional cloning of the constitutional 3;8 translocation breakpoints revealed that the *FHIT* gene spanned the chromosome 3 breakpoint (Ohta et al., 1996). The gene co-localises with *FRA3B,* which is the most common inducible fragile site within the human genome (Ong et al., 1997). Hemi- or homozygous deletion of *FHIT* and reduced expression of the gene had been reported in several neoplasms including kidney, lung, cervix, esophagus, colon, stomach and pancreas tumours, implicating a role in tumour development (Sozzi et al., 1996; Virgilio et al., 1996; Druck et al., 1997; Hadaczek et al., 1999; Eyzaguirre et al., 1999). The chromosome

8 breakpoint disrupted the *TRC8* gene (Gemmill et al., 1998) and this gene may also function as a tumour suppressor gene (Teh et al., 1999).

Two Dutch families were also reported to display an association between constitutional chromosome 3 translocations and RCC. The first one involved five members over three generations carrying a constitutional t(2;3)(q35;q21) who developed RCC (Koolen, et al., 1998; Bodmer et al., 1998). In the second family, a t(3;6)(q12;q15) was transmitted and four members were diagnosed with cRCC (Eleveld et al., 2001). Other families have also been reported with different translocations e.g. t(3;4)(p13;p16), t(2;3)(q33;q21) and t(1;3)(q32;q13.3) (van Kessel et al., 1999; Kanayama et al., 2001; Podolski et al., 2001). Positional cloning of the familial t(2;3)(q35;q21) breakpoint revealed disruption of *DIRC2* which resides on chromosome 3 (Bodmer et al., 2002) while in the t(2;3)(q33;q21) family, *DIRC1* on chromosome 2 was found to be disrupted (Druck et al., 2001).

Although in some of the cases of familial cRCC associated with constitutional chromosome 3 translocations characterisation of the translocation breakpoint has revealed presence of a putative tumour suppressor gene for example (e.g. *FHIT, TRC8, DIRC1, DIRC2, NORE1* and *LSAMP*) (Ohta et al., 1996; Gemmill et al., 1998; Druck et al., 2001; Bodmer et al., 2002; Chen et al., 2003; Poland et al., 2007) or fusion transcript, in some cases no gene is disrupted or the disrupted gene does not appear a likely candidate tumour suppressor gene (Gemmill et al., 1998; Bodmer et al., 2002; Bugert et al., 2007). Hence in some cases it has been suggested that RCC susceptibility results not from direct disruption of a gene but from instability of the derivative chromosome 3 such that loss of the derivative chromosome 3 (that contains a *VHL* allele) through nondisjunction and subsequent somatic *VHL* gene mutation on the non-translocated chromosome 3

homologue. This process would result in homozygous loss of *VHL* function and has been termed a three-step model of tumourigenesis (Schmidt et al., 1995; Bodmer et al., 1998; Bodmer et al., 2002). Thus the first hit would be the occurrence of a germ line chromosome 3 translocation. Non-disjunctional loss of the derivative chromosome that carries the 3p segment would represent the second step. Finally, the third step would involve a somatic mutation in the remaining 3p allele of an RCC-related tumour suppressor gene (TSG) such as *VHL*.

Recently developed high resolution methods for genomic copy number analysis such as array based comparative genomic hybridisation (aCGH) can offer a high resolution information on copy number changes in cancer on a genome-wide level. Genomic DNA copy number alterations (CNA) have been shown to be a contributing factor in the development and progression of cancer. In cRCC, common somatic chromosomal changes in sporadic cases include loss of 3p, 4q, 6q, 8p, 9q and 14 and gain of 5q and 7 have been reported (Sanjmyatav et al., 2005).

5.1.3 Inherited renal cell carcinoma

A number of inherited disorders may predispose to RCC. Inherited RCC is characterised by an earlier age at diagnosis than in sporadic and inherited tumours are often multicentric and/or bilateral. Von Hippel-Lindau disease, hereditary type 1 papillary renal carcinoma (HPRC1), hereditary leiomyomatosis and renal cell carcinoma (HLRCC), Birt-Hogg-Dubé syndrome are examples of inherited disorders predisposing to renal cell carcinoma.

5.1.3.1 Hereditary papillary renal carcinoma (HPRC)

HPRC is very rare with an approximate incidence 1 per 10 million persons. It is an autosomal dominant hereditary cancer syndrome, a highly penetrant disease in which patients have a high risk of developing bilateral and multifocal type 1 papillary RCC (pRCC) (Zbar et al., 1994). The tumours are most often well differentiated, malignant and can metastasize. Genetic studies in kindreds with familial pRCC led to the identification of *MET* proto-oncogene located on the long arm of chromosome 7 (Schmidt et al., 1997). *MET* mutations are rare in sporadic pRCC, only about 5% of the cases (Schmidt et al., 1997; Schmidt et al., 1999). Furthermore, about 75% of sporadic pRCC cases have trisomy of chromosome 7 (Cohen and McGovern, 2005).

5.1.3.2 Hereditary leiomyomatosis renal cell carcinoma (HLRCC)

HLRCC is rare and dominantly inherited disorder caused by germline mutations in the fumarate hydratase gene (*FH*) (Tomlinson et al., 2002). Fumarate hydratase is a key component of the tricarboxylic acid cycle (Krebs cycle) and catalyses the conversion of fumarate to malate. HLRCC was first described in a Finnish family in which eleven members had uterine leiomyomas, two had uterine leiomyosarcoma and seven individuals had a history of cutaneous nodules (two of which were confirmed to be cutaneous leiomyomatosis). In addition, four kidney cancer cases occurred in young (33-48 years old) females and the tumours are different from those that appear in patients with VHL, HPRC and BHD. Kidney cancers in HLRCC displayed a distinct papillary histology (type 2 pRCC) and presented as unilateral solitary lesions that had metastasized at the time of diagnosis (Launonen et al., 2001).

5.1.3.3 Birt-Hogg-Dubé (BHD) syndrome

BHD is a hereditary cancer syndrome with an autosomal dominant inheritance pattern. It is characterised by a cutaneous tumours (typically fibrofolliculomas), multiple lung cysts, spontaneous pneumothorax and renal tumours (Menko et al., 2009). Approximately a quarter of patients with BHD have RCC (mean age at diagnosis 50 years) with the youngest affected individual at 20 years (Menko et al., 2002; Toro et al., 2008). Chromophobe RCC and mixed chromophobe/oncocytic tumours are typical for BHD but the histopathology is variable and other histological subtypes including clear cell have been reported (Pavlovich et al., 2002). The BHD gene maps to 17p11.2 (Schmidt et al., 2001; Khoo et al., 2001) and germline mutations in a novel gene, *FLCN*, that encodes for folliculin was identified (Nickerson et al., 2002).

5.1.3.4 Von Hippel-Lindau (VHL) disease

Von Hippel-Lindau (VHL) disease (MIM number 193300) is a dominantly inherited familial cancer syndrome that affects approximately 1 in 36,000 individuals and ~20% of cases arise as *de novo* mutations without a family history (Maher et al., 1991a; Richards et al., 1995). It was first reported in the medical literature more than 100 years ago by Treacher Collins who described bilateral vascular growths in the retinas of two siblings (Collins E, *1894*). Ten years later, a similar observation was described in another family by a German ophthalmologist, Eugene von Hippel (*Hippel Ev, 1904*). Arvid Lindau, a Swedish pathologist, had noted that these retinal lesions were associated with an increased risk of developing hemangioblastoma of the brain and spinal cord (*Lindau A, 1927*). The disease was then referred as 'Lindau's disease' until 1936 when Charles Davison first used the eponym 'von Hippel-Lindau disease' (Davison et al., 1936).

Individuals with VHL disease carry one wild-type *VHL* allele and one inactivated *VHL* allele i.e. VHL patients are *VHL* heterozygotes. Tumour or cyst development in VHL disease is linked to somatic inactivation or loss of the remaining wild-type *VHL* allele. Patients affected by VHL are at a high risk of developing clear cell RCC (>70% lifetime risk), retinal and cerebellar haemangioblastomas, phaeochromocytomas and renal, pancreatic and epididymal cysts (Maher, 2004). *VHL*-associated renal tumours are uniformly of clear cell renal carcinoma and is often multifocal and bilateral (Mandriota et al., 2002). The age at which clinical symptoms or signs develop is highly variable and the most common causes of death are unresectable hemangioblastoma or late diagnosed cRCC (Maher and Kaelin, 1997). It has been estimated that the risk of renal cell carcinoma in VHL disease is >70% by the age of 60 years (Maher et al., 1990b).

Clinically, VHL families can be subdivided into type 1 or type 2 based on the absence or presence of pheochromocytoma. Type 1 is characterized by a low risk of pheochromocytoma. It is associated with large deletions and truncating mutations typically predispose to hemangioblastomas and RCC but not pheochromocytoma (Crossey et al., 1994; Maher et al., 1996b; Zbar et al., 1996). Type 2 is usually caused by surface missense mutations and is associated with high risk of pheochromocytoma. An explanation for these findings would be that pheochromocytoma development is due to a mutant pVHL 'gain-of-function' or complete loss of pVHL functions is incompatible with pheochromocytoma development (Kondo and Kaelin, 2001). Type 2 can be further divided into type 2A, type 2B and type 2C. Type 2A has a low risk of RCC while type 2B has a high risk of RCC. Type 2C is associated with familial pheochromocytoma without the other stigmata of VHL disease (Crossey et al., 1995; Eng et al., 1995; Ritter et al., 1996; Woodward et al., 1997; Neumann et al., 1998; van der Harst et al., 1998).

Essentially, all VHL patients have a mutation in the *VHL* gene which resides in 3p25. *VHL* gene mutations have been reported in >500 VHL kindreds (Latif et al., 1993; Crossey et al., 1994; Chen et al., 1995; Zbar et al., 1996; Maher et al., 1996b; http://www.umd.necker.fr). Among patients with VHL disease, ~40% of mutations are genomic deletions and the rest are protein truncating mutations (nonsense, frameshift insertions and deletions, splice site mutations) or intragenic missense mutations. Recurrent missense mutations were also noted in some families which occur at a CpG mutation hotspot at codon 167, for example p.R167W and p.R167Q (Richards et al., 1995). Although a wide variety of mutations have been described, no mutations have been reported in the first 53 amino acids of $pVHL_{30}$ (Woodward and Maher, 2006).

5.1.4 Von Hippel-Lindau (*VHL*) gene

Linkage analysis of VHL kindreds mapped the *VHL* locus to chromosome 3p25 (Seizinger et al., 1988). The gene, *VHL*, was isolated in 1993 using a positional cloning strategy through an international collaboration led by Eamonn Maher (University of Cambridge, England), Michael Lerman, Marston Linehan and Berton Zbar (National Cancer Institute, United States)(Latif et al., 1993). The *VHL* gene contains three exons and encodes an mRNA of approximately 4.5 kb with a long 3'-untranslated region (Latif et al., 1993; Renbaum, 1996). The *VHL* mRNA encodes a protein (pVHL) that contains 213 amino acid residues and migrates with apparent molecular weight of about 24 to 30 kDa (VHL_{30}) (Iliopoulos et al., 1995). The primary sequence of pVHL does not closely resemble any of other known proteins. A second pVHL isoform of approximately 19kDa (VHL_{19}) is produced as a result of internal translational initiation at an in-frame start codon (ATG) at codon 54 (Schoenfeld et al., 1998; Iliopoulos et al., 1998; Blankenship et al., 1999). pVHL

shuttles between the nucleus and cytoplasm (Duan et al., 1995; Lee et al., 1996; Ye et al., 1998; Lee et al., 1999).

Knowledge of the function of the *VHL* tumour suppressor gene product (pVHL) was derived from a number of strategies including observing the effects of reintroducing the wild-type *VHL* gene into cultures of cells which lack functional pVHL. Thus in sporadic clear cell RCC cell lines with pVHL inactivation, the reintroduction of wild-type pVHL into the *VHL* null RCC cell lines restored normal oxygen-dependent regulation of vascular endothelial growth factor (VEGF) and other hypoxia-inducible RNAs (Siemeister et al., 1996; Gnarra et al., 1996; Levy et al., 1996). Iliopoulos et al (1995) demonstrated that *VHL* was a tumour suppressor gene as, when introduced to *VHL* deficient cells, it suppressed tumour growth in nude mice. pVHL is regarded as a 'gatekeeper' tumour suppressor gene product rather than a 'caretaker' due to its ability to suppress growth of fully transformed cells.

Both *VHL* gene products, $pVHL_{30}$ and $pVHL_{19}$ can inhibit the production of the hypoxia-inducible proteins when reintroduced into renal carcinoma cells that lack the wild-type *VHL* allele. The relationship between VHL disease and HIF-α in RCC was first described by Maxwell et al (1999). They reported that cells lacking pVHL are unable to degrade HIF-α under both normoxic and hypoxic conditions, thus cells deficient in pVHL behave as being hypoxic (pseudohypoxic) even in normoxic conditions due to continuous HIF-α activation (Maxwell et al., 1999; Cohen and McGovern, 2005; Weiss and Lin, 2006). The fact that only a subgroup of *VHL* mutation carriers develop RCC and about 25%-30% of sporadic cRCC do not involved alterations in the *VHL* gene suggests involvement of other genes responsible for tumourigenesis of cRCC that might affect the same signalling

pathway as *VHL* or other mechanisms to inactivate *VHL* for example biallelic VHL inactivation due to loss of heterozygosity or methylation (Young et al., 2009).

5.1.5 Function of the VHL protein (pVHL)

The VHL protein (pVHL) has been implicated in several processes but the most well-defined is its role in regulating proteolytic degradation of the α subunits of the hypoxia inducible factor (HIF), HIF-1 and HIF-2 transcription factors. pVHL has two distinct protein binding domains: an α domain interacts with the elongin C protein, which in turn interacts with elongin B and Cullin-2 to form a tetrameric VCBC complex, and a β domain surface binding site which binds HIF-1α and HIF-2α subunits (Pause et al., 1997; Lonergan et al., 1998; Maxwell et al., 1999). Moreover, the Rbx-1 protein was then shown to associate with the VCBC complex (Kamura et al., 1999).

Hemangioblastoma and other *VHL*-related tumours are highly vascular and demonstrate over-production of hypoxia-inducible mRNAs such as vascular endothelial growth factor (VEGF) (Wizigmann-Voos et al., 1995). Many hypoxia-inducible mRNAs are under the control of heterodimeric transcription factors (HIF-1 and HIF-2), which consist of a degradable α subunit and a stable constitutively expressed beta subunit (Schofield and Ratcliffe, 2004). Under normoxic conditions, HIF-1α and HIF-2α are bound by VHL and VCBC complex induces polyubiquitylation and proteosomal degradation (Maxwell et al., 1999; Cockman et al., 2000; Kamura et al., 2000) but under hypoxic conditions the α subunits are stabilised and HIF-1 and HIF-2 activate transcription of a wide repertoire of hypoxia-inducible mRNAs (Schofield and Ratcliffe, 2004). In the absence of functioning pVHL (mutant pVHL), HIF-1 and HIF-2 expression is upregulated, leading to upregulation in expression of hypoxia-inducible mRNAs (Maxwell et al., 1999; Cockman

et al., 2000) (Figure 5.3). The oxygen-dependent interaction of pVHL with HIF-α is provided by the hydroxylation status of key HIF-α proline residues (Pro-402 and Pro-564) (Ivan et al., 2001; Jaakkola et al., 2001; Masson et al., 2001; Yu et al., 2001). Thus, in the presence of oxygen, HIF-α subunits are hydroxylated at the conserved prolyl residues by members of the egg laying defective nine (EGLN) family (also known as the PHD family) (Bruick and McKnight 2001; Epstein et al., 2001). Molecular oxygen and 2-oxoglutarate are essential cosubstrates and iron is an essential cofactor (Epstein et al., 2001; Schofield and Ratcliffe, 2004) and, in the absence of these, hydroxylation does not occur and pVHL is unable to bind the alpha subunits. In humans, three EGLN homologues have been implicated in HIF-α modification (PHD1/EglN2/HIFPH1, PHD2/EglN1/HIFPH2 and PHD3/EglN3/HIFPH3) (Bruick and McKnight 2001; Epstein et al., 2001).

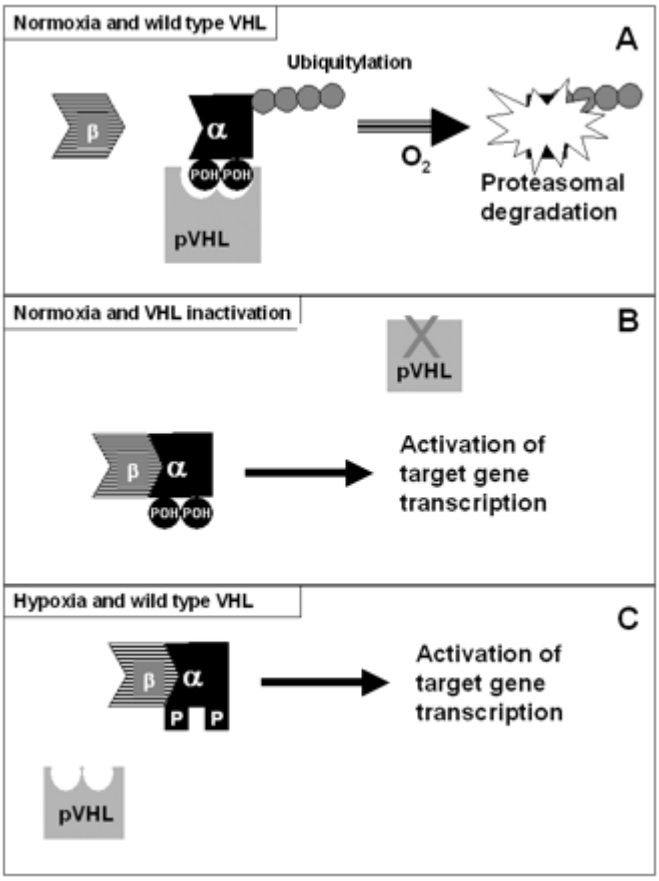

Figure 5.3: Relationship between VHL protein (pVHL) and regulation of hypoxia-inducible factor α subunits. **(A)** Under normoxic conditions, pVHL binds to HIF-α subunits leading to ubiquitylation and proteosomal degradation. The ability of pVHL to bind an HIF-α subunit is dependent on hydroxylation of two proline residues (POH). **(B)** In a tumour with pVHL inactivation, the lack of wild-type pVHL allows HIF-α and HIF-ß subunits to interact and the heterodimeric transcription factors activate expression of a wide repertoire of hypoxia-inducible genes. **(C)** In hypoxia, the two critical proline residues in the α subunit are not hydroxylated (P) and pVHL is unable to bind HIF-α, leading to activation of the hypoxia-inducible gene response. (Adapted from: Woodward and Maher, 2006)

5.1.6 Clear cell renal cell carcinoma and *VHL* tumour suppressor gene

Mutations in the *VHL* gene are mostly restricted to cRCC (Banks et al., 2006) and RCC in patients with VHL disease are always of clear cell histology. Germline inactivation of the *VHL* causes the von Hippel-Lindau disease, and somatic mutations of the remaining wild type of this gene have been linked to the development of tumour or cyst in VHL disease (Kim and Kaelin, 2004). Thus VHL disease conforms to the Knudson 2-hit model

(Knudson, 1971). In sporadic form of cRCC, biallelic *VHL* inactivation (due to hypermeyhylation or mutation) is also common whereby both the first hit and second hit occur somatically ie. after conception rather than in the germline.

Mutations in *VHL* are extremely heterogenous: 20-37% of VHL patients have large or partial germline deletion, 30-38% have missense mutations and 23-27% have nonsense or frameshift mutations (Maher and Kaelin, 1997; Stolle et al., 1998). The mutations are distributed throughout the coding sequence except that intragenic missense mutations are rarely observed in the first 50 codons (Zbar et al., 1996). Furthermore, type 2 VHL patients almost invariably harbour *VHL* missense mutations while patients with type 1 frequently harbour *VHL* deletions or truncation mutations (Crossey et al., 1994; Chen et al., 1995; Maher et al., 1996b; Zbar et al., 1996).

Kidneys removed from VHL patients typically contain a multitude of smaller lesions or preneoplastic renal cysts of varying sizes and renal cell carcinomas. Immunohistochemical and genetic evaluation of the epithelial cells lining these renal cysts show early loss of *VHL* and overexpression of HIF and HIF target genes such as *VEGF* (Zhuang et al., 1994; Zhuang et al., 1996; Lubensky et al., 1996; Wiesener et al., 2001; Mandriota et al., 2002). Overexpression of HIF-responsive growth factors, as well as their receptors, is also a feature of renal carcinomas (Mydlo et al., 1989; Lubensky et al., 1996). Thus, *VHL* likely serves as an early "gatekeeper" tumour suppressor gene for renal cell carcinoma and it is presumed that further genetic alterations are needed for progression of preneoplastic renal cysts to renal carcinomas (figure 5.4).

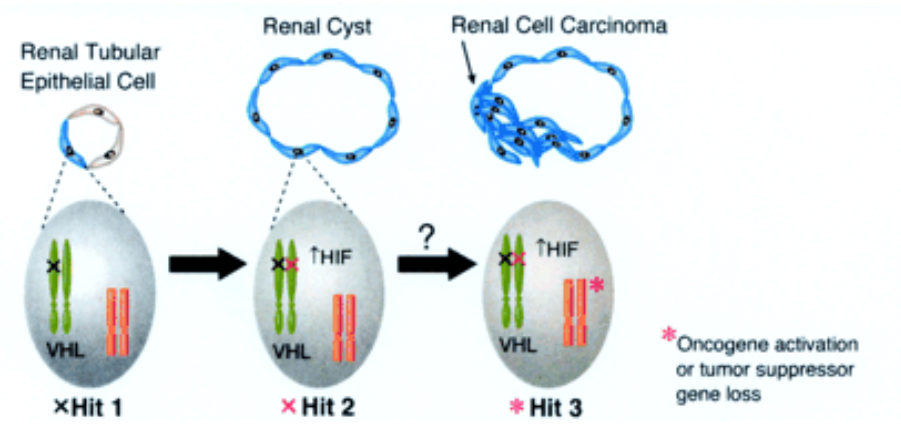

Figure 5.4: Pathogenesis of von Hippel-Lindau (VHL) disease-associated renal cell carcinoma. Biallelic *VHL* inactivation in a renal tubular epithelial cell stabilizes HIF, correlating with the formation a premalignant renal cyst. Alterations at other loci are probably required for carcinoma development. In VHL disease, the first *VHL* mutation (hit) is present in the germline.
(Adapted from Kim and Kaelin, 2004)

This study is aim to identify copy number changes and characterise chromosomal changes in primary tumours of clear cell renal cell carcinoma from sporadic, VHL disease and renal cell carcinoma cell lines using 250K SNP Array.

5.2 Materials and methods

5.2.1 DNA samples

Genomic DNA was extracted from primary renal cancers (sporadic and VHL) and cell lines by standard methods and stored at -80^{o}C. Three groups of renal cancers were investigated: (a) 21 clear cell RCC from 21 patients with von Hippel-Lindau disease, (b) 13 sporadic clear cell RCC without evidence of somatic *VHL* mutations or promoter methylation (details of mutation and methylation analyses have been reported previously (McRonald et al., 2009) (c) 23 RCC cell lines which include 786O, 769P, A498, A704, ACHN, Caki1, Caki2, CAL54, KTCL26, KTCL140, RCC1, RCC4, RCC6, RCC11, RCC12, RCC48, SKRC18, SKRC39, SKRC45, SKRC47, SKRC54, UMRC2 and UMRC3. Ethical approval for collection of clinical material was obtained from the South Birmingham Ethics Committee and relevant local ethics committees. DNA concentrations were measured with Nanodrop model ND-1000 spectrophotometer (NanoDrop Technologies, Wilmington, DE).

5.2.2 Affymetrix GeneChip 250K mapping arrays

Experiments were performed according to standard protocols for Affymetrix GeneChip Mapping 250K sty1 arrays (Gene Chip Mapping 500K Assay Manual (P/N 701930 Rev2., Affymetrix Santa Clara, CA). Quality control, genotype calling, and probe level normalization were made in the Affymetrix GeneChip Genotyping Analysis Software (GTYPE) 4.1. The Dynamic Model (DM) algorithm was used to perform quality control, a call rate >93% was required. Genotype calls were made using the BRLMM algorithm (Rabbee and Speed, 2006). Subsequent analysis, including copy number normalization to produce log2 ratios was performed using the genotyping console (GTC) v2.0. The

reference set was 48 samples from the HapMap project (www.hapmap.org/downloads/raw_data/affy500k/).

5.2.3 MLPA analysis

MLPA was applied to confirm some of the deletions and duplications identified from SNP microarray. The MLPA Kit used was SALSA P007-A1 Human Chromosome Kit (MRC Holland, Amsterdam, The Netherlands) that contains probes for 40 different target sequences (refer appendix A5). Among these are many genes that are often deleted or amplified in various tumours. The analysis was performed according to the manufacturer's instructions. The ligation products were amplified on a Tetrad thermal cycler (Peltier 225 from MJR). PCR products were then separated by capillary electrophoresis on a Beckman Coulter CEQ 8000 genetic analyser. Electropherograms were analysed using GeneMarker MLPA Analysis (SoftGenetics, LLC, USA). Deletions were indicated by a value of <0.785 and duplications by >1.33.

5.3 Results of copy number changes of sporadic clear cell renal cell carcinoma (cRCC) using 250K SNP array

Clear cell renal cell carcinoma (cRCC) is genetically complex involving a large number of chromosome aberrations throughout the whole genome. Of the 13 cases of sporadic cRCC without *VHL* inactivation analysed using Affymetrix 250K SNP array, only one showed no copy number changes. Another one sample was not included because of excess background signal. The reference set for 250K Sty1 mapping arrays was 48 samples from the HapMap project (www.hapmap.org/downloads/raw_data/affy500k/) and six normal controls were used for MLPA, The average call rate of the 12 samples was 95.7±2.18.

Most of the changes involved large segments (> 10.5 Mb) of chromosome arm or the whole chromosome arm or even the whole chromosome (table 5.1 and figure 5.5). Whole arm/large fragment (≥10 Mb) deletions were seen slightly less frequent compared to duplications/amplifications with a total number of 62 and 70 respectively, making an average of deletions 5.2 and duplications/amplifications 5.8 per tumour. Similar findings were also observed with small (<10 Mb) changes; 7 deletions and 13 gains. The most common chromosome deletion was at 3p (6 cases, 50.0%). Among the 3 cases with whole 3p deletion, 1(LS16) also had whole 3q loss (table 5.1 and table 5.2). Complete loss of chromosome arm was also found in 1p, 1q, 6p, 6q, 8p, 14q (table 5.1). Loss of 1p and 14q were the second most common deletion (5 cases, 41.7%) involving only large fragments/whole chromosome arm (table 5.1 and figure 5.5). Of the 5 cases of 1p deletion, 2 cases (LS7 and LS21) were found to have complete loss of the chromosome while in chromosome 14, 3 cases were identified to have a total loss of the long arm of the chromosome (table 5.1 and table 5.2). Deletions were the sole event seen in 6q as well as in 10q and 17p, although at a lower frequencies, ~8.3%-25%. However, deletions were not detected in chromosomes 5, 7, 12, 15q, 19q and 20. Small deletions were identified in chromosomes 3q, 6p, 9p, 11p, 12p, 16p, 22q in only a handful of cases and at a very low frequency.

Table 5.1: Chromosome gains and losses in primary tumours of sporadic cRCC

Chrom. arm	Losses				Gains			
	Whole arm	Fragment ≥10 Mb	Frequency	Fragment <10 Mb	Whole arm	Fragment ≥10 Mb	Frequency	Fragment <10 Mb
1p	2	3	5	0	0	1	1	0
1q	2	1	3	0	0	1	1	0
2p	1	0	1	0	1	1	2	0
2q	1	2	3	0	1	1	2	0
3p	3	3	6	0	1	0	1	0
3q	1	1	2	1	1	3	4	0
4p	1	0	1	0	2	0	2	0
4q	1	1	2	0	2	0	2	0
5p	0	0	0	0	2	1	3	0
5q	0	0	0	0	2	4*	6	2
6p	2	1*	3	1	0	1	1	0
6q	2	1	3	0	0	0	0	0
7p	0	0	0	0	2	0	2	0
7q	0	0	0	0	2	0	2	0
8p	3	0	3	0	0	1	1	1
8q	1	2	3	0	0	5	5	0
9p	1	1	2	1	1	0	1	0
9q	1	2	3	0	1	1	2	2*
10p	1	0	1	0	1	0	1	0
10q	1	0	1	0	0	0	0	0
11p	0	1	1	1	1	0	1	0
11q	0	2	2	1	1	0	1	0
12p	0	0	0	0	3	0	3	0
12q	0	0	0	0	3	0	3	0
13q	0	3	3	0	0	1	1	0
14q	3	2	5	0	1	0	1	0
15q	0	0	0	0	2	0	2	0
16p	0	1	1	1	1	1	2	1
16q	0	1	1	0	1	2	3	0
17p	1	0	1	0	0	0	0	0
17q	1	0	1	0	0	0	0	1
18p	1	0	1	0	0	1	1	0
18q	1	1	2	0	0	2	2	1
19p	0	1	1	0	0	0	0	3*
19q	0	0	0	0	0	1	1	0
20p	0	0	0	0	2	1	3	0
20q	0	0	0	0	2	2	4	2
21q	1	0	1	0	1	1	2	0
22q	0	0	0	0	1	0	1	0

*contain region ≥4 copies

Abbreviations*:* p, short arm; q, long arm; Mb, megabase; Chrom, chromosome

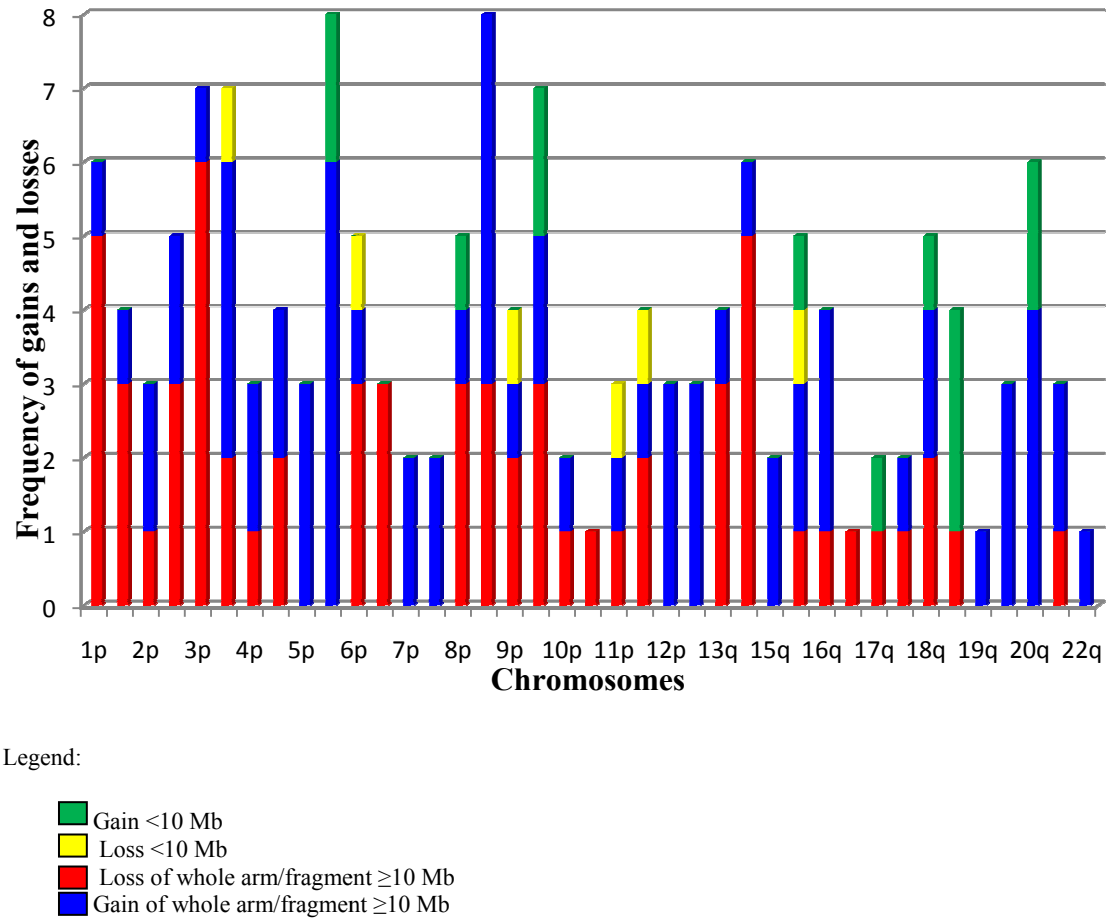

Figure 5.5: Frequency of gains and losses in sporadic cRCC.

Overall, large gains involved all autosomes except 6q, 10q, 17 and 19p (table 5.1 and figure 5.5). In addition, chromosome gains involving large and small fragments were observed as the only event in chromosomes 5, 7, 12, 15q, 19q and 20. The most chromosome gain encountered in 5q consisting of 6 large fragments/whole arm and 2 small fragments. Of the six cases, 2 had whole gain of 5p with 1 (LS7) showed gain of the whole chromosome. Region of amplification (≥4 copies) was detected in 5q31.3-q35.1 (39.1 Mb). The two small gains were identified in 5q21.1-q21.3 (5.2 Mb) and 5q35.3 (2.9 Mb). All the regions of gain in 8q (5 cases, 41.7%) involved large fragments ranging from 14.4 Mb to 98.5 Mb. Among the 4 cases which showed gain in 3q, 1 (LS7) had gain of the

whole chromosome 3 (table 5.1 and table 5.2). Of the 4 cases with gain 20q, two (LS8 and LS16) showed gain of the whole chromosome 20 (table 5.2). Gain of whole chromosome 12 was detected in cases LS3, LS7 and LS8. Gain in chromosome 7 involved the whole chromosome which was found in two cases (LS7 and LS8). Other gains of whole chromosome arms included 5p, 16q, and 20p in ~25% of the csases.

Table 5.2: Whole chromosome loss and gain in sporadic cRCC

	Cases										
	JS259	LS3	LS7	LS8	LS9	LS10	LS16	LS17	LS18	LS20	LS21
CHR1			loss								loss
CHR2			loss				gain				
CHR3			gain				loss				
CHR4			gain		loss		gain				
CHR5			gain								
CHR6			loss				loss				
CHR7			gain	gain							
CHR8										loss	
CHR9			gain		loss						
CHR10			loss								
CHR11			gain								
CHR12		Gain	gain	gain							
CHR13											
CHR14			gain		loss		loss				loss
CHR15			gain	gain							
CHR16			gain								
CHR17			loss	loss							
CHR18											
CHR19											
CHR20				gain			gain				
CHR21				gain							loss
CHR22			gain								

Amplification in small regions was found in 9q33.2-q34.11 (8.1 Mb) and 19p12 (1.7 Mb). All except one of the cases with deletion 3p involved large fragments involving deletion of *VHL* gene. Among the 6 cases, 3 showed complete 3p loss, 2 with almost complete loss 3p (spanning 3p12.1-p26.3) and 1 with interstitial deletion in 3p11.2-p13 (not including *VHL* gene in 3p25). In addition to large duplications in 5q, 2 small duplications were identified

in 5q21.1-q21.3 and 5q35.3 with a size of ~5.2 Mb and ~2.9 Mb respectively. There was a region of amplification spanning 5q31.3-q35.1 (39.1 Mb). Details of the overlapping regions in chromosomes 3 and 5 as well as other chromosomes together with MLPA analysis for confirmation in some of the regions are shown in table 5.3. Microarray and the MLPA copy number analysis results were concordant.

Table 5.3: Overlap regions of gains and losses in ≥33% of sporadic cRCC cases

Chrom.	Region	Start	End	Size (Mb)	MLPA probes
Gain					
3q	3q24-q29	146,340,000	196,600,000	49.7	
5q	5q31.3-q35.1	141,500,000	180,625,000	39.1*	IL12B (5q33.1)
5q	5q35.3	178,000,000	180,857,866	2.9	
8q	8q11.21-q13.2	49,000,000	70,000,000	21.0	
8q	8q21.3-q24.3	90,800,000	146,264,000	55.5	
16p	16p11.2	28,450,000	31,325,000	2.9	MVP (16p11.2)
20q	20q11.22-q11.23	32,170,000	35,980,000	3.8	
20q	20q13.2-q13.33	50,270,000	62,435,964	12.2	
Loss					
1p	1p13.3-p31.1	83,500,000	110,650,000	27.2	
1p	1p34.2-p36.33	0	43,200,000	43.2	CTPS (1p34.2)
3p	3p12.1-p13	73,000,000	84,000,000	11.0	
3p	3p13-p26.3	0	73,000,000	73.0	
6p	6p21.2-p21.33	30,000,000	38,460,000	8.5	LTA (6p21.3), CDKN1A (6p21.2)
14q	14q12-q31.2	25,380,000	82,685,000	57.3	NFKBIA (14q13)

*≥4 copies (amplification)
Abbreviations*:* p, short arm; q, long arm; Mb, megabase; Chrom, chromosome

Some of the overlapping regions of deletion harboured known tumour suppressor genes, for example *TP73* at 1p36.32 or oncogene such as *myc* at 8q24.21.

5.4 Discussion

Previous reported cytogenetic and copy number analyses of sporadic RCC (Klatte et al., 2009, Dalgliesh et al., 2010) will have comprised mainly clear cell RCC with *VHL* inactivation. For example, in an analysis of 282 tumours of unselected RCC, Klatte et al (2009) had identified the most frequent cytogenetic changes were loss of 3p (60%), 14q (28%), 8p (20%), 6q (17%), loss of 9p (16%) and 4p (13%), gain of 5q (33%) and trisomy 7 (26%). Similarly, copy number analysis of sporadic RCC using high resolution SNP arrays abnormalities demonstrated recurrent losses on 3p, 4, 6q, 8p, 9p and 14q and recurrent gains on 1q, 2, 5q, 7 and 12 (Dalgleish et al 2010). In the present study, twelve cases of cRCC without evidence of *VHL* mutations or methylation were analysed for copy number changes using high resolution 250K SNP microarray. Large gains and losses were frequent and often involved the whole chromosome arm or the whole chromosome. Deletion 3p was found in 50% of the cases (5/6 tumours with 3p25 loss and 1/6 with 3p11.2-p13 loss). The fact that one of the *VHL* was deleted and the other was retained (without evidence of mutations or methylation) in these tumours is interesting and suggests several possible explanations. Firstly a *VHL* mutation might be present but not detectable by standard analysis (e.g. if located in an intron). Alternatively, other 3p TSGs may be implicated in these cases. Thus Bodmer et al (2002) suggested that region 3p12-p14 might contain gene(s) involved in tumour development and allele loss at 3p21/methylation of *RASSF1A* has also been implicated in RCC (Clifford et al., 1998, Morrissey et al., 2001). However, my findings suggest that there could be another group of cRCC which does not involved mutations, methylation or deletions of *VHL* as shown in the *VHL* wild type cRCC cases which do not have deletion 3p. Thus, suggesting alternative non-*VHL* independent pathway(s) as the mechanism in promoting tumourigenesis in this group of cRCC.

Large gain 5q was encountered in 6/12 (50%) of the cases with 5q35.3 as the smallest overlapping region. Among the genes that reside in the region is *MAPK9* which are involved in a wide variety of cellular processes such as proliferation, differentiation, transcription regulation and development, thus might be a candidate gene for cRCC. Similar finding was observed by Chen et al (2009) using Ilumina's 317K high resolution SNP arrays in a study of 80 patients with cRCC. Another common region in 5q was identified in 5q31.3-q35.1 (table 5.3). Gain in 5q31-qter had been associated with favourable prognosis in cRCC (Gunawan et al., 2001). Another interesting study had revealed *TGFBI* which resides in 5q31.1 may be a putative oncogene for cRCC (Matsuda et al., 2008). However, the region identified in the present study does not support the finding.

The second most common gain was observed in chromosome 8q. All the five cases involved gain of large fragments (≥10 Mb). Minimal common gain was identified in two regions; 8q11.21-q13.2 and 8q21.3-q24.3 (table 5.3). One of the known proto-oncogene in 8q24.21 is *MYC* and the gene was shown to be consistently overexpressed in tumours with 8q24 amplification (Beroukhim et al., 2009).

Deletion in chromosome 1p was also common in this study, 5/12 (41.7%) of the cases. Two cases showed deletion of the whole chromosome, one case with interstitial deletion spanning 1p12-p31.1 and the other two were terminal deletions. Two regions of common deletions in all of the five cases were shown to be in 1p13.3-p31.1 and 1p34.2-p36.33. Beroukhim et al (2009) carried out copy number and gene expression analysis on 90 cRCC tumours of both sporadic and VHL disease and identified gene *RUNX3* (in 1p36.11) as a candidate gene for cRCC. This gene encodes a member of the runt domain-containing

family of transcription factors. It functions as a tumour suppressor and is frequently deleted or transcriptionally silenced in cancer.

With the same frequency as in deletion 1p, deletion 14q was another common finding in this study. Of the five cases, three had deletion in the whole 14q and two with almost all of chromosome 14q deleted. Beroukhim et al (2009) had identified region 14q31.1 to be deleted in 42% of the cases and Toma et al (2008) found deletion 14q in 36% of cRCC cases. A positive correlation between allelic loss and chromosome 14q especially 14q24-q31 and 14q31-q32 and poor prognosis were described (Mitsumori et al., 2002; Kaku et al., 2004; Alimov et al., 2004).

Gain of chromosome 20q was found in four cases (33.3%). Two cases had duplication of the whole chromosome, two cases with interstitial and terminal duplications. Minimal overlap region of the four cases was identified in 20q11.22-q11.23 (~3.8 Mb) and 20q13.2-q13.33 (~12.2 Mb). In another study, gain in 20q13.33 was identified in 20% of cRCC cases (Beroukhim et al., 2009). However, gain of chromosome 20q was shown to be more frequently detected in papillary RCC (Sanders et al., 2002; Brunelli et al., 2003). Deletion in other chromosomes were also found at a lower frequency (~25%) which includes 1q, 2q, 6p, 6q, 8p, 8q and 9q and gain of 5p, 12p, 12q and 16q.

High resolution methods such as microarrays have facilitated the investigation of copy number changes in this study. At present the most widely detected copy number changes are large with deletion 3p, 1p and 14q and gain 5q and 8q as the most frequent changes. This study also suggests that there is a subset of cRCC without biallelic inactivation of *VHL*, similar to the findings made by Beroukhim et al (2009). Based on the expression

profiles and copy number changes, they separate the cRCC without biallelic inactivation into two groups: one with expression profiles including *HIF*-responsive genes, different from the majority of cRCC and the other with similar copy number and expression profiles to tumours with such inactivation. The observation in the latter group raises the possibility that the former group has unobserved genetic alterations of the *VHL* pathway and may respond to treatment targeting this pathway.

Interestingly, present study also suggests another group of cRCC with non-*VHL* inactivation i.e. $VHL^{+}/^{+}$. Further investigations including expression study or application of higher resolution arrays and massive parallel sequencing techniques will give information as to whether this group really represent another group of cRCC or has unidentified *VHL* inactivation.

5.5 Results of copy number changes of clear cell renal cell carcinoma (cRCC) in VHL using 250K SNP array

The reference set for 250K Sty1 mapping arrays was 48 samples from the HapMap project (www.hapmap.org/downloads/raw_data/affy500k/). A total of 21 samples of cRCC from VHL patients were analysed. The average call rate of the samples was 97.19±1.47. In general, copy number changes in VHL cRCC were not complex. The majority of the cases had large deletion in 3p (15 cases, 71%) and duplication in 5q (13 cases, 62%) (table 5.4). Changes in the other chromosomes were also observed but not as frequent (<23%). Deletions of whole arm/fragment ≥10 Mb were encountered more than duplications, 62 and 59 respectively. These tumours have on average 2.9 deletions and 2.8 duplications. Data in table 5.4 is summarized in figure 5.6.

Table 5.4: Chromosome gains and losses identified in cRCC of the VHL tumours

Chrom. arm	**Losses**				**Gains**			
	Whole arm	Fragment ≥10 Mb	Frequency	Fragment <10 Mb	Whole arm	Fragment ≥10 Mb	Frequency	Fragment <10 Mb
1p	0	3	3	0	0	0	0	0
1q	0	0	0	0	0	3	3	1
2p	0	0	0	0	3	0	3	0
2q	0	0	0	0	3	1	4	0
3p	7	10	17	0	0	1	1	0
3q	0	4	4	0	0	2	2	2
4p	2	1	3	0	0	1	1	0
4q	2	1	3	0	0	0	0	0
5p	1	0	1	0	2	0	2	0
5q	0	1	1	0	0	13	13	0
6p	0	1	1	0	1	0	1	0
6q	0	0	0	0	1	0	1	0
7p	0	0	0	0	5	0	5	0
7q	0	1	1	0	3	1	4	0
8p	1	3	4	0	0	0	0	1*
8q	0	1	1	0	0	3	3	0
9p	1	0	1	0	1	0	1	0
9q	1	0	1	2	1	0	1	0

10p	0	0	0	0	0	1	1	0
10q	0	3	3	0	0	0	0	0
11p	0	0	0	0	2	0	2	0
11q	0	0	0	0	2	0	2	0
12p	0	0	0	0	0	0	0	0
12q	0	1	1	0	0	0	0	0
13q	1	1	2	0	0	3	3	0
14q	3	0	3	0	1	0	1	0
15q	1	0	1	3	0	0	0	0
16p	0	1	1	0	0	0	0	1
16q	0	2	2	0	0	1	1	0
17p	0	0	0	1	0	0	0	2
17q	0	0	0	0	0	1	1	0
18p	1	0	1	0	0	0	0	0
18q	1	0	1	0	0	0	0	0
19p	1	0	1	1	0	1	1	0
19q	1	1	2	0	0	0	0	0
20p	0	0	0	0	1	0	1	0
20q	0	0	0	0	1	0	1	0
21q	0	1	1	0	1	0	1	0
22q	1	1	2	1	0	0	0	0

* Contain ≥ 4 copies

Abbreviations: p, short arm; q, long arm; Mb, megabase; Chrom, chromosome

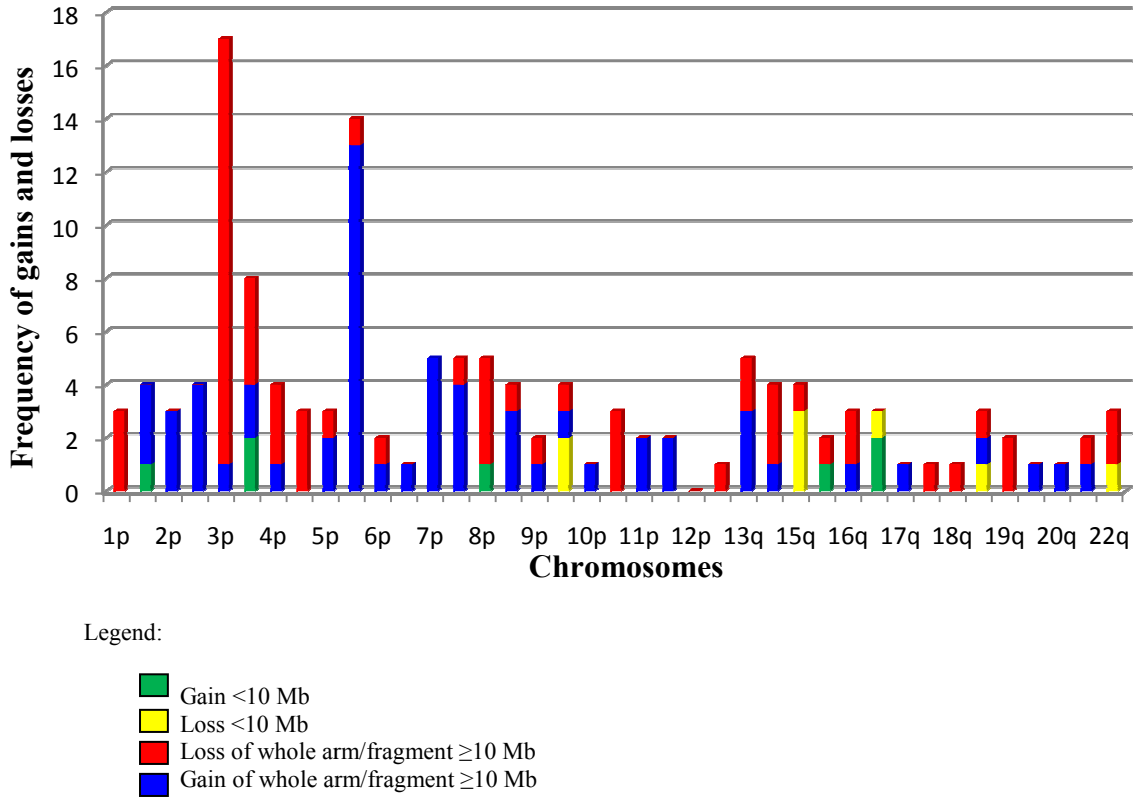

Figure 5.6: Frequency of gains and losses of cRCC in VHL

Deletions in 3p involved whole arm/large fragment and among the 15 cases, 2 had two large deletions on the chromosome arm (making it a total of 17, see table 5.4) and 7 showed complete loss of 3p. Two recurrent duplications on 5q were identified in 5q32-q35.3 (~37.7 Mb) and 5q21.1-q35.3 (~78.6 Mb). Gain of 7p was observed in 5/21 (23.8%) and involved the whole chromosome arm. Deletion 3q, 8p and gain 2q, 7q were not as common as shown in only about 19% of the tumours. Details of overlapping regions were shown in table 5.5. MLPA analysis was done to verify the changes in some of the regions. Microarray and the MLPA copy number analysis results were concordant.

Table 5.5: Overlapping regions of gains and losses in ≥19% of cRCC in the VHL tumours studied

Chrom.	Region	Start	End	Size (Mb)	MLPA probes
Gain					
2q	2q23.3-q37.3	153,000,000	242,951,149	89.9	
5q	5q32-q35.3	143,200,000	180,857,866	37.7	IL12B (5q33.1)
7p	7p11.2-p22.3	0	57,500,000	57.5	
7q	7q11.21-q22.1	64,000,000	99,370,000	35.3	
7q	7q32.1-q36.3	127,600,000	158,821,424	31.2	CASP2 (7q35)
Loss					
3p	3p14.2-p21.1	52,000,000	61,820,000	9.8	
3p	3p21.31-p26.3	0	44,750,000	44.7	
3q	3q13.11-q13.31	104,880,000	116,409,600	11.5	
3q	3q11.2-q13.11	95,350,000	104,880,000	9.5	
8p	8p12-p23.3	0	34,880,000	34.9	

Abbreviations: p, short arm; q, long arm; Mb, megabase; Chrom, chromosome

5.6 Discussion

This is the second array-based genome wide analysis of copy number abnormalities in VHL disease associated cRCC. Beroukhim et al (2009) had analysed 36 metachronous primary tumours from 12 patients with VHL disease (in addition to 54 sporadic cRCC) using the same platform. The most frequent copy number change (86% of VHL RCC) was 3p loss including the *VHL* tumour suppressor gene. 5q gain was the second most common with the smallest overlapping region identified in 5q32-q35.3. Similarly, the present study also observed deletion 3p as the most frequent (76.2%) and gain 5q (61.9%) as the second most common. Also common is gain 7p which was observed in 5 cases (23.8%) and all of them involved the whole short arm of the chromosome. Gain in chromosomes 1q, 2p, 2q, 7q, 8q, 13q and deletion in 1p, 3q, 4p, 4q, 8p, 10q and 14q were encountered at a lower frequency ~14%-19% of the cases. Genome wide analysis of the previous studies were of

unselected cRCC (i.e. unspecified whether the tumours were from VHLs or sporadics). Comparing the findings of the present study with the previous reports (Cifola et al., 2007; Toma et al., 2008; Matsuda et al., 2008; Beroukhim et al., 2009) all of the changes observed were similar except gain 2p and 13q and loss 3q and 4p were identified only in the present study (table 5.6).

Table 5.6: Previous studies of copy number changes in cRCC

Author (year)	Sample	Method	Chrom. Gain	Chrom. Loss	LOH
Cifola et al (2007)	27 cRCC tumour tissue	Affymetrix 100K SNP array	4p15.1-q13.1	1p36.32-p36.31	1p36.22-36.21
			4q26-q28.3	1p36.11	2q36.3
			5p15.1-p14.1	3p26.3-p26.2	3p26.3
			5q11.2-q12.3	3p25.3-p25.1	3p26.2-p25.3
			5q14.3-q21.3	9q33.3-q34.11	3p24.3
			5q23.1-q34	22q13.1-q13.2	3p14.3
			7p21.3-p21.2		3q22.1
			7q21.11		6q16.1
			7q31.31-q31.32		6q22.1-q22.31
			11p15.1-q12.1		6q22.31
			11q14.2-q22.3		6q22.33-q23.2
			12q12-q15		6q25.2-q25.3
			12q21.31-q23.1		6q26
			14q21.1-q21.3		9q31.1-q31.2
			16p11.2-q11.1		13q33.2
			19p12-p11		
			22p13-p11.2		
Toma et al (2008)	22 primary cRCC and matched normal kidney tissue	Affymetrix 10K SNP array	5q23.3-5qter	3pter-3p21.31	3p
			7q11.21-7qter	14q23.3-14q.32.31	9
				9pter-9qter	14
				6q23.2-6q26	
Matsuda et al (2008)	35 cRCC tissue and 7 normal controls	Affymetrix 100K SNP array	3	1p	
			5q22-qter	3p	
			5q23.2-q34	10q	
			7q31-q34	19p	
			7p	6q	
			8q	9p	
			12q	11p	
			16	13q	

			17	14q	
				18	
				22q	
Beroukhim et al (2009)	90 cRCC tumours (sporadics and VHLs)	Affymetrix 250K SNP array	1q	1p	
			2q	3p	
			5q	4q	
			7q	6q	
			8q	8p	
			12p	9p	
			20q	14q	

The VHL tumours without 3p deletion showed no LOH in the region (data not shown). In these cases, it is possible that the wild type VHL allele is inactivated by somatic mutation or exon deletion or promoter methylation that would not be detected by LOH analysis. Other 3p tumour suppressor genes (e.g. *RASSF1A*) might also be inactivated in a similar manner (though *RASSF1A* is usually inactivated by methylation rather than mutation (Morrissey et al., 2001).

5.7 Results of copy number changes of RCC cell lines using 250K SNP Array

The average call rate (%) for the 23 samples was 96.2±2.15. All of the 23 RCC cell lines exhibited copy number changes with majority involving large/whole arm deletions and/or duplications (table 5.7, figure 5.7). Deletions of whole arm/large fragments were observed less than duplications/amplifications of whole arm/large fragments, 301 and 331 respectively, making an average of 13.1 deletions and 14.4 duplications/amplifications per cell line. Deletion 14q was seen in all of the lines and most (21/23, 91.3%) involved almost the whole long arm. All of the cell lines except one (SKRC47) showed deletions in 3p. Of these, 19 (86.3%) showed *VHL* deletion and the remaining 3 cell lines had deletion in 3p12.3-p21.31, 3p13-p22.2 and 3p14.2 respectively. Evidence of homozygous deletion in 3p14.2 which harboured *FHIT* gene was found in RCC48.

Frequent loss of large fragment/whole arm was also detected in other chromosomes which includes 4q (18/23, 78.3%), 18q (18/23, 78.3%), 13q (16/23, 69.6%), 1p (16/23, 69.6%), 4p (12/23, 52.2%), 8p (12/23, 52.2%), 9p (12/23, 52.2%), 9q (11/23, 47.8%), 15q (11/23, 47.8%). Among the 12 cell lines with deletion 4p, 11 showed complete loss of chromosome 4. The 9 cell lines which showed a complete loss of 18p also had a complete loss of 18q. Similar finding was observed in chromosome 9 where 5 of the cell lines showed a complete loss of the chromosome. In addition, homozygous deletion at 9p21.3 was identified in 8 cell lines (ACHN, Caki1, CAL54, RCC1, RCC11, RCC4, RCC6 and SKRC54) and at 9p23-p24.1 in 3 cell lines (Caki1, RCC1 and RCC6). The former region with the size of an ~0.4 Mb contains 3 genes (*MTAP, CDKN2A, CDKN2B*) and the latter ~1.0 Mb contains only 1 gene (*PTPRD*).

The most common chromosomal gain were seen in chromosomes 7p (21/23, 91.3%), 7q (20/23, 86.9%), 12q (18/23, 78.3%), 8q (17/23, 73.9%), 5q (17/23, 73.9%), 2q (15/23, 65.2%), 20q (15/23, 65.2%), 16p (14/23, 60.9%), 5p (13/23, 56.5%), 17q (13/23, 56.5%), 16q (13/23, 56.5%), 1q (13/23, 56.5%), 3q (12/23, 52.2%), 20p (12/23, 52.2%), 2p (11/23, 47.8%). Some of them also involved whole gain of the chromosome, for example in chromosomes 7 (14/23), 12 (8/23), 16 (9/23), 20 (11/23) (table 5.7).

Table 5.7: Chromosome gains and losses identified in the RCC cell lines

Chr. arm	Losses				Gains			
	Whole arm	Fragment ≥10 Mb	Frequency	Fragment <10 Mb	Whole arm	Fragment ≥10 Mb	Frequency	Fragment <10 Mb
1p	2	14	16	0	0	9	9	0
1q	2	5	7	0	0	13*	13	0
2p	0	6	6	0	5	6	11	0
2q	0	3	3	3	5	10	15	0
3p	4	18	22	1**	0	5	5	1
3q	4	4	8	1	0	10*	10	1
4p	11	1	12	0	0	4	4	0
4q	11	7	18	0	0	3	3	1
5p	2	2	4	0	5	8*	13	1*
5q	2	5	7	1	5	12	17	1
6p	5	0	5	0	3	3	6	2
6q	5	4	9	0	3	6	9	0
7p	0	1	1	0	14*	7	21	1*
7q	0	1	1	0	14	6*	20	2*
8p	0	12	12	0	2	1	3	0
8q	0	3	3	1	2	15	17	1
9p	5	7	12	11**	1	1*	2	0
9q	5	6	11	0	1	5	6	0
10p	3	6	9	0	2	1	3	2*
10q	3	0	3	1	2	6	8	0
11p	3	4	7	0	1	4	5	0
11q	3	7	10	0	1	2	3	0
12p	0	1	1	0	8	2	10	2
12q	0	1	1	1	8	10*	18	0
13q	0	16	16	1	0	3	3	1
14q	0	23	23	0	0	0	0	0
15q	0	11	11	0	0	3	3	2
16p	1	2	3	0	9	5	14	0
16q	1	2	3	2**	9	4	13	0
17p	0	7	7	0	5	4	9	2*
17q	0	1	1	2	5	8*	13	6
18p	9	1	10	0	0	2	2	1
18q	9	9	18	0	0	0	0	0
19p	0	2	2	4	1	2	3	2
19q	0	2	2	0	1	4	5	4
20p	1	3	4	3	11	1	12	1
20q	1	0	1	0	11	4	15	1
21q	0	7	7	0	0	3	3	0
22q	0	4	4	0	0	3	3	0

*contain ≥4 copies (amplification) ** contain homozygous deletion
Abbreviations: p, short arm; q, long arm; Mb, megabase; Chr, chromosome

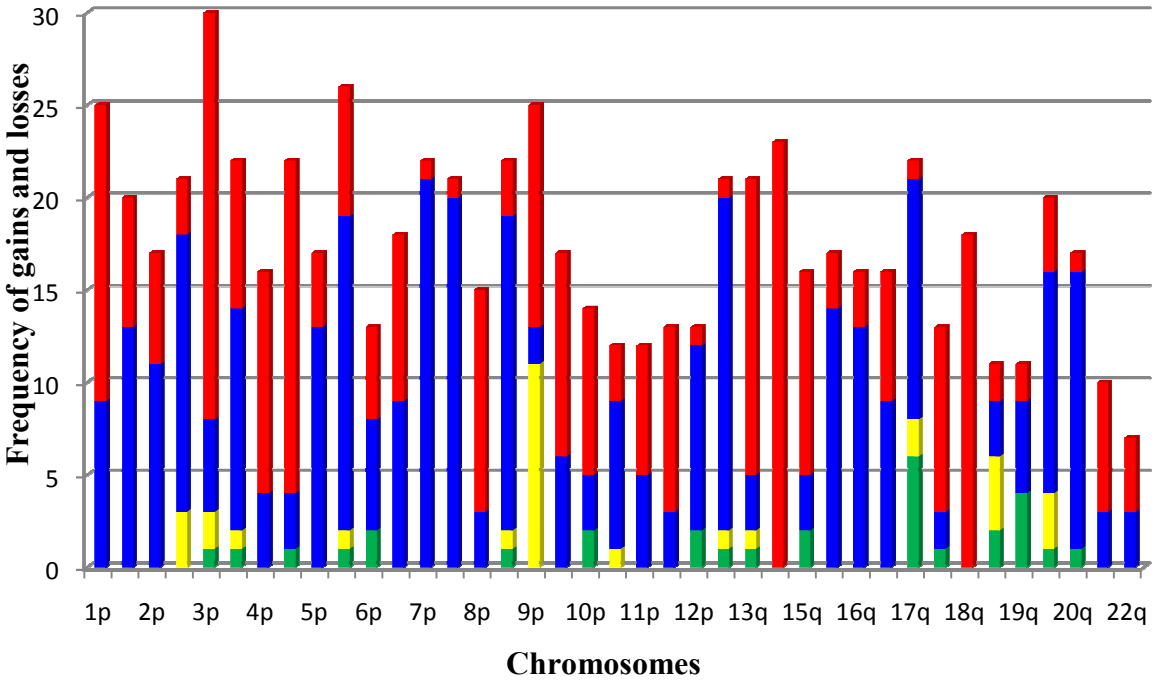

Legend:

Gain <10 Mb
Loss <10 Mb
Loss of whole arm/fragment ≥10 Mb
Gain of whole arm/fragment ≥10 Mb

Figure 5.7: Frequency of gains and losses in RCC cell lines

Minimal overlapping region of the most common (>43%) copy number changes which include gain 2q, 5q, 7, 8q, 12q, 20q and loss 1p, 3p, 4q, 9p, 13q, 14q and 18q is shown in table 5.8.

Table 5.8: Minimal overlapping region of gains and losses in the RCC cell lines

Chr.	Location	Start position	End position	Size (Mb)	Frequency (%)
Gain					
2	2q35-q36.3	216,000,000	228,800,000	12.8	11 (47.8)
	2q24.3-q33.3	164,000,000	206,271,500	42.3	12 (52.2)
	2q11.2-q14.3	95,000,000	122,660,000	27.7	12 (52.2)
3	3q22.1-q29	133,228,000	199,501,827	66.2	10 (43.5)
5	5q34-q35.3	164,700,000	180,857,866	16.2	17 (73.9)
7	7p11.2-p12.1[a]	53,000,000	57,500,000	4.5	18 (78.3)
	7p21.2-p22.3[b]	0	15,000,000	15.0	18 (78.3)
	7q34-q36.3	138,434,000	158,821,424	20.4	18 (78.3)
	7q11.21-11.22 [c]	61,500,000	68,635,000	7.1	18 (78.3)
8	8q24.12-q24.3	120,000,000	146,274,826	26.2	16 (69.6)
12	12q24.22-q24.33	116,500,000	132,349,534	15.8	12 (52.2)
	12q12-q13.2	37,200,000	54,900,000	17.7	14 (60.9)
16	16p11.2-p13.3	0	31,500,000	31.5	14(60.9)
20	20q11.21-q11.23	29,340,000	34,349,000	5.0	16 (69.6)
Loss					
1	1p35.3-p36.33	0	28,800,000	28.8	13 (56.5)
3	3p14.2 [d]	59,500,000	60,100,000	0.6	20 (87.0)
	3p21.2-p26.3	0	51,680,000	51.6	19 (82.6)
	3p11.2-p13	73,000,000	89,400,000	16.4	20 (87.0)
4	4q12-q13.1	56,330,000	65,000,000	8.6	15 (65.2)
	4q31.22-q35.2	146,000,000	191,273,063	45.2	16 (69.6)
8	8p21.3-p23.3	0	23,300,000	23.3	12 (52.2)
9	9p21.3 [e]	21,800,000	22,200,000	0.4	17 (73.9)
	9p23-p24.1[f]	9,000,000	10,000,000	1.0	14 (60.9)
13	q12.1-q13.1	18,000,000	32,000,000	14.0	15 (65.2)
14	q11.2-q13.1	20,000,000	32,000,000	12.0	23 (100)
	q23.1-q32.33	56,000,000	106,368,585	50.4	22 (95.7)
18	q22.3-q23	67,400,000	76,117,153	8.7	17 (73.9)

Abbreviations*:* p, short arm; q, long arm; Mb, megabase; Chr, chromosome
[a] contain ≥4 copies (amplification) in 2/18 cases
[b] contain ≥4 copies (amplification) in 1/18 cases
[c] contain ≥4 copies (amplification) in 3/18 cases
[d] homozygous deletion in 1/20 cases
[e] homozygous deletion in 7/17 cases
[f] homozygous deletion in 2/14 cases

The most copy number changes were found in Caki2 (24 gains and 22 losses) and the least in KTCL140 (4 gains and 5 losses) (figure 5.8, table 5.9). Other cell lines which showed a high number of gains and losses (total gains and losses of 33- 40) include UMRC2, UMRC3, SKRC39, SKRC45, RCC 48 and Caki1. Total changes between 21 and 28 were seen in SKRC47, SKRC 54, SKRC18, RCC6, RCC1, RCC11, RCC12, CAL54 and A498. Cell lines 769P, A704, RCC4, 786O, ACHN and KTCL 26 had 15 to 20 chromosomal changes (figure 5.8, table 5.9).

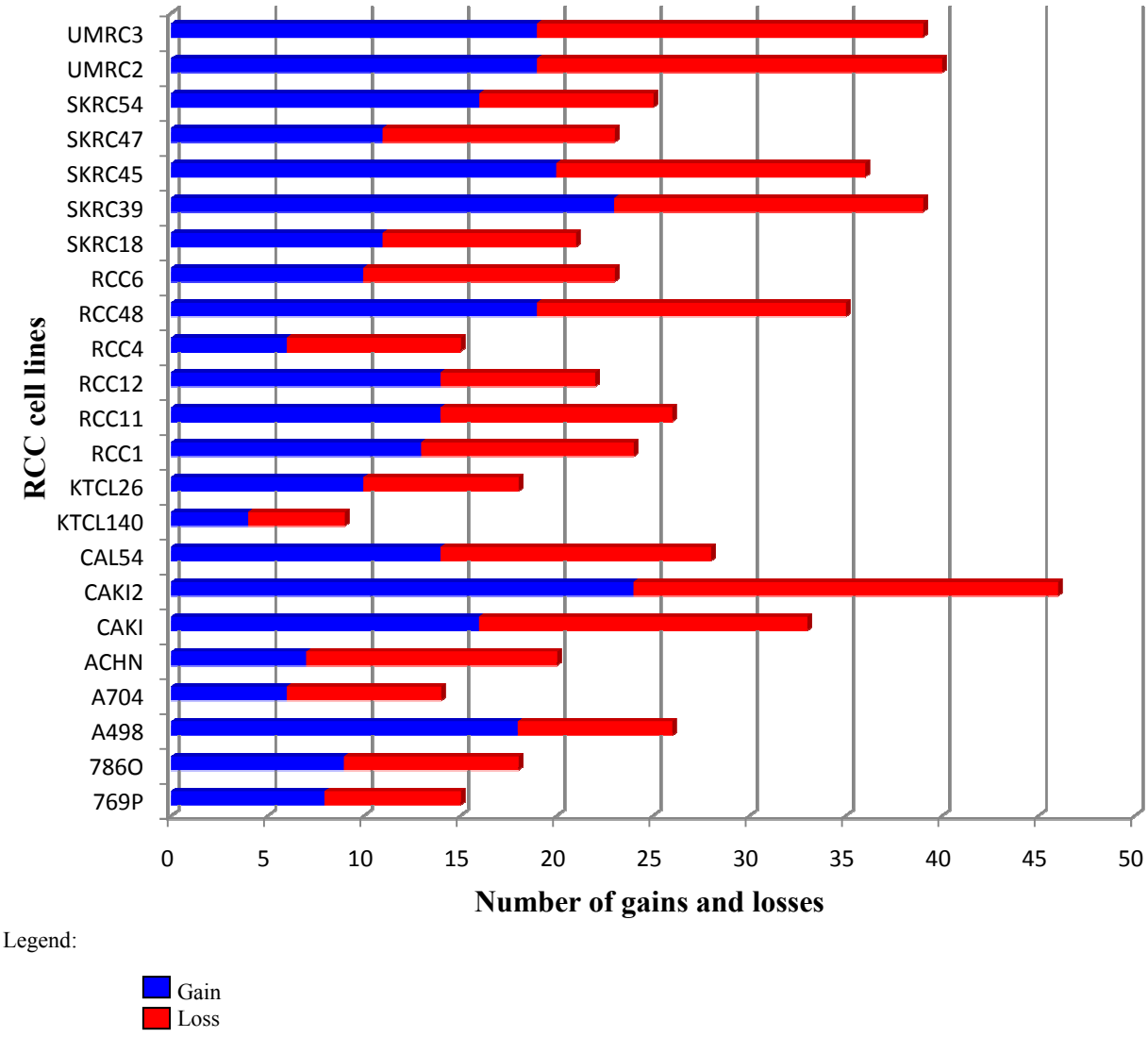

Figure 5.8: Number of gains and losses of the 23 RCC cell lines studied

Table 5.9: Details of chromosome regions of gains and losses of the RCC cell lines

Cell line	Gains	Total gain	Losses	Total loss
769P	1q23.1-q44, 2, 5q31.2-q35.3, 7, 8q11.22-q24.3, 12, 17	8	1p35.3-p36.33, 3, 6, 9p21.3-p22.3, 9q12-q21.11, 11q14.1-q25, 14q11.2-q32.33	7
786O	2p11.2-p24.3, 2q11-q37.3, 5p12-p15.33, 5p12, 7, 8q11.21-q24.3, 9q21.13-q34.3, 20q11.21-q13.33,	9	3p11.2-p13, 3p21.2-p26.3, 4q31.22-q35.2, 5q11.2-q21.1, 8p11.21-p23.3, 13q12.11-q34, 14q11.2-q32.33, 18q12.2-q23, 19q13.11-q13.42	9
A498	1q21.2-q44, 2p11.2-p25.3, 2q11.2-q34, 5p12-p15.33, 7, 8q11.21-q24.3, 9, 11p11.2-p15.5, 16, 17, 19p12, 19q12, 19q13.11-q13.12, 19q13.33-q13.43, 20p12.2-p11.21, 20q11.21-q13.33, 21q11.2-22.3	18	1p35.1-p36.33, 2q22.1, 3p21.2-p26.3, 6, 11q11.2-q25, 14q11.2-q32.33, 18q11.32-q23, 20p12.2-p13	8
A704	3p12.1, 5q15-q35.3, 7, 12, 16p11.2-p13.3	6	1p35.1-p36.13, 3p12.3-p26.3, 4, 6q21-q27, 9, 14q11.2-q32.33, 16q12.1-q24.3, 20p21	8
ACHN	1q21.1-q44, 2, 7, 10q11.21-q26.3, 12, 16, 17	7	1p35.1-p36.33, 3, 4, 5, 6, 8p11.21-p23.3, 8q11.21-q21.11, 9p21.3, 13q12.11-q32.3, 15q11.2-q26.3, 14q11.2-q32.33, 18q12.2-q23, 20	13
Caki1	1q21.1-q44, 3q12.1-q29, 4p12-p16.3, 4q12-q13.3, 5p14.3-p15.33, 5p12-p13.1, 5q15-q35.3, 7q22.3-q36.3, 8q11.21-q24.3, 12q12-q24.33,16q12.1-q24.3, 17q11.2-q22, 17q22-q25.3, 18p11.21-p11.32, 19p13.3, 20q11.21-q11.23	16	1p21.3-p31.1, 3p12.3-p26.3, 6q22.32-q27, 9p23-p24.1, 9p21.3, 9q12-q21.11, 11q14.1-q25, 12p11.21-p13.33, 13q12.1-q13.1, 15q11.2-q22.2, 14q11.2-q32.33, 17p11.2-p13.3, 18q11.2-q23, 19p13.3, 20p11.21-p13, 21q11.2-q22.3, 22q11.21-q13.33	17
Caki2	1q21.1-q44, 2p11.2-p25.3, 2q11.2-q14.3, 2q24.3-q33.3, 2q37.1-q37.3, 3q22.1-q29, 4q12, 5q33.2-q35.3, 6p11.2-p12.1, 6q12-q13, 6q16.1-q21, 6q22.31-q24.1, 7, 12p11.21-p11.22, 12q12-q14.2, 12q14.2-q21.32, 12q24.22-q24.33, 15q26.1-	24	1p12-p31.3, 2q37.1-q37.3, 3p11.2-p26.3, 3q11.2-q21.3, 4q12-q13.1, 6q25.1-q27, 8p11.21-p23.3, 8q11.21-q12.1, 9p11.2-p24.3, 9q12-q21.33, 11p11.12-p14.1, 11q12.1-q25, 12q21.32-	22

	q26.3, 16p11.2-p13.3, 17q11.2-q25.33, 19p12-p13.2, 19q12-q13.43, 20, 22q11.21-q13.33		q24.22, 13q12.11-q34, 14q11.2-q13.1, 14q23.1-q32.33, 16q11.2-q21, 16q21, 17p11.2-p13.3, 18q11.2-q23, 19p13.3, 19p13.2-p13.3	
CAL54	2, 3p11.2-p12.3, 3q11.2-q29, 7p15.2-p22.3, 7p11.2-p14.3, 7q11.21-q34, 7q34-q36.3, 8, 9q22.31-q34.3, 12, 16, 17, 20	14	1, 3p12.3-p26.3, 4, 5, 6, 9p11.2-p24.3, 9q12-q22.31, 10, 11, 13q12.11-q34, 15q11.2-q26.3, 14q11.2-q32.33, 18, 21q11.2-q22.3	14
KTCL140	5q21.3-q35.3, 15q11.2, 17q24.3-q25.3	4	1p35.2-p36.33, 3p14.1-p26.3, 4, 5q11.2-q21.3, 14q11.2-q32.33	5
KTCL26	1p21.3-p31.3, 1q25.2-q44, 5, 6, 7, 8q11.23-q24.23, 9q21.13-q34.3, 11p11.2-p15.5, 16q12.1-q24.3, 20,	10	2p11.2-p25.3, 3, 4, 9p11.2-p24.3, 10p11.22-p15.3, 11q22.3-q25, 13q12.11-q14.3, 14q21.3-q32.33	8
RCC1	1p11.2-p31.1, 3q22.1, 3q22.1-q29, 5, 6p21.1, 6q14.1-q27, 7, 8q11.23-q24.23, 10, 19p12-p13.3, 19q13.12-q13.43, 20q11.21-q13.33, 22q11.21-q13.33	13	1q21.1-31.1, 3p11.2-p26.3, 3q11.2-q21.3, 4, 8p11.21-p23.3, 9, 15q25.3-q26.3, 14q11.2-q32.33, 16, 18, 21q11.2-q22.3	11
RCC11	1p12-p33, 1q21.1-q44, 2, 5q21.3-q35.3, 6, 7, 8q11.23-q24.23, 12p11.21-p13.33, 15q11.2-q26.3, 16, 17, 20, 21q11.2-q22.3, 22q11.21-q13.33	14	1p35.1-p36.33, 3, 4, 5p12-p15.33, 5q11.2-q21.1, 8p11.21-p23.3, 9, 10, 11, 13q12.11-q34, 14q11.2-q32.33, 18	12
RCC12	2, 4p14-p16.3, 5q21.1-q35.3, 6p12.1-p25.3, 6q12-q22.33, 7, 8q11.21-q24.3, 9q21.13-q31.2, 11, 12, 13q14.12-q21.33, 16p11.2-p13.3,16q21-q23.1	14	3p12.2-p26.3, 4q12-q35.2, 8p11.21-p23.3, 9p13.1-p24.3, 14q11.2-q32.33, 15q11.2-q26.3, 14q11.2-q32.33, 17p11.2-p13.2	8
RCC4	1p32.2-p35.1, 5q23.3-q35.3, 6, 16, 20	6	1p35.1-p36.33, 3p12.3-p29, 4,9p13.1-p22.3, 9q12-q34.3, 13q12.11-q21.1, 15q11.2-q26.3, 14q11.2-q32.33, 21q11.2-q22.3	9
RCC48	1p11.2-p35.3, 1q32.2-q44, 2q11-q37.3, 3q11.2-q29, 5p12-p15.33, 5q34-q35.3, 6p12.1-p25.3, 6q12-q25.2, 7, 8q11.21-q24.3, 11p11.22-p15.5, 12p11.21-p13.33, 12q12-q13.2, 12q21.1-q21.32, 15q11.2-q26.3, 17q21.31-q25.1, 17q25.3, 20	19	1p35.3-p36.33, 1q21.1-q32.1, 2p11.2-p25.3, 2q22.3, 3p12.3-p26.3, 4, 9, 10, 12q14.2-q21.1, 13q12.11-q34, 14q11.2-q32.33, 16q24.1-q24.3, 17p11.2-p13.1, 18, 19p12-p13.3, 19q12-q13.32	16

RCC6	2p11.2-p25.3, 2q11.2-q24.1, 2q35-q36.3, 3q21.1-q29, 5, 6p12.1-p25.3, 7, 8q11.21-q24.3, 12p13.33-q24.33, 16, 20	10	1, 2q24.2-q34, 2q36.3-q37.3, 3p12.3-p26.3, 3q11.2-q21.1, 4, 8p12-p23.3, 9, 13q12.11-q34, 14q11.2-q32.33, 17p11.2-p13.3, 18, 22q11.22-q12.3	13
SKRC18	3q11.2-q29, 5, 7, 8q11.21-q24.3, 10q11.21-q26.3, 12p11.21, 12q12-q24.33, 16p11.2-p13.3, 17p11.2-p13.3, 19q13.42-q13.43, 20	11	1p32.3-p36.33, 1q23.3-q25.2, 3p12.3-p21.31, 11q13.2-q25, 13q12.11-q34, 15q11.2-q22.31, 14q11.2-q23.1, 17q25.3, 18q11.2-q23, 22q11.22-q13.33	10
SKRC39	1p31.3-p13.1, 1q25.2-q44, 2q11-q37.3, 3p22.3-p26.3, 3p11.2-p12.3, 5p12-p15.33, 5q15-q35.3, 7p11.2-p22.3, 7q11.21-q34, 8q11.23-q21.11, 8q24.12-q24.3, 10p11.21-p11.22, 12q12-q23.3, 16, 17p11.2, 17p13.2-p13.3, 17p13.1, 17q21.32, 17q21.32-q21.33, 17q24.2, 17q25.2-q25.3, 20,	23	3p13-p22.2, 4q12-q35.2, 6q26-q27, 7q35-q36.3, 8p12-p23.3, 8q11.21-q11.23, 9p13.1-p24.3, 10p11.22-p15.3, 11p11.12-p15.5, 13q12.11-q21.31, 13q33.3-q34, 15q11.2-q21.1, 14q12-q32.33, 18, 21q11.2-q21.1, 21q22.2-q22.3,	16
SKRC45	3p21.31-p26.3, 3p11.2-p14.1, 3q21.1-q29, 3q11.2-q11.2, 4q26-q31.23, 5q21.2-q21.3, 5q21.1-q35.3, 7p11.2-p22.3, 7q11.21-q11.22, 8q21.3-q24.3, 9p23-p24.3, 10q11.21-q26.3, 11q12.1-q25, 12, 13q31.2-q31.3, 16p11.2-p13.3, 16q12.1-q23.2, 17q21.31-q25.3, 18p11.21-p11.32, 21q11.2-q22.3	20	3p14.2, 3q13.32-q21.1, 3q26.1, 4p12-p16.3, 4q12-q26, 5q11.2-q21.2, 5q21.3-q22.1, 8p12-p23.3, 9p13.1-p23, 10p11.21-p15.3, 11p13-p15.1, 15q11.2-q26.3, 14q11.2-q32.33, 18q12.1-q22.1, 20p11.22-p13, 22q11.22-q13.33	16
SKRC47	5,7q34-q36.3, 10q11.21-q26.3, 11p15.1-p15.5, 12q12-q23.1, 13q12.11-q34, 17p11.2-p13.3, 19q12-q13.2, 19q13.43, 20,	11	1q24.2-q41, 2p24.1-p25.3, 4, 8p11.21-p23.3, 9p21.3-p24.3, 10p11.21-p15.3, 15q11.2-q26.3, 14q11.2-q32.33, 16p11.2-p13.3, 17q11.2-q25.33, 18q21.33-q23, 19p12-p13.3	12
SKRC54	1q31.3-q44, 3q11.2-q29, 5p12-p15.33, 7p11.2-p22.3, 7q11.21-q11.22, 7q11.22-q36.3, 8q13.2-q21.3, 10p12.31-p14, 10p11.1-p11.22, 10q11.21-q26.3, 12, 16, 17p11.2-p13.3, 19, 20	16	3p12.3-p26.3, 8p11.21-p23.3, 8q11.21-q13.1, 9p21.3, 9q13-q31.1, 10p14-p15.3, 13q12.11-q34, 14q11.2-q32.33, 18	9
UMRC2	1p31.3-p34.2, 1p11.2-p13.2, 1q21.1-q44, 2q22.1-q37.3, 3q11.2-q29, 4p12-p16.3, 4q12-q21.3,	19	1p34.3-p36.33, 1p13.3-p31.3, 2p11.2-p25.3, 2q11.2-q22.1, 3p12.3-p26.3, 4q22.1-	21

	5q14.3-q35.3, 7, 8, 9q32-q34.3, 10, 11q13.1-q25, 12, 15q11.2-q25.3, 16, 17q11.2, 17q12-q25.3, 18p11.21		q35.2, 5p12-p14.3, 5q11.2-q14.1, 6, 11p11.12-p15.5, 11q12.1-q13.1, 13q12.11-q34, 15q25.3-q26.3, 14q11.2-q32.33, 17p11.2-p13.3, 17q11.2-q12, 18p11.21-p11.32, 18q11.2-q23, 19p13.12-p13.3, 21q11.2-q22.3, 22q11.22-q13.33	
UMRC3	1p22.3-p34.3, 1q31.2-q42.2, 1q42.3-q44, 2p16.3-p24.1, 2p13.2-p14, 2q11.2-q37.3, 3q11.2-q29, 4p12-p16.3, 4q12-q24, 5p12-p15.33, 8p11.21-p12, 8q24.21-q24.3, 10q11.23-q24.2, 12q21.31-q24.33, 13q31.1-q33.3, 17q12-q25.3, 20p11.21-p11.23, 20q11.21-q13.33	19	1p12-p22.3, 1q12-q31.1, 2p24.1-p25.3, 2p12-p13.2, 3p12.3-p26.3, 4q25-q35.2, 7p11.2-p22.3, 8p21.3-p23.3, 9p13.1-p24.3, 10p11.21-p15.3, 10q11.23-q11.21, 11, 13q12.11-q22.2, 13q33.3-q34, 14q11.2-q32.33, 16q11.2-q24.3, 17p11.2-p13.3, 18q22.3-q23, 20p12.3-p13, 20p12.1	20

Abbreviations*:* p, short arm; q, long arm

5.8 Discussion

Copy number changes in the 23 RCC cell lines detected in the present study appears complex, involving the whole genome (table 5.7, figure 5.7). The changes were also most frequently involved large fragments (>10 Mb) with gains detected more frequently than losses (average of 14.4 duplications/amplifications and 13.1 deletions per cell line). Earlier report by Pavlovich et al (2003) had identified deletion 3p, gain 5q and trisomy 7 as the most common findings in 10 RCC cell lines and 5 renal tumours using spectral karyotyping (SKY) and comparative genomic hybridisation (CGH) methods. Strefford et al (2005) applied CGH on 19 RCC cell lines (of which nine of them were also investigated in the present study). Many of the findings are in agreement with the present report for example gain 1q, 5q, 7 and loss 1p, 3p, 14q. However, the increased resolution of 250K SNP array applied in the present study has allowed the detection of more regions of gains and losses on the chromosomes (table 5.10 and 5.11). Thus the use of microarray has given more information about the chromosomal changes associated with RCC.

Table 5.10: Regions of gain in the RCC cell lines identified by Strefford et al (2005) compared with the present study

Cell line	Gains (Strefford et al., 2005)	Gains (present study)
SKRC45	5q21~qter,7q21.1~pter,8q23~q24.3, 9q,11q,13	3p21.31-p26.3, 3p11.2-p14.1, 3q21.1-q29, 3q11.2-q11.2, 4q26-q31.23, 5q21.2-q21.3, 5q21.1-q35.3, 7p11.2-p22.3, 7q11.21-q11.22, 8q21.3-q24.3, 9p23-p24.3, 10q11.21-q26.3, 11q12.1-q25, 12, 13q31.2-q31.3, 16p11.2-p13.3, 16q12.1-q23.2, 17q21.31-q25.3, 18p11.21-p11.32, 21q11.2-q22.3
769P	1q25~qtel,4q28~qtel,5p15.1~ptel, 5q31~qtel,8q21.3~qtel,12q14~ptel	1q23.1-q44, 2, 5q31.2-q35.3, 7, 8q11.22-q24.3, 12, 17
786O	1q32~qter,4p15.1~q21,5p10~pter,7q10~qter,8q10~qter,12q21.1~pter	2p11.2-p24.3, 2q11-q37.3, 5p12-p15.33, 5p12, 7, 8q11.21-q24.3, 9q21.13-q34.3, 20q11.21-q13.33
A498	1q32~qter,2p10~pter,4q28~qter,5p10~pter,5q23.3~qter,7,8q21.3~qter,9q31~q34.1,17q21.3~qter,20q10~qter	1q21.2-q44, 2p11.2-p25.3, 2q11.2-q34, 5p12-p15.33, 7, 8q11.21-q24.3, 9, 11p11.2-p15.5, 16, 17, 19p12, 19q12, 19q13.11-q13.12, 19q13.33-q13.43, 20p12.2-p11.21, 20q11.21-q13.33, 21q11.2-22.3
A704	1q32~qter,5q14~qter,7,11q10~qter,12, 20q10~qter	3p12.1, 5q15-q35.3, 7, 12, 16p11.2-p13.3
ACHN	1q32~qter,2p10~pter,5p10~pter,7,12,16, 17p10~pter	1q21.1-q44, 2, 7, 10q11.21-q26.3, 12, 16, 17
Caki1	1q21.3~qter,5q13~pter,7q21.2~qter, 8q13~qter,11p12~pter,17q21.3~qter	1q21.1-q44, 3q12.1-q29, 4p12-p16.3, 4q12-q13.3, 5p14.3-p15.33, 5p12-p13.1, 5q15-q35.3, 7q22.3-q36.3, 8q11.21-q24.3, 12q12-q24.33,16q12.1-q24.3, 17q11.2-q22, 17q22-q25.3, 18p11.21-p11.32, 19p13.3, 20q11.21-q11.23
Caki2	7p15~pter,8q22.3~qter,12q13.3~qter,20, 21,22q13.1~qter	1q21.1-q44, 2p11.2-p25.3, 2q11.2-q14.3, 2q24.3-q33.3, 2q37.1-q37.3, 3q22.1-q29, 4q12, 5q33.2-q35.3, 6p11.2-p12.1, 6q12-q13, 6q16.1-q21, 6q22.31-q24.1, 7, 12p11.21-p11.22, 12q12-q14.2, 12q14.2-q21.32, 12q24.22-q24.33, 15q26.1-q26.3, 16p11.2-p13.3, 17q11.2-q25.33, 19p12-p13.2, 19q12-q13.43, 20, 22q11.21-q13.33
CAL54	7,12q13.3~qter,20	2, 3p11.2-p12.3, 3q11.2-q29, 7p15.2-p22.3, 7p11.2-p14.3, 7q11.21-q34, 7q34-q36.3, 8, 9q22.31-q34.3, 12, 16, 17, 20

Abbreviations: p, short arm; q, long arm; chrom., chromosome; ter, terminal

Table 5.11: Regions of loss in the RCC cell lines identified by Strefford et al (2005) compared with the present study

Cell line	Losses (Strefford et al., 2005)	Losses (present study)
SKRC45	1p31.1~pter,3p14.1~p21.3,6,8q21.1~pter,9q,14,15,16q22~qter,18q12.3~qter,19,22	3p14.2, 3q13.32-q21.1, 3q26.1, 4p12-p16.3, 4q12-q26, 5q11.2-q21.2, 5q21.3-q22.1, 8p12-p23.3, 9p13.1-p23, 10p11.21-p15.3, 11p13-p15.1, 15q11.2-q26.3, 14q11.2-q32.33, 18q12.1-q22.1, 20p11.22-p13, 22q11.22-q13.33
769P	1p34.6~ptel,3p13~ptel,11q14.3~qtel, 14q13~qtel,Y	1p35.3-p36.33, 3, 6, 9p21.3-p22.3, 9q12-q21.11, 11q14.1-q25, 14q11.2-q32.33
786O	1p32~pter,3p14.1~p22,4q32~qter,8p10~pter, 10p10~ptel,14q13~qter,18q21.3~pter	3p11.2-p13, 3p21.2-p26.3, 4q31.22-q35.2, 5q11.2-q21.1, 8p11.21-p23.3, 13q12.11-q34,14q11.2-q32.33, 18q12.2-q23, 19q13.11-q13.42
A498	1p32~pter,3p12~q25,6q15~qter,11q14.3~qter, 18,19q10~qter,Xq24~qter	1p35.1-p36.33, 2q22.1, 3p21.2-p26.3, 6, 11q11.2-q25, 14q11.2-q32.33, 18q11.32-q23, 20p12.2-p13
A704	3p10~pter,6q10~qter,9,14,16q13~qter, 22q13.1~qter	1p35.1-p36.13, 3p12.3-p26.3, 4, 6q21-q27, 9, 14q11.2-q32.33, 16q12.1-q24.3, 20p21
ACHN	4q10~qter,9p10~pter,Y	1p35.1-p36.33, 3, 4, 5, 6, 8p11.21-p23.3, 8q11.21-q21.11, 9p21.3, 13q12.11-q32.3, 15q11.2-q26.3, 14q11.2-q32.33, 18q12.2-q23, 20
Caki1	3p14.2~p23,6,9p12~p21,14q11.2~qter,15, 18q10~qter,22q11.2~qter,Y	1p21.3-p31.1, 3p12.3-p26.3, 6q22.32-q27, 9p23-p24.1, 9p21.3, 9q12-q21.11, 11q14.1-q25, 12p11.21-p13.33, 13q12.1-q13.1, 15q11.2-q22.2, 14q11.2-q32.33, 17p11.2-p13.3, 18q11.2-q23, 19p13.3, 20p11.21-p13, 21q11.2-q22.3, 22q11.21-q13.33
Caki2	3p14.2~p23,9p10~pter,11q13.5~qter, 13q23.3~qter,17p10~pter,18q10~qter	1p12-p31.3, 2q37.1-q37.3, 3p11.2-p26.3, 3q11.2-q21.3, 4q12-q13.1, 6q25.1-q27, 8p11.21-p23.3, 8q11.21-q12.1, 9p11.2-p24.3, 9q12-q21.33, 11p11.12-p14.1, 11q12.1-q25, 12q21.32-q24.22, 13q12.11-q34, 14q11.2-q13.1, 14q23.1-q32.33, 16q11.2-q21, 16q21, 17p11.2-p13.3, 18q11.2-q23, 19p13.3, 19p13.2-p13.3
CAL54	3p12~p21.3,9p10~pter,10q21.2~qter, 13q21.1~q1	1, 3p12.3-p26.3, 4, 5, 6, 9p11.2-p24.3, 9q12-q22.31, 10, 11, 13q12.11-q34, 15q11.2-q26.3, 14q11.2-q32.33, 18, 21q11.2-q22.3

Abbreviations: p, short arm; q, long arm; chrom., chromosome; ter, terminal

Deletion 1p, 3p, 4q, 9p, 13q 14q and 18q and gain 1q, 2q, 5p, 5q, 7p, 7q, 8q, 12q, 16p, 16q, 17q, 20p and 20q were the most common changes (>52%) observed in the present study. A previous analysis of a very large number of unselected RCC tumours reported that the most frequent cytogenetic changes were loss of 3p (60%), 14q (28%), 8p (20%), 6q (17%), loss of 9p (16%) and 4p (13%), gain of 5q (33%) and trisomy 7 (26%) (Klatte et al., 2009). Similarly, copy number analysis of sporadic RCC tumours using high resolution SNP arrays abnormalities demonstrated recurrent losses on 3p, 4, 6q, 8p, 9p and 14q and recurrent gains on 1q, 2, 5q, 7 and 12 (Dalgliesh et al., 2010) and Beroukhim et al (2009) reported amplification 1q, 2q, 5q, 7q, 8q, 12p and 20q and deletion 1p, 3p, 4q, 6q, 8p, 9p and 14q as the most frequent copy number changes in cRCC tumours (sporadics and VHLs). All of the changes found in the present study were also found in the previous reports (Beroukhim et al., 2009; Klatte et al., 2009; Dalgliesh et al., 2010) except deletion 13q, 18q and gain 16, 17q and 20p. These might reflect changes associated with the different subtype of RCC other than the clear cell. For example, large deletion 13q was associated with chromophobe subtype of RCC (Schwerdtle et al., 1996).

Deletion 14q was seen in all of the cell lines studied with all having large deletions. A similar study by Strefford et al (2005) identified deletion 14qtel in more than 63% of the 19 RCC cell lines. Although it had also been detected in cRCC tumours but the frequency was not as high, for example Beroukhim et al (2009) detected deletion in 14q31.1 in 42% of the 90 cRCC tumours from sporadic and VHL, Toma et al (2008) found deletion 14q23.3-q32.31 in 36% of the 22 cRCC tumour samples. Deletion 14q had been related with a sarcomatoid component in RCC which is usually aggressive, potentially metastatic and associate with poor prognosis (Matsuda et al., 2008). LOH in 14q was shown to be

related with tumour aggressiveness and poor survival in RCC (Mitsumori et al., 2002; Alimov et al., 2004).

All except one cell line (22/23, 95.7%) showed deletion in 3p. Most of the deletions involved large fragments and of the 22 cell lines, 19 (86.4%) showed deletion of the *VHL* gene which maps to 3p25.3. This study has identified three most frequently deleted regions on 3p; 3p14.2, 3p21.2-p26.3, 3p11.2-p13 (table 5.8). Many reports before have focused on three regions as rearrangements have been repeatedly observed in them: 3p12-p14, 3p21 and 3p25-p26 (Lubinski et al., 1994; van den Berg and Buys, 1997). Deletion in either 3p25 or 3p12-14 occurred in adenomas whereas carcinomas occurred in 3p21 together with losses in 3p25 or 3p12-14 or both. In the present study, most of the deletion involved long and terminal 3p thus supporting the previous observation (Chudek et al., 1997; Alimov et al., 2000; Sukosd et al., 2003). In addition, one of the cell lines, SKRC45, had a focal interstitial deletion in 3p14.2, without deletion in the other two regions (3p21.2-p26.3 and 3p11.2-p13). The only gene which resides in the region is *FHIT* and this suggests that deletion of the gene alone can implicate cRCC. Another cell line, RCC48 had a homozygous deletion in the same region with the same size (~0.6 Mb), although deletions in the other two regions were also observed. The *FHIT* gene is a putative tumour suppressor factor that has been related to malignancies of the lungs, head and neck, breast carcinoma, Merkel cell carcinoma, colon tumours, cervical carcinomas and renal carcinomas (Virgilio et al., 1996; Sozzi et al., 1996; Ohta et al., 1996; Negrini et al., 1996; Hadaczek et al., 1998; Luceri et al., 2000).

Previous reports had identified deletions or loss of heterozygosity in the 3p14.2 region and altered expression of the FHIT protein occurs in kidney cancers (Hadaczek et al., 1999;

Velickovic et al., 1999; Sukosd et al., 2003). The *FHIT* gene has been shown to suppress growth of cancer cells *in vitro* and *in vivo* (Roz et al., 2002) and restoration of *FHIT* gene expression in *FHIT*-deficient mice prevents tumour development (Dumon et al., 2001). Reports by Chudek et al (1997) and Sukosd et al (2003) described a terminal 3p deletion in most of the cases they studied and concluded that interstitial deletions did not exist in cRCC and that the interstitial 3p deletions identified by some of the studies could be due to technical artifacts. The number of cell lines involved with interstitial 3p deletions in the present study were too low (3/22), therefore it cannot be concluded whether the observation reflect the true genetic mechanism or only an artifact.

The next most common changes were gain of chromosome 7p and 7q with most of the cell lines showing whole chromosome gain (table 5.7). Minimal overlap region was found in 7p11.2-p12.1, 7p21.2-p22.3, 7q11.21-11.22 and 7q34-7q36.3 with the first three regions showing amplification. One of the many genes in 7p11.2-p12.1 is *EGFR*, a cell surface protein that binds to epidermal growth factor which then induces receptor dimerization and tyrosine autophosphorylation and leads to cell proliferation. Mutations in this gene are associated with a number of cancers including lung cancer and anal cancer (Kobayashi et al., 2005; Walker et al., 2009). Furthermore, *EGFR* was previously described only in primary papillary RCC (Kovacs et al., 1991) but other study have also revealed high frequency of gain (Strefford et al., 2005) and increased levels of the gene in RCC (Moch et al., 1998). Gain on chromosome 7 were also related with high grade clear cell carcinoma (Matsuda et al., 2008) and duplication/amplification of *MET* at 7q31-q34 have been identified in cRCC (Pavlovich et al., 2003). There was also a positive correlation observed between *MET* expression and high nuclear grade (Choi et al., 2006).

Gain of 5q was found in 73.9% of the cell lines with the minimal overlap region identified in 5q34-q35.3 (table 5.8). Beroukhim et al (2009) have analysed 90 cRCC tumours (both sporadic and VHL-disease associated tumours) using the same platform and found gain 5q as the second most common changes after deletion 3p. They used GISTIC-based analysis to point the peak region and the region identified on 5q was in 5q35.3. However, no oncogene or TSG detected in that region. Gain of 5q after the initial loss of 3p may contribute to tumour progression in cRCC (Brauch et al., 1994; Meloni et al., 2002; Nagao et al., 2005). Nagao et al (2005) also concluded that allelic loss of 3p25 including the *VHL* gene is thought to be an immediate event in the development of cRCC and copy number gains or losses of 5q21 approximately q23 are thought to be events that lead to tumour progression although the clinical significance of either gains or losses is not well known. Other regions identified were in 5q33-q35 (Strefford et al., 2005; Toma et al., 2008) and 5q22.1-q23.2 (Toma et al., 2008). Gain of 5q is associated with t(3;5) which is common in cRCC and patients with deletion 3p and gain 5q22.3-q23.3 have been associated with better disease-free survival compared to those who had the deletion without the gain (Nagao et al., 2005).

In addition to duplication 5q34-q35.3, an interstitial gain in 5q21.2-q21.3 with the size ~4.3 Mb was detected in 1 case, SKRC45. Other cell lines which overlap the region were identified in 10 cases. The region contains three genes; *RAB9P1, EFNA5* and *FBXL17*. *RAB9P1* is a member of RAS oncogene family, *FBXL17* is a member of the F-box protein family and interact with SKP1 through the F box, and they interact with ubiquitination targets through other protein interaction domains (Jin et al., 2004) and *EFNA5* is a member of the ephrin gene family, prevents axon bundling in cocultures of cortical neurons with

astrocytes, a model of late stage nervous system development and differentiation. Further investigation of the genes is important to elucidate its function in relation to RCC.

Other copy number alterations ocurred in ~65%-78% of the cell lines were loss of 1p, 4q, 18q and gain of 2q, 8q, 12q and 20q. Deletion 4q is associated with sarcomatoid transformation in RCCs and one of the most frequently encountered chromosomal changes in papillary renal cell carcinoma (Jiang et al., 1998). The region of deletion on 18q found in this study (18q22.3-q23) is not in the same region identified by the previous reports. Both Hirata et al (2005) and Strefford et al (2005) identified LOH and deletion in 18q21.1-q21.3. The putative TSGs identified in the region include *SMAD4, BCL2* and *DCC*. Possible reasons that might contribute to the discrepancies seen are the differences in the methods applied, the sample size and the differences in the samples used, for example Strefford et al (2005) applied comparative genomic hybridisation (CGH) in their study.

1p35.3-p36.33 was identified as one of the most common region loss in the present study. Cifola et al (2008) and Beroukhim et al (2009) had each identified deletion in 1p36.11-p36.32 and 1p36.11 in cRCC tumours and RCC cell lines respectively. Among the many genes in the region is *RUNX3* which resides in 1p36.11 and has been shown to suffer gene silencing, homozygous deletion, hypermethylated or protein mislocalization to the cytoplasm in a variety of cancers (Li et al., 2002; Ito et al., 2005; Imamura et al., 2005; Vogiatzi et al., 2006; Tsunematsu et al., 2009). Gain of chromosomes 2, 12 and 20 were shown to be associated with papillary RCC (Brunelli et al., 2003; Matsuda et al., 2008). Complete gain of chromosome 20 (found in 11/23, 47.8% of the cell lines) and 12 (found in 8/23, 34.8% of the cell lines) were frequently encountered in this study (table 5.7).

The minimal common gain region in the 16/23 (69.6%) of the cases with gain of chromosome 8q was identified in 8q24.12-q24.3 where *MYC* resides. The gene participates in most aspects of cellular function, including replication, growth, metabolism, differentiation and apoptosis (Packham and Cleveland 1995; Hoffman and Liebermann 1998; Dang 1999; Elend and Eilers 1999; Prendergast, 1999). It has been shown to be amplified and/or overexpressed in numerous human cancers such as breast cancer, urothelial carcinoma, metastatic prostatic carcinoma, small cell lung cancer (Johnson et al., 1992; Jenkins et al., 1997; Christoph et al., 1999; Liao and Dickson, 2000; Naidu et al., 2002). Regions of homozygous deletion were seen in 9p21.3 and 9p23-p24.1 in 7/17 and 2/14 of the cases respectively. Three genes reside in the 9p21.3 are *MTAP, CDKN2A, CDKN2B* which were reported to be deficient in many cancers. *PTPRD* is the only gene in 9p22-p23 and the protein encoded by this gene regulates a variety of processes including cell growth, differentiation, mitotic cycle and oncogenic transformation. A study carried out by Grady et al (2001) on renal cell carcinoma has revealed a high incidence of LOH on chromosome 9 particularly 9p21 and 9p22-p23 suggesting several putative TSGs in the regions. It has also been shown that LOH on chromosome 9 have a higher risk of recurrence, poor prognosis and shorter tumour-specific survival (Schraml et al., 2001; Presti et al., 2002; Toma et al., 2008).

At present, copy number changes observed in RCC cell lines usually are large with frequent loss detected in 1p, 3p, 4q, 9p, 13q, 14q and 18q and gain 1q, 2q, 5p, 5q, 7p, 7q, 8q, 12q, 16p, 16q, 17q, 20p and 20q. These changes were also found in primary RCC tumours, therefore RCC cell lines represent a useful model for studying renal cancer. Although the aberrations identified in the cell lines could also be associated with *in vitro* karyotype evolution, it retains much of the genetic information of the primary tumour as

shown in the present study and the previous report (Pavlovich et al., 2003). High resolution 250K SNP microarrays is a useful method which allows detail characterisation of RCC to be carried out as shown in the results of this study.

5.9 Comparison of copy number changes identified in primary tumours and RCC cell lines

Overall, the RCC cell lines have more copy number changes than the primary tumours and more changes were seen in the cRCC sporadic tumours than in the VHLs (table 5.12). Overlapping changes that were common to the two sets of tumours and the cell lines are loss of 3p and gain of 5q. Gain of 2q, 7 and loss of 3q, 8p were more common in VHL (≥19%) than in sporadic tumours. On the other hand, gain 3q, 8q, 16p, 20q and loss 1p, 6p and 14q were observed more frequently (≥33%) in the sporadic than in the VHL tumours. However, the findings observed were not statistically significant except for gain 20q.

Table 5.12: Most common regions of gains and losses identified in cRCC primary tumours (sporadics and VHLs) and RCC cell lines using 250K SNP array

	cRCC		RCC cell line
	sporadic	**VHL**	
gain		2q23.3-q37.3	2q35-q36.3
			2q24.3-q33.3
			2q11.2-q14.3
	3q24-q29		3q22.1-q29
	5q31.3-q35.1	5q32-q35.3	5q34-q35.3
	5q35.3		
		7p11.2-p22.3	7p11.2-p12.1
		7q11.21-q22.1	7p21.2-p22.3
		7q32.1-q36.3	7q34-q36.3
			7q11.21-11.22
	8q11.21-q13.2		8q24.12-q24.3
	8q21.3-q24.3		
			12q24.22-q24.33
			12q12-q13.2
	16p11.2		16p11.2-p13.3

	20q11.22-q11.23		20q11.21-q11.23
	20q13.2-q13.33		
loss	1p13.3-p31.1		1p35.3-p36.33
	1p34.2-p36.33		
	3p12.1-p13	3p14.2-p21.1	3p14.2
	3p13-p26.3	3p21.31-p26.3	3p21.2-p26.3
		3q13.11-q13.31 3q11.2-q13.11	3p11.2-p13
			4q12-q13.1
			4q31.22-q35.2
	6p21.2-p21.33		
		8p12-p23.3	8p21.3-p23.3
			9p21.3
			9p23-p24.1
			13q12.1-q13.1
	14q12-q31.2		14q11.2-q13.1
			14q23.1-q32.33
			18q22.3-q23

Abbreviations: p, short arm; q, long arm

Most VHL associated RCC are detected presymptomatically and removed when the tumour reaches ~3 cm. In contrast, only a minority of sporadic RCC is detected presymptomatically and so, on average, sporadic tumours are larger. Hence genetic differences between VHL cRCC and sporadic *VHL* wild type cRCC might reflect (a) differences in stage of tumourigenesis (i.e. later in sporadic cases), (b) differences in mechanisms of tumourigenesis according to the presence or absence of *VHL* mutations. Deletion 3p including the *VHL* gene, was detected in 71% of the VHL tumours, 50% of the sporadic tumours and 95.7% of the cell lines.

Gain of 5q35.3 was common both in the primary tumours and the cell lines. Among the genes that reside in the region is *MAPK9* which are involved in a wide variety of cellular processes such as proliferation, differentiation, transcription regulation and development, thus might be a candidate gene for RCC.

High resolution SNP array has allowed detailed analysis of copy number changes in the cRCC primary tumours (sporadic and VHLs) and RCC cell lines as demonstrated in the present study. Most often the changes identified are large and in some cases involve the whole arm or the whole chromosome. Although there is overlap between the copy number changes detected in VHL cRCC and sporadic cRCC, some changes (e.g. 1p, 14q loss and 8q, 20q gain) are preferentially associated with the latter. Further studies are required to determine the potential role of individual gene within these regions with the use of more advanced methods such as higher resolution arrays and massive parallel sequencing techniques.

6 Identification of copy number changes in sporadic clear cell renal cell carcinoma (cRCC) using high resolution array SNP6.0

6.1 Introduction

Human cancers are partly due to irreversible structural mutations which can produce DNA copy number alterations at distinct locations in the genome (Albertson et al., 2003). In most solid tumours, copy number alterations are shown to be a common feature (Weir et al., 2004; Kops et al., 2005; Albertson, 2006). Chromosome segments that are deleted or duplicated/amplified harbour tumour suppressor genes (TSG) or oncogenes respectively. For example, small single nucleotide mutation can inactivate TSG on an allele and hemizygous deletion can remove the other allele to achieve functional inactivation. This results in loss of heterozygosity (LOH) across the loci. LOH can also be due to homozygous deletion (deletion on both alleles), uniparental disomy (UPD), mitotic recombination or gene conversions. Conversely, genomic amplification of oncogenes contributes to uncontrolled positive growth signaling. These alterations contribute to tumourigenesis and progression by enabling the aberrant function of genes that positively and negatively regulate aspects of cell proliferation, apoptosis, genome stability, angiogenesis, invasion and metastasis (Hanahan and Weinberg, 2000). Measuring gene dosage at high resolution and with accuracy is very important for dissecting the mechanism of cancer development (Garraway et al., 2005). Thus identifying these changes offer a basis for a better understanding of cancer development and subsequently improved tools for clinical management such as new diagnostics and therapeutic targets.

Comparative genomic hybridisation (CGH) was the first developed technique for genome wide characterisation of copy number changes especially in cancer (Kallionemi et al., 1992). Subsequently, higher resolution array-based CGH methods were introduced

replacing target metaphase spreads used in CGH with a large number of discrete genomic or cDNA clones (Albertson et al., 2000; Hodgson et al., 2001; Pollack et al., 2002). For example, arrays consisting of 32,433 bacterial artificial chromosomes (BAC) clones spanning the entire human genome, with a resolution of less than 100 kb allowing comprehensive analyses of cancer genomes (Ishkanian et al., 2004). More recent technology using synthetic high-density oligonucleotide microarrays (Lieberfarb et al., 2003; Bignell et al., 2004; Huang et al., 2004; Janne et al., 2004; Rauch et al., 2004; Wong et al., 2004; Zhao et al., 2004; Zhou et al., 2004) has enabled LOH and copy number changes to be identified simultaneously at even higher resolution than the previous methods. These high throughput microarrays are commercially available and designed to genotype thousands of single nucleotide polymorphisms (SNPs) in human genomic DNA. Among the different proposed platforms, Affymetrix Human Mapping Array offers genome wide studies using 25 nucleotides long probes and developed different types of SNP microarrays; 10K array - an array covering 10,204 SNPs (GeneChip Human Mapping 10K), 100K array - a pair of arrays covering 116, 204 SNPs (GeneChip Human Mapping 50K Xba array and Hind Array) and 500K array - a pair of arrays covering 504,152 SNPs (GeneChip Human Mapping 250K Nsp Array and Sty Array). These Affymetrix SNP arrays were designed so that each SNP is interrogated by 24 to 40 unique probes. Of these, half are perfectly complementary to the sequence harbouring the SNP site (perfect match probes), while half mismatch the sequence at the probe's middle nucleotide (mismatch probes). The mismatch probes were intended to capture background effects such as cross-hybridization. For the Affymetrix GeneChip 500K, SNPs have a median spacing of 2.5 kb. However, the probes are not uniformly distributed across the genome and are particularly sparse in regions of segmental duplication and complex CNV. These create problems for the design of robust genotyping SNP assays in these regions. As a result, the resolution of

the array is variable across the genome and CNV detection has a lower limit of 10–40 kb (Carter, 2007). Therefore, Affymetrix has included additional nonpolymorphic probes on their latest SNP Array 6.0 to overcome the problem.

The SNP Array 6.0, which interrogates nearly one million SNPs and differs fundamentally from previous versions. First, each SNP on the 6.0 array is interrogated only by six or eight perfect match probes - three or four replicates of the same probe sequence for each of the two alleles. Therefore, intensity data for each SNP consist of three or four repeated pairs of measurements. Second, the SNP probe sets are augmented with nearly one million CNV probes, which are meant to interrogate regions of the genome that do not harbour SNPs, but that may be polymorphic with regard to copy number. Each such CNV site is interrogated by only one probe. The Affymetrix SNP array 6.0 (Genome-Wide Human SNP Array 6.0) (McCarroll et al, 2008) contains more than 1.8 million markers; 906,600 single nucleotide polymorphisms (SNPs) and more than 946,000 probes for the detection of copy number variation, thus providing the highest physical coverage of the genome with median marker spacing of 680 bases (GenomeWide Human SNP Array 6.0 (Affymetrix) http://www.affymetrix.com/products_services/arrays/specific/genome_wide_snp6/genome_wide_snp_6.affx). Details of the SNPs selection and its description for array SNP6.0 are available from http://www.affymetrix.com/support/support_result.affx. The SNP6.0 arrays have been applied for studies of common diseases such as diabetes and heart disease (McPherson et al., 2007; Saxena et al., 2007; Zeggini et al., 2007), detection of UPD and characterisation of chromosome breakpoint in chronic lymphocytic leukemia (Hagenkord et al., 2010) and identification of copy number alterations and LOH in tumours (Greenman et al., 2010; Gorringe et al., 2009). The arrays were also successfully applied on fresh frozen tissue (Tuefferd et al, 2008) as well as archived samples (Tuefferd et al., 2008;

Bucasas et al, 2009). The Birdseed algorithm (Korn et al, 2008) is specifically designed for the Genome-Wide Human SNP Array 6.0 to process data from the arrays.

The main aim of this study is to precisely characterise and identify copy number changes associated with sporadic clear cell renal cell carcinoma (cRCC). Therefore, I took advantage of the latest microarray technology, Affymetrix array SNP6.0, to study copy number changes of 37 samples of sporadic cRCC. The data was then compared with the results of sporadic cRCC obtained using the 250K SNP array.

6.2 Materials and methods

6.2.1 DNA sample

A total of 37 genomic DNA from sporadic primary clear cell renal cell carcinoma tumours were studied. Genomic DNA was extracted following standard methods and stored at -80^{o}C.

6.2.2 SNP Array 6.0 analysis

The methods were described in detail in sections 2.1 and 2.2. The SNP Array 6.0 platform offers the genotype calling algorithm "Birdseed" to determine the genotypes of 909,622 SNPs (Affymetrix, Inc. http://www.affymetrix.com/index.affx). The Birdseed algorithm performs a multiple-chip analysis to estimate signal intensity for each allele of each SNP, fitting probe-specific effects to increase precision, and then makes genotype calls by fitting a Gaussian mixture model in the two-dimensional A-signal vs. B-signal space, using SNP-specific models to improve accuracy. In addition, this array also contains 945,826 copy number probes designed to interrogate CNVs in the genome; 115,000 of these probes interrogate previously identified CNVs while the remaining 831,000 are distributed across

the genome for improved CNV detection (Affymetrix, Inc. http://www.affymetrix.com/index.affx). Copy number analysis was performed with Affymetrix Genotyping Console v3.0.2 (GTC v3.0.2).

6.2.3 MLPA analysis

MLPA was applied on 20 samples to confirm some of the deletions and duplications identified from the array SNP6.0 microarray. The MLPA Kit used was SALSA P007-A1 Human Chromosome Kit (MRC Holland, Amsterdam, The Netherlands) that contains probes for 40 different target sequences (appendix A5). Among these are many genes that are often deleted or amplified in various tumours. The analysis was performed according to the manufacturer's instructions. The ligation products were amplified on a Tetrad thermal cycler (Peltier 225 from MJR). PCR products were then separated by capillary electrophoresis on a Beckman Coulter CEQ 8000 genetic analyzer. Electropherograms were analyzed using GeneMarker MLPA Analysis (SoftGenetics, LLC, USA). Deletions were indicated by a value of <0.785 and duplications by >1.33.

6.3 Results

6.3.1 SNP Array 6.0 analysis

The reference set for 250K Sty1 mapping arrays was 48 samples from the HapMap project (www.hapmap.org/downloads/raw_data/affy500k/) and 270 HapMap individuals of various populations for SNP 6.0 (Goldstein and Cavalleri, 2005). Six normal controls were used for MLPA. The average call rate of the 37 samples was 95.13±1.78. Overall, 325 gains (mean per tumour was 8.78) and 269 losses (mean per tumour was 7.27) were detected with majority of them involved the whole chromosome arm or segments ≥10 Mb (table 6.1 and figure 6.1). Small deletions and duplications were not a common feature and

all of the small regions (<10 Mb) identified were not recurrent. Deletion 3p was the most frequently encountered aberrations, seen in 28(75.7%) of the cases and all of them involved deletion of the whole 3p or segments ≥10 Mb. Gain of 5q was encountered in 16(43.2%) of the cases and among these, 8 cases showed deletion in 3p. Loss of chromosome 1, 3, 6, 9, 14 and gain of chromosome 5, 7, 11, 12, 17 were observed in ~19%-32% of the cases. Loss of whole 8p and 14q were seen in 13(35.1%) and 12(32.4%) respectively. In addition, small deleted regions (<10 Mb) were identified in 14q11.2 (7.6 Mb), 8p21.2 containing 7 genes, 8p12 containing 15 genes and 1p36.11-p36.12 containing 43 genes.

Gain of 16q were found as frequently as gain 5q and the small gain segments identified in 16q came from the same sample at different regions on the chromosome. Gain of chromosome 7, 11, 12 and 17q were also fairly common, encountered in 29.7%-37.8% of the cases (table 6.1).

Table 6.1: Chromosome gains and losses in the 37 samples of sporadic cRCC analysed with array SNP6.0

Chrom.	Loss				Gain			
	Whole chrom. arm	**≥10 Mb**	**<10 Mb**	**Total**	**Whole chrom. arm**	**≥10 Mb**	**<10 Mb**	**Total**
1p	13	3	1	17	2	2	0	4
1q	12	0	0	12	5	0	0	5
2p	5	0	0	5	3	0	0	3
2q	5	1	0	6	3	1	0	4
3p	13	15	0	28	6	4	1	11
3q	10	0	0	10	7	1	0	8
4p	3	2	0	5	6	1	0	7
4q	3	1	0	4	7	0	0	7
5p	3	0	1	4	9	2	0	11
5q	4	0	0	4	9	7	0	16
6p	10	1	0	11	6	2	0	8
6q	10	2	0	12	6	0	0	6
7p	0	2	0	2	14	0	0	14
7q	0	3	0	3	14	0	0	14
8p	13	0	2	15	5	0	1	6
8q	6	2	1	9	7	3	0	10
9p	7	0	0	7	5	0	1	6
9q	7	0	0	7	5	0	2	7
10p	6	0	0	6	5	0	0	5
10q	7	0	0	7	5	1	0	6
11p	2	0	0	2	11	0	0	11
11q	2	1	0	3	10	0	0	10
12p	0	3	0	3	10	0	1	11
12q	0	1	0	1	10	1	0	11
13q	6	1	0	7	11	0	0	11
14q	12	2	1	15	4	0	1	5
15q	3	1	0	4	5	1	0	6
16p	0	0	0	0	6	0	0	6
16q	0	2	2	4	8	2	6	16
17p	5	1	1	7	8	0	0	8
17q	5	0	0	5	8	3	0	11
18p	3	0	0	3	6	0	0	6
18q	3	4	0	7	6	0	0	6
19p	5	1	1	7	3	1	1	5
19q	5	0	0	5	3	1	1	5
20p	0	0	0	0	3	2	0	5
20q	0	0	0	0	3	1	1	5
21q	5	0	1	6	4	0	2	6
22q	4	0	0	4	5	0	0	5

Abbreviations: p, short arm; q, long arm; chrom., chromosome; Mb, megabase

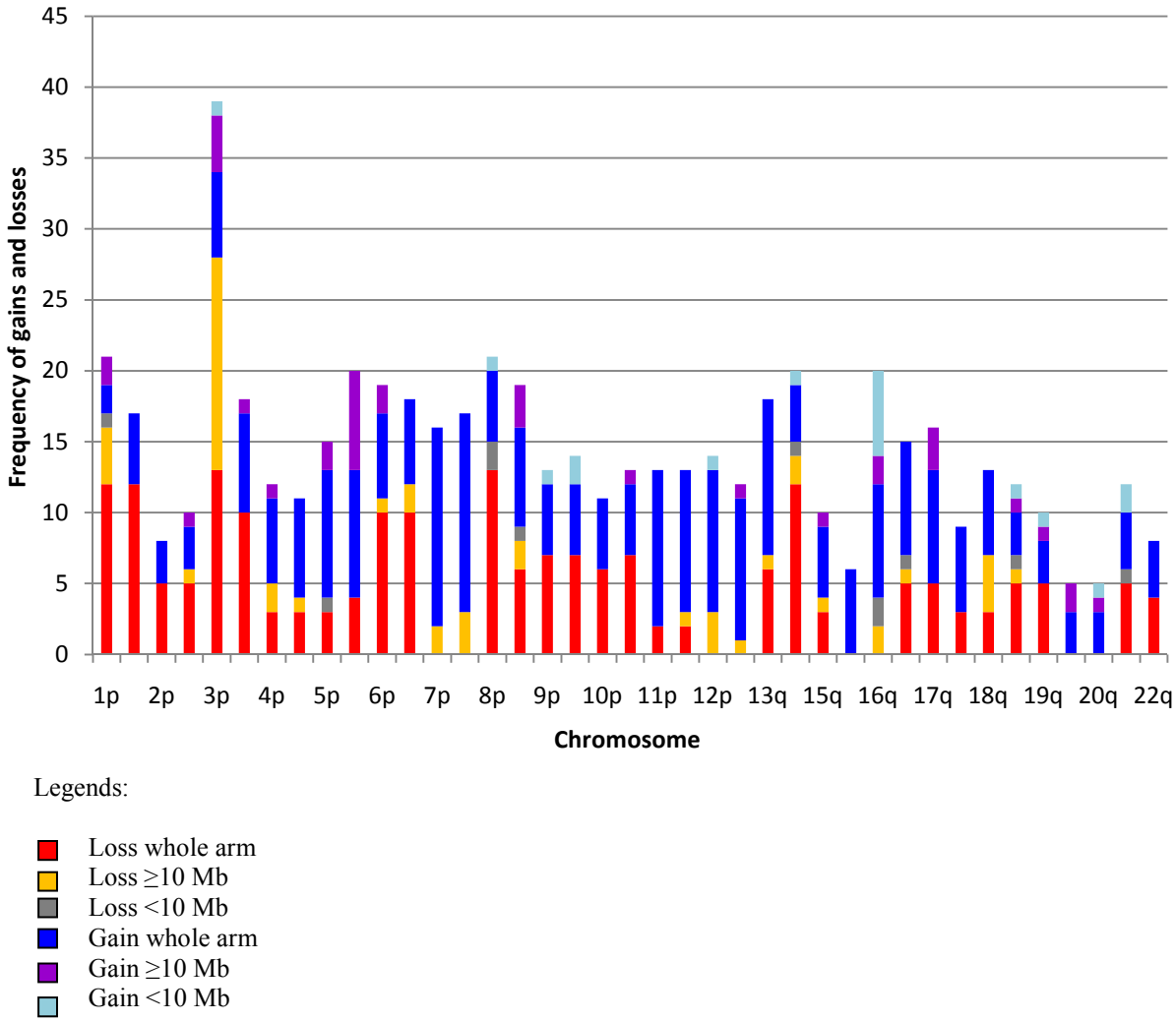

Figure 6.1: Frequency of chromosome gains and losses identified in the 37 samples of sporadic cRCC studied.

Minimal overlapping regions of the most common (>27%) copy number changes is shown in table 6.2. MLPA analysis was done to verify the changes in some of the regions. Microarray and the MLPA copy number analysis results was concordant (table 6.2).

Table 6.2: Minimal overlapping regions of gains and losses of the most common copy number changes in the sporadic cRCC studied.

	Affected region	Start pos.	End pos.	Size (Mb)	MLPA probes
Loss	1p22.3-p31.3	65,000,000	87,285,000	22.28	
	3p14.3-p26.3	0	55,280,000	55	
	6q16.3-q27	103,700,000	170,899,992	67.19	
	6p21.1-p25.3	0	40,000,000	40	CDKN1A (6p21.2), LTA (6p21.3)
	8p12	36,000,000	38,000,000	2	
	8p21.2	23,680,000	25,060,000	13.8	
	14q11.2	18,000,000	25,626,000	7.62	
	14q23.2-q32.33	63,212,700	106,368,585	43.15	
Gain	3p11.2	87,450,000	90,400,000	29.5	
	3p22.2-p24.1	28,400,000	38,680,000	10.28	
	5p15.1-p15.33	0	18,000,000	18	
	5q31.1-q35.3	131,000,000	180,857,866	49.85	IL12B (5q33.1)
	8q11.21-q21.1	47,000,000	76,200,000	29.2	
	8q21.11-q22.3	76,200,000	106,000,000	29.8	
	8q23.1-q24.3	106,100,000	145,200,000	39.1	MYC(8q24.12), PTK2 (8q24), SLA (8q24.2)
	11p11.12-p15.5	0	51,400,000	51	
	12p13.32-p13.33	0	4,400,000	4	
	12q12-q21.32	37,636,000	86,175,000	48.54	
	16q12.1	45,000,000	46,200,000	1.2	
	16q12.1	49,200,000	49,885,000	0.68	
	16q12.1-q12.2	50,000,000	53,700,000	3.7	
	16q12.2-q21	53,700,000	59,000,000	6.7	
	16q21-q22.3	59,200,000	70,000,000	10.8	
	16q22.3	70,180,000	71,000,000	1.18	
	17q24.1-q25.3	60,900,000	78,774,742	17.87	
	17q21.2-q24.2	35,075,000	61,863,600	26.78	TOP2A (17q21.2)

Abbreviations: p, short arm; q, long arm; pos, position; Mb, megabase

In the present study, there were 18 small gain regions (<10Mb) and 11 small loss regions identified. Four regions of amplification (≥4 copies) were identified on chromosome 16q (table 6.3).

Table 6.3: Small regions (<10 Mb) of gains and losses in the 37 samples sporadic cRCC studied with array SNP6.0

Gain (<10 Mb)				Loss (<10 Mb)			
Chrom. band	**Start pos.**	**End pos.**	**Size (Mb)**	**Chrom. band**	**Start pos.**	**End pos.**	**Size (Mb)**
3p11.2	87.45	90.40	2.95	1p36.11-p36.12	21.89	24.25	2.36
8p21.1-p21.2	26.80	29.06	2.26	5p14.1	26.75	29.14	2.39
9p11.2	40.50	47.20	6.70	8p12	36.00	38.00	2.0
9q12	65.34	69.26	3.92	8p21.2	23.68	25.06	1.38
9q34.2-q34.3	136.40	140.27	3.87	8q11.21-q11.22	48.00	50.80	2.80
12p13.32-p13.33	0	7.24	7.24	14q11.2	18.00	25.63	7.63
14q32.33	105.00	106.37	1.37	16q12.1	46.55	48.95	2.40
16q12.1*	45.00	46.20	1.20	16q23.2-q24.3	79.20	88.83	9.63
16q12.1*	49.20	49.89	0.69	17p12	14.00	15.43	1.43
16q12.1-q12.2	50.00	53.70	3.70	19p12	22.00	24.26	2.26
16q22.3*	70.18	71.00	0.82	21q11.2	13.30	14.18	0.88
16q23.1*	75.25	76.09	0.84				
16q23.1-q23.2	77.35	78.97	1.62				
19p13.3	0	3.00	3.00				
19q13.31-q13.32	48.93	51.60	2.67				
20q13.33	59.80	62.44	2.64				
21q21.2-q21.3	24.25	26.00	1.75				
21q22.11-q22.12	33.50	35.37	1.87				

*contain ≥4 copies

Abbreviations: p, short arm; q, long arm; chrom., chromosome; pos., position; Mb, megabase

6.3.2 Comparison of copy number changes identified in sporadic cRCC using array SNP6.0 and 250K SNP array

Both methods have shown that gains involving large segments (>10 Mb) were more common than deletions. Deletion 3p, 1p, 14q and gain 5q were the most frequently encountered alterations, found in >40% of the cases. Both methods also agree that deletion 20 was not associated with RCC and gain in chromosome 7 usually involved the whole chromosome. Gain of whole chromosome 7 and 16q and deletion 8p were shown as a common event (~37%-43% of the cases) in sporadic cRCC by SNP6.0, however, results from 250K array identified the aberrations not as common (<26% of the cases). Other fairly common aberrations, encountered in ~27%-32% of the cases with SNP6.0 were loss of 1q, 3q, 6 and gain of 3p, 5p, 8q, 11, 12, 13q and 17q. These aberrations were seen in ~8%-25% of the cases identified by 250K SNP array except gain 8q which was encountered in 41.6% of the cases. In general more copy number abnormalities were observed in sporadic group than VHLs. This could reflect the use of SNP 6.0 arrays or the fact that in general, sporadic tumours will be at a more advanced stage at operation. Some of the differences (e.g. gain 16q, loss 1p, loss 1q and loss 6q were statistically significant) after allowance for multiple testing (Bonferroni corrected P value ~0.0024).

Small regions of deletion and gain were identified using both arrays; Array SNP6.0 has identified 11 small deletions and 18 small gains while 250K SNP array has detected 7 small deletions and 13 small gains (table 6.4). Mean size of the smallest region identified with SNP6.0 was 2.90 and 4.65 for 250K array. Almost all of the small regions identified with 250K arrays were not in the same regions detected using SNP6.0 except for gain in the regions 9q and 19p (table 6.4). These might reflect the heterogenous characteristic of these tumours or it could be due to the smaller sample size analysed by 250K compared to

array SNP6.0. Therefore, copy number changes in sporadic RCC for this study are combined results obtained using 250K and SNP6.0 arrays.

Table 6.4: Small regions (<10 Mb) of gains and losses detected in sporadic cRCC using 250K SNP array and array SNP6.0

	250K SNP array		SNP6.0 array	
	Chrom. band	**Size (Mb)**	**Chrom. band**	**Size (Mb)**
Loss	3q11.2	2.7	1p36.11-p36.12	2.36
	6p21.2-p21.33	8.46	5p14.1	2.39
	9p13.1-p21.1	6	8p12	2
	11p11.12-p11.2	4.71	8p21.2	1.38
	11q14.1-q14.3	7.1	8q11.21-q11.22	2.8
	11q12.1-q12.2	3.3	14q11.2	7.63
	16p13.2-p13.3	1	16q12.1	2.4
			16q23.2-q24.3	9.63
			17p12	1.43
			19p12	2.26
			21q11.2	0.88
Gain	5q21.1-q21.3	5.16	3p11.2	2.95
	5q35.3	2.86	8p21.1-p21.2	2.26
	8p11.21-p12	9.97	9p11.2	6.7
	6p12.3-p21.2*	8.2	9q12	3.92
	9q33.2-q34.11*	8.14	9q34.2-q34.3	3.87
	9q34.3	1.87	12p13.32-p13.33	7.24
	16p11.2	2.88	14q32.33	1.37
	17q21.33-q22	1.67	16q12.1*	1.2
	18q11.2-q12.1	8.45	16q12.1*	0.69
	19p13.13-p13.2	2.13	16q12.1-q12.2	3.7
	19p12-p13.11	3.8	16q22.3*	0.82
	19p12*	1.73	16q23.1*	0.84
	20q11.21-q11.23	6.45	16q23.1-q23.2	1.62
			19p13.3	3
			19q13.31-q13.32	2.67
			20q13.33	2.64
			21q21.2-q21.3	1.75
			21q22.11-q22.12	1.87

*contain ≥4 copies
Abbreviations: chrom., chromosome; Mb, megabase

6.4 Discussion

It is evidence from both of the 250K SNP array and SNP6.0 arrays data that copy number changes in sporadic cRCC tumours most frequently involved large segments of the chromosomes and with preference to chromosome gains. This suggests that cRCC tumourigenesis requires elimination and gain of multiple genes on many chromosomes which also involved many 'passenger' and 'driver' events.

Recent findings have shown that known cancer genes that are frequently mutated in other adult epithelial cancers, for example the *RAS* genes, *BRAF*, *TP53*, *RB* (also known as *RB1*), *CDKN2A*, *PIK3CA*, *PTEN*, *EGFR* and *ERBB2*, make only a small contribution to cRCC (http://www.sanger.ac.uk/genetics/CGP/cosmic/). Deletion 3p which is a hallmark of cRCC was detected in 50% and 75.5% of the sporadic cRCC cases using 250K SNP array and SNP6.0 array, respectively, making it the most common findings, thus supporting previous reports (Banks et al., 2006; Monzon et al, 2009; Beroukhim et al., 2009; Klatte et al., 2009). The deletion contributed to the loss of function of the *VHL* gene (maps to 3p25.3), a step known to be an important event in the pathogenesis of cRCC (Zbar et al., 2003). However, it has been shown that *VHL* inactivation alone induces senescence, therefore a requirement for further mutations to further promote ccRCC development is required (Young et al., 2008).

The present study shows that almost all of the chromosomes were involved in the copy number alterations, with some more common than the other (table 6.1). Large deletion 1p, 14q and gain 5q were also found to be strongly related with cRCC as demonstrated by ~40%-50% of the cases having these alterations from the results of both arrays. In addition, gain of chromosome 7 and 16q and deletion 8p identified using array SNP6.0 and

gain 8q identified by 250K SNP array were also a common alteration in cRCC, seen in ~37%-42% of the cases. Other fairly common alterations (~32%-33% of the cases) include deletion 1q and 6q detected by array SNP6.0 and gain 20q detected by 250K SNP array. These results are in agreement with the previous report (Beroukhim et al, 2009), except for chromosome 1q which was found to be frequently deleted in this study was shown to be among the most commonly amplified chromosomes in the report. The frequently found alterations indicate that the genes in that particular chromosome are highly implicated in cRCC. Only one alteration, deletion 20p, does not seem to play a role in cRCC as demonstrated by both arrays.

Since most of the deletion on 3p involved large segments, it is thought that additional TSGs on the chromosome must have contributed to the cRCC tumourigenesis. Our data supports this idea as majority of the cases from both arrays with 3p deletion involved the whole arm or large segments. Mapping studies have shown the presence of additional TSGs in more centromeric regions of 3p particularly 3p12-p14 and 3p21 (van den Berg and Buys, 1997). A number of other genes have been identified as a candidate of TSGs on 3p, including *FHIT, ROBO* and *RASSF1A*. *RASSF1A* maps to 3p21.3 and was reported inactivated by promoter methylation and epigenetic silencing in 40%-50% of cRCC. The gene product appears to have multiple functions and modulates apoptosis, cell motility, cell cycle and microtubule stability (Agathanggelou et al, 2005). *FHIT* located in 3p14.2 is altered by deletion or translocation in many types of cancer including lung, cervix, esophagus, bladder and kidney carcinoma (Ohta et al, 1996; Virgilio et al, 1996; Sozzi et al, 1996; Druck et al, 1997; Mori et al, 2000; Baffa et al, 2000). Most recently, a new report identified *SETD2* as a novel 3p TSG in cRCC (Duns et al., 2010).

Identification of small regions may lead to important discovery of TSGs or oncogenes implicated with the cancer. Array SNP6.0 has identified copy number changes in more chromosome regions compared to 250K SNP array due to its higher resolution and the larger number of samples analysed compared to 250K SNP array. This was demonstrated by the higher number of small regions detected by the array (table 6.3). However, the majority of the small regions were not recurrent and all of them occurred together with large deletions or gains. Therefore, it was difficult to unequivocally assess the significance of these findings and associate the small regions with candidate TSGs or oncogene. A possible explanation to the observation is that the various regions of small gains and losses may represent random changes from genomic instability or it could be that some changes reflect rare CNVs and ideally constitutional DNA should be investigated at the same time (however large (≥690 kb) constitutional CNVs are rare and none of the copy number gains or losses identified in my studies corresponded to those identified in a recent publication of constitutional DNAs analysed with the Affymetrix 6.0 array platform (Närvä et al, 2010)).

In conclusion, copy number changes in sporadic cRCC usually involved large segments and chromosome gains were more common than chromosome loss. Eleven copy number changes were identified including 6 regions of deletion on chromosome 3p, 1q, 14q, 8p, 1q, 6q and 5 regions of gain including chromosome 5q, 7, 16q, 8q, 20q. More chromosomal changes were revealed in this study as the application of high resolution array SNP6.0 as well as the use of a larger number of samples has assists in the identification of the changes associated with cRCC.

7 Future works and recent developments

One of the important factors in determining accurate results in cancer studies is the purity of the DNA used. An alternative to the method applied in this study for obtaining the DNA from cancer samples with minimal contamination of normal cells is the use of laser microdissection to isolate specific cells of interest from microscopic regions of tissue or cell or organisms (Emmert-Buck et al., 1996; Espina et al., 2007). The tool has been applied in various cancer studies and on a variety of tissue samples such as solid tissues, cell cultures, cytologic preparations, frozen and paraffin embedded tissue (Wild et al., 2000; Orba et al., 2003; Dahl et al., 2006; Korekane et al., 2007; Kawamura et al., 2010). Due to the high degree of purity (95%) in the cell populations obtained using the tool, Nakamura et al (2004) have detected a large proportion of genes that were upregulated or downregulated in pancreatic cancers that were different from those reported in previous studies. They suggests laser microdissection is useful in providing important information for finding candidate genes whose products might serve as specific tumour markers and/or as molecular targets for treatment of patients with pancreatic cancer.

Genetic aberrations associated with cRCC are complex as demonstrated by the present study as well as previous reports. Identifying copy number changes is one genetic aspect of the cancer but to understand the precise genetic basis and the mechanisms involved requires a comprehensive knowledge of mutational, transcriptional, epigenetic and copy number status of individual genes. Further advances in the evaluation of gene copy number analysis for example higher resolution arrays and massive parallel sequencing techniques (also referred to as next-generation or second-generation sequencing) will facilitate the investigation on copy number status of individual genes. The next-generation sequencing

technology available commercially are for example 454 sequencing (used in the 454 Genome Sequencers, Roche Applied Science, Basel), Solexa technology (used in the Illumina (San Diego, Genome Analyzer), the SOLiD platform (Applied Biosystems, Foster City, CA, USA), the Polonator (Dover/Harvard) and the HeliScope Single Molecule Sequencer technology (Helicos, Cambridge, MA, USA). These platforms rely on sequencing by synthesis (i.e. serial extension of primed templates) using either polymerase (Mitra et al., 2003; Turcatti et al., 2008) or a ligase (Brenner, et al., 2000; Shendure et al., 2005) as the enzyme. This new technology has been applied in various aspects of cancer studies such as targeted gene re-sequencing, mutation detection, copy number variation (CNV), single nucleotide polymorphism (SNP), changes in chromatin architecture, and epigenetic changes such as methylation pattern alteration (Thomas et al., 2006; Chen et al., 2008; Jones et al., 2008; Parsons et al., 2008; Sugarbaker et al., 2008; Chiang et al., 2009; Maher et al., 2009; Stephens et al., 2009). With the ability to analyse entire genomes, these technologies hold promise to global mapping of normal variation and mutations of all types for correlation with disease propensity, diagnosis, treatment, prognosis as well as identification of new targets for interventional therapy discovery and development (Mullighan et al., 2007; Jones et al., 2008; Sugarbaker et al., 2008).

8 Conclusions

The application of high resolution and high throughput SNP microarray has significantly contributed to the knowledge of constitutional disorders such as 3p deletion syndrome and Beckwith-Wiedemann syndrome (BWS) as well as cancer studies of cRCC (in VHL and sporadic) as demonstrated in the present study. Current evidence suggests *SRGAP3* as the major determinant of psychomotor retardation in 3p deletion syndrome. A region for congenital heart disease (CHD) was identified in an interval ~200 Kb (between 11.15 Mb and 11.35 Mb), however the two genes (*HRH1* and *ATG7)* contained in the region are not associated with cardiovascular development. Thus, further investigations on a larger number of samples using a more comprehensive approach that includes mutational, transcriptional, epigenetic and copy number analysis of individual genes may help to understand the genetic basis of CHD and 3p deletion syndrome. Combination of FISH and microarray methods has successfully characterised chromosome aberrations on 11p15.4-p15.5 in six BWS patients. Breakpoint in *ZNF215* is very rare and to date, this is the second to report such findings. Therefore, further investigation of the gene is important to know its relation with BWS.

Within the limitations of the analysis, imposed by both the unknown ploidy of the cancer samples and the variable degree of contamination by normal cells, the overall pattern of copy number changes in the primary tumours involved large regions, most often the whole chromosome arm or the whole chromosome. Copy number changes pattern in VHL were more homogenous in contrast to sporadic cRCC. In addition to deletion 3p and gain 5q as the most common findings in both sets of the tumours, gain of 2q, 7 and loss of 3q, 8p were more common in VHL cRCC. Sporadic tumours appeared to have more changes (for

example loss of 1p, 14q, 6p and gain of 8q, 16p, 20q). As the changes observed in the primary tumours overlap with the cell lines, therefore RCC cell lines can be used as a model for studying cRCC.

References

Agathanggelou, A., Cooper, W. N. & Latif, F. Role of the Ras-association domain family 1 tumour suppressor gene in human cancers. Cancer Res 2005;65:3497-508.

Aitman, T. J., Dong, R., Vyse, T. J., Norsworthy, P. J., Johnson, M. D., Smith, J., Mangion, J., Roberton-Lowe, C., Marshall, A. J., Petretto, E., Hodges, M. D., Bhangal, G., Patel, S. G., Sheehan-Rooney, K., Duda, M., Cook, P. R., Evans, D. J., Domin, J., Flint, J., Boyle, J. J., Pusey, C. D. & Cook, H. T. Copy number polymorphism in Fcgr3 predisposes to glomerulonephritis in rats and humans. Nature 2006;439:851-5.

Albertson, D. G., Ylstra, B., Segraves, R., Collins, C., Dairkee, S. H., Kowbel, D., Kuo, W. L., Gray, J. W. & Pinkel, D. Quantitative mapping of amplicon structure by array CGH identifies CYP24 as a candidate oncogene. Nat Genet 2000;25:144-6.

Albertson, D. G. & Pinkel, D. Genomic microarrays in human genetic disease and cancer. Hum Mol Genet 2003;12 Spec No 2:R145-52.

Albertson, D. G., Collins, C., Mccormick, F. & Gray, J. W. Chromosome aberrations in solid tumours. Nat Genet 2003;34:369-76.

Albertson, D. G. Gene amplification in cancer. Trends Genet 2006;22:447-55.

Alders, M., Ryan, A., Hodges, M., Bliek, J., Feinberg, A. P., Privitera, O., Westerveld, A., Little, P. F. & Mannens, M. Disruption of a novel imprinted zinc-finger gene, ZNF215, in Beckwith-Wiedemann syndrome. Am J Hum Genet 2000;66:1473-84.

Aldred, M. A., Vijayakrishnan, J., James, V., Soubrier, F., Gomez-Sanchez, M. A., Martensson, G., Galie, N., Manes, A., Corris, P., Simonneau, G., Humbert, M., Morrell, N. W. & Trembath, R. C. BMPR2 gene rearrangements account for a significant proportion of mutations in familial and idiopathic pulmonary arterial hypertension. Hum Mutat 2006;27:212-3.

Algar, E. M., St Heaps, L., Darmanian, A., Dagar, V., Prawitt, D., Peters, G. B. & Collins, F. Paternally inherited submicroscopic duplication at 11p15.5 implicates insulin-like growth factor II in overgrowth and Wilms' tumourigenesis. Cancer Res 2007;67:2360-5.

Alimov, A., Kost-Alimova, M., Liu, J., Li, C., Bergerheim, U., Imreh, S., Klein, G. & Zabarovsky, E. R. Combined LOH/CGH analysis proves the existence of interstitial 3p deletions in renal cell carcinoma. Oncogene 2000;19:1392-9.

Alimov, A., Sundelin, B., Wang, N., Larsson, C. & Bergerheim, U. Loss of 14q31-q32.2 in renal cell carcinoma is associated with high malignancy grade and poor survival. Int J Oncol 2004;25:179-85.

Amin, M. B., Corless, C. L., Renshaw, A. A., Tickoo, S. K., Kubus, J. & Schultz, D. S. Papillary (chromophil) renal cell carcinoma: histomorphologic characteristics and evaluation of conventional pathologic prognostic parameters in 62 cases. Am J Surg Pathol 1997;21:621-35.

Angeloni, D., Lindor, N. M., Pack, S., Latif, F., Wei, M. H. & Lerman, M. I. CALL gene is haploinsufficient in a 3p- syndrome patient. Am J Med Genet 1999;86:482-5.

Anglard, P., Tory, K., Brauch, H., Weiss, G. H., Latif, F., Merino, M. J., Lerman, M. I., Zbar, B. & Linehan, W. M. Molecular analysis of genetic changes in the origin and development of renal cell carcinoma. Cancer Res 1991;51:1071-7.

Aretz, S., Stienen, D., Uhlhaas, S., Stolte, M., Entius, M. M., Loff, S., Back, W., Kaufmann, A., Keller, K. M., Blaas, S. H., Siebert, R., Vogt, S., Spranger, S., Holinski-Feder, E., Sunde, L., Propping, P. & Friedl, W. High proportion of large

genomic deletions and a genotype phenotype update in 80 unrelated families with juvenile polyposis syndrome. J Med Genet 2007;44:702-9.

Argani, P., Antonescu, C. R., Illei, P. B., Lui, M. Y., Timmons, C. F., Newbury, R., Reuter, V. E., Garvin, A. J., Perez-Atayde, A. R., Fletcher, J. A., Beckwith, J. B., Bridge, J. A. & Ladanyi, M. Primary renal neoplasms with the ASPL-TFE3 gene fusion of alveolar soft part sarcoma: a distinctive tumour entity previously included among renal cell carcinomas of children and adolescents. Am J Pathol 2001;159:179-92.

Baffa, R., Gomella, L. G., Vecchione, A., Bassi, P., Mimori, K., Sedor, J., Calviello, C. M., Gardiman, M., Minimo, C., Strup, S. E., Mccue, P. A., Kovatich, A. J., Pagano, F., Huebner, K. & Croce, C. M. Loss of FHIT expression in transitional cell carcinoma of the urinary bladder. Am J Pathol 2000;156:419-24.

Bajolle, F., Rullier, J., Picard, A. M. & Legrele, G. [Partial trisomy for the distal part of the short arm of chromosome 11 due to paternal translocations 11/5]. Ann Genet 1978;21:181-5.

Ballif BC, Hornor SA, Jenkins E, Madan-Khetarpal S, Surti U, Jackson KE, Asamoah A, Brock PL, Gowans GC, Conway RL, Graham JM Jr, Medne L, Zackai EH, Shaikh TH, Geoghegan J, Selzer RR, Eis PS, Bejjani BA, Shaffer LG. 2007. Discovery of a previously unrecognized microdeletion syndrome of 16p11.2-p12.2. Nat Genet 39:1071–1073.

Bandyopadhyay, R., Mcquillan, C., Page, S. L., Choo, K. H. & Shaffer, L. G. Identification and characterization of satellite III subfamilies to the acrocentric chromosomes. Chromosome Res 2001;9:223-33.

Bandyopadhyay, R., Heller, A., Knox-Dubois, C., Mccaskill, C., Berend, S. A., Page, S. L. & Shaffer, L. G. Parental origin and timing of de novo Robertsonian translocation formation. Am J Hum Genet 2002;71:1456-62.

Banks, R. E., Tirukonda, P., Taylor, C., Hornigold, N., Astuti, D., Cohen, D., Maher, E. R., Stanley, A. J., Harnden, P., Joyce, A., Knowles, M. & Selby, P. J. Genetic and epigenetic analysis of von Hippel-Lindau (VHL) gene alterations and relationship with clinical variables in sporadic renal cancer. Cancer Res 2006;66:2000-11.

Barber JCK. 2008. Terminal 3p deletions: Phenotypic variability, chromosomal non-penetrance or gene modification? Am Med Genet Part A 146A:1899–1901.

Barlow, D. P. Imprinting: a gamete's point of view. Trends Genet 1994;10:194-9.

Barton, S. C., Surani, M. A. & Norris, M. L. Role of paternal and maternal genomes in mouse development. Nature 1984;311:374-6.

Beckwith, J. Bruce (1963). "Extreme cytomegaly of the adrenal fetal cortex, omphalocele, hyperplasia of kidneys and pancreas, and Leydig cell hyperplasia - another syndrome?". Annual Meeting of the Western Society for Pediatric Research. Los Angeles.

Bejjani, B. A., Saleki, R., Ballif, B. C., Rorem, E. A., Sundin, K., Theisen, A., Kashork, C. D. & Shaffer, L. G. Use of targeted array-based CGH for the clinical diagnosis of chromosomal imbalance: is less more? Am J Med Genet A 2005;134:259-67.

Bejjani, B. A. & Shaffer, L. G. Application of array-based comparative genomic hybridization to clinical diagnostics. J Mol Diagn 2006;8:528-33.

Bell, A. C. & Felsenfeld, G. Methylation of a CTCF-dependent boundary controls imprinted expression of the Igf2 gene. Nature 2000;405:482-5.

Benedict, W. F., Murphree, A. L., Banerjee, A., Spina, C. A., Sparkes, M. C. & Sparkes, R. S. Patient with 13 chromosome deletion: evidence that the retinoblastoma gene is a recessive cancer gene. Science 1983;219:973-5.

Benini, D., Vino, L., Vecchini, S. & Fanos, V. 46, XY, del (3) (pter-->p25) syndrome: further delineation of the clinical phenotype. Eur J Pediatr 1999;158:955-7.

Beroukhim, R., Lin, M., Park, Y., Hao, K., Zhao, X., Garraway, L. A., Fox, E. A., Hochberg, E. P., Mellinghoff, I. K., Hofer, M. D., Descazeaud, A., Rubin, M. A., Meyerson, M., Wong, W. H., Sellers, W. R. & Li, C. Inferring loss-of-heterozygosity from unpaired tumours using high-density oligonucleotide SNP arrays. PLoS Comput Biol 2006;2:e41.

Beroukhim, R., Brunet, J. P., Di Napoli, A., Mertz, K. D., Seeley, A., Pires, M. M., Linhart, D., Worrell, R. A., Moch, H., Rubin, M. A., Sellers, W. R., Meyerson, M., Linehan, W. M., Kaelin, W. G., Jr. & Signoretti, S. Patterns of gene expression and copy-number alterations in von-hippel lindau disease-associated and sporadic clear cell carcinoma of the kidney. Cancer Res 2009;69:4674-81.

Bhalla, K., Phillips, H. A., Crawford, J., Mckenzie, O. L., Mulley, J. C., Eyre, H., Gardner, A. E., Kremmidiotis, G. & Callen, D. F. The de novo chromosome 16 translocations of two patients with abnormal phenotypes (mental retardation and epilepsy) disrupt the A2BP1 gene. J Hum Genet 2004;49:308-11.

Bhuiyan, Z. A., Yatsuki, H., Sasaguri, T., Joh, K., Soejima, H., Zhu, X., Hatada, I., Morisaki, H., Morisaki, T. & Mukai, T. Functional analysis of the p57KIP2 gene mutation in Beckwith-Wiedemann syndrome. Hum Genet 1999;104:205-10.

Bien-Willner, G. A., Stankiewicz, P. & Lupski, J. R. SOX9cre1, a cis-acting regulatory element located 1.1 Mb upstream of SOX9, mediates its enhancement through the SHH pathway. Hum Mol Genet 2007;16:1143-56.

Bignell, G. R., Huang, J., Greshock, J., Watt, S., Butler, A., West, S., Grigorova, M., Jones, K. W., Wei, W., Stratton, M. R., Futreal, P. A., Weber, B., Shapero, M. H. & Wooster, R. High-resolution analysis of DNA copy number using oligonucleotide microarrays. Genome Res 2004;14:287-95.

Bjorge, T., Tretli, S. & Engeland, A. Relation of height and body mass index to renal cell carcinoma in two million Norwegian men and women. Am J Epidemiol 2004;160:1168-76.

Blankenship, C., Naglich, J. G., Whaley, J. M., Seizinger, B. & Kley, N. Alternate choice of initiation codon produces a biologically active product of the von Hippel Lindau gene with tumour suppressor activity. Oncogene 1999;18:1529-35.

Bliek, J., Maas, S. M., Ruijter, J. M., Hennekam, R. C., Alders, M., Westerveld, A. & Mannens, M. M. Increased tumour risk for BWS patients correlates with aberrant H19 and not KCNQ1OT1 methylation: occurrence of KCNQ1OT1 hypomethylation in familial cases of BWS. Hum Mol Genet 2001;10:467-76.

Bliek, J., Gicquel, C., Maas, S., Gaston, V., Le Bouc, Y. & Mannens, M. Epigenotyping as a tool for the prediction of tumour risk and tumour type in patients with Beckwith-Wiedemann syndrome (BWS). J Pediatr 2004;145:796-9.

Bliek, J., Snijder, S., Maas, S. M., Polstra, A., Van Der Lip, K., Alders, M., Knegt, A. C. & Mannens, M. M. Phenotypic discordance upon paternal or maternal transmission of duplications of the 11p15 imprinted regions. Eur J Med Genet 2009;52:404-8.

Blouin, J. L., Binkert, F. & Antonarakis, S. E. Biparental inheritance of chromosome 21 polymorphic markers indicates that some Robertsonian translocations t(21;21) occur postzygotically. Am J Med Genet 1994;49:363-8.

Bocciardi, R., Giorda, R., Marigo, V., Zordan, P., Montanaro, D., Gimelli, S., Seri, M., Lerone, M., Ravazzolo, R. & Gimelli, G. Molecular characterization of a t(2;6) balanced translocation that is associated with a complex phenotype and leads to truncation of the TCBA1 gene. Hum Mutat 2005;26:426-36.

Bodmer, D., Eleveld, M. J., Ligtenberg, M. J., Weterman, M. A., Janssen, B. A., Smeets, D. F., De Wit, P. E., Van Den Berg, A., Van Den Berg, E., Koolen, M. I. & Geurts Van Kessel, A. An alternative route for multistep tumourigenesis in a novel case of hereditary renal cell cancer and a t(2;3)(q35;q21) chromosome translocation. Am J Hum Genet 1998;62:1475-83.

Bodmer, D., Eleveld, M., Kater-Baats, E., Janssen, I., Janssen, B., Weterman, M., Schoenmakers, E., Nickerson, M., Linehan, M., Zbar, B. & Van Kessel, A. G. Disruption of a novel MFS transporter gene, DIRC2, by a familial renal cell carcinoma-associated t(2;3)(q35;q21). Hum Mol Genet 2002;11:641-9.

Brauch, H., Pomer, S., Hieronymus, T., Schadt, T., Lohrke, H. & Komitowski, D. Genetic alterations in sporadic renal-cell carcinoma: molecular analyses of tumour suppressor gene harboring chromosomal regions 3p, 5q, and 17p. World J Urol 1994;12:162-8.

Brinkley, B. R. Managing the centrosome numbers game: from chaos to stability in cancer cell division. Trends Cell Biol 2001;11:18-21.

Brookes, A. J. The essence of SNPs. Gene 1999;234:177-86.

Brown, K. W., Gardner, A., Williams, J. C., Mott, M. G., Mcdermott, A. & Maitland, N. J. Paternal origin of 11p15 duplications in the Beckwith-Wiedemann syndrome. A new case and review of the literature. Cancer Genet Cytogenet 1992;58:66-70.

Brown, K. W., Villar, A. J., Bickmore, W., Clayton-Smith, J., Catchpoole, D., Maher, E. R. & Reik, W. Imprinting mutation in the Beckwith-Wiedemann syndrome leads to biallelic IGF2 expression through an H19-independent pathway. Hum Mol Genet 1996;5:2027-32.

Bruder, C. E., Hirvela, C., Tapia-Paez, I., Fransson, I., Segraves, R., Hamilton, G., Zhang, X. X., Evans, D. G., Wallace, A. J., Baser, M. E., Zucman-Rossi, J., Hergersberg, M., Boltshauser, E., Papi, L., Rouleau, G. A., Poptodorov, G., Jordanova, A., Rask-Andersen, H., Kluwe, L., Mautner, V., Sainio, M., Hung, G., Mathiesen, T., Moller, C., Pulst, S. M., Harder, H., Heiberg, A., Honda, M., Niimura, M., Sahlen, S., Blennow, E., Albertson, D. G., Pinkel, D. & Dumanski, J. P. High resolution deletion analysis of constitutional DNA from neurofibromatosis type 2 (NF2) patients using microarray-CGH. Hum Mol Genet 2001;10:271-82.

Bruick, R. K. & Mcknight, S. L. A conserved family of prolyl-4-hydroxylases that modify HIF. Science 2001;294:1337-40.

Brunelli, M., Eble, J. N., Zhang, S., Martignoni, G. & Cheng, L. Gains of chromosomes 7, 17, 12, 16, and 20 and loss of Y occur early in the evolution of papillary renal cell neoplasia: a fluorescent in situ hybridization study. Mod Pathol 2003;16:1053-9.

Bucasas, K. L., Pandya, G. A., Pradhan, S., Fleischmann, R. D., Peterson, S. N. & Belmont, J. W. Assessing the utility of whole-genome amplified serum DNA for array-based high throughput genotyping. BMC Genet 2009;10:85.

Buckley, P. G., Mantripragada, K. K., Benetkiewicz, M., Tapia-Paez, I., Diaz De Stahl, T., Rosenquist, M., Ali, H., Jarbo, C., De Bustos, C., Hirvela, C., Sinder Wilen, B., Fransson, I., Thyr, C., Johnsson, B. I., Bruder, C. E., Menzel, U., Hergersberg, M., Mandahl, N., Blennow, E., Wedell, A., Beare, D. M., Collins, J. E., Dunham, I., Albertson, D., Pinkel, D., Bastian, B. C., Faruqi, A. F., Lasken, R. S., Ichimura, K., Collins, V. P. & Dumanski, J. P. A full-coverage, high-resolution human

chromosome 22 genomic microarray for clinical and research applications. Hum Mol Genet 2002;11:3221-9.
Bugert, P., Wilhelm, M. & Kovacs, G. FHIT gene and the FRA3B region are not involved in the genetics of renal cell carcinomas. Genes Chromosomes Cancer 1997;20:9-15.
Cai, W. W., Mao, J. H., Chow, C. W., Damani, S., Balmain, A. & Bradley, A. Genome-wide detection of chromosomal imbalances in tumours using BAC microarrays. Nat Biotechnol 2002;20:393-6.
Cargile, C. B., Goh, D. L., Goodman, B. K., Chen, X. N., Korenberg, J. R., Semenza, G. L. & Thomas, G. H. Molecular cytogenetic characterization of a subtle interstitial del(3)(p25.3p26.2) in a patient with deletion 3p syndrome. Am J Med Genet 2002;109:133-8.
Carlson, C., Sirotkin, H., Pandita, R., Goldberg, R., Mckie, J., Wadey, R., Patanjali, S. R., Weissman, S. M., Anyane-Yeboa, K., Warburton, D., Scambler, P., Shprintzen, R., Kucherlapati, R. & Morrow, B. E. Molecular definition of 22q11 deletions in 151 velo-cardio-facial syndrome patients. Am J Hum Genet 1997;61:620-9.
Carter, N. P. Methods and strategies for analyzing copy number variation using DNA microarrays. Nat Genet 2007;39:S16-21.
Caspersson, T., Zech, L. & Johansson, C. Analysis of human metaphase chromosome set by aid of DNA-binding fluorescent agents. Exp Cell Res 1970;62:490-2.
Caspersson, T., Lomakka, G. & Zech, L. The 24 fluorescence patterns of the human metaphase chromosomes - distinguishing characters and variability. Hereditas 1972;67:89-102.
Catchpoole, D., Lam, W. W., Valler, D., Temple, I. K., Joyce, J. A., Reik, W., Schofield, P. N. & Maher, E. R. Epigenetic modification and uniparental inheritance of H19 in Beckwith-Wiedemann syndrome. J Med Genet 1997;34:353-9.
Cavenee, W. K., Dryja, T. P., Phillips, R. A., Benedict, W. F., Godbout, R., Gallie, B. L., Murphree, A. L., Strong, L. C. & White, R. L. Expression of recessive alleles by chromosomal mechanisms in retinoblastoma. Nature 1983;305:779-84.
Charalambous, M., Da Rocha, S. T. & Ferguson-Smith, A. C. Genomic imprinting, growth control and the allocation of nutritional resources: consequences for postnatal life. Curr Opin Endocrinol Diabetes Obes 2007;14:3-12.
Chen, F., Kishida, T., Yao, M., Hustad, T., Glavac, D., Dean, M., Gnarra, J. R., Orcutt, M. L., Duh, F. M., Glenn, G. & Et Al. Germline mutations in the von Hippel-Lindau disease tumour suppressor gene: correlations with phenotype. Hum Mutat 1995;5:66-75.
Chen, J., Lui, W. O., Vos, M. D., Clark, G. J., Takahashi, M., Schoumans, J., Khoo, S. K., Petillo, D., Lavery, T., Sugimura, J., Astuti, D., Zhang, C., Kagawa, S., Maher, E. R., Larsson, C., Alberts, A. S., Kanayama, H. O. & Teh, B. T. The t(1;3) breakpoint-spanning genes LSAMP and NORE1 are involved in clear cell renal cell carcinomas. Cancer Cell 2003;4:405-13.
Chen, K. S., Gunaratne, P. H., Hoheisel, J. D., Young, I. G., Miklos, G. L., Greenberg, F., Shaffer, L. G., Campbell, H. D. & Lupski, J. R. The human homologue of the Drosophila melanogaster flightless-I gene (flil) maps within the Smith-Magenis microdeletion critical region in 17p11.2. Am J Hum Genet 1995;56:175-82.
Chen, K. S., Manian, P., Koeuth, T., Potocki, L., Zhao, Q., Chinault, A. C., Lee, C. C. & Lupski, J. R. Homologous recombination of a flanking repeat gene cluster is a mechanism for a common contiguous gene deletion syndrome. Nat Genet 1997;17:154-63.

Chen, M., Ye, Y., Yang, H., Tamboli, P., Matin, S., Tannir, N. M., Wood, C. G., Gu, J. & Wu, X. Genome-wide profiling of chromosomal alterations in renal cell carcinoma using high-density single nucleotide polymorphism arrays. Int J Cancer 2009;125:2342-8.

Chen, W., Kalscheuer, V., Tzschach, A., Menzel, C., Ullmann, R., Schulz, M. H., Erdogan, F., Li, N., Kijas, Z., Arkesteijn, G., Pajares, I. L., Goetz-Sothmann, M., Heinrich, U., Rost, I., Dufke, A., Grasshoff, U., Glaeser, B., Vingron, M. & Ropers, H. H. Mapping translocation breakpoints by next-generation sequencing. Genome Res 2008;18:1143-9.

Chen, Y. H., Xu, S. J., Bendahhou, S., Wang, X. L., Wang, Y., Xu, W. Y., Jin, H. W., Sun, H., Su, X. Y., Zhuang, Q. N., Yang, Y. Q., Li, Y. B., Liu, Y., Xu, H. J., Li, X. F., Ma, N., Mou, C. P., Chen, Z., Barhanin, J. & Huang, W. KCNQ1 gain-of-function mutation in familial atrial fibrillation. Science 2003;299:251-4.

Chiang, D. Y., Getz, G., Jaffe, D. B., O'kelly, M. J., Zhao, X., Carter, S. L., Russ, C., Nusbaum, C., Meyerson, M. & Lander, E. S. High-resolution mapping of copy-number alterations with massively parallel sequencing. Nat Methods 2009;6:99-103.

Christ, L. A., Crowe, C. A., Micale, M. A., Conroy, J. M. & Schwartz, S. Chromosome breakage hotspots and delineation of the critical region for the 9p-deletion syndrome. Am J Hum Genet 1999;65:1387-95.

Christian, S. L., Robinson, W. P., Huang, B., Mutirangura, A., Line, M. R., Nakao, M., Surti, U., Chakravarti, A. & Ledbetter, D. H. Molecular characterization of two proximal deletion breakpoint regions in both Prader-Willi and Angelman syndrome patients. Am J Hum Genet 1995;57:40-8.

Christoph, F., Schmidt, B., Schmitz-Drager, B. J. & Schulz, W. A. Over-expression and amplification of the c-myc gene in human urothelial carcinoma. Int J Cancer 1999;84:169-73.

Choi, J. S., Kim, M. K., Seo, J. W., Choi, Y. L., Kim, D. H., Chun, Y. K. & Ko, Y. H. MET expression in sporadic renal cell carcinomas. J Korean Med Sci 2006;21:672-7.

Chudek, J., Wilhelm, M., Bugert, P., Herbers, J. & Kovacs, G. Detailed microsatellite analysis of chromosome 3p region in non-papillary renal cell carcinomas. Int J Cancer 1997;73:225-9.

Chung, W. Y., Yuan, L., Feng, L., Hensle, T. & Tycko, B. Chromosome 11p15.5 regional imprinting: comparative analysis of KIP2 and H19 in human tissues and Wilms' tumours. Hum Mol Genet 1996;5:1101-8.

Cifola, I., Spinelli, R., Beltrame, L., Peano, C., Fasoli, E., Ferrero, S., Bosari, S., Signorini, S., Rocco, F., Perego, R., Proserpio, V., Raimondo, F., Mocarelli, P. & Battaglia, C. Genome-wide screening of copy number alterations and LOH events in renal cell carcinomas and integration with gene expression profile. Mol Cancer 2008;7:6.

Clarke, A. R., Purdie, C. A., Harrison, D. J., Morris, R. G., Bird, C. C., Hooper, M. L. & Wyllie, A. H. Thymocyte apoptosis induced by p53-dependent and independent pathways. Nature 1993;362:849-52.

Clifford, S. C., Prowse, A. H., Affara, N. A., Buys, C. H. & Maher, E. R. Inactivation of the von Hippel-Lindau (VHL) tumour suppressor gene and allelic losses at chromosome arm 3p in primary renal cell carcinoma: evidence for a VHL-independent pathway in clear cell renal tumourigenesis. Genes Chromosomes Cancer 1998;22:200-9.

Cockman, M. E., Masson, N., Mole, D. R., Jaakkola, P., Chang, G. W., Clifford, S. C., Maher, E. R., Pugh, C. W., Ratcliffe, P. J. & Maxwell, P. H. Hypoxia inducible factor-alpha binding and ubiquitylation by the von Hippel-Lindau tumour suppressor protein. J Biol Chem 2000;275:25733-41.

Cohen, A. J., Li, F. P., Berg, S., Marchetto, D. J., Tsai, S., Jacobs, S. C. & Brown, R. S. Hereditary renal-cell carcinoma associated with a chromosomal translocation. N Engl J Med 1979;301:592-5.

Cohen, H. T. & Mcgovern, F. J. Renal-cell carcinoma. N Engl J Med 2005;353:2477-90.

Collins E, intra ocular growths (two cases, brother and sister with peculiar vascular new growth probably retinal affecting both eyes) Trans Ophthalmol Soc U K 14:141-149, 1894

Cook, E. H., Jr. & Scherer, S. W. Copy-number variations associated with neuropsychiatric conditions. Nature 2008;455:919-23.

Cooper, W. N., Luharia, A., Evans, G. A., Raza, H., Haire, A. C., Grundy, R., Bowdin, S. C., Riccio, A., Sebastio, G., Bliek, J., Schofield, P. N., Reik, W., Macdonald, F. & Maher, E. R. Molecular subtypes and phenotypic expression of Beckwith-Wiedemann syndrome. Eur J Hum Genet 2005;13:1025-32.

Cooper, W. N., Curley, R., Macdonald, F. & Maher, E. R. Mitotic recombination and uniparental disomy in Beckwith-Wiedemann syndrome. Genomics 2007;89:613-7.

Coppes, M. J., Arnold, M., Beckwith, J. B., Ritchey, M. L., D'angio, G. J., Green, D. M. & Breslow, N. E. Factors affecting the risk of contralateral Wilms tumour development: a report from the National Wilms Tumour Study Group. Cancer 1999;85:1616-25.

Crossey, P. A., Foster, K., Richards, F. M., Phipps, M. E., Latif, F., Tory, K., Jones, M. H., Bentley, E., Kumar, R., Lerman, M. I. & Et Al. Molecular genetic investigations of the mechanism of tumourigenesis in von Hippel-Lindau disease: analysis of allele loss in VHL tumours. Hum Genet 1994;93:53-8.

Crossey, P. A., Eng, C., Ginalska-Malinowska, M., Lennard, T. W., Wheeler, D. C., Ponder, B. A. & Maher, E. R. Molecular genetic diagnosis of von Hippel-Lindau disease in familial phaeochromocytoma. J Med Genet 1995;32:885-6.

Cotter, P. D., Kaffe, S., Mccurdy, L. D., Jhaveri, M., Willner, J. P. & Hirschhorn, K. Paternal uniparental disomy for chromosome 14: a case report and review. Am J Med Genet 1997;70:74-9.

Crolla, J. A. & Van Heyningen, V. Frequent chromosome aberrations revealed by molecular cytogenetic studies in patients with aniridia. Am J Hum Genet 2002;71:1138-49.

Crotty, T. B., Farrow, G. M. & Lieber, M. M. Chromophobe cell renal carcinoma: clinicopathological features of 50 cases. J Urol 1995;154:964-7.

Cui, H., Niemitz, E. L., Ravenel, J. D., Onyango, P., Brandenburg, S. A., Lobanenkov, V. V. & Feinberg, A. P. Loss of imprinting of insulin-like growth factor-II in Wilms' tumour commonly involves altered methylation but not mutations of CTCF or its binding site. Cancer Res 2001;61:4947-50.

Dalgliesh, G. L., Furge, K., Greenman, C., Chen, L., Bignell, G., Butler, A., Davies, H., Edkins, S., Hardy, C., Latimer, C., Teague, J., Andrews, J., Barthorpe, S., Beare, D., Buck, G., Campbell, P. J., Forbes, S., Jia, M., Jones, D., Knott, H., Kok, C. Y., Lau, K. W., Leroy, C., Lin, M. L., Mcbride, D. J., Maddison, M., Maguire, S., Mclay, K., Menzies, A., Mironenko, T., Mulderrig, L., Mudie, L., O'meara, S., Pleasance, E., Rajasingham, A., Shepherd, R., Smith, R., Stebbings, L., Stephens, P., Tang, G., Tarpey, P. S., Turrell, K., Dykema, K. J., Khoo, S. K., Petillo, D.,

Wondergem, B., Anema, J., Kahnoski, R. J., Teh, B. T., Stratton, M. R. & Futreal, P. A. Systematic sequencing of renal carcinoma reveals inactivation of histone modifying genes. Nature 2010;463:360-3.

Dang, C. V. c-Myc target genes involved in cell growth, apoptosis, and metabolism. Mol Cell Biol 1999;19:1-11.

Davies, H., Bignell, G. R., Cox, C., Stephens, P., Edkins, S., Clegg, S., Teague, J., Woffendin, H., Garnett, M. J., Bottomley, W., Davis, N., Dicks, E., Ewing, R., Floyd, Y., Gray, K., Hall, S., Hawes, R., Hughes, J., Kosmidou, V., Menzies, A., Mould, C., Parker, A., Stevens, C., Watt, S., Hooper, S., Wilson, R., Jayatilake, H., Gusterson, B. A., Cooper, C., Shipley, J., Hargrave, D., Pritchard-Jones, K., Maitland, N., Chenevix-Trench, G., Riggins, G. J., Bigner, D. D., Palmieri, G., Cossu, A., Flanagan, A., Nicholson, A., Ho, J. W., Leung, S. Y., Yuen, S. T., Weber, B. L., Seigler, H. F., Darrow, T. L., Paterson, H., Marais, R., Marshall, C. J., Wooster, R., Stratton, M. R. & Futreal, P. A. Mutations of the BRAF gene in human cancer. Nature 2002;417:949-54.

Davison C, Brock S, Cyke CG: retinal and central nervous hemangioblastomatosis with visceral changes (von Hippel Lindau's disease) Bull Neurol Inst New York 5:72-93, 1936

DeBaun, M. R., Siegel, M. J. & Choyke, P. L. Nephromegaly in infancy and early childhood: a risk factor for Wilms tumour in Beckwith-Wiedemann syndrome. J Pediatr 1998;132:401-4.

DeBaun, M. R., Niemitz, E. L., Mcneil, D. E., Brandenburg, S. A., Lee, M. P. & Feinberg, A. P. Epigenetic alterations of H19 and LIT1 distinguish patients with Beckwith-Wiedemann syndrome with cancer and birth defects. Am J Hum Genet 2002;70:604-11.

De Braekeleer, M. & Dao, T. N. Cytogenetic studies in male infertility: a review. Hum Reprod 1991;6:245-50.

De Vries, B. B., Pfundt, R., Leisink, M., Koolen, D. A., Vissers, L. E., Janssen, I. M., Reijmersdal, S., Nillesen, W. M., Huys, E. H., Leeuw, N., Smeets, D., Sistermans, E. A., Feuth, T., Van Ravenswaaij-Arts, C. M., Van Kessel, A. G., Schoenmakers, E. F., Brunner, H. G. & Veltman, J. A. Diagnostic genome profiling in mental retardation. Am J Hum Genet 2005;77:606-16.

Delahunt, B., Eble, J. N., Mccredie, M. R., Bethwaite, P. B., Stewart, J. H. & Bilous, A. M. Morphologic typing of papillary renal cell carcinoma: comparison of growth kinetics and patient survival in 66 cases. Hum Pathol 2001;32:590-5.

Delicado, A., Lapunzina, P., Palomares, M., Molina, M. A., Galan, E. & Lopez Pajares, I. Beckwith-Wiedemann syndrome due to 11p15.5 paternal duplication associated with Klinefelter syndrome and a "de novo" pericentric inversion of chromosome Y. Eur J Med Genet 2005;48:159-66.

Depienne, C., Heron, D., Betancur, C., Benyahia, B., Trouillard, O., Bouteiller, D., Verloes, A., Leguern, E., Leboyer, M. & Brice, A. Autism, language delay and mental retardation in a patient with 7q11 duplication. J Med Genet 2007;44:452-8.

Dhote, R., Pellicer-Coeuret, M., Thiounn, N., Debre, B. & Vidal-Trecan, G. Risk factors for adult renal cell carcinoma: a systematic review and implications for prevention. BJU Int 2000;86:20-7.

Diaz-Meyer, N., Day, C. D., Khatod, K., Maher, E. R., Cooper, W., Reik, W., Junien, C., Graham, G., Algar, E., Der Kaloustian, V. M. & Higgins, M. J. Silencing of CDKN1C (p57KIP2) is associated with hypomethylation at KvDMR1 in Beckwith-Wiedemann syndrome. J Med Genet 2003;40:797-801.

Dijkhuizen, T., Van Essen, T., Van Der Vlies, P., Verheij, J. B., Sikkema-Raddatz, B., Van Der Veen, A. Y., Gerssen-Schoorl, K. B., Buys, C. H. & Kok, K. FISH and array-CGH analysis of a complex chromosome 3 aberration suggests that loss of CNTN4 and CRBN contributes to mental retardation in 3pter deletions. Am J Med Genet A 2006;140:2482-7.

Druck, T., Hadaczek, P., Fu, T. B., Ohta, M., Siprashvili, Z., Baffa, R., Negrini, M., Kastury, K., Veronese, M. L., Rosen, D., Rothstein, J., Mccue, P., Cotticelli, M. G., Inoue, H., Croce, C. M. & Huebner, K. Structure and expression of the human FHIT gene in normal and tumour cells. Cancer Res 1997;57:504-12.

Druck, T., Podolski, J., Byrski, T., Wyrwicz, L., Zajaczek, S., Kata, G., Borowka, A., Lubinski, J. & Huebner, K. The DIRC1 gene at chromosome 2q33 spans a familial RCC-associated t(2;3)(q33;q21) chromosome translocation. J Hum Genet 2001;46:583-9.

Drumheller, T., Mcgillivray, B. C., Behrner, D., Macleod, P., Mcfadden, D. E., Roberson, J., Venditti, C., Chorney, K., Chorney, M. & Smith, D. I. Precise localisation of 3p25 breakpoints in four patients with the 3p-syndrome. J Med Genet 1996;33:842-7.

Drut, R. M. & Drut, R. Nonimmune fetal hydrops and placentomegaly: diagnosis of familial Wiedemann-Beckwith syndrome with trisomy 11p15 using FISH. Am J Med Genet 1996;62:145-9.

Duan, D. R., Humphrey, J. S., Chen, D. Y., Weng, Y., Sukegawa, J., Lee, S., Gnarra, J. R., Linehan, W. M. & Klausner, R. D. Characterization of the VHL tumour suppressor gene product: localization, complex formation, and the effect of natural inactivating mutations. Proc Natl Acad Sci U S A 1995;92:6459-63.

Dumon, K. R., Ishii, H., Fong, L. Y., Zanesi, N., Fidanza, V., Mancini, R., Vecchione, A., Baffa, R., Trapasso, F., During, M. J., Huebner, K. & Croce, C. M. FHIT gene therapy prevents tumour development in Fhit-deficient mice. Proc Natl Acad Sci U S A 2001;98:3346-51.

Duns, G., Van Den Berg, E., Van Duivenbode, I., Osinga, J., Hollema, H., Hofstra, R. M. & Kok, K. Histone methyltransferase gene SETD2 is a novel tumour suppressor gene in clear cell renal cell carcinoma. Cancer Res 2010;70:4287-91.

Dutly, F., Baumer, A., Kayserili, H., Yuksel-Apak, M., Zerova, T., Hebisch, G. & Schinzel, A. Seven cases of Wiedmann-Beckwith syndrome, including the first reported case of mosaic paternal isodisomy along the whole chromosome 11. Am J Med Genet 1998;79:347-53.

Edelmann, L., Pandita, R. K. & Morrow, B. E. Low-copy repeats mediate the common 3-Mb deletion in patients with velo-cardio-facial syndrome. Am J Hum Genet 1999a;64:1076-86.

Edelmann, L., Spiteri, E., Mccain, N., Goldberg, R., Pandita, R. K., Duong, S., Fox, J., Blumenthal, D., Lalani, S. R., Shaffer, L. G. & Morrow, B. E. A common breakpoint on 11q23 in carriers of the constitutional t(11;22) translocation. Am J Hum Genet 1999b;65:1608-16.

Edwards, J. H., Harnden, D. G., Cameron, A. H., Crosse, V. M. & Wolff, O. H. A new trisomic syndrome. Lancet 1960;1:787-90.

Eggermann, T., Wollmann, H. A., Kuner, R., Eggermann, K., Enders, H., Kaiser, P. & Ranke, M. B. Molecular studies in 37 Silver-Russell syndrome patients: frequency and etiology of uniparental disomy. Hum Genet 1997;100:415-9.

Eggermann, T., Schonherr, N., Meyer, E., Obermann, C., Mavany, M., Eggermann, K., Ranke, M. B. & Wollmann, H. A. Epigenetic mutations in 11p15 in Silver-Russell

syndrome are restricted to the telomeric imprinting domain. J Med Genet 2006;43:615-6.
Elend, M. & Eilers, M. Cell growth: downstream of Myc - to grow or to cycle? Curr Biol 1999;9:R936-8.
Eleveld, M. J., Bodmer, D., Merkx, G., Siepman, A., Sprenger, S. H., Weterman, M. A., Ligtenberg, M. J., Kamp, J., Stapper, W., Jeuken, J. W., Smeets, D., Smits, A. & Geurts Van Kessel, A. Molecular analysis of a familial case of renal cell cancer and a t(3;6)(q12;q15). Genes Chromosomes Cancer 2001;31:23-32.
Elliott, M. & Maher, E. R. Beckwith-Wiedemann syndrome. J Med Genet 1994;31:560-4.
Emmert-Buck, M. R., Bonner, R. F., Smith, P. D., Chuaqui, R. F., Zhuang, Z., Goldstein, S. R., Weiss, R. A. & Liotta, L. A. Laser capture microdissection. Science 1996;274:998-1001.
Endris, V., Wogatzky, B., Leimer, U., Bartsch, D., Zatyka, M., Latif, F., Maher, E. R., Tariverdian, G., Kirsch, S., Karch, D. & Rappold, G. A. The novel Rho-GTPase activating gene MEGAP/ srGAP3 has a putative role in severe mental retardation. Proc Natl Acad Sci U S A 2002;99:11754-9.
Eng, C., Crossey, P. A., Mulligan, L. M., Healey, C. S., Houghton, C., Prowse, A., Chew, S. L., Dahia, P. L., O'riordan, J. L., Toledo, S. P. & Et Al. Mutations in the RET proto-oncogene and the von Hippel-Lindau disease tumour suppressor gene in sporadic and syndromic phaeochromocytomas. J Med Genet 1995;32:934-7.
Engel, J. R., Smallwood, A., Harper, A., Higgins, M. J., Oshimura, M., Reik, W., Schofield, P. N. & Maher, E. R. Epigenotype-phenotype correlations in Beckwith-Wiedemann syndrome. J Med Genet 2000;37:921-6.
Epstein, A. C., Gleadle, J. M., Mcneill, L. A., Hewitson, K. S., O'rourke, J., Mole, D. R., Mukherji, M., Metzen, E., Wilson, M. I., Dhanda, A., Tian, Y. M., Masson, N., Hamilton, D. L., Jaakkola, P., Barstead, R., Hodgkin, J., Maxwell, P. H., Pugh, C. W., Schofield, C. J. & Ratcliffe, P. J. C. elegans EGL-9 and mammalian homologs define a family of dioxygenases that regulate HIF by prolyl hydroxylation. Cell 2001;107:43-54.
Espina, V., Heiby, M., Pierobon, M. & Liotta, L. A. Laser capture microdissection technology. Expert Rev Mol Diagn 2007;7:647-57.
Estabrooks L.L, Lamb A.N, Kirkman H.N, et al. Beckwith-Wiedemann syndrome in twins with a duplication of chromosome 15(qll.2-qI3)mat. AmI 7 Humn Genet 1989;45:A75
Eyzaguirre, E. J., Miettinen, M., Norris, B. A. & Gatalica, Z. Different immunohistochemical patterns of Fhit protein expression in renal neoplasms. Mod Pathol 1999;12:979-83.
Falk, R. E., Carrel, R. E., Valente, M., Crandall, B. F. & Sparkes, R. S. Partial trisomy of chromosome 11: a case report. Am J Ment Defic 1973;77:383-8.
Ferlay J et al., GLOBOCAN 2002: Cancer incidence, mortality and prevalence worldwide, IARC Press, Lyon, 2004).
Fernandez, T., Morgan, T., Davis, N., Klin, A., Morris, A., Farhi, A., Lifton, R. P. & State, M. W. Disruption of contactin 4 (CNTN4) results in developmental delay and other features of 3p deletion syndrome. Am J Hum Genet 2004;74:1286-93.
Fero, M. L., Randel, E., Gurley, K. E., Roberts, J. M. & Kemp, C. J. The murine gene p27Kip1 is haplo-insufficient for tumour suppression. Nature 1998;396:177-80.
Fert-Ferrer, S., Guichet, A., Tantau, J., Delezoide, A. L., Ozilou, C., Romana, S. P., Gosset, P., Viot, G., Loison, S., Moraine, C., Morichon-Delvallez, N., Turleau, C., Vekemans, M. & Prieur, M. Subtle familial unbalanced translocation

t(8;11)(p23.2;p15.5) in two fetuses with Beckwith-Wiedemann features. Prenat Diagn 2000;20:511-5.

Fiegler, H., Carr, P., Douglas, E. J., Burford, D. C., Hunt, S., Scott, C. E., Smith, J., Vetrie, D., Gorman, P., Tomlinson, I. P. & Carter, N. P. DNA microarrays for comparative genomic hybridization based on DOP-PCR amplification of BAC and PAC clones. Genes Chromosomes Cancer 2003;36:361-74.

Fisher, A. M., Thomas, N. S., Cockwell, A., Stecko, O., Kerr, B., Temple, I. K. & Clayton, P. Duplications of chromosome 11p15 of maternal origin result in a phenotype that includes growth retardation. Hum Genet 2002;111:290-6.

Fitzpatrick, G. V., Soloway, P. D. & Higgins, M. J. Regional loss of imprinting and growth deficiency in mice with a targeted deletion of KvDMR1. Nat Genet 2002;32:426-31.

Flint, J., Craddock, C. F., Villegas, A., Bentley, D. P., Williams, H. J., Galanello, R., Cao, A., Wood, W. G., Ayyub, H. & Higgs, D. R. Healing of broken human chromosomes by the addition of telomeric repeats. Am J Hum Genet 1994;55:505-12.

Ford, C. E., Jones, K. W., Polani, P. E., De Almeida, J. C. & Briggs, J. H. A sex-chromosome anomaly in a case of gonadal dysgenesis (Turner's syndrome). Lancet 1959;1:711-3.

Forozan, F., Karhu, R., Kononen, J., Kallioniemi, A. & Kallioniemi, O. P. Genome screening by comparative genomic hybridization. Trends Genet 1997;13:405-9.

Foster, K., Prowse, A., Van Den Berg, A., Fleming, S., Hulsbeek, M. M., Crossey, P. A., Richards, F. M., Cairns, P., Affara, N. A., Ferguson-Smith, M. A. & Et Al. Somatic mutations of the von Hippel-Lindau disease tumour suppressor gene in non-familial clear cell renal carcinoma. Hum Mol Genet 1994;3:2169-73.

Fraccaro, M., Lindsten, J., Ford, C. E. & Iselius, L. The 11q;22q translocation: a European collaborative analysis of 43 cases. Hum Genet 1980;56:21-51.

Friend, S. H., Bernards, R., Rogelj, S., Weinberg, R. A., Rapaport, J. M., Albert, D. M. & Dryja, T. P. A human DNA segment with properties of the gene that predisposes to retinoblastoma and osteosarcoma. Nature 1986;323:643-6.

Garraway, L. A., Widlund, H. R., Rubin, M. A., Getz, G., Berger, A. J., Ramaswamy, S., Beroukhim, R., Milner, D. A., Granter, S. R., Du, J., Lee, C., Wagner, S. N., Li, C., Golub, T. R., Rimm, D. L., Meyerson, M. L., Fisher, D. E. & Sellers, W. R. Integrative genomic analyses identify MITF as a lineage survival oncogene amplified in malignant melanoma. Nature 2005;436:117-22.

Gaston, V., Le Bouc, Y., Soupre, V., Burglen, L., Donadieu, J., Oro, H., Audry, G., Vazquez, M. P. & Gicquel, C. Analysis of the methylation status of the KCNQ1OT and H19 genes in leukocyte DNA for the diagnosis and prognosis of Beckwith-Wiedemann syndrome. Eur J Hum Genet 2001;9:409-18.

Gemmill, R. M., West, J. D., Boldog, F., Tanaka, N., Robinson, L. J., Smith, D. I., Li, F. & Drabkin, H. A. The hereditary renal cell carcinoma 3;8 translocation fuses FHIT to a patched-related gene, TRC8. Proc Natl Acad Sci U S A 1998;95:9572-7.

Gerdes, T., Kirchhoff, M., Lind, A. M., Larsen, G. V., Schwartz, M. & Lundsteen, C. Computer-assisted prenatal aneuploidy screening for chromosome 13, 18, 21, X and Y based on multiplex ligation-dependent probe amplification (MLPA). Eur J Hum Genet 2005;13:171-5.

Gibbs, J. R. & Singleton, A. Application of genome-wide single nucleotide polymorphism typing: simple association and beyond. PLoS Genet 2006;2:e150.

Gille, J. J., Hogervorst, F. B., Pals, G., Wijnen, J. T., Van Schooten, R. J., Dommering, C. J., Meijer, G. A., Craanen, M. E., Nederlof, P. M., De Jong, D., Mcelgunn, C. J., Schouten, J. P. & Menko, F. H. Genomic deletions of MSH2 and MLH1 in colorectal cancer families detected by a novel mutation detection approach. Br J Cancer 2002;87:892-7.

Glaser, R. L., Ramsay, J. P. & Morison, I. M. The imprinted gene and parent-of-origin effect database now includes parental origin of de novo mutations. Nucleic Acids Res 2006;34:D29-31.

Gnarra, J. R., Tory, K., Weng, Y., Schmidt, L., Wei, M. H., Li, H., Latif, F., Liu, S., Chen, F., Duh, F. M. & Et Al. Mutations of the VHL tumour suppressor gene in renal carcinoma. Nat Genet 1994;7:85-90.

Gnarra, J. R., Zhou, S., Merrill, M. J., Wagner, J. R., Krumm, A., Papavassiliou, E., Oldfield, E. H., Klausner, R. D. & Linehan, W. M. Post-transcriptional regulation of vascular endothelial growth factor mRNA by the product of the VHL tumour suppressor gene. Proc Natl Acad Sci U S A 1996;93:10589-94.

Gonzalez, E., Kulkarni, H., Bolivar, H., Mangano, A., Sanchez, R., Catano, G., Nibbs, R. J., Freedman, B. I., Quinones, M. P., Bamshad, M. J., Murthy, K. K., Rovin, B. H., Bradley, W., Clark, R. A., Anderson, S. A., O'connell R, J., Agan, B. K., Ahuja, S. S., Bologna, R., Sen, L., Dolan, M. J. & Ahuja, S. K. The influence of CCL3L1 gene-containing segmental duplications on HIV-1/AIDS susceptibility. Science 2005;307:1434-40.

Gorringe, K. L., Ramakrishna, M., Williams, L. H., Sridhar, A., Boyle, S. E., Bearfoot, J. L., Li, J., Anglesio, M. S. & Campbell, I. G. Are there any more ovarian tumour suppressor genes? A new perspective using ultra high-resolution copy number and loss of heterozygosity analysis. Genes Chromosomes Cancer 2009;48:931-42.

Gottlieb, E., Haffner, R., King, A., Asher, G., Gruss, P., Lonai, P. & Oren, M. Transgenic mouse model for studying the transcriptional activity of the p53 protein: age- and tissue-dependent changes in radiation-induced activation during embryogenesis. EMBO J 1997;16:1381-90.

Grady, B., Goharderakhshan, R., Chang, J., Ribeiro-Filho, L. A., Perinchery, G., Franks, J., Presti, J., Carroll, P. & Dahiya, R. Frequently deleted loci on chromosome 9 may harbor several tumour suppressor genes in human renal cell carcinoma. J Urol 2001;166:1088-92.

Green, E. K., Priestley, M. D., Waters, J., Maliszewska, C., Latif, F. & Maher, E. R. Detailed mapping of a congenital heart disease gene in chromosome 3p25. J Med Genet 2000;37:581-7.

Greenberg, F., Guzzetta, V., Montes De Oca-Luna, R., Magenis, R. E., Smith, A. C., Richter, S. F., Kondo, I., Dobyns, W. B., Patel, P. I. & Lupski, J. R. Molecular analysis of the Smith-Magenis syndrome: a possible contiguous-gene syndrome associated with del(17)(p11.2). Am J Hum Genet 1991;49:1207-18.

Greenman, C. D., Bignell, G., Butler, A., Edkins, S., Hinton, J., Beare, D., Swamy, S., Santarius, T., Chen, L., Widaa, S., Futreal, P. A. & Stratton, M. R. PICNIC: an algorithm to predict absolute allelic copy number variation with microarray cancer data. Biostatistics 2010;11:164-75.

Grossman, E., Messerli, F. H. & Goldbourt, U. Does diuretic therapy increase the risk of renal cell carcinoma? Am J Cardiol 1999;83:1090-3.

Grossman, E., Messerli, F. H., Boyko, V. & Goldbourt, U. Is there an association between hypertension and cancer mortality? Am J Med 2002;112:479-86.

Grundy, R. G., Aledo, R. & Cowell, J. K. Characterization of the breakpoints in unbalanced t(5;11)(p15;p15) constitutional chromosome translocations in two patients with beckwith-wiedemann syndrome using fluorescence in situ hybridisation. Int J Mol Med 1998;1:801-8.

Gunawan, B., Huber, W., Holtrup, M., Von Heydebreck, A., Efferth, T., Poustka, A., Ringert, R. H., Jakse, G. & Fuzesi, L. Prognostic impacts of cytogenetic findings in clear cell renal cell carcinoma: gain of 5q31-qter predicts a distinct clinical phenotype with favorable prognosis. Cancer Res 2001;61:7731-8.

Gupta, K., Miller, J. D., Li, J. Z., Russell, M. W. & Charbonneau, C. Epidemiologic and socioeconomic burden of metastatic renal cell carcinoma (mRCC): a literature review. Cancer Treat Rev 2008;34:193-205.

Guzzetta, V., Franco, B., Trask, B. J., Zhang, H., Saucedo-Cardenas, O., Montes De Oca-Luna, R., Greenberg, F., Chinault, A. C., Lupski, J. R. & Patel, P. I. Somatic cell hybrids, sequence-tagged sites, simple repeat polymorphisms, and yeast artificial chromosomes for physical and genetic mapping of proximal 17p. Genomics 1992;13:551-9.

Haas, O. A., Zoubek, A., Grumayer, E. R. & Gadner, H. Constitutional interstitial deletion of 11p11 and pericentric inversion of chromosome 9 in a patient with Wiedemann-Beckwith syndrome and hepatoblastoma. Cancer Genet Cytogenet 1986;23:95-104.

Hadaczek, P., Kovatich, A., Gronwald, J., Lubinski, J., Huebner, K. & Mccue, P. A. Loss or reduction of Fhit expression in renal neoplasias: correlation with histogenic class. Hum Pathol 1999;30:1276-83.

Hagenkord, J. M., Monzon, F. A., Kash, S. F., Lilleberg, S., Xie, Q. & Kant, J. A. Array-based karyotyping for prognostic assessment in chronic lymphocytic leukemia: performance comparison of affymetrix 10K2.0, 250K Nsp, and SNP6.0 arrays. J Mol Diagn 2010;12:184-96.

Hamerton, J. L., Canning, N., Ray, M. & Smith, S. A cytogenetic survey of 14,069 newborn infants. I. Incidence of chromosome abnormalities. Clin Genet 1975;8:223-43.

Han, J. Y., Shin, J. H., Han, M. S., Je, G. H. & Shaffer, L. G. Microarray detection of a de novo der(X)t(X;11)(q28;p13) in a girl with premature ovarian failure and features of Beckwith-Wiedemann syndrome. J Hum Genet 2006;51:641-3.

Hanahan, D. & Weinberg, R. A. The hallmarks of cancer. Cell 2000;100:57-70.

Hao, Y., Crenshaw, T., Moulton, T., Newcomb, E. & Tycko, B. Tumour-suppressor activity of H19 RNA. Nature 1993;365:764-7.

Hark, A. T., Schoenherr, C. J., Katz, D. J., Ingram, R. S., Levorse, J. M. & Tilghman, S. M. CTCF mediates methylation-sensitive enhancer-blocking activity at the H19/Igf2 locus. Nature 2000;405:486-9.

Hatada, I., Ohashi, H., Fukushima, Y., Kaneko, Y., Inoue, M., Komoto, Y., Okada, A., Ohishi, S., Nabetani, A., Morisaki, H., Nakayama, M., Niikawa, N. & Mukai, T. An imprinted gene p57KIP2 is mutated in Beckwith-Wiedemann syndrome. Nat Genet 1996;14:171-3.

Healey, S., Powell, F., Battersby, M., Chenevix-Trench, G. & Mcgill, J. Distinct phenotype in maternal uniparental disomy of chromosome 14. Am J Med Genet 1994;51:147-9.

Helman, L. J. & Meltzer, P. Mechanisms of sarcoma development. Nat Rev Cancer 2003;3:685-94.

Henry, I., Bonaiti-Pellie, C., Chehensse, V., Beldjord, C., Schwartz, C., Utermann, G. & Junien, C. Uniparental paternal disomy in a genetic cancer-predisposing syndrome. Nature 1991;351:665-7.

Henry, I., Puech, A., Riesewijk, A., Ahnine, L., Mannens, M., Beldjord, C., Bitoun, P., Tournade, M. F., Landrieu, P. & Junien, C. Somatic mosaicism for partial paternal isodisomy in Wiedemann-Beckwith syndrome: a post-fertilization event. Eur J Hum Genet 1993;1:19-29.

Higgins, J. J., Pucilowska, J., Lombardi, R. Q. & Rooney, J. P. Candidate genes for recessive non-syndromic mental retardation on chromosome 3p (MRT2A). Clin Genet 2004;65:496-500.

Hill, A. S., Foot, N. J., Chaplin, T. L. & Young, B. D. The most frequent constitutional translocation in humans, the t(11;22)(q23;q11) is due to a highly specific alu-mediated recombination. Hum Mol Genet 2000;9:1525-32.

Hippel Ev, Ueber eine sehr seltene erkrankung der nethaut. Graefe Arch Ophthalmol 59:83-106, 1904)

Hirata, H., Matsuyama, H., Matsumoto, H., Korenaga, Y., Ohmi, C., Sakano, S., Yoshihiro, S. & Naito, K. Deletion mapping of 18q in conventional renal cell carcinoma. Cancer Genet Cytogenet 2005;163:101-5.

Hirschhorn, K., Cooper, H. L. & Firschein, I. L. Deletion of short arms of chromosome 4-5 in a child with defects of midline fusion. Humangenetik 1965;1:479-82.

Hodgson, G., Hager, J. H., Volik, S., Hariono, S., Wernick, M., Moore, D., Nowak, N., Albertson, D. G., Pinkel, D., Collins, C., Hanahan, D. & Gray, J. W. Genome scanning with array CGH delineates regional alterations in mouse islet carcinomas. Nat Genet 2001;29:459-64.

Hoffman, B. & Liebermann, D. A. The proto-oncogene c-myc and apoptosis. Oncogene 1998;17:3351-7.

Hoovers, J. M., Kalikin, L. M., Johnson, L. A., Alders, M., Redeker, B., Law, D. J., Bliek, J., Steenman, M., Benedict, M., Wiegant, J., Lengauer, C., Taillon-Miller, P., Schlessinger, D., Edwards, M. C., Elledge, S. J., Ivens, A., Westerveld, A., Little, P., Mannens, M. & Feinberg, A. P. Multiple genetic loci within 11p15 defined by Beckwith-Wiedemann syndrome rearrangement breakpoints and subchromosomal transferable fragments. Proc Natl Acad Sci U S A 1995;92:12456-60.

Horike, S., Mitsuya, K., Meguro, M., Kotobuki, N., Kashiwagi, A., Notsu, T., Schulz, T. C., Shirayoshi, Y. & Oshimura, M. Targeted disruption of the human LIT1 locus defines a putative imprinting control element playing an essential role in Beckwith-Wiedemann syndrome. Hum Mol Genet 2000;9:2075-83.

Huang, J., Wei, W., Zhang, J., Liu, G., Bignell, G. R., Stratton, M. R., Futreal, P. A., Wooster, R., Jones, K. W. & Shapero, M. H. Whole genome DNA copy number changes identified by high density oligonucleotide arrays. Hum Genomics 2004;1:287-99.

Huebner, K. Tumour suppressors on 3p: a neoclassic quartet. Proc Natl Acad Sci U S A 2001;98:14763-5.

Hunt, J. D., Van Der Hel, O. L., Mcmillan, G. P., Boffetta, P. & Brennan, P. Renal cell carcinoma in relation to cigarette smoking: meta-analysis of 24 studies. Int J Cancer 2005;114:101-8.

Iliopoulos, O., Kibel, A., Gray, S. & Kaelin, W. G., Jr. Tumour suppression by the human von Hippel-Lindau gene product. Nat Med 1995;1:822-6.

Iliopoulos, O., Ohh, M. & Kaelin, W. G., Jr. pVHL19 is a biologically active product of the von Hippel-Lindau gene arising from internal translation initiation. Proc Natl Acad Sci U S A 1998;95:11661-6.

Imamura, Y., Hibi, K., Koike, M., Fujiwara, M., Kodera, Y., Ito, K. & Nakao, A. RUNX3 promoter region is specifically methylated in poorly-differentiated colorectal cancer. Anticancer Res 2005;25:2627-30.

Iselius, L., Lindsten, J., Aurias, A., Fraccaro, M., Bastard, C., Bottelli, A. M., Bui, T. H., Caufin, D., Dalpra, L., Delendi, N. & Et Al. The 11q;22q translocation: a collaborative study of 20 new cases and analysis of 110 families. Hum Genet 1983;64:343-55.

Ishikawa, I., Saito, Y., Asaka, M., Tomosugi, N., Yuri, T., Watanabe, M. & Honda, R. Twenty-year follow-up of acquired renal cystic disease. Clin Nephrol 2003;59:153-9.

Ishikawa, S., Komura, D., Tsuji, S., Nishimura, K., Yamamoto, S., Panda, B., Huang, J., Fukayama, M., Jones, K. W. & Aburatani, H. Allelic dosage analysis with genotyping microarrays. Biochem Biophys Res Commun 2005;333:1309-14.

Ishkanian, A. S., Malloff, C. A., Watson, S. K., Deleeuw, R. J., Chi, B., Coe, B. P., Snijders, A., Albertson, D. G., Pinkel, D., Marra, M. A., Ling, V., Macaulay, C. & Lam, W. L. A tiling resolution DNA microarray with complete coverage of the human genome. Nat Genet 2004;36:299-303.

Itoh, N., Becroft, D. M., Reeve, A. E. & Morison, I. M. Proportion of cells with paternal 11p15 uniparental disomy correlates with organ enlargement in Wiedemann-beckwith syndrome. Am J Med Genet 2000;92:111-6.

Ivan, M., Kondo, K., Yang, H., Kim, W., Valiando, J., Ohh, M., Salic, A., Asara, J. M., Lane, W. S. & Kaelin, W. G., Jr. HIFalpha targeted for VHL-mediated destruction by proline hydroxylation: implications for O2 sensing. Science 2001;292:464-8.

Jaakkola, P., Mole, D. R., Tian, Y. M., Wilson, M. I., Gielbert, J., Gaskell, S. J., Kriegsheim, A., Hebestreit, H. F., Mukherji, M., Schofield, C. J., Maxwell, P. H., Pugh, C. W. & Ratcliffe, P. J. Targeting of HIF-alpha to the von Hippel-Lindau ubiquitylation complex by O2-regulated prolyl hydroxylation. Science 2001;292:468-72.

Jacobs, P. A., Baikie, A. G., Brown, W. M., Macgregor, T. N., Maclean, N. & Harnden, D. G. Evidence for the existence of the human "super female". Lancet 1959;2:423-5.

Jacobs, P. A. & Strong, J. A. A case of human intersexuality having a possible XXY sex-determining mechanism. Nature 1959;183:302-3.

Jacobs, P. A., Browne, C., Gregson, N., Joyce, C. & White, H. Estimates of the frequency of chromosome abnormalities detectable in unselected newborns using moderate levels of banding. J Med Genet 1992;29:103-8.

Janne, P. A., Li, C., Zhao, X., Girard, L., Chen, T. H., Minna, J., Christiani, D. C., Johnson, B. E. & Meyerson, M. High-resolution single-nucleotide polymorphism array and clustering analysis of loss of heterozygosity in human lung cancer cell lines. Oncogene 2004;23:2716-26.

Jeffries, A. R., Mungall, A. J., Dawson, E., Halls, K., Langford, C. F., Murray, R. M., Dunham, I. & Powell, J. F. beta-1,3-Glucuronyltransferase-1 gene implicated as a candidate for a schizophrenia-like psychosis through molecular analysis of a balanced translocation. Mol Psychiatry 2003;8:654-63.

Jenkins, R. B., Qian, J., Lieber, M. M. & Bostwick, D. G. Detection of c-myc oncogene amplification and chromosomal anomalies in metastatic prostatic carcinoma by fluorescence in situ hybridization. Cancer Res 1997;57:524-31.

Jervis GA, Newkirk P, Kousseff BG. 2002. Deletion 3p25.3 in a mother and daughter with normal phenotype. Am J Hum Genet 71:294 (Abstract #717).

Jiang, F., Moch, H., Richter, J., Egenter, C., Gasser, T., Bubendorf, L., Gschwind, R., Sauter, G. & Mihatsch, M. J. Comparative genomic hybridization reveals frequent chromosome 13q and 4q losses in renal carcinomas with sarcomatoid transformation. J Pathol 1998;185:382-8.

Jin, J., Cardozo, T., Lovering, R. C., Elledge, S. J., Pagano, M. & Harper, J. W. Systematic analysis and nomenclature of mammalian F-box proteins. Genes Dev 2004;18:2573-80.

Johnson, B. E., Brennan, J. F., Ihde, D. C. & Gazdar, A. F. myc family DNA amplification in tumours and tumour cell lines from patients with small-cell lung cancer. J Natl Cancer Inst Monogr 1992:39-43.

Jones, C., Slijepcevic, P., Marsh, S., Baker, E., Langdon, W. Y., Richards, R. I. & Tunnacliffe, A. Physical linkage of the fragile site FRA11B and a Jacobsen syndrome chromosome deletion breakpoint in 11q23.3. Hum Mol Genet 1994;3:2123-30.

Jones, C., Penny, L., Mattina, T., Yu, S., Baker, E., Voullaire, L., Langdon, W. Y., Sutherland, G. R., Richards, R. I. & Tunnacliffe, A. Association of a chromosome deletion syndrome with a fragile site within the proto-oncogene CBL2. Nature 1995;376:145-9.

Jones, C., Mullenbach, R., Grossfeld, P., Auer, R., Favier, R., Chien, K., James, M., Tunnacliffe, A. & Cotter, F. Co-localisation of CCG repeats and chromosome deletion breakpoints in Jacobsen syndrome: evidence for a common mechanism of chromosome breakage. Hum Mol Genet 2000;9:1201-8.

Jones, S., Zhang, X., Parsons, D. W., Lin, J. C., Leary, R. J., Angenendt, P., Mankoo, P., Carter, H., Kamiyama, H., Jimeno, A., Hong, S. M., Fu, B., Lin, M. T., Calhoun, E. S., Kamiyama, M., Walter, K., Nikolskaya, T., Nikolsky, Y., Hartigan, J., Smith, D. R., Hidalgo, M., Leach, S. D., Klein, A. P., Jaffee, E. M., Goggins, M., Maitra, A., Iacobuzio-Donahue, C., Eshleman, J. R., Kern, S. E., Hruban, R. H., Karchin, R., Papadopoulos, N., Parmigiani, G., Vogelstein, B., Velculescu, V. E. & Kinzler, K. W. Core signaling pathways in human pancreatic cancers revealed by global genomic analyses. Science 2008;321:1801-6.

Journel, H., Lucas, J., Allaire, C., Le Mee, F., Defawe, G., Lecornu, M., Jouan, H., Roussey, M. & Le Marec, B. Trisomy 11p15 and Beckwith-Wiedemann syndrome. Report of two new cases. Ann Genet 1985;28:97-101.

Joyce, J. A., Lam, W. K., Catchpoole, D. J., Jenks, P., Reik, W., Maher, E. R. & Schofield, P. N. Imprinting of IGF2 and H19: lack of reciprocity in sporadic Beckwith-Wiedemann syndrome. Hum Mol Genet 1997;6:1543-8.

Junien, C. Beckwith-Wiedemann syndrome, tumourigenesis and imprinting. Curr Opin Genet Dev 1992;2:431-8.

Juyal, R. C., Kuwano, A., Kondo, I., Zara, F., Baldini, A. & Patel, P. I. Mosaicism for del(17)(p11.2p11.2) underlying the Smith-Magenis syndrome. Am J Med Genet 1996;66:193-6.

Kajii, T. & Ohama, K. Androgenetic origin of hydatidiform mole. Nature 1977;268:633-4.

Kaku, H., Ito, S., Ebara, S., Ouchida, M., Nasu, Y., Tsushima, T., Kumon, H. & Shimizu, K. Positive correlation between allelic loss at chromosome 14q24-31 and poor prognosis of patients with renal cell carcinoma. Urology 2004;64:176-81.

Kallioniemi, A., Kallioniemi, O. P., Sudar, D., Rutovitz, D., Gray, J. W., Waldman, F. & Pinkel, D. Comparative genomic hybridization for molecular cytogenetic analysis of solid tumours. Science 1992;258:818-21.

Kamura, T., Koepp, D. M., Conrad, M. N., Skowyra, D., Moreland, R. J., Iliopoulos, O., Lane, W. S., Kaelin, W. G., Jr., Elledge, S. J., Conaway, R. C., Harper, J. W. & Conaway, J. W. Rbx1, a component of the VHL tumour suppressor complex and SCF ubiquitin ligase. Science 1999;284:657-61.

Kamura, T., Sato, S., Iwai, K., Czyzyk-Krzeska, M., Conaway, R. C. & Conaway, J. W. Activation of HIF1alpha ubiquitination by a reconstituted von Hippel-Lindau (VHL) tumour suppressor complex. Proc Natl Acad Sci U S A 2000;97:10430-5.

Kanayama, H., Lui, W. O., Takahashi, M., Naroda, T., Kedra, D., Wong, F. K., Kuroki, Y., Nakahori, Y., Larsson, C., Kagawa, S. & Teh, B. T. Association of a novel constitutional translocation t(1q;3q) with familial renal cell carcinoma. J Med Genet 2001;38:165-70.

Kanno, J., Hutchin, T., Kamada, F., Narisawa, A., Aoki, Y., Matsubara, Y. & Kure, S. Genomic deletion within GLDC is a major cause of non-ketotic hyperglycinaemia. J Med Genet 2007;44:e69.

Kariya, S., Aoji, K., Akagi, H., Fukushima, K., Chikumoto, E., Ogawa, T., Karaki, M. & Nishizaki, K. A terminal deletion of the short arm of chromosome 3: karyotype 46, XY, del (3) (p25-pter); a case report and literature review. Int J Pediatr Otorhinolaryngol 2000;56:71-8.

Kawamura, T., Nomura, M., Tojo, H., Fujii, K., Hamasaki, H., Mikami, S., Bando, Y., Kato, H. & Nishimura, T. Proteomic analysis of laser-microdissected paraffin-embedded tissues: (1) Stage-related protein candidates upon non-metastatic lung adenocarcinoma. J Proteomics 2010;73:1089-99.

Khoo, S. K., Bradley, M., Wong, F. K., Hedblad, M. A., Nordenskjold, M. & Teh, B. T. Birt-Hogg-Dube syndrome: mapping of a novel hereditary neoplasia gene to chromosome 17p12-q11.2. Oncogene 2001;20:5239-42.

Kim, W. Y. & Kaelin, W. G. Role of VHL gene mutation in human cancer. J Clin Oncol 2004;22:4991-5004.

Kinzler, K. W. & Vogelstein, B. Cancer-susceptibility genes. Gatekeepers and caretakers. Nature 1997;386:761, 763.

Kirov, G., Gumus, D., Chen, W., Norton, N., Georgieva, L., Sari, M., O'donovan, M. C., Erdogan, F., Owen, M. J., Ropers, H. H. & Ullmann, R. Comparative genome hybridization suggests a role for NRXN1 and APBA2 in schizophrenia. Hum Mol Genet 2008;17:458-65.

Klar, J., Asling, B., Carlsson, B., Ulvsback, M., Dellsen, A., Strom, C., Rhedin, M., Forslund, A., Anneren, G., Ludvigsson, J. F. & Dahl, N. RAR-related orphan receptor A isoform 1 (RORa1) is disrupted by a balanced translocation t(4;15)(q22.3;q21.3) associated with severe obesity. Eur J Hum Genet 2005;13:928-34.

Klatte, T., Rao, P. N., De Martino, M., Larochelle, J., Shuch, B., Zomorodian, N., Said, J., Kabbinavar, F. F., Belldegrun, A. S. & Pantuck, A. J. Cytogenetic profile predicts prognosis of patients with clear cell renal cell carcinoma. J Clin Oncol 2009;27:746-53.

Kloth, J. N., Oosting, J., Van Wezel, T., Szuhai, K., Knijnenburg, J., Gorter, A., Kenter, G. G., Fleuren, G. J. & Jordanova, E. S. Combined array-comparative genomic hybridization and single-nucleotide polymorphism-loss of heterozygosity analysis reveals complex genetic alterations in cervical cancer. BMC Genomics 2007;8:53.

Kluwe, L., Nygren, A. O., Errami, A., Heinrich, B., Matthies, C., Tatagiba, M. & Mautner, V. Screening for large mutations of the NF2 gene. Genes Chromosomes Cancer 2005;42:384-91.

Knight, L. A., Yong, M. H., Tan, M. & Ng, I. S. Del(3) (p25.3) without phenotypic effect. J Med Genet 1995;32:994-5.

Knight, S. J., Regan, R., Nicod, A., Horsley, S. W., Kearney, L., Homfray, T., Winter, R. M., Bolton, P. & Flint, J. Subtle chromosomal rearrangements in children with unexplained mental retardation. Lancet 1999;354:1676-81.

Knudson, A. G., Jr. Mutation and cancer: statistical study of retinoblastoma. Proc Natl Acad Sci U S A 1971;68:820-3.

Knuutila, S., Bjorkqvist, A. M., Autio, K., Tarkkanen, M., Wolf, M., Monni, O., Szymanska, J., Larramendy, M. L., Tapper, J., Pere, H., El-Rifai, W., Hemmer, S., Wasenius, V. M., Vidgren, V. & Zhu, Y. DNA copy number amplifications in human neoplasms: review of comparative genomic hybridization studies. Am J Pathol 1998;152:1107-23.

Kobayashi, S., Boggon, T. J., Dayaram, T., Janne, P. A., Kocher, O., Meyerson, M., Johnson, B. E., Eck, M. J., Tenen, D. G. & Halmos, B. EGFR mutation and resistance of non-small-cell lung cancer to gefitinib. N Engl J Med 2005;352:786-92.

Kondo, K. & Kaelin, W. G., Jr. The von Hippel-Lindau tumour suppressor gene. Exp Cell Res 2001;264:117-25.

Koolen, M. I., Van Der Meyden, A. P., Bodmer, D., Eleveld, M., Van Der Looij, E., Brunner, H., Smits, A., Van Den Berg, E., Smeets, D. & Geurts Van Kessel, A. A familial case of renal cell carcinoma and a t(2;3) chromosome translocation. Kidney Int 1998;53:273-5.

Kops, G. J., Weaver, B. A. & Cleveland, D. W. On the road to cancer: aneuploidy and the mitotic checkpoint. Nat Rev Cancer 2005;5:773-85.

Korekane, H., Shida, K., Murata, K., Ohue, M., Sasaki, Y., Imaoka, S. & Miyamoto, Y. Evaluation of laser microdissection as a tool in cancer glycomic studies. Biochem Biophys Res Commun 2007;352:579-86.

Korn, J. M., Kuruvilla, F. G., Mccarroll, S. A., Wysoker, A., Nemesh, J., Cawley, S., Hubbell, E., Veitch, J., Collins, P. J., Darvishi, K., Lee, C., Nizzari, M. M., Gabriel, S. B., Purcell, S., Daly, M. J. & Altshuler, D. Integrated genotype calling and association analysis of SNPs, common copy number polymorphisms and rare CNVs. Nat Genet 2008;40:1253-60.

Kotzot, D., Schmitt, S., Bernasconi, F., Robinson, W. P., Lurie, I. W., Ilyina, H., Mehes, K., Hamel, B. C., Otten, B. J., Hergersberg, M. & Et Al. Uniparental disomy 7 in Silver-Russell syndrome and primordial growth retardation. Hum Mol Genet 1995;4:583-7.

Kovacs, G. & Frisch, S. Clonal chromosome abnormalities in tumour cells from patients with sporadic renal cell carcinomas. Cancer Res 1989;49:651-9.

Kovacs, G., Fuzesi, L., Emanual, A. & Kung, H. F. Cytogenetics of papillary renal cell tumours. Genes Chromosomes Cancer 1991;3:249-55.

Kovacs, G., Akhtar, M., Beckwith, B. J., Bugert, P., Cooper, C. S., Delahunt, B., Eble, J. N., Fleming, S., Ljungberg, B., Medeiros, L. J., Moch, H., Reuter, V. E., Ritz, E., Roos, G., Schmidt, D., Srigley, J. R., Storkel, S., Van Den Berg, E. & Zbar, B. The Heidelberg classification of renal cell tumours. J Pathol 1997;183:131-3.

Koyle, M. A., Hatch, D. A., Furness, P. D., Lovell, M. A., Odom, L. F. & Kurzrock, E. A. Long-term urological complications in survivors younger than 15 months of advanced stage abdominal neuroblastoma. J Urol 2001;166:1455-8.

Kozlowski, P., Bissler, J., Pei, Y. & Kwiatkowski, D. J. Analysis of PKD1 for genomic deletion by multiplex ligation-dependent probe assay: absence of hot spots. Genomics 2008;91:203-8.

Krajewska-Walasek, M., Gutkowska, A., Mospinek-Krasnopolska, M. & Chrzanowska, K. A new case of Beckwith-Wiedemann syndrome with an 11p15 duplication of paternal origin [46,XY,-21,+der(21), t(11;21)(p15.2;q22.3)pat]. Acta Genet Med Gemellol (Roma) 1996;45:245-50.

Kraus, J., Pantel, K., Pinkel, D., Albertson, D. G. & Speicher, M. R. High-resolution genomic profiling of occult micrometastatic tumour cells. Genes Chromosomes Cancer 2003;36:159-66.

Krimpenfort, P., Quon, K. C., Mooi, W. J., Loonstra, A. & Berns, A. Loss of p16Ink4a confers susceptibility to metastatic melanoma in mice. Nature 2001;413:83-6.

Kruglyak, L. Prospects for whole-genome linkage disequilibrium mapping of common disease genes. Nat Genet 1999;22:139-44.

Kruglyak, L. & Nickerson, D. A. Variation is the spice of life. Nat Genet 2001;27:234-6.

Kubota, T., Saitoh, S., Matsumoto, T., Narahara, K., Fukushima, Y., Jinno, Y. & Niikawa, N. Excess functional copy of allele at chromosomal region 11p15 may cause Wiedemann-Beckwith (EMG) syndrome. Am J Med Genet 1994;49:378-83.

Kurahashi, H., Shaikh, T. H., Hu, P., Roe, B. A., Emanuel, B. S. & Budarf, M. L. Regions of genomic instability on 22q11 and 11q23 as the etiology for the recurrent constitutional t(11;22). Hum Mol Genet 2000;9:1665-70.

Laframboise, T. Single nucleotide polymorphism arrays: a decade of biological, computational and technological advances. Nucleic Acids Res 2009;37:4181-93.

Lam, W. W., Hatada, I., Ohishi, S., Mukai, T., Joyce, J. A., Cole, T. R., Donnai, D., Reik, W., Schofield, P. N. & Maher, E. R. Analysis of germline CDKN1C (p57KIP2) mutations in familial and sporadic Beckwith-Wiedemann syndrome (BWS) provides a novel genotype-phenotype correlation. J Med Genet 1999;36:518-23.

Lamb, J., Harris, P. C., Wilkie, A. O., Wood, W. G., Dauwerse, J. G. & Higgs, D. R. De novo truncation of chromosome 16p and healing with (TTAGGG)n in the alpha-thalassemia/mental retardation syndrome (ATR-16). Am J Hum Genet 1993;52:668-76.

Latif, F., Tory, K., Gnarra, J., Yao, M., Duh, F. M., Orcutt, M. L., Stackhouse, T., Kuzmin, I., Modi, W., Geil, L. & Et Al. Identification of the von Hippel-Lindau disease tumour suppressor gene. Science 1993;260:1317-20.

Launonen, V., Vierimaa, O., Kiuru, M., Isola, J., Roth, S., Pukkala, E., Sistonen, P., Herva, R. & Aaltonen, L. A. Inherited susceptibility to uterine leiomyomas and renal cell cancer. Proc Natl Acad Sci U S A 2001;98:3387-92.

Lee, M. H., Reynisdottir, I. & Massague, J. Cloning of p57KIP2, a cyclin-dependent kinase inhibitor with unique domain structure and tissue distribution. Genes Dev 1995;9:639-49.

Lee, M. P., Hu, R. J., Johnson, L. A. & Feinberg, A. P. Human KVLQT1 gene shows tissue-specific imprinting and encompasses Beckwith-Wiedemann syndrome chromosomal rearrangements. Nat Genet 1997;15:181-5.

Lee, M. P., Debaun, M. R., Mitsuya, K., Galonek, H. L., Brandenburg, S., Oshimura, M. & Feinberg, A. P. Loss of imprinting of a paternally expressed transcript, with antisense orientation to KVLQT1, occurs frequently in Beckwith-Wiedemann

syndrome and is independent of insulin-like growth factor II imprinting. Proc Natl Acad Sci U S A 1999;96:5203-8.
Lee, S., Chen, D. Y., Humphrey, J. S., Gnarra, J. R., Linehan, W. M. & Klausner, R. D. Nuclear/cytoplasmic localization of the von Hippel-Lindau tumour suppressor gene product is determined by cell density. Proc Natl Acad Sci U S A 1996;93:1770-5.
Lee, S., Neumann, M., Stearman, R., Stauber, R., Pause, A., Pavlakis, G. N. & Klausner, R. D. Transcription-dependent nuclear-cytoplasmic trafficking is required for the function of the von Hippel-Lindau tumour suppressor protein. Mol Cell Biol 1999;19:1486-97.
Lejeune, J., Gautier, M., Lafourcade, J., Berger, R. & Turpin, R. [Partial Deletion of the Short Arm of the 5 Chromosome: The 5th Case of Crying Cat Syndrome.]. Ann Genet 1964;7:7-10.
Lejeune, J., Lafourcade, J., Berger, R., Vialatte, J., Boeswillwald, M., Seringe, P. & Turpin, R. [3 Cases of Partial Deletion of the Short Arm of a 5 Chromosome.]. C R Hebd Seances Acad Sci 1963;257:3098-102.
Lejeune, J., Turpin, R. & Gautier, M. [Mongolism; a chromosomal disease (trisomy).]. Bull Acad Natl Med 1959;143:256-65.
Lengauer, C., Kinzler, K. W. & Vogelstein, B. Genetic instabilities in human cancers. Nature 1998;396:643-9.
Levan, A. Chromosome studies on some human tumours and tissues of normal origin, grown in vivo and in vitro at the Sloan-Kettering Institute. Cancer 1956;9:648-63.
Levan, A. Some current problems of cancer cytogenetics. Hereditas 1967;57:343-55.
Levy, A. P., Levy, N. S. & Goldberg, M. A. Post-transcriptional regulation of vascular endothelial growth factor by hypoxia. J Biol Chem 1996;271:2746-53.
Lewis, A. & Murrell, A. Genomic imprinting: CTCF protects the boundaries. Curr Biol 2004;14:R284-6.
Lewis R.. Human Genetics: Concepts and Applications, 6th Ed 2005. McGraw Hill, New York
Li, M., Squire, J. A. & Weksberg, R. Molecular genetics of Wiedemann-Beckwith syndrome. Am J Med Genet 1998;79:253-9.
Liao, D. J. & Dickson, R. B. c-Myc in breast cancer. Endocr Relat Cancer 2000;7:143-64.
Lichter, P., Joos, S., Bentz, M. & Lampel, S. Comparative genomic hybridization: uses and limitations. Semin Hematol 2000;37:348-57.
Lieberfarb, M. E., Lin, M., Lechpammer, M., Li, C., Tanenbaum, D. M., Febbo, P. G., Wright, R. L., Shim, J., Kantoff, P. W., Loda, M., Meyerson, M. & Sellers, W. R. Genome-wide loss of heterozygosity analysis from laser capture microdissected prostate cancer using single nucleotide polymorphic allele (SNP) arrays and a novel bioinformatics platform dChipSNP. Cancer Res 2003;63:4781-5.
Lindau A: zur frage der angiomatosis retinal und ihrer hirncomplikation. Acta Ophthalmol 4:193-226, 1927
Lindblad, P. Epidemiology of renal cell carcinoma. Scand J Surg 2004;93:88-96.
Lindblad-Toh, K., Tanenbaum, D. M., Daly, M. J., Winchester, E., Lui, W. O., Villapakkam, A., Stanton, S. E., Larsson, C., Hudson, T. J., Johnson, B. E., Lander, E. S. & Meyerson, M. Loss-of-heterozygosity analysis of small-cell lung carcinomas using single-nucleotide polymorphism arrays. Nat Biotechnol 2000;18:1001-5.
Linder, D. & Gartler, S. M. Distribution of Glucose-6-Phosphate Dehydrogenase Electrophoretic Variants in Different Tissues of Heterozygotes. Am J Hum Genet 1965;17:212-20.

Linder, D., Mccaw, B. K. & Hecht, F. Parthenogenic origin of benign ovarian teratomas. N Engl J Med 1975;292:63-6.
Linehan, W. M., Walther, M. M. & Zbar, B. The genetic basis of cancer of the kidney. J Urol 2003;170:2163-72.
Lipworth, L., Tarone, R. E. & Mclaughlin, J. K. The epidemiology of renal cell carcinoma. J Urol 2006;176:2353-8.
Lonergan, K. M., Iliopoulos, O., Ohh, M., Kamura, T., Conaway, R. C., Conaway, J. W. & Kaelin, W. G., Jr. Regulation of hypoxia-inducible mRNAs by the von Hippel-Lindau tumour suppressor protein requires binding to complexes containing elongins B/C and Cul2. Mol Cell Biol 1998;18:732-41.
Look, A. T. Oncogenic transcription factors in the human acute leukemias. Science 1997;278:1059-64.
Lubensky, I. A., Gnarra, J. R., Bertheau, P., Walther, M. M., Linehan, W. M. & Zhuang, Z. Allelic deletions of the VHL gene detected in multiple microscopic clear cell renal lesions in von Hippel-Lindau disease patients. Am J Pathol 1996;149:2089-94.
Lubinski, J., Hadaczek, P., Podolski, J., Toloczko, A., Sikorski, A., Mccue, P., Druck, T. & Huebner, K. Common regions of deletion in chromosome regions 3p12 and 3p14.2 in primary clear cell renal carcinomas. Cancer Res 1994;54:3710-3.
Luceri, C., Guglielmi, F., De Filippo, C., Caderni, G., Mini, E., Biggeri, A., Napoli, C., Tonelli, F., Cianchi, F. & Dolara, P. Clinicopathologic features and FHIT gene expression in sporadic colorectal adenocarcinomas. Scand J Gastroenterol 2000;35:637-41.
Lupski, J. R., Roth, J. R. & Weinstock, G. M. Chromosomal duplications in bacteria, fruit flies, and humans. Am J Hum Genet 1996;58:21-7.
Lupski, J. R. Genomic disorders: structural features of the genome can lead to DNA rearrangements and human disease traits. Trends Genet 1998;14:417-22.
Lupski, J. R. Genomic rearrangements and sporadic disease. Nat Genet 2007;39:S43-7.
Maher, C. A., Kumar-Sinha, C., Cao, X., Kalyana-Sundaram, S., Han, B., Jing, X., Sam, L., Barrette, T., Palanisamy, N. & Chinnaiyan, A. M. Transcriptome sequencing to detect gene fusions in cancer. Nature 2009;458:97-101.
Maher, E. R., Yates, J. R. & Ferguson-Smith, M. A. Statistical analysis of the two stage mutation model in von Hippel-Lindau disease, and in sporadic cerebellar haemangioblastoma and renal cell carcinoma. J Med Genet 1990a;27:311-4.
Maher, E. R., Yates, J. R., Harries, R., Benjamin, C., Harris, R., Moore, A. T. & Ferguson-Smith, M. A. Clinical features and natural history of von Hippel-Lindau disease. Q J Med 1990b;77:1151-63.
Maher, E. R., Iselius, L., Yates, J. R., Littler, M., Benjamin, C., Harris, R., Sampson, J., Williams, A., Ferguson-Smith, M. A. & Morton, N. Von Hippel-Lindau disease: a genetic study. J Med Genet 1991a;28:443-7.
Maher, E. R. Inherited renal cell carcinoma. Br J Urol 1996a;78:542-5.
Maher, E. R., Webster, A. R., Richards, F. M., Green, J. S., Crossey, P. A., Payne, S. J. & Moore, A. T. Phenotypic expression in von Hippel-Lindau disease: correlations with germline VHL gene mutations. J Med Genet 1996b;33:328-32.
Maher, E. R. & Kaelin, W. G., Jr. von Hippel-Lindau disease. Medicine (Baltimore) 1997;76:381-91.
Maher, E. R. & Reik, W. Beckwith-Wiedemann syndrome: imprinting in clusters revisited. J Clin Invest 2000;105:247-52.
Maher, E. R. Von Hippel-Lindau disease. Curr Mol Med 2004;4:833-42.

Malcolm, S., Clayton-Smith, J., Nichols, M., Robb, S., Webb, T., Armour, J. A., Jeffreys, A. J. & Pembrey, M. E. Uniparental paternal disomy in Angelman's syndrome. Lancet 1991;337:694-7.

Malmgren, H., Sahlen, S., Wide, K., Lundvall, M. & Blennow, E. Distal 3p deletion syndrome: detailed molecular cytogenetic and clinical characterization of three small distal deletions and review. Am J Med Genet A 2007;143A:2143-9.

Mandriota, S. J., Turner, K. J., Davies, D. R., Murray, P. G., Morgan, N. V., Sowter, H. M., Wykoff, C. C., Maher, E. R., Harris, A. L., Ratcliffe, P. J. & Maxwell, P. H. HIF activation identifies early lesions in VHL kidneys: evidence for site-specific tumour suppressor function in the nephron. Cancer Cell 2002;1:459-68.

Mann, G., Trebo, M. M., Haas, O. A., Grumayer-Panzer, E. R., Dworzak, M. N., Lion, T. & Gadner, H. Philadelphia chromosome-positive mature B-cell (Burkitt cell) leukaemia. Br J Haematol 2002;118:559-62.

Mannens, M., Hoovers, J. M., Redeker, E., Verjaal, M., Feinberg, A. P., Little, P., Boavida, M., Coad, N., Steenman, M., Bliek, J. & Et Al. Parental imprinting of human chromosome region 11p15.3-pter involved in the Beckwith-Wiedemann syndrome and various human neoplasia. Eur J Hum Genet 1994;2:3-23.

Martinez, A., Fullwood, P., Kondo, K., Kishida, T., Yao, M., Maher, E. R. & Latif, F. Role of chromosome 3p12-p21 tumour suppressor genes in clear cell renal cell carcinoma: analysis of VHL dependent and VHL independent pathways of tumourigenesis. Mol Pathol 2000;53:137-44.

Masson, N., Willam, C., Maxwell, P. H., Pugh, C. W. & Ratcliffe, P. J. Independent function of two destruction domains in hypoxia-inducible factor-alpha chains activated by prolyl hydroxylation. EMBO J 2001;20:5197-206.

Matsuda, D., Khoo, S. K., Massie, A., Iwamura, M., Chen, J., Petillo, D., Wondergem, B., Avallone, M., Kloostra, S. J., Tan, M. H., Koeman, J., Zhang, Z., Kahnoski, R. J., Baba, S. & Teh, B. T. Identification of copy number alterations and its association with pathological features in clear cell and papillary RCC. Cancer Lett 2008;272:260-7.

Matsuoka, S., Edwards, M. C., Bai, C., Parker, S., Zhang, P., Baldini, A., Harper, J. W. & Elledge, S. J. p57KIP2, a structurally distinct member of the p21CIP1 Cdk inhibitor family, is a candidate tumour suppressor gene. Genes Dev 1995;9:650-62.

Mathew, A., Devesa, S. S., Fraumeni, J. F., Jr. & Chow, W. H. Global increases in kidney cancer incidence, 1973-1992. Eur J Cancer Prev 2002;11:171-8.

Maxwell, P. H., Wiesener, M. S., Chang, G. W., Clifford, S. C., Vaux, E. C., Cockman, M. E., Wykoff, C. C., Pugh, C. W., Maher, E. R. & Ratcliffe, P. J. The tumour suppressor protein VHL targets hypoxia-inducible factors for oxygen-dependent proteolysis. Nature 1999;399:271-5.

McCarroll, S. A., Kuruvilla, F. G., Korn, J. M., Cawley, S., Nemesh, J., Wysoker, A., Shapero, M. H., De Bakker, P. I., Maller, J. B., Kirby, A., Elliott, A. L., Parkin, M., Hubbell, E., Webster, T., Mei, R., Veitch, J., Collins, P. J., Handsaker, R., Lincoln, S., Nizzari, M., Blume, J., Jones, K. W., Rava, R., Daly, M. J., Gabriel, S. B. & Altshuler, D. Integrated detection and population-genetic analysis of SNPs and copy number variation. Nat Genet 2008;40:1166-74.

McClure, R. J., Telford, N. & Newell, S. J. A mild phenotype associated with der(9)t(3;9)(p25;p23). J Med Genet 1996;33:625-7.

McCredie, M., Pommer, W., Mclaughlin, J. K., Stewart, J. H., Lindblad, P., Mandel, J. S., Mellemgaard, A., Schlehofer, B. & Niwa, S. International renal-cell cancer study. II. Analgesics. Int J Cancer 1995;60:345-9.

McGrath, J. & Solter, D. Completion of mouse embryogenesis requires both the maternal and paternal genomes. Cell 1984;37:179-83.

McLaughlin, J. K., Chow, W. H., Mandel, J. S., Mellemgaard, A., Mccredie, M., Lindblad, P., Schlehofer, B., Pommer, W., Niwa, S. & Adami, H. O. International renal-cell cancer study. VIII. Role of diuretics, other anti-hypertensive medications and hypertension. Int J Cancer 1995;63:216-21.

McPherson, R., Pertsemlidis, A., Kavaslar, N., Stewart, A., Roberts, R., Cox, D. R., Hinds, D. A., Pennacchio, L. A., Tybjaerg-Hansen, A., Folsom, A. R., Boerwinkle, E., Hobbs, H. H. & Cohen, J. C. A common allele on chromosome 9 associated with coronary heart disease. Science 2007;316:1488-91.

McRonald, F. E., Morris, M. R., Gentle, D., Winchester, L., Baban, D., Ragoussis, J., Clarke, N. W., Brown, M. D., Kishida, T., Yao, M., Latif, F. & Maher, E. R. CpG methylation profiling in VHL related and VHL unrelated renal cell carcinoma. Mol Cancer 2009;8:31.

Mellemgaard, A. Human renal-cell carcinoma--epidemiological and mechanistic aspects. IARC Sci Publ 1999:69-80.

Meloni-Ehrig, A. M. Renal cancer: cytogenetic and molecular genetic aspects. Am J Med Genet 2002;115:164-72.

Menko, F. H., Van Steensel, M. A., Giraud, S., Friis-Hansen, L., Richard, S., Ungari, S., Nordenskjold, M., Hansen, T. V., Solly, J. & Maher, E. R. Birt-Hogg-Dube syndrome: diagnosis and management. Lancet Oncol 2009;10:1199-206.

Merrild, U., Berggreen, S., Hansen, L., Mikkelsen, M. & Henningsen, K. Partial deletion of the short arm of chromosome 3. Eur J Pediatr 1981;136:211-6.

Mertens, F., Johansson, B., Hoglund, M. & Mitelman, F. Chromosomal imbalance maps of malignant solid tumours: a cytogenetic survey of 3185 neoplasms. Cancer Res 1997;57:2765-80.

Mikhail, F. M., Sathienkijkanchai, A., Robin, N. H., Prucka, S., Biggerstaff, J. S., Komorowski, J., Andersson, R., Bruder, C. E., Piotrowski, A., Diaz De Stahl, T., Dumanski, J. P. & Carroll, A. J. Overlapping phenotype of Wolf-Hirschhorn and Beckwith-Wiedemann syndromes in a girl with der(4)t(4;11)(pter;pter). Am J Med Genet A 2007;143A:1760-6.

Mitelman, F., Johansson, B. & Mertens, F. Fusion genes and rearranged genes as a linear function of chromosome aberrations in cancer. Nat Genet 2004;36:331-4.

Mitsumori, K., Kittleson, J. M., Itoh, N., Delahunt, B., Heathcott, R. W., Stewart, J. H., Mccredie, M. R. & Reeve, A. E. Chromosome 14q LOH in localized clear cell renal cell carcinoma. J Pathol 2002;198:110-4.

Moch, H., Sauter, G., Gasser, T. C., Bubendorf, L., Richter, J., Presti, J. C., Jr., Waldman, F. M. & Mihatsch, M. J. EGF-r gene copy number changes in renal cell carcinoma detected by fluorescence in situ hybridization. J Pathol 1998;184:424-9.

Monzon, F. A., Alvarez, K., Gatalica, Z., Bridge, J. A., Nelson, M., Kim, H. J. & Hagenkord, J. M. Detection of chromosomal aberrations in renal tumours: a comparative study of conventional cytogenetics and virtual karyotyping with single-nucleotide polymorphism microarrays. Arch Pathol Lab Med 2009;133:1917-22.

Moorhead, P. S., Nowell, P. C., Mellman, W. J., Battips, D. M. & Hungerford, D. A. Chromosome preparations of leukocytes cultured from human peripheral blood. Exp Cell Res 1960;20:613-6.

Mori, M., Mimori, K., Shiraishi, T., Alder, H., Inoue, H., Tanaka, Y., Sugimachi, K., Huebner, K. & Croce, C. M. Altered expression of Fhit in carcinoma and precarcinomatous lesions of the esophagus. Cancer Res 2000;60:1177-82.

Morison, I. M. & Reeve, A. E. A catalogue of imprinted genes and parent-of-origin effects in humans and animals. Hum Mol Genet 1998;7:1599-609.

Morison, I. M., Ramsay, J. P. & Spencer, H. G. A census of mammalian imprinting. Trends Genet 2005;21:457-65.

Morris, C. A. & Mervis, C. B. Williams syndrome and related disorders. Annu Rev Genomics Hum Genet 2000;1:461-84.

Morrissey, C., Martinez, A., Zatyka, M., Agathanggelou, A., Honorio, S., Astuti, D., Morgan, N. V., Moch, H., Richards, F. M., Kishida, T., Yao, M., Schraml, P., Latif, F. & Maher, E. R. Epigenetic inactivation of the RASSF1A 3p21.3 tumour suppressor gene in both clear cell and papillary renal cell carcinoma. Cancer Res 2001;61:7277-81.

Morrow, B., Goldberg, R., Carlson, C., Das Gupta, R., Sirotkin, H., Collins, J., Dunham, I., O'donnell, H., Scambler, P., Shprintzen, R. & Et Al. Molecular definition of the 22q11 deletions in velo-cardio-facial syndrome. Am J Hum Genet 1995;56:1391-403.

Motzer, R. J., Bander, N. H. & Nanus, D. M. Renal-cell carcinoma. N Engl J Med 1996;335:865-75.

Mowrey, P. N., Chorney, M. J., Venditti, C. P., Latif, F., Modi, W. S., Lerman, M. I., Zbar, B., Robins, D. B., Rogan, P. K. & Ladda, R. L. Clinical and molecular analyses of deletion 3p25-pter syndrome. Am J Med Genet 1993;46:623-9.

Mullighan, C. G., Goorha, S., Radtke, I., Miller, C. B., Coustan-Smith, E., Dalton, J. D., Girtman, K., Mathew, S., Ma, J., Pounds, S. B., Su, X., Pui, C. H., Relling, M. V., Evans, W. E., Shurtleff, S. A. & Downing, J. R. Genome-wide analysis of genetic alterations in acute lymphoblastic leukaemia. Nature 2007;446:758-64.

Murrell, A., Heeson, S. & Reik, W. Interaction between differentially methylated regions partitions the imprinted genes Igf2 and H19 into parent-specific chromatin loops. Nat Genet 2004;36:889-93.

Mutirangura, A., Jayakumar, A., Sutcliffe, J. S., Nakao, M., Mckinney, M. J., Buiting, K., Horsthemke, B., Beaudet, A. L., Chinault, A. C. & Ledbetter, D. H. A complete YAC contig of the Prader-Willi/Angelman chromosome region (15q11-q13) and refined localization of the SNRPN gene. Genomics 1993;18:546-52.

Mydlo, J. H., Michaeli, J., Cordon-Cardo, C., Goldenberg, A. S., Heston, W. D. & Fair, W. R. Expression of transforming growth factor alpha and epidermal growth factor receptor messenger RNA in neoplastic and nonneoplastic human kidney tissue. Cancer Res 1989;49:3407-11.

Nagao, K., Yamaguchi, S., Matsuyama, H., Korenaga, Y., Hirata, H., Yoshihiro, S., Fukunaga, K., Oba, K. & Naito, K. Allelic loss of 3p25 associated with alterations of 5q22.3 approximately q23.2 may affect the prognosis of conventional renal cell carcinoma. Cancer Genet Cytogenet 2005;160:43-8.

Naidu, R., Wahab, N. A., Yadav, M. & Kutty, M. K. Protein expression and molecular analysis of c-myc gene in primary breast carcinomas using immunohistochemistry and differential polymerase chain reaction. Int J Mol Med 2002;9:189-96.

Nakamura, T., Furukawa, Y., Nakagawa, H., Tsunoda, T., Ohigashi, H., Murata, K., Ishikawa, O., Ohgaki, K., Kashimura, N., Miyamoto, M., Hirano, S., Kondo, S., Katoh, H., Nakamura, Y. & Katagiri, T. Genome-wide cDNA microarray analysis of gene expression profiles in pancreatic cancers using populations of tumour cells and normal ductal epithelial cells selected for purity by laser microdissection. Oncogene 2004;23:2385-400.

Narahara, K., Kikkawa, K., Murakami, M., Hiramoto, K., Namba, H., Tsuji, K., Yokoyama, Y. & Kimoto, H. Loss of the 3p25.3 band is critical in the manifestation of del(3p) syndrome: karyotype-phenotype correlation in cases with deficiency of the distal portion of the short arm of chromosome 3. Am J Med Genet 1990;35:269-73.

Närvä E, Autio R, Rahkonen N, Kong L, Harrison N, Kitsberg D, Borghese L,Itskovitz-Eldor J, Rasool O, Dvorak P, Hovatta O, Otonkoski T, Tuuri T, Cui W, Brüstle O, Baker D, Maltby E, Moore HD, Benvenisty N, Andrews PW, Yli-Harja O, Lahesmaa R. High-resolution DNA analysis of human embryonic stem cell lines reveals culture-induced copy number changes and loss of heterozygosity. Nat Biotechnol. 2010;28:371-7

Negrini, M., Monaco, C., Vorechovsky, I., Ohta, M., Druck, T., Baffa, R., Huebner, K. & Croce, C. M. The FHIT gene at 3p14.2 is abnormal in breast carcinomas. Cancer Res 1996;56:3173-9.

Neumann, H. P., Bender, B. U., Berger, D. P., Laubenberger, J., Schultze-Seemann, W., Wetterauer, U., Ferstl, F. J., Herbst, E. W., Schwarzkopf, G., Hes, F. J., Lips, C. J., Lamiell, J. M., Masek, O., Riegler, P., Mueller, B., Glavac, D. & Brauch, H. Prevalence, morphology and biology of renal cell carcinoma in von Hippel-Lindau disease compared to sporadic renal cell carcinoma. J Urol 1998;160:1248-54.

Newsham, I., Kindler-Rohrborn, A., Daub, D. & Cavenee, W. A constitutional BWS-related t(11;16) chromosome translocation occurring in the same region of chromosome 16 implicated in Wilms' tumours. Genes Chromosomes Cancer 1995;12:1-7.

Neyroud, N., Tesson, F., Denjoy, I., Leibovici, M., Donger, C., Barhanin, J., Faure, S., Gary, F., Coumel, P., Petit, C., Schwartz, K. & Guicheney, P. A novel mutation in the potassium channel gene KVLQT1 causes the Jervell and Lange-Nielsen cardioauditory syndrome. Nat Genet 1997;15:186-9.

Nicholls, R. D., Knoll, J. H., Glatt, K., Hersh, J. H., Brewster, T. D., Graham, J. M., Jr., Wurster-Hill, D., Wharton, R. & Latt, S. A. Restriction fragment length polymorphisms within proximal 15q and their use in molecular cytogenetics and the Prader-Willi syndrome. Am J Med Genet 1989;33:66-77.

Nicholls, R. D., Pai, G. S., Gottlieb, W. & Cantu, E. S. Paternal uniparental disomy of chromosome 15 in a child with Angelman syndrome. Ann Neurol 1992;32:512-8.

Nicholls, R. D. The impact of genomic imprinting for neurobehavioral and developmental disorders. J Clin Invest 2000;105:413-8.

Nickerson, M. L., Warren, M. B., Toro, J. R., Matrosova, V., Glenn, G., Turner, M. L., Duray, P., Merino, M., Choyke, P., Pavlovich, C. P., Sharma, N., Walther, M., Munroe, D., Hill, R., Maher, E., Greenberg, C., Lerman, M. I., Linehan, W. M., Zbar, B. & Schmidt, L. S. Mutations in a novel gene lead to kidney tumours, lung wall defects, and benign tumours of the hair follicle in patients with the Birt-Hogg-Dube syndrome. Cancer Cell 2002;2:157-64.

Nielsen, J. & Wohlert, M. Chromosome abnormalities found among 34,910 newborn children: results from a 13-year incidence study in Arhus, Denmark. Hum Genet 1991;87:81-3.

Niemitz, E. L., Debaun, M. R., Fallon, J., Murakami, K., Kugoh, H., Oshimura, M. & Feinberg, A. P. Microdeletion of LIT1 in familial Beckwith-Wiedemann syndrome. Am J Hum Genet 2004;75:844-9.

Nienhaus, H., Mau, U. & Zang, K. D. Infant with del(3) (p25-pter): karyotype-phenotype correlation and review of previously reported cases. Am J Med Genet 1992;44:573-5.

Niikawa, N., Ishikiriyama, S., Takahashi, S., Inagawa, A., Tonoki, H., Ohta, Y., Hase, N., Kamei, T. & Kajii, T. The Wiedemann-Beckwith syndrome: pedigree studies on five families with evidence for autosomal dominant inheritance with variable expressivity. Am J Med Genet 1986;24:41-55.

Niimura, Y. & Gojobori, T. In silico chromosome staining: reconstruction of Giemsa bands from the whole human genome sequence. Proc Natl Acad Sci U S A 2002;99:797-802.

Norman, A. M., Read, A. P., Clayton-Smith, J., Andrews, T. & Donnai, D. Recurrent Wiedemann-Beckwith syndrome with inversion of chromosome (11)(p11.2p15.5). Am J Med Genet 1992;42:638-41.

Nowak, M. A., Michor, F., Komarova, N. L. & Iwasa, Y. Evolutionary dynamics of tumour suppressor gene inactivation. Proc Natl Acad Sci U S A 2004;101:10635-8.

Nowell, P. C. & Hungerford, D. A. Chromosome studies on normal and leukemic human leukocytes. J Natl Cancer Inst 1960;25:85-109.

Nussbaum RL, McInnes RR, Willard HF, Genetic Variation in Individuals: Mutation and Polymorphism, Thompson & Thompson Genetics in Medicine, 6th edition Philadelphia, PA: W.B. Saunders; 2001, pg 84.

Nystrom, A., Cheetham, J. E., Engstrom, W. & Schofield, P. N. Molecular analysis of patients with Wiedemann-Beckwith syndrome. II. Paternally derived disomies of chromosome 11. Eur J Pediatr 1992;151:511-4.

Ogawa, O., Eccles, M. R., Szeto, J., Mcnoe, L. A., Yun, K., Maw, M. A., Smith, P. J. & Reeve, A. E. Relaxation of insulin-like growth factor II gene imprinting implicated in Wilms' tumour. Nature 1993;362:749-51.

Ohta, M., Inoue, H., Cotticelli, M. G., Kastury, K., Baffa, R., Palazzo, J., Siprashvili, Z., Mori, M., Mccue, P., Druck, T., Croce, C. M. & Huebner, K. The FHIT gene, spanning the chromosome 3p14.2 fragile site and renal carcinoma-associated t(3;8) breakpoint, is abnormal in digestive tract cancers. Cell 1996;84:587-97.

Okano, Y., Osasa, Y., Yamamoto, H., Hase, Y., Tsuruhara, T. & Fujita, H. An infant with Beckwith-Wiedemann syndrome and chromosomal duplication 11p13----pter.: correlation of symptoms between 11p trisomy and Beckwith-Wiedemann syndrome. Jinrui Idengaku Zasshi 1986;31:365-72.

Ong, S. T., Fong, K. M., Bader, S. A., Minna, J. D., Le Beau, M. M., Mckeithan, T. W. & Rassool, F. V. Precise localization of the FHIT gene to the common fragile site at 3p14.2 (FRA3B) and characterization of homozygous deletions within FRA3B that affect FHIT transcription in tumour cell lines. Genes Chromosomes Cancer 1997;20:16-23.

Orba, Y., Tanaka, S., Nishihara, H., Kawamura, N., Itoh, T., Shimizu, M., Sawa, H. & Nagashima, K. Application of laser capture microdissection to cytologic specimens

for the detection of immunoglobulin heavy chain gene rearrangement in patients with malignant lymphoma. Cancer 2003;99:198-204.

Packham, G. & Cleveland, J. L. c-Myc and apoptosis. Biochim Biophys Acta 1995;1242:11-28.

Page, S. L., Shin, J. C., Han, J. Y., Choo, K. H. & Shaffer, L. G. Breakpoint diversity illustrates distinct mechanisms for Robertsonian translocation formation. Hum Mol Genet 1996;5:1279-88.

Page, S. L. & Shaffer, L. G. Nonhomologous Robertsonian translocations form predominantly during female meiosis. Nat Genet 1997;15:231-2.

Pandita, A., Zielenska, M., Thorner, P., Bayani, J., Godbout, R., Greenberg, M. & Squire, J. A. Application of comparative genomic hybridization, spectral karyotyping, and microarray analysis in the identification of subtype-specific patterns of genomic changes in rhabdomyosarcoma. Neoplasia 1999;1:262-75.

Paris, P. L., Albertson, D. G., Alers, J. C., Andaya, A., Carroll, P., Fridlyand, J., Jain, A. N., Kamkar, S., Kowbel, D., Krijtenburg, P. J., Pinkel, D., Schroder, F. H., Vissers, K. J., Watson, V. J., Wildhagen, M. F., Collins, C. & Van Dekken, H. High-resolution analysis of paraffin-embedded and formalin-fixed prostate tumours using comparative genomic hybridization to genomic microarrays. Am J Pathol 2003;162:763-70.

Parsons, D. W., Jones, S., Zhang, X., Lin, J. C., Leary, R. J., Angenendt, P., Mankoo, P., Carter, H., Siu, I. M., Gallia, G. L., Olivi, A., Mclendon, R., Rasheed, B. A., Keir, S., Nikolskaya, T., Nikolsky, Y., Busam, D. A., Tekleab, H., Diaz, L. A., Jr., Hartigan, J., Smith, D. R., Strausberg, R. L., Marie, S. K., Shinjo, S. M., Yan, H., Riggins, G. J., Bigner, D. D., Karchin, R., Papadopoulos, N., Parmigiani, G., Vogelstein, B., Velculescu, V. E. & Kinzler, K. W. An integrated genomic analysis of human glioblastoma multiforme. Science 2008;321:1807-12.

Patau, K., Smith, D. W., Therman, E., Inhorn, S. L. & Wagner, H. P. Multiple congenital anomaly caused by an extra autosome. Lancet 1960;1:790-3.

Pause, A., Lee, S., Worrell, R. A., Chen, D. Y., Burgess, W. H., Linehan, W. M. & Klausner, R. D. The von Hippel-Lindau tumour-suppressor gene product forms a stable complex with human CUL-2, a member of the Cdc53 family of proteins. Proc Natl Acad Sci U S A 1997;94:2156-61.

Pavlovich, C. P., Walther, M. M., Eyler, R. A., Hewitt, S. M., Zbar, B., Linehan, W. M. & Merino, M. J. Renal tumours in the Birt-Hogg-Dube syndrome. Am J Surg Pathol 2002;26:1542-52.

Pavlovich, C. P., Padilla-Nash, H., Wangsa, D., Nickerson, M. L., Matrosova, V., Linehan, W. M., Ried, T. & Phillips, J. L. Patterns of aneuploidy in stage IV clear cell renal cell carcinoma revealed by comparative genomic hybridization and spectral karyotyping. Genes Chromosomes Cancer 2003;37:252-60.

Peoples, R., Franke, Y., Wang, Y. K., Perez-Jurado, L., Paperna, T., Cisco, M. & Francke, U. A physical map, including a BAC/PAC clone contig, of the Williams-Beuren syndrome--deletion region at 7q11.23. Am J Hum Genet 2000;66:47-68.

Pettenati, M. J., Haines, J. L., Higgins, R. R., Wappner, R. S., Palmer, C. G. & Weaver, D. D. Wiedemann-Beckwith syndrome: presentation of clinical and cytogenetic data on 22 new cases and review of the literature. Hum Genet 1986;74:143-54.

Phipps, M. E., Latif, F., Prowse, A., Payne, S. J., Dietz-Band, J., Leversha, M., Affara, N. A., Moore, A. T., Tolmie, J., Schinzel, A. & Et Al. Molecular genetic analysis of the 3p- syndrome. Hum Mol Genet 1994;3:903-8.

Pinkel, D., Segraves, R., Sudar, D., Clark, S., Poole, I., Kowbel, D., Collins, C., Kuo, W. L., Chen, C., Zhai, Y., Dairkee, S. H., Ljung, B. M., Gray, J. W. & Albertson, D. G. High resolution analysis of DNA copy number variation using comparative genomic hybridization to microarrays. Nat Genet 1998;20:207-11.

Pinkel, D. & Albertson, D. G. Array comparative genomic hybridization and its applications in cancer. Nat Genet 2005;37 Suppl:S11-7.

Pinto, D., Pagnamenta, A. T., Klei, L., Anney, R., Merico, D., Regan, R., Conroy, J., Magalhaes, T. R., Correia, C., Abrahams, B. S., Almeida, J., Bacchelli, E., Bader, G. D., Bailey, A. J., Baird, G., Battaglia, A., Berney, T., Bolshakova, N., Bolte, S., Bolton, P. F., Bourgeron, T., Brennan, S., Brian, J., Bryson, S. E., Carson, A. R., Casallo, G., Casey, J., Chung, B. H., Cochrane, L., Corsello, C., Crawford, E. L., Crossett, A., Cytrynbaum, C., Dawson, G., De Jonge, M., Delorme, R., Drmic, I., Duketis, E., Duque, F., Estes, A., Farrar, P., Fernandez, B. A., Folstein, S. E., Fombonne, E., Freitag, C. M., Gilbert, J., Gillberg, C., Glessner, J. T., Goldberg, J., Green, A., Green, J., Guter, S. J., Hakonarson, H., Heron, E. A., Hill, M., Holt, R., Howe, J. L., Hughes, G., Hus, V., Igliozzi, R., Kim, C., Klauck, S. M., Kolevzon, A., Korvatska, O., Kustanovich, V., Lajonchere, C. M., Lamb, J. A., Laskawiec, M., Leboyer, M., Le Couteur, A., Leventhal, B. L., Lionel, A. C., Liu, X. Q., Lord, C., Lotspeich, L., Lund, S. C., Maestrini, E., Mahoney, W., Mantoulan, C., Marshall, C. R., Mcconachie, H., Mcdougle, C. J., Mcgrath, J., Mcmahon, W. M., Merikangas, A., Migita, O., Minshew, N. J., Mirza, G. K., Munson, J., Nelson, S. F., Noakes, C., Noor, A., Nygren, G., Oliveira, G., Papanikolaou, K., Parr, J. R., Parrini, B., Paton, T., Pickles, A., Pilorge, M., et al. Functional impact of global rare copy number variation in autism spectrum disorders. Nature 2010;466:368-72.

Podolski, J., Byrski, T., Zajaczek, S., Druck, T., Zimonjic, D. B., Popescu, N. C., Kata, G., Borowka, A., Gronwald, J., Lubinski, J. & Huebner, K. Characterization of a familial RCC-associated t(2;3)(q33;q21) chromosome translocation. J Hum Genet 2001;46:685-93.

Poland, K. S., Azim, M., Folsom, M., Goldfarb, R., Naeem, R., Korch, C., Drabkin, H. A., Gemmill, R. M. & Plon, S. E. A constitutional balanced t(3;8)(p14;q24.1) translocation results in disruption of the TRC8 gene and predisposition to clear cell renal cell carcinoma. Genes Chromosomes Cancer 2007;46:805-12.

Pollack, J. R., Perou, C. M., Alizadeh, A. A., Eisen, M. B., Pergamenschikov, A., Williams, C. F., Jeffrey, S. S., Botstein, D. & Brown, P. O. Genome-wide analysis of DNA copy-number changes using cDNA microarrays. Nat Genet 1999;23:41-6.

Pollack, J. R., Sorlie, T., Perou, C. M., Rees, C. A., Jeffrey, S. S., Lonning, P. E., Tibshirani, R., Botstein, D., Borresen-Dale, A. L. & Brown, P. O. Microarray analysis reveals a major direct role of DNA copy number alteration in the transcriptional program of human breast tumours. Proc Natl Acad Sci U S A 2002;99:12963-8.

Potocki, L., Chen, K. S., Park, S. S., Osterholm, D. E., Withers, M. A., Kimonis, V., Summers, A. M., Meschino, W. S., Anyane-Yeboa, K., Kashork, C. D., Shaffer, L. G. & Lupski, J. R. Molecular mechanism for duplication 17p11.2- the homologous recombination reciprocal of the Smith-Magenis microdeletion. Nat Genet 2000;24:84-7.

Prawitt, D., Enklaar, T., Gartner-Rupprecht, B., Spangenberg, C., Oswald, M., Lausch, E., Schmidtke, P., Reutzel, D., Fees, S., Lucito, R., Korzon, M., Brozek, I., Limon, J., Housman, D. E., Pelletier, J. & Zabel, B. Microdeletion of target sites for insulator

protein CTCF in a chromosome 11p15 imprinting center in Beckwith-Wiedemann syndrome and Wilms' tumour. Proc Natl Acad Sci U S A 2005;102:4085-90.

Preece, M. A., Price, S. M., Davies, V., Clough, L., Stanier, P., Trembath, R. C. & Moore, G. E. Maternal uniparental disomy 7 in Silver-Russell syndrome. J Med Genet 1997;34:6-9.

Prendergast, G. C. Mechanisms of apoptosis by c-Myc. Oncogene 1999;18:2967-87.

Presti, J. C., Jr., Moch, H., Gelb, A. B., Huynh, D. & Waldman, F. M. Initiating genetic events in small renal neoplasms detected by comparative genomic hybridization. J Urol 1998;160:1557-61.

Presti, J. C., Jr., Wilhelm, M., Reuter, V., Russo, P., Motzer, R. & Waldman, F. Allelic loss on chromosomes 8 and 9 correlates with clinical outcome in locally advanced clear cell carcinoma of the kidney. J Urol 2002;167:1464-8.

Pueschel, S. M. & Padre-Mendoza, T. Chromosome 11 and Beckwith-Wiedemann syndrome. J Pediatr 1984;104:484-5.

Rainier, S., Johnson, L. A., Dobry, C. J., Ping, A. J., Grundy, P. E. & Feinberg, A. P. Relaxation of imprinted genes in human cancer. Nature 1993;362:747-9.

Rakowski, S. K., Winterkorn, E. B., Paul, E., Steele, D. J., Halpern, E. F. & Thiele, E. A. Renal manifestations of tuberous sclerosis complex: Incidence, prognosis, and predictive factors. Kidney Int 2006;70:1777-82.

Rauch, A., Ruschendorf, F., Huang, J., Trautmann, U., Becker, C., Thiel, C., Jones, K. W., Reis, A. & Nurnberg, P. Molecular karyotyping using an SNP array for genomewide genotyping. J Med Genet 2004;41:916-22.

Redeker, E., Alders, M., Hoovers, J. M., Richard, C. W., 3rd, Westerveld, A. & Mannens, M. Physical mapping of 3 candidate tumour suppressor genes relative to Beckwith-Wiedemann syndrome associated chromosomal breakpoints at 11p15.3. Cytogenet Cell Genet 1995;68:222-5.

Redeker, E. J., De Visser, A. S., Bergen, A. A. & Mannens, M. M. Multiplex ligation-dependent probe amplification (MLPA) enhances the molecular diagnosis of aniridia and related disorders. Mol Vis 2008;14:836-40.

Redon, R., Ishikawa, S., Fitch, K. R., Feuk, L., Perry, G. H., Andrews, T. D., Fiegler, H., Shapero, M. H., Carson, A. R., Chen, W., Cho, E. K., Dallaire, S., Freeman, J. L., Gonzalez, J. R., Gratacos, M., Huang, J., Kalaitzopoulos, D., Komura, D., Macdonald, J. R., Marshall, C. R., Mei, R., Montgomery, L., Nishimura, K., Okamura, K., Shen, F., Somerville, M. J., Tchinda, J., Valsesia, A., Woodwark, C., Yang, F., Zhang, J., Zerjal, T., Armengol, L., Conrad, D. F., Estivill, X., Tyler-Smith, C., Carter, N. P., Aburatani, H., Lee, C., Jones, K. W., Scherer, S. W. & Hurles, M. E. Global variation in copy number in the human genome. Nature 2006;444:444-54.

Reik, W. & Maher, E. R. Imprinting in clusters: lessons from Beckwith-Wiedemann syndrome. Trends Genet 1997;13:330-4.

Renbaum, P., Duh, F. M., Latif, F., Zbar, B., Lerman, M. I. & Kuzmin, I. Isolation and characterization of the full-length 3' untranslated region of the human von Hippel-Lindau tumour suppressor gene. Hum Genet 1996;98:666-71.

Richards, F. M., Payne, S. J., Zbar, B., Affara, N. A., Ferguson-Smith, M. A. & Maher, E. R. Molecular analysis of de novo germline mutations in the von Hippel-Lindau disease gene. Hum Mol Genet 1995;4:2139-43.

Risch, N., Kidd, K. K. & Tishkoff, S. A. Response: genetic data and the african origin of humans. Science 1996;274:1548b-9b.

Ritter, M. M., Frilling, A., Crossey, P. A., Hoppner, W., Maher, E. R., Mulligan, L., Ponder, B. A. & Engelhardt, D. Isolated familial pheochromocytoma as a variant of von Hippel-Lindau disease. J Clin Endocrinol Metab 1996;81:1035-7.

Robinson, W. P., Bottani, A., Xie, Y. G., Balakrishman, J., Binkert, F., Machler, M., Prader, A. & Schinzel, A. Molecular, cytogenetic, and clinical investigations of Prader-Willi syndrome patients. Am J Hum Genet 1991;49:1219-34.

Robinson, S. W., Morris, C. D., Goldmuntz, E., Reller, M. D., Jones, M. A., Steiner, R. D. & Maslen, C. L. Missense mutations in CRELD1 are associated with cardiac atrioventricular septal defects. Am J Hum Genet 2003;72:1047-52.

Roohi, J., Montagna, C., Tegay, D. H., Palmer, L. E., Devincent, C., Pomeroy, J. C., Christian, S. L., Nowak, N. & Hatchwell, E. Disruption of contactin 4 in three subjects with autism spectrum disorder. J Med Genet 2009;46:176-82.

Rowley, J. D. Letter: A new consistent chromosomal abnormality in chronic myelogenous leukaemia identified by quinacrine fluorescence and Giemsa staining. Nature 1973;243:290-3.

Rowley, J. D. Chromosome translocations: dangerous liaisons revisited. Nat Rev Cancer 2001;1:245-50.

Roz, L., Gramegna, M., Ishii, H., Croce, C. M. & Sozzi, G. Restoration of fragile histidine triad (FHIT) expression induces apoptosis and suppresses tumourigenicity in lung and cervical cancer cell lines. Proc Natl Acad Sci U S A 2002;99:3615-20.

Rumpelt, H. J., Storkel, S., Moll, R., Scharfe, T. & Thoenes, W. Bellini duct carcinoma: further evidence for this rare variant of renal cell carcinoma. Histopathology 1991;18:115-22.

Russo A, Migliavacca M, Zanna I, Macaluso M, Gebbia N and Bazan V. (2003). *Encycl. Hum. Genome*. John Wiley & Sons Ltd

Russo, S., Finelli, P., Recalcati, M. P., Ferraiuolo, S., Cogliati, F., Dalla Bernardina, B., Tibiletti, M. G., Agosti, M., Sala, M., Bonati, M. T. & Larizza, L. Molecular and genomic characterisation of cryptic chromosomal alterations leading to paternal duplication of the 11p15.5 Beckwith-Wiedemann region. J Med Genet 2006;43:e39.

Sait, S. N., Nowak, N. J., Singh-Kahlon, P., Weksberg, R., Squire, J., Shows, T. B. & Higgins, M. J. Localization of Beckwith-Wiedemann and rhabdoid tumour chromosome rearrangements to a defined interval in chromosome band 11p15.5. Genes Chromosomes Cancer 1994;11:97-105.

Sandberg, A. A. & Hossfeld, D. K. Chromosomal abnormalities in human neoplasia. Annu Rev Med 1970;21:379-408.

Sanders, M. E., Mick, R., Tomaszewski, J. E. & Barr, F. G. Unique patterns of allelic imbalance distinguish type 1 from type 2 sporadic papillary renal cell carcinoma. Am J Pathol 2002;161:997-1005.

Sanguinetti, M. C. Long QT syndrome: ionic basis and arrhythmia mechanism in long QT syndrome type 1. J Cardiovasc Electrophysiol 2000;11:710-2.

Sanjmyatav, J., Schubert, J. & Junker, K. Comparative study of renal cell carcinoma by CGH, multicolor-FISH and conventional cytogenic banding analysis. Oncol Rep 2005;14:1183-7.

Sanlaville, D., Aubry, M. C., Dumez, Y., Nolen, M. C., Amiel, J., Pinson, M. P., Lyonnet, S., Munnich, A., Vekemans, M. & Morichon-Delvallez, N. Maternal uniparental heterodisomy of chromosome 14: chromosomal mechanism and clinical follow up. J Med Genet 2000;37:525-8.

Saunders, W. Centrosomal amplification and spindle multipolarity in cancer cells. Semin Cancer Biol 2005;15:25-32.

Saxena, R., Voight, B. F., Lyssenko, V., Burtt, N. P., De Bakker, P. I., Chen, H., Roix, J. J., Kathiresan, S., Hirschhorn, J. N., Daly, M. J., Hughes, T. E., Groop, L., Altshuler, D., Almgren, P., Florez, J. C., Meyer, J., Ardlie, K., Bengtsson Bostrom, K., Isomaa, B., Lettre, G., Lindblad, U., Lyon, H. N., Melander, O., Newton-Cheh, C., Nilsson, P., Orho-Melander, M., Rastam, L., Speliotes, E. K., Taskinen, M. R., Tuomi, T., Guiducci, C., Berglund, A., Carlson, J., Gianniny, L., Hackett, R., Hall, L., Holmkvist, J., Laurila, E., Sjogren, M., Sterner, M., Surti, A., Svensson, M., Tewhey, R., Blumenstiel, B., Parkin, M., Defelice, M., Barry, R., Brodeur, W., Camarata, J., Chia, N., Fava, M., Gibbons, J., Handsaker, B., Healy, C., Nguyen, K., Gates, C., Sougnez, C., Gage, D., Nizzari, M., Gabriel, S. B., Chirn, G. W., Ma, Q., Parikh, H., Richardson, D., Ricke, D. & Purcell, S. Genome-wide association analysis identifies loci for type 2 diabetes and triglyceride levels. Science 2007;316:1331-6.

Schappert-Kimmijser, J., Hemmes, G. D. & Nijland, R. The heredity of retinoblastoma. Ophthalmologica 1966;151:197-213.

Schmidt, L., Li, F., Brown, R. S., Berg, S., Chen, F., Wei, M. H., Tory, K., Lerman, I. & Zbar, B. Mechanism of tumourigenesis of renal carcinomas associated with the constitutional chromosome 3;8 translocation. Cancer J Sci Am 1995;1:191-5.

Schmidt, L., Duh, F. M., Chen, F., Kishida, T., Glenn, G., Choyke, P., Scherer, S. W., Zhuang, Z., Lubensky, I., Dean, M., Allikmets, R., Chidambaram, A., Bergerheim, U. R., Feltis, J. T., Casadevall, C., Zamarron, A., Bernues, M., Richard, S., Lips, C. J., Walther, M. M., Tsui, L. C., Geil, L., Orcutt, M. L., Stackhouse, T., Lipan, J., Slife, L., Brauch, H., Decker, J., Niehans, G., Hughson, M. D., Moch, H., Storkel, S., Lerman, M. I., Linehan, W. M. & Zbar, B. Germline and somatic mutations in the tyrosine kinase domain of the MET proto-oncogene in papillary renal carcinomas. Nat Genet 1997;16:68-73.

Schmidt, L., Junker, K., Nakaigawa, N., Kinjerski, T., Weirich, G., Miller, M., Lubensky, I., Neumann, H. P., Brauch, H., Decker, J., Vocke, C., Brown, J. A., Jenkins, R., Richard, S., Bergerheim, U., Gerrard, B., Dean, M., Linehan, W. M. & Zbar, B. Novel mutations of the MET proto-oncogene in papillary renal carcinomas. Oncogene 1999;18:2343-50.

Schmidt, L. S., Warren, M. B., Nickerson, M. L., Weirich, G., Matrosova, V., Toro, J. R., Turner, M. L., Duray, P., Merino, M., Hewitt, S., Pavlovich, C. P., Glenn, G., Greenberg, C. R., Linehan, W. M. & Zbar, B. Birt-Hogg-Dube syndrome, a genodermatosis associated with spontaneous pneumothorax and kidney neoplasia, maps to chromosome 17p11.2. Am J Hum Genet 2001;69:876-82.

Schmutz, S. M. Deletion of chromosome 11(p11p13) in a patient with Beckwith-Wiedemann syndrome. Clin Genet 1986;30:154-6.

Schnedl, W. Banding pattern of human chromosomes. Nat New Biol 1971;233:93-4.

Schneid, H., Holthuizen, P. E. & Sussenbach, J. S. Differential promoter activation in two human insulin-like growth factor-II-producing tumour cell lines. Endocrinology 1993;132:1145-50.

Schoenfeld, A., Davidowitz, E. J. & Burk, R. D. A second major native von Hippel-Lindau gene product, initiated from an internal translation start site, functions as a tumour suppressor. Proc Natl Acad Sci U S A 1998;95:8817-22.

Schofield, C. J. & Ratcliffe, P. J. Oxygen sensing by HIF hydroxylases. Nat Rev Mol Cell Biol 2004;5:343-54.

Schoumans, J., Ruivenkamp, C., Holmberg, E., Kyllerman, M., Anderlid, B. M. & Nordenskjold, M. Detection of chromosomal imbalances in children with idiopathic mental retardation by array based comparative genomic hybridisation (array-CGH). J Med Genet 2005;42:699-705.

Schouten, J. P., Mcelgunn, C. J., Waaijer, R., Zwijnenburg, D., Diepvens, F. & Pals, G. Relative quantification of 40 nucleic acid sequences by multiplex ligation-dependent probe amplification. Nucleic Acids Res 2002;30:e57.

Schraml, P., Struckmann, K., Bednar, R., Fu, W., Gasser, T., Wilber, K., Kononen, J., Sauter, G., Mihatsch, M. J. & Moch, H. CDKNA2A mutation analysis, protein expression, and deletion mapping of chromosome 9p in conventional clear-cell renal carcinomas: evidence for a second tumour suppressor gene proximal to CDKN2A. Am J Pathol 2001;158:593-601.

Schwerdtle, R. F., Storkel, S., Neuhaus, C., Brauch, H., Weidt, E., Brenner, W., Hohenfellner, R., Huber, C. & Decker, H. J. Allelic losses at chromosomes 1p, 2p, 6p, 10p, 13q, 17p, and 21q significantly correlate with the chromophobe subtype of renal cell carcinoma. Cancer Res 1996;56:2927-30

Schwyzer, U., Binkert, F., Caflisch, U., Baumgartner, B. & Schinzel, A. Terminal deletion of the short arm of chromosome 3, del(3pter-p25): a recognizable syndrome. Helv Paediatr Acta 1987;42:309-15.

Seabright, M. A rapid banding technique for human chromosomes. Lancet 1971;2:971-2.

Seabright, M. The use of proteolytic enzymes for the mapping of structural rearrangements in the chromosomes of man. Chromosoma 1972;36:204-10.

Sebat, J., Lakshmi, B., Malhotra, D., Troge, J., Lese-Martin, C., Walsh, T., Yamrom, B., Yoon, S., Krasnitz, A., Kendall, J., Leotta, A., Pai, D., Zhang, R., Lee, Y. H., Hicks, J., Spence, S. J., Lee, A. T., Puura, K., Lehtimaki, T., Ledbetter, D., Gregersen, P. K., Bregman, J., Sutcliffe, J. S., Jobanputra, V., Chung, W., Warburton, D., King, M. C., Skuse, D., Geschwind, D. H., Gilliam, T. C., Ye, K. & Wigler, M. Strong association of de novo copy number mutations with autism. Science 2007;316:445-9.

Seizinger, B. R., Rouleau, G. A., Ozelius, L. J., Lane, A. H., Farmer, G. E., Lamiell, J. M., Haines, J., Yuen, J. W., Collins, D., Majoor-Krakauer, D. & Et Al. Von Hippel-Lindau disease maps to the region of chromosome 3 associated with renal cell carcinoma. Nature 1988;332:268-9.

Shaffer, L. G., Jackson-Cook, C. K., Stasiowski, B. A., Spence, J. E. & Brown, J. A. Parental origin determination in thirty de novo Robertsonian translocations. Am J Med Genet 1992;43:957-63.

Shaffer, L. G. & Lupski, J. R. Molecular mechanisms for constitutional chromosomal rearrangements in humans. Annu Rev Genet 2000;34:297-329.

Shaikh, T. H., Budarf, M. L., Celle, L., Zackai, E. H. & Emanuel, B. S. Clustered 11q23 and 22q11 breakpoints and 3:1 meiotic malsegregation in multiple unrelated t(11;22) families. Am J Hum Genet 1999;65:1595-607.

Shaikh, T. H., Kurahashi, H., Saitta, S. C., O'hare, A. M., Hu, P., Roe, B. A., Driscoll, D. A., Mcdonald-Mcginn, D. M., Zackai, E. H., Budarf, M. L. & Emanuel, B. S. Chromosome 22-specific low copy repeats and the 22q11.2 deletion syndrome: genomic organization and deletion endpoint analysis. Hum Mol Genet 2000;9:489-501.

Shaw-Smith, C., Redon, R., Rickman, L., Rio, M., Willatt, L., Fiegler, H., Firth, H., Sanlaville, D., Winter, R., Colleaux, L., Bobrow, M. & Carter, N. P. Microarray based comparative genomic hybridisation (array-CGH) detects submicroscopic

chromosomal deletions and duplications in patients with learning disability/mental retardation and dysmorphic features. J Med Genet 2004;41:241-8.

Shrimpton, A. E., Jensen, K. A. & Hoo, J. J. Karyotype-phenotype analysis and molecular delineation of a 3p26 deletion/8q24.3 duplication case with a virtually normal phenotype and mild cognitive deficit. Am J Med Genet A 2006;140:388-91.

Shuib, S., Mcmullan, D., Rattenberry, E., Barber, R. M., Rahman, F., Zatyka, M., Chapman, C., Macdonald, F., Latif, F., Davison, V. & Maher, E. R. Microarray based analysis of 3p25-p26 deletions (3p- syndrome). Am J Med Genet A 2009;149A:2099-105.

Siebert, R., Matthiesen, P., Harder, S., Zhang, Y., Borowski, A., Zuhlke-Jenisch, R., Metzke, S., Joos, S., Weber-Matthiesen, K., Grote, W. & Schlegelberger, B. Application of interphase fluorescence in situ Hybridization for the detection of the Burkitt translocation t(8;14)(q24;q32) in B-cell lymphomas. Blood 1998;91:984-90.

Siemeister, G., Weindel, K., Mohrs, K., Barleon, B., Martiny-Baron, G. & Marme, D. Reversion of deregulated expression of vascular endothelial growth factor in human renal carcinoma cells by von Hippel-Lindau tumour suppressor protein. Cancer Res 1996;56:2299-301.

Sklower-Brooks S, Pappas J, Duncan C, Genovese M, Gu H, Jenkins EC.2002. Deletion 3p25 in a mother and child. Am J Hum Genet 71:301(Abstract #751).

Slatter, R. E., Elliott, M., Welham, K., Carrera, M., Schofield, P. N., Barton, D. E. & Maher, E. R. Mosaic uniparental disomy in Beckwith-Wiedemann syndrome. J Med Genet 1994;31:749-53.

Slavotinek, A., Gaunt, L. & Donnai, D. Paternally inherited duplications of 11p15.5 and Beckwith-Wiedemann syndrome. J Med Genet 1997;34:819-26.

Slebos, R. J., Kibbelaar, R. E., Dalesio, O., Kooistra, A., Stam, J., Meijer, C. J., Wagenaar, S. S., Vanderschueren, R. G., Van Zandwijk, N., Mooi, W. J. & Et Al. K-ras oncogene activation as a prognostic marker in adenocarcinoma of the lung. N Engl J Med 1990;323:561-5.

Smilinich, N. J., Day, C. D., Fitzpatrick, G. V., Caldwell, G. M., Lossie, A. C., Cooper, P. R., Smallwood, A. C., Joyce, J. A., Schofield, P. N., Reik, W., Nicholls, R. D., Weksberg, R., Driscoll, D. J., Maher, E. R., Shows, T. B. & Higgins, M. J. A maternally methylated CpG island in KvLQT1 is associated with an antisense paternal transcript and loss of imprinting in Beckwith-Wiedemann syndrome. Proc Natl Acad Sci U S A 1999;96:8064-9.

Smith, D. W., Patau, K., Therman, E. & Inhorn, S. L. A new autosomal trisomy syndrome: multiple congenital anomalies caused by an extra chromosome. J Pediatr 1960;57:338-45.

Snijders, A. M., Nowak, N., Segraves, R., Blackwood, S., Brown, N., Conroy, J., Hamilton, G., Hindle, A. K., Huey, B., Kimura, K., Law, S., Myambo, K., Palmer, J., Ylstra, B., Yue, J. P., Gray, J. W., Jain, A. N., Pinkel, D. & Albertson, D. G. Assembly of microarrays for genome-wide measurement of DNA copy number. Nat Genet 2001;29:263-4.

Solinas-Toldo, S., Lampel, S., Stilgenbauer, S., Nickolenko, J., Benner, A., Dohner, H., Cremer, T. & Lichter, P. Matrix-based comparative genomic hybridization: biochips to screen for genomic imbalances. Genes Chromosomes Cancer 1997;20:399-407.

Sotelo-Avila, C., Gonzalez-Crussi, F. & Fowler, J. W. Complete and incomplete forms of Beckwith-Wiedemann syndrome: their oncogenic potential. J Pediatr 1980;96:47-50.

Sozzi, G., Veronese, M. L., Negrini, M., Baffa, R., Cotticelli, M. G., Inoue, H., Tornielli, S., Pilotti, S., De Gregorio, L., Pastorino, U., Pierotti, M. A., Ohta, M., Huebner, K. & Croce, C. M. The FHIT gene 3p14.2 is abnormal in lung cancer. Cell 1996;85:17-26.

Sparago, A., Cerrato, F., Vernucci, M., Ferrero, G. B., Silengo, M. C. & Riccio, A. Microdeletions in the human H19 DMR result in loss of IGF2 imprinting and Beckwith-Wiedemann syndrome. Nat Genet 2004;36:958-60.

Speicher, M. R., Gwyn Ballard, S. & Ward, D. C. Karyotyping human chromosomes by combinatorial multi-fluor FISH. Nat Genet 1996;12:368-75.

Speicher, M. R. & Carter, N. P. The new cytogenetics: blurring the boundaries with molecular biology. Nat Rev Genet 2005;6:782-92.

Spitz, F., Montavon, T., Monso-Hinard, C., Morris, M., Ventruto, M. L., Antonarakis, S., Ventruto, V. & Duboule, D. A t(2;8) balanced translocation with breakpoints near the human HOXD complex causes mesomelic dysplasia and vertebral defects. Genomics 2002;79:493-8.

Srigley, J. R. & Eble, J. N. Collecting duct carcinoma of kidney. Semin Diagn Pathol 1998;15:54-67.

St Clair, D. Copy number variation and schizophrenia. Schizophr Bull 2009;35:9-12.

Stehelin, D., Guntaka, R. V., Varmus, H. E. & Bishop, J. M. Purification of DNA complementary to nucleotide sequences required for neoplastic transformation of fibroblasts by avian sarcoma viruses. J Mol Biol 1976a;101:349-65.

Stehelin, D., Varmus, H. E., Bishop, J. M. & Vogt, P. K. DNA related to the transforming gene(s) of avian sarcoma viruses is present in normal avian DNA. Nature 1976b;260:170-3.

Stehelin, D., Fujita, D. J., Padgett, T., Varmus, H. E. & Bishop, J. M. Detection and enumeration of transformation-defective strains of avian sarcoma virus with molecular hybridization. Virology 1977;76:675-84.

Stephens, P. J., Mcbride, D. J., Lin, M. L., Varela, I., Pleasance, E. D., Simpson, J. T., Stebbings, L. A., Leroy, C., Edkins, S., Mudie, L. J., Greenman, C. D., Jia, M., Latimer, C., Teague, J. W., Lau, K. W., Burton, J., Quail, M. A., Swerdlow, H., Churcher, C., Natrajan, R., Sieuwerts, A. M., Martens, J. W., Silver, D. P., Langerod, A., Russnes, H. E., Foekens, J. A., Reis-Filho, J. S., Van 'T Veer, L., Richardson, A. L., Borresen-Dale, A. L., Campbell, P. J., Futreal, P. A. & Stratton, M. R. Complex landscapes of somatic rearrangement in human breast cancer genomes. Nature 2009;462:1005-10.

Stolle, C., Glenn, G., Zbar, B., Humphrey, J. S., Choyke, P., Walther, M., Pack, S., Hurley, K., Andrey, C., Klausner, R. & Linehan, W. M. Improved detection of germline mutations in the von Hippel-Lindau disease tumour suppressor gene. Hum Mutat 1998;12:417-23.

Storkel, S., Eble, J. N., Adlakha, K., Amin, M., Blute, M. L., Bostwick, D. G., Darson, M., Delahunt, B. & Iczkowski, K. Classification of renal cell carcinoma: Workgroup No. 1. Union Internationale Contre le Cancer (UICC) and the American Joint Committee on Cancer (AJCC). Cancer 1997;80:987-9.

Strefford, J. C., Stasevich, I., Lane, T. M., Lu, Y. J., Oliver, T. & Young, B. D. A combination of molecular cytogenetic analyses reveals complex genetic alterations in conventional renal cell carcinoma. Cancer Genet Cytogenet 2005;159:1-9.

Sugarbaker, D. J., Richards, W. G., Gordon, G. J., Dong, L., De Rienzo, A., Maulik, G., Glickman, J. N., Chirieac, L. R., Hartman, M. L., Taillon, B. E., Du, L., Bouffard, P., Kingsmore, S. F., Miller, N. A., Farmer, A. D., Jensen, R. V., Gullans, S. R. & Bueno, R. Transcriptome sequencing of malignant pleural mesothelioma tumours. Proc Natl Acad Sci U S A 2008;105:3521-6.

Sukosd, F., Kuroda, N., Beothe, T., Kaur, A. P. & Kovacs, G. Deletion of chromosome 3p14.2-p25 involving the VHL and FHIT genes in conventional renal cell carcinoma. Cancer Res 2003;63:455-7.

Sulis, M. L. & Parsons, R. PTEN: from pathology to biology. Trends Cell Biol 2003;13:478-83.

Sumner, A. T., Evans, H. J. & Buckland, R. A. New technique for distinguishing between human chromosomes. Nat New Biol 1971;232:31-2.

Sun, F. L., Dean, W. L., Kelsey, G., Allen, N. D. & Reik, W. Transactivation of Igf2 in a mouse model of Beckwith-Wiedemann syndrome. Nature 1997;389:809-15.

Squire, J. A., Li, M., Perlikowski, S., Fei, Y. L., Bayani, J., Zhang, Z. M. & Weksberg, R. Alterations of H19 imprinting and IGF2 replication timing are infrequent in Beckwith-Wiedemann syndrome. Genomics 2000;65:234-42.

Swartz, M. A., Karth, J., Schneider, D. T., Rodriguez, R., Beckwith, J. B. & Perlman, E. J. Renal medullary carcinoma: clinical, pathologic, immunohistochemical, and genetic analysis with pathogenetic implications. Urology 2002;60:1083-9.

Szuhai, K. & Tanke, H. J. COBRA: combined binary ratio labeling of nucleic-acid probes for multi-color fluorescence in situ hybridization karyotyping. Nat Protoc 2006;1:264-75.

Takagishi J, Rauen KA, Drumheller T, Kousseff B, Sutcliffe M. 2006.Chromosome 3p25 deletion in mother and daughter with minimal phenotypic effect. Am J Med Genet Part A 140A:1587–1593.

Tan, T. Y. & Amor, D. J. Tumour surveillance in Beckwith-Wiedemann syndrome and hemihyperplasia: a critical review of the evidence and suggested guidelines for local practice. J Paediatr Child Health 2006;42:486-90.

Tanida I, Tanida-Miyake T, Ueno T, Kominami E. 2001. The human homolog of Saccharomyces cerevisiae Apg7p is a protein-activating enzyme for multiple substrates including human Apg12p, GATE-16, GABARAP, and MAP-LC3. J Biol Chem 276:1701–1706.

Taylor, C. F., Charlton, R. S., Burn, J., Sheridan, E. & Taylor, G. R. Genomic deletions in MSH2 or MLH1 are a frequent cause of hereditary non-polyposis colorectal cancer: identification of novel and recurrent deletions by MLPA. Hum Mutat 2003;22:428-33.

Teh, B. T., Giraud, S., Sari, N. F., Hii, S. I., Bergerat, J. P., Larsson, C., Limacher, J. M. & Nicol, D. Familial non-VHL non-papillary clear-cell renal cancer. Lancet 1997;349:848-9.

Tester, D. J., Will, M. L., Haglund, C. M. & Ackerman, M. J. Compendium of cardiac channel mutations in 541 consecutive unrelated patients referred for long QT syndrome genetic testing. Heart Rhythm 2005;2:507-17.

Therman, E., Susman, B. & Denniston, C. The nonrandom participation of human acrocentric chromosomes in Robertsonian translocations. Ann Hum Genet 1989;53:49-65.

Thoenes, W., Storkel, S. & Rumpelt, H. J. Histopathology and classification of renal cell tumours (adenomas, oncocytomas and carcinomas). The basic cytological and

histopathological elements and their use for diagnostics. Pathol Res Pract 1986;181:125-43.

Thomas, R. K., Nickerson, E., Simons, J. F., Janne, P. A., Tengs, T., Yuza, Y., Garraway, L. A., Laframboise, T., Lee, J. C., Shah, K., O'neill, K., Sasaki, H., Lindeman, N., Wong, K. K., Borras, A. M., Gutmann, E. J., Dragnev, K. H., Debiasi, R., Chen, T. H., Glatt, K. A., Greulich, H., Desany, B., Lubeski, C. K., Brockman, W., Alvarez, P., Hutchison, S. K., Leamon, J. H., Ronan, M. T., Turenchalk, G. S., Egholm, M., Sellers, W. R., Rothberg, J. M. & Meyerson, M. Sensitive mutation detection in heterogeneous cancer specimens by massively parallel picoliter reactor sequencing. Nat Med 2006;12:852-5.

Toma, M. I., Grosser, M., Herr, A., Aust, D. E., Meye, A., Hoefling, C., Fuessel, S., Wuttig, D., Wirth, M. P. & Baretton, G. B. Loss of heterozygosity and copy number abnormality in clear cell renal cell carcinoma discovered by high-density affymetrix 10K single nucleotide polymorphism mapping array. Neoplasia 2008;10:634-42.

Tomlinson, I. P., Alam, N. A., Rowan, A. J., Barclay, E., Jaeger, E. E., Kelsell, D., Leigh, I., Gorman, P., Lamlum, H., Rahman, S., Roylance, R. R., Olpin, S., Bevan, S., Barker, K., Hearle, N., Houlston, R. S., Kiuru, M., Lehtonen, R., Karhu, A., Vilkki, S., Laiho, P., Eklund, C., Vierimaa, O., Aittomaki, K., Hietala, M., Sistonen, P., Paetau, A., Salovaara, R., Herva, R., Launonen, V. & Aaltonen, L. A. Germline mutations in FH predispose to dominantly inherited uterine fibroids, skin leiomyomata and papillary renal cell cancer. Nat Genet 2002;30:406-10.

Tommerup, N., Brandt, C. A., Pedersen, S., Bolund, L. & Kamper, J. Sex dependent transmission of Beckwith-Wiedemann syndrome associated with a reciprocal translocation t(9;11)(p11.2;p15.5). J Med Genet 1993;30:958-61.

Tonoki, H., Narahara, K., Matsumoto, T. & Niikawa, N. Regional mapping of the parathyroid hormone gene (PTH) by cytogenetic and molecular studies. Cytogenet Cell Genet 1991;56:103-4.

Toro, J. R., Wei, M. H., Glenn, G. M., Weinreich, M., Toure, O., Vocke, C., Turner, M., Choyke, P., Merino, M. J., Pinto, P. A., Steinberg, S. M., Schmidt, L. S. & Linehan, W. M. BHD mutations, clinical and molecular genetic investigations of Birt-Hogg-Dube syndrome: a new series of 50 families and a review of published reports. J Med Genet 2008;45:321-31.

Trask, B. J., Mefford, H., Van Den Engh, G., Massa, H. F., Juyal, R. C., Potocki, L., Finucane, B., Abuelo, D. N., Witt, D. R., Magenis, E., Baldini, A., Greenberg, F., Lupski, J. R. & Patel, P. I. Quantification by flow cytometry of chromosome-17 deletions in Smith-Magenis syndrome patients. Hum Genet 1996;98:710-8.

Trotman, L. C., Niki, M., Dotan, Z. A., Koutcher, J. A., Di Cristofano, A., Xiao, A., Khoo, A. S., Roy-Burman, P., Greenberg, N. M., Van Dyke, T., Cordon-Cardo, C. & Pandolfi, P. P. Pten dose dictates cancer progression in the prostate. PLoS Biol 2003;1:E59.

Tsunematsu, T., Kudo, Y., Iizuka, S., Ogawa, I., Fujita, T., Kurihara, H., Abiko, Y. & Takata, T. RUNX3 has an oncogenic role in head and neck cancer. PLoS One 2009;4:e5892.

Tuefferd, M., De Bondt, A., Van Den Wyngaert, I., Talloen, W., Verbeke, T., Carvalho, B., Clevert, D. A., Alifano, M., Raghavan, N., Amaratunga, D., Gohlmann, H., Broet, P. & Camilleri-Broet, S. Genome-wide copy number alterations detection in fresh frozen and matched FFPE samples using SNP 6.0 arrays. Genes Chromosomes Cancer 2008;47:957-64.

Tunnacliffe, A., Jones, C., Le Paslier, D., Todd, R., Cherif, D., Birdsall, M., Devenish, L., Yousry, C., Cotter, F. E. & James, M. R. Localization of Jacobsen syndrome breakpoints on a 40-Mb physical map of distal chromosome 11q. Genome Res 1999;9:44-52.

Turleau, C., De Grouchy, J., Chavin-Colin, F., Martelli, H., Voyer, M. & Charlas, R. Trisomy 11p15 and Beckwith-Wiedemann syndrome. A report of two cases. Hum Genet 1984;67:219-21.

Tycko, B., Trasler, J. & Bestor, T. Genomic imprinting: gametic mechanisms and somatic consequences. J Androl 1997;18:480-6.

Van Den Berg, A. & Buys, C. H. Involvement of multiple loci on chromosome 3 in renal cell cancer development. Genes Chromosomes Cancer 1997;19:59-76.

Van Der Harst, E., De Krijger, R. R., Dinjens, W. N., Weeks, L. E., Bonjer, H. J., Bruining, H. A., Lamberts, S. W. & Koper, J. W. Germline mutations in the vhl gene in patients presenting with phaeochromocytomas. Int J Cancer 1998;77:337-40.

Van Dijk, B. A., Schouten, L. J., Kiemeney, L. A., Goldbohm, R. A. & Van Den Brandt, P. A. Relation of height, body mass, energy intake, and physical activity to risk of renal cell carcinoma: results from the Netherlands Cohort Study. Am J Epidemiol 2004;160:1159-67.

Van Dijk, M. C., Rombout, P. D., Boots-Sprenger, S. H., Straatman, H., Bernsen, M. R., Ruiter, D. J. & Jeuken, J. W. Multiplex ligation-dependent probe amplification for the detection of chromosomal gains and losses in formalin-fixed tissue. Diagn Mol Pathol 2005;14:9-16.

Van Dyke, D. L., Weiss, L., Roberson, J. R. & Babu, V. R. The frequency and mutation rate of balanced autosomal rearrangements in man estimated from prenatal genetic studies for advanced maternal age. Am J Hum Genet 1983;35:301-8.

Van Houwelingen, K. P., Van Dijk, B. A., Hulsbergen-Van De Kaa, C. A., Schouten, L. J., Gorissen, H. J., Schalken, J. A., Van Den Brandt, P. A. & Oosterwijk, E. Prevalence of von Hippel-Lindau gene mutations in sporadic renal cell carcinoma: results from The Netherlands cohort study. BMC Cancer 2005;5:57.

Van Kessel, A. G., Wijnhoven, H., Bodmer, D., Eleveld, M., Kiemeney, L., Mulders, P., Weterman, M., Ligtenberg, M., Smeets, D. & Smits, A. Renal cell cancer: chromosome 3 translocations as risk factors. J Natl Cancer Inst 1999;91:1159-60.

Velagaleti, G. V., Bien-Willner, G. A., Northup, J. K., Lockhart, L. H., Hawkins, J. C., Jalal, S. M., Withers, M., Lupski, J. R. & Stankiewicz, P. Position effects due to chromosome breakpoints that map approximately 900 Kb upstream and approximately 1.3 Mb downstream of SOX9 in two patients with campomelic dysplasia. Am J Hum Genet 2005;76:652-62.

Velickovic, M., Delahunt, B. & Grebe, S. K. Loss of heterozygosity at 3p14.2 in clear cell renal cell carcinoma is an early event and is highly localized to the FHIT gene locus. Cancer Res 1999;59:1323-6.

Veltman, J. A., Schoenmakers, E. F., Eussen, B. H., Janssen, I., Merkx, G., Van Cleef, B., Van Ravenswaaij, C. M., Brunner, H. G., Smeets, D. & Van Kessel, A. G. High-throughput analysis of subtelomeric chromosome rearrangements by use of array-based comparative genomic hybridization. Am J Hum Genet 2002;70:1269-76.

Veltman, J. A., Jonkers, Y., Nuijten, I., Janssen, I., Van Der Vliet, W., Huys, E., Vermeesch, J., Van Buggenhout, G., Fryns, J. P., Admiraal, R., Terhal, P., Lacombe, D., Van Kessel, A. G., Smeets, D., Schoenmakers, E. F. & Van

Ravenswaaij-Arts, C. M. Definition of a critical region on chromosome 18 for congenital aural atresia by arrayCGH. Am J Hum Genet 2003;72:1578-84.

Venkatachalam, S., Shi, Y. P., Jones, S. N., Vogel, H., Bradley, A., Pinkel, D. & Donehower, L. A. Retention of wild-type p53 in tumours from p53 heterozygous mice: reduction of p53 dosage can promote cancer formation. EMBO J 1998;17:4657-67.

Verjaal, M. & De Nef, M. B. A patient with a partial deletion of the short arm of chromosome 3. Am J Dis Child 1978;132:43-5.

Vermeesch, J. R., Fiegler, H., De Leeuw, N., Szuhai, K., Schoumans, J., Ciccone, R., Speleman, F., Rauch, A., Clayton-Smith, J., Van Ravenswaaij, C., Sanlaville, D., Patsalis, P. C., Firth, H., Devriendt, K. & Zuffardi, O. Guidelines for molecular karyotyping in constitutional genetic diagnosis. Eur J Hum Genet 2007;15:1105-14.

Virgilio, L., Shuster, M., Gollin, S. M., Veronese, M. L., Ohta, M., Huebner, K. & Croce, C. M. FHIT gene alterations in head and neck squamous cell carcinomas. Proc Natl Acad Sci U S A 1996;93:9770-5.

Vissers, L. E., De Vries, B. B., Osoegawa, K., Janssen, I. M., Feuth, T., Choy, C. O., Straatman, H., Van Der Vliet, W., Huys, E. H., Van Rijk, A., Smeets, D., Van Ravenswaaij-Arts, C. M., Knoers, N. V., Van Der Burgt, I., De Jong, P. J., Brunner, H. G., Van Kessel, A. G., Schoenmakers, E. F. & Veltman, J. A. Array-based comparative genomic hybridization for the genomewide detection of submicroscopic chromosomal abnormalities. Am J Hum Genet 2003;73:1261-70.

Vogel, F. [New studies on the genetics of retinoblastoma; glioma retinae.]. Z Mensch Vererb Konstitutionsl 1957;34:205-36.

Vogelstein, B. & Kinzler, K. W. Cancer genes and the pathways they control. Nat Med 2004;10:789-99.

Vogiatzi, P., De Falco, G., Claudio, P. P. & Giordano, A. How does the human RUNX3 gene induce apoptosis in gastric cancer? Latest data, reflections and reactions. Cancer Biol Ther 2006;5:371-4.

Wales, J. K., Walker, V., Moore, I. E. & Clayton, P. T. Bronze baby syndrome, biliary hypoplasia, incomplete Beckwith-Wiedemann syndrome and partial trisomy 11. Eur J Pediatr 1986;145:141-3.

Walker, F., Abramowitz, L., Benabderrahmane, D., Duval, X., Descatoire, V., Henin, D., Lehy, T. & Aparicio, T. Growth factor receptor expression in anal squamous lesions: modifications associated with oncogenic human papillomavirus and human immunodeficiency virus. Hum Pathol 2009;40:1517-27.

Wang, D. G., Fan, J. B., Siao, C. J., Berno, A., Young, P., Sapolsky, R., Ghandour, G., Perkins, N., Winchester, E., Spencer, J., Kruglyak, L., Stein, L., Hsie, L., Topaloglou, T., Hubbell, E., Robinson, E., Mittmann, M., Morris, M. S., Shen, N., Kilburn, D., Rioux, J., Nusbaum, C., Rozen, S., Hudson, T. J., Lipshutz, R., Chee, M. & Lander, E. S. Large-scale identification, mapping, and genotyping of single-nucleotide polymorphisms in the human genome. Science 1998;280:1077-82.

Warburton, D. De novo balanced chromosome rearrangements and extra marker chromosomes identified at prenatal diagnosis: clinical significance and distribution of breakpoints. Am J Hum Genet 1991;49:995-1013.

Waziri, M., Patil, S. R., Hanson, J. W. & Bartley, J. A. Abnormality of chromosome 11 in patients with features of Beckwith-Wiedemann syndrome. J Pediatr 1983;102:873-6.

Weir, B., Zhao, X. & Meyerson, M. Somatic alterations in the human cancer genome. Cancer Cell 2004;6:433-8.
Weiss, R. H. & Lin, P. Y. Kidney cancer: identification of novel targets for therapy. Kidney Int 2006;69:224-32.
Weksberg, R., Shen, D. R., Fei, Y. L., Song, Q. L. & Squire, J. Disruption of insulin-like growth factor 2 imprinting in Beckwith-Wiedemann syndrome. Nat Genet 1993;5:143-50.
Weksberg, R., Nishikawa, J., Caluseriu, O., Fei, Y. L., Shuman, C., Wei, C., Steele, L., Cameron, J., Smith, A., Ambus, I., Li, M., Ray, P. N., Sadowski, P. & Squire, J. Tumour development in the Beckwith-Wiedemann syndrome is associated with a variety of constitutional molecular 11p15 alterations including imprinting defects of KCNQ1OT1. Hum Mol Genet 2001;10:2989-3000.
Weksberg, R., Smith, A. C., Squire, J. & Sadowski, P. Beckwith-Wiedemann syndrome demonstrates a role for epigenetic control of normal development. Hum Mol Genet 2003;12 Spec No 1:R61-8.
Weksberg, R., Shuman, C. & Smith, A. C. Beckwith-Wiedemann syndrome. Am J Med Genet C Semin Med Genet 2005;137C:12-23.
Wiedemann HR (September 1964). "Familial malformation complex with umbilical hernia and macroglossia - a "new syndrome"?" (in French). Journal de génétique humaine 13: 223–32.
Wiesener, M. S., Munchenhagen, P. M., Berger, I., Morgan, N. V., Roigas, J., Schwiertz, A., Jurgensen, J. S., Gruber, G., Maxwell, P. H., Loning, S. A., Frei, U., Maher, E. R., Grone, H. J. & Eckardt, K. U. Constitutive activation of hypoxia-inducible genes related to overexpression of hypoxia-inducible factor-1alpha in clear cell renal carcinomas. Cancer Res 2001;61:5215-22.
Wild, P., Knuechel, R., Dietmaier, W., Hofstaedter, F. & Hartmann, A. Laser microdissection and microsatellite analyses of breast cancer reveal a high degree of tumour heterogeneity. Pathobiology 2000;68:180-90.
Wilhelm, M., Veltman, J. A., Olshen, A. B., Jain, A. N., Moore, D. H., Presti, J. C., Jr., Kovacs, G. & Waldman, F. M. Array-based comparative genomic hybridization for the differential diagnosis of renal cell cancer. Cancer Res 2002;62:957-60.
Wilkie, A. O., Lamb, J., Harris, P. C., Finney, R. D. & Higgs, D. R. A truncated human chromosome 16 associated with alpha thalassaemia is stabilized by addition of telomeric repeat (TTAGGG)n. Nature 1990;346:868-71.
Wizigmann-Voos, S., Breier, G., Risau, W. & Plate, K. H. Up-regulation of vascular endothelial growth factor and its receptors in von Hippel-Lindau disease-associated and sporadic hemangioblastomas. Cancer Res 1995;55:1358-64.
Wolf, U., Reinwein, H., Porsch, R., Schroter, R. & Baitsch, H. [Deficiency on the short arms of a chromosome No. 4]. Humangenetik 1965;1:397-413.
Wolk, A., Lindblad, P. & Adami, H. O. Nutrition and renal cell cancer. Cancer Causes Control 1996;7:5-18.
Wong, K. K., Tsang, Y. T., Shen, J., Cheng, R. S., Chang, Y. M., Man, T. K. & Lau, C. C. Allelic imbalance analysis by high-density single-nucleotide polymorphic allele (SNP) array with whole genome amplified DNA. Nucleic Acids Res 2004;32:e69.
Woodward, E. R., Eng, C., Mcmahon, R., Voutilainen, R., Affara, N. A., Ponder, B. A. & Maher, E. R. Genetic predisposition to phaeochromocytoma: analysis of candidate genes GDNF, RET and VHL. Hum Mol Genet 1997;6:1051-6.

Woodward, E. R., Buchberger, A., Clifford, S. C., Hurst, L. D., Affara, N. A. & Maher, E. R. Comparative sequence analysis of the VHL tumour suppressor gene. Genomics 2000a;65:253-65.

Woodward, E. R. & Maher, E. R. Von Hippel-Lindau disease and endocrine tumour susceptibility. Endocr Relat Cancer 2006;13:415-25.

Wu, Y. Q., Heilstedt, H. A., Bedell, J. A., May, K. M., Starkey, D. E., Mcpherson, J. D., Shapira, S. K. & Shaffer, L. G. Molecular refinement of the 1p36 deletion syndrome reveals size diversity and a preponderance of maternally derived deletions. Hum Mol Genet 1999;8:313-21.

Yan, Y., Frisen, J., Lee, M. H., Massague, J. & Barbacid, M. Ablation of the CDK inhibitor p57Kip2 results in increased apoptosis and delayed differentiation during mouse development. Genes Dev 1997;11:973-83.

Ye, Y., Vasavada, S., Kuzmin, I., Stackhouse, T., Zbar, B. & Williams, B. R. Subcellular localization of the von Hippel-Lindau disease gene product is cell cycle-dependent. Int J Cancer 1998;78:62-9.

Young, A. C., Craven, R. A., Cohen, D., Taylor, C., Booth, C., Harnden, P., Cairns, D. A., Astuti, D., Gregory, W., Maher, E. R., Knowles, M. A., Joyce, A., Selby, P. J. & Banks, R. E. Analysis of VHL Gene Alterations and their Relationship to Clinical Parameters in Sporadic Conventional Renal Cell Carcinoma. Clin Cancer Res 2009;15:7582-7592.

Yu, F., White, S. B., Zhao, Q. & Lee, F. S. HIF-1alpha binding to VHL is regulated by stimulus-sensitive proline hydroxylation. Proc Natl Acad Sci U S A 2001;98:9630-5.

Yu, W., Ballif, B. C., Kashork, C. D., Heilstedt, H. A., Howard, L. A., Cai, W. W., White, L. D., Liu, W., Beaudet, A. L., Bejjani, B. A., Shaw, C. A. & Shaffer, L. G. Development of a comparative genomic hybridization microarray and demonstration of its utility with 25 well-characterized 1p36 deletions. Hum Mol Genet 2003;12:2145-52.

Yuan, J. M., Castelao, J. E., Gago-Dominguez, M., Yu, M. C. & Ross, R. K. Tobacco use in relation to renal cell carcinoma. Cancer Epidemiol Biomarkers Prev 1998;7:429-33.

Yunis, J. J. High resolution of human chromosomes. Science 1976;191:1268-70.

Zackai, E. H. & Emanuel, B. S. Site-specific reciprocal translocation, t(11;22) (q23;q11), in several unrelated families with 3:1 meiotic disjunction. Am J Med Genet 1980;7:507-21.

Zatyka M, Priestley M, Ladusans EJ, Fryer AE, Mason J, Latif F, Maher ER. 2005. Analysis of CRELD1 as a candidate 3p25 atrioventicular septal defect locus (AVSD2). Clin Genet 67:526–528.

Zbar, B., Brauch, H., Talmadge, C. & Linehan, M. Loss of alleles of loci on the short arm of chromosome 3 in renal cell carcinoma. Nature 1987;327:721-4.

Zbar, B., Tory, K., Merino, M., Schmidt, L., Glenn, G., Choyke, P., Walther, M. M., Lerman, M. & Linehan, W. M. Hereditary papillary renal cell carcinoma. J Urol 1994;151:561-6.

Zbar, B., Kishida, T., Chen, F., Schmidt, L., Maher, E. R., Richards, F. M., Crossey, P. A., Webster, A. R., Affara, N. A., Ferguson-Smith, M. A., Brauch, H., Glavac, D., Neumann, H. P., Tisherman, S., Mulvihill, J. J., Gross, D. J., Shuin, T., Whaley, J., Seizinger, B., Kley, N., Olschwang, S., Boisson, C., Richard, S., Lips, C. H., Lerman, M. & Et Al. Germline mutations in the Von Hippel-Lindau disease (VHL)

gene in families from North America, Europe, and Japan. Hum Mutat 1996;8:348-57.

Zbar, B., Klausner, R. & Linehan, W. M. Studying cancer families to identify kidney cancer genes. Annu Rev Med 2003;54:217-33.

Zeggini, E., Weedon, M. N., Lindgren, C. M., Frayling, T. M., Elliott, K. S., Lango, H., Timpson, N. J., Perry, J. R., Rayner, N. W., Freathy, R. M., Barrett, J. C., Shields, B., Morris, A. P., Ellard, S., Groves, C. J., Harries, L. W., Marchini, J. L., Owen, K. R., Knight, B., Cardon, L. R., Walker, M., Hitman, G. A., Morris, A. D., Doney, A. S., Mccarthy, M. I. & Hattersley, A. T. Replication of genome-wide association signals in UK samples reveals risk loci for type 2 diabetes. Science 2007;316:1336-41.

Zhang, P., Liegeois, N. J., Wong, C., Finegold, M., Hou, H., Thompson, J. C., Silverman, A., Harper, J. W., Depinho, R. A. & Elledge, S. J. Altered cell differentiation and proliferation in mice lacking p57KIP2 indicates a role in Beckwith-Wiedemann syndrome. Nature 1997;387:151-8.

Zhao, X., Li, C., Paez, J. G., Chin, K., Janne, P. A., Chen, T. H., Girard, L., Minna, J., Christiani, D., Leo, C., Gray, J. W., Sellers, W. R. & Meyerson, M. An integrated view of copy number and allelic alterations in the cancer genome using single nucleotide polymorphism arrays. Cancer Res 2004;64:3060-71.

Zhou, X., Mok, S. C., Chen, Z., Li, Y. & Wong, D. T. Concurrent analysis of loss of heterozygosity (LOH) and copy number abnormality (CNA) for oral premalignancy progression using the Affymetrix 10K SNP mapping array. Hum Genet 2004;115:327-30.

Zhuang, Z., Roth, M. J., Emmert-Buck, M. R., Lubensky, I. A., Liotta, L. A. & Solomon, D. Detection of the von Hippel-Lindau gene deletion in cytologic specimens using microdissection and the polymerase chain reaction. Acta Cytol 1994;38:671-5.

Zhuang, Z., Gnarra, J. R., Dudley, C. F., Zbar, B., Linehan, W. M. & Lubensky, I. A. Detection of von Hippel-Lindau disease gene mutations in paraffin-embedded sporadic renal cell carcinoma specimens. Mod Pathol 1996;9:838-42.

Zollino, M., Orteschi, D., Marangi, G., De Crescenzo, A., Pecile, V., Riccio, A. & Neri, G. A case of Beckwith-Wiedemann syndrome caused by a cryptic 11p15 deletion encompassing the centromeric imprinted domain of the BWS locus. J Med Genet 2010 Jun;47(6):429-32. Epub 2009 Oct 20.

Appendix A1

GENOMIC DNA GENERAL REQUIREMENTS FOR 250K SNP ARRAY AND SNP 6.0 ARRAY

• DNA must be double-stranded (not single-stranded).

This requirement relates to the restriction enzyme digestion step in the protocol.

• DNA must be free of PCR inhibitors.

Examples of inhibitors include high concentrations of heme (from blood) and high concentrations of chelating agents (i.e., EDTA). The genomic DNA extraction/purification method should render DNA that is generally salt-free because high concentrations of certain salts can also inhibit PCR and other enzyme reactions.

• DNA must not be contaminated with other human genomic DNA sources, or with genomic DNA from other organisms. PCR amplification of the ligated genomic DNA is not human specific, so sufficient quantities of nonhuman DNA may also be amplified and could potentially result in compromised genotype calls. Contaminated or mixed DNA may manifest as high detection rates and low call rates.

• DNA must not be highly degraded. For any particular SNP, the genomic DNA fragment containing the SNP must have Nsp I (or Sty I) restriction sites intact so that ligation can occur on both ends of the fragment and PCR can be successful. The approximate average size of genomic DNA may be assessed on a 1% or 2% agarose gel using an appropriate size standard control. Ref 103 can be run on the same gel for side-by-side comparison. High quality genomic DNA will run as a major band at approximately 10-20 kb on the gel. Pre-amplification methods or pre-digestion with restriction enzymes other than Nsp I or Sty I have not been tested by Affymetrix. If other methods are desired, it is recommended conducting experiments to evaluate their performance with this assay.

Sources of Human Genomic DNA

The following sources of human genomic DNA have been successfully tested in the laboratories at Affymetrix for DNA that meets the requirements described in the section

• blood

• cell line

Success with other types of samples such as saliva will depend on quality (degree of degradation, degree of inhibitors present, etc.), quantity of genomic DNA extracted, and purity of these types of samples

Genomic DNA Extraction/Purification Methods

Genomic DNA extraction and purification methods that meet the general requirements outlined above should yield successful results. Methods that include boiling or strong denaturants are not acceptable, because the DNA would be rendered single-stranded. Genomic DNA extracted using the following methods have been tested at Affymetrix:

SDS/ProK digestion, phenol-chloroform extraction, Microcon® or Centricon® (Millipore) ultrapurification and concentration.

QIAGEN; QIAamp® DNA Blood Maxi Kit

DNA Cleanup

If a genomic DNA preparation is suspected to contain inhibitors, the following cleanup procedure can be used:

1. Add 0.5 volumes of 7.5 M NH4OAc, 2.5 volumes of absolute ethanol (stored at –20°C), and 0.5 µL of glycogen (5 mg/mL) to 250 ng genomic DNA.

2. Vortex and incubate at –20°C for 1 hr.

3. Centrifuge at 12,000x g in a microcentrifuge at room temperature for 20 min.

4. Remove supernatant and wash pellet with 0.5 mL of 80% ethanol.

5. Centrifuge at 12,000x g at room temperature for 5 min.

6. Remove the 80% ethanol and repeat the 80% ethanol wash one more time.

7. Resuspend the pellet in reduced EDTA TE buffer (10 mM Tris, pH 8.0, 0.1 mM EDTA, pH 8.0).

Appendix A2

Shutting Down the Fluidics Station

1. After removing a probe array from the probe array holder, the LCD window displays the message ENGAGE WASHBLOCK.

2. For the FS-450, gently lift up the cartridge lever to engage or close, the washblock.

The fluidics station automatically performs a Cleanout procedure. The LCD window indicates the progress of the Cleanout procedure.

3. When the fluidics station LCD window indicates REMOVE VIALS, the Cleanout procedure is complete.

4. Remove the sample microcentrifuge vial(s) from the sample holder(s).

5. If no other processing is to be performed, place wash lines into a bottle filled with deionized water.

6. Choose Shutdown_450 for all modules from the drop-down Protocol list in the Fluidics Station dialog box. Click the Run button for all modules. The Shutdown protocol is critical to instrument reliability.

7. After Shutdown protocol is complete, flip the ON/OFF switch of the fluidics station to the OFF position.

8. Place buffer lines in a different bottle of deionized water than the one used for the shutdown protocol.

Appendix A3

Preparation of low-C dNTPs

The reagents required are: 10 mM dCTP
10 mM dTTP
10mM dATP
10 mM dGTP
Sterile water for injections

The 10 mM dNTPs (Sigma-Aldrich Inc., USA) were retrieved from the -20°C freezer and thawed at room temperature. They were then briefly vortexed, spun and placed in a tube rack. 150 ul of sterile water, 100 ul of dTTP, 100 ul of dATP, 100 ul of dGTP and 50 ul of dCTP were pippetted into a 1.5 ml eppendorf tube. The solution was vortexed and aliquoted 50 ul into 0.5 ml eppendorf tubes. The tubes were stored in -20°C freezer until required.

Appendix A4

Preparation of washing solution

0.4XSSC/0.3% NP-40

20 ml 20XSSC and 950 ml distilled water were mixed together in a sterile glass bottle. 3 ml of NP-40 (Roche Ltd., Basel, Switzerland) was added and mixed thoroughly. The solution was adjusted to pH 7.0-7.5 with NaOH. Distilled water was added to make 1 litre final volume. The solution was kept at room temperature and discarded after 6 months.

2XSSC/0.1% NP-40

100 ml 20XSSC and 850 ml distilled water was mixed together in a sterile glass bottle. 1 ml of NP-40 (Roche Ltd., Basel, Switzerland) was added to the solution and mixed thoroughly. The pH was adjusted to 7.0-7.5 with NaOH. Distilled water was added to make 1 litre final volume. The solution was kept at room temperature and discarded after 6 months.

Appendix A5

SALSA MLPA kit P007 Human Chromosomal Abberation-3 probe mix

Length (nt)	SALSA MLPA probe	Chromosomal position
64-70-76-82	Q-fragments: DNA quantity; only visible with less than 100 ng sample DNA	
88-92-96	D-fragments: Low signal of 88 or 96 nt fragment indicates incomplete denaturation	
136	**LTA**00662-L00158	06p21.3
142	**CFLAR**00663-L00074	02q33.1
148‡	**PTEN**00522-L00387	10q23.3
154	**MYC**00580-L00145	08q24.12
160	**BCL**2L100843-L00105	20q11.21
166	**TNFRSF1B**00553-L00122	01p36.22
175	**TNFRSF1A**00554-L00123	12p13.31
184	**CASP1**00559-L00128	11q22.3
194	**B2M**00349-L00175	15q21.1
202	**MME**00487-L00069	03q25.1
211	**IFNG**00472-L00088	12q14
220	**SLA**00488-L00080	08q24.2
229*	**LHX1**10813-L12283	17q12
238	**TINF2**00974-L00561	14q12
247	**MSH2**00911-L00499	02p21
256	**TOP2A**01055-L00628	17q21.2
265	**THBD**00474-L00388	20p11.2
274	**BCL2**01019-L00365	18q21.33
283	**FMR2**00493-L00369	Xq28
292‡	**TFF1**00509-L02263	21q22.3
301	**BCL6**00494-L00072	03q27
310	**IL1**800471-L00054	11q23.1
319	**CTPS1**0812-L00143	1p34.2
328	**CDKN1A**00543-L00370	06p21.2
337	**Hs.57051800497**-L00071	03q26
346	**MVP**00550-L00372	16p11.2
355	**BIRC2**00547-L00116	11q22
364	**MDM2**00337-L00163	12q14.3
373	**IL2**00655-L00183	04q26
382	**IL12B**00470-L00053	05q33.1
391	**NFKBIA**00478-L00061	14q13
400	**PRKDC**00545-L00114	08q11
409	**CD44**00669-L00373	11p12
418	**HLAF**00656-L00393	06p21.3
427	**CASP2**00680-L00121	07q35

435	**NCOA3**01015-L00595	20q13.12
445	**ING1**00802-L00320	13q34
454	**IGF1R**00605-L00018	15q26
461	**TP53**00844-L00302	17p13.1
470	**PTK2**01021-L00188	08q24

* New in lot 0108; replaces the 17q12 probe for SCYA3 present in previous lots.
‡ Small change in length or peak height, no change in sequence detected as compared to previous lots.